

LOSSLESS COUPLED NONUNIFORM LINES AND THEIR APPLICATIONS
TO DIRECTIONAL COUPLERS AND ALL-PASS NETWORKS

Satchandi Narayan Verma

A THESIS
in
The Faculty
of
Engineering

Presented in Partial Fulfillment of the Requirements for
the Degree of Doctor of Engineering at
Sir George Williams University
Montreal, Canada

September, 1972

7

IN MEMORY OF MY FATHER

NIRANJAN LAL VERMA

TABLE OF CONTENTS

LIST OF TABLES	vii
LIST OF FIGURES	ix
LIST OF IMPORTANT SYMBOLS AND ABBREVIATIONS	xvii
ACKNOWLEDGEMENTS	xxii
ABSTRACT	xxiii
1. INTRODUCTION	1
1.1 General	1
1.2 Lossless Transmission Lines	2
1.3 Lossless Coupled Lines	4
1.4 Scope of the Thesis	14
2. DECOUPLING OF LOSSLESS COUPLED NONUNIFORM TRANSMISSION LINES	16
2.1 Introduction	16
2.2 Decoupling of Coupled Lines	16
2.3 Coupled Line Immittance and Chain Matrices	21
2.4 Coupled Line Transfer Scattering Matrix	26
2.5 Conclusions	31
3. COUPLED NONUNIFORM TRANSMISSION LINE DIRECTIONAL COUPLERS	32

3.1 Introduction	32
3.2 Four-port Codirectional Coupler	32
3.3 Coupled Lines as Codirectional Couplers	36
3.4 Coupled Line Codirectional Coupler Characteristics	44
3.5 Four-port Contradirectional Coupler	46
3.6 Coupled Lines as Contradirectional Couplers	49
3.7 Coupled Line Contradirectional Couplers with 'Basic lines' as Decoupled Lines	60
3.8 Coupled Line Contradirectional Couplers with 0, 90 or 180 Degrees Phase Shifts	83
3.9 Conclusions	91
4. COUPLED NONUNIFORM TRANSMISSION LINE FOLDED ALL-PASS NETWORKS	94
4.1 Introduction	94
4.2 Lossless All-pass Two-port Networks	94
4.3 Coupled Lines as Folded All-pass Networks	97
4.4 Folded All-pass Networks with 'Basic lines' as Decoupled Lines	114
4.4.1 Phase Characteristics	114
4.4.2 Delay Characteristics	140
4.5 Conclusions	150
5. CONCLUSIONS	152

REFERENCES	156
APPENDIX A	171
APPENDIX B	176
APPENDIX C	177

LIST OF TABLES

Table 3.1	Chain Matrices of the Basic Lines with Hyperbolic Solutions	62
Table 3.2	Chain Matrices of the Duals of the Basic Lines Considered in Table 3.1	63
Table 3.3	ϵ for Contradirectional Couplers with Basic Lines as Decoupled Lines	64
Table 3.4	Decoupled Line Tapers for Various Couplers	66
Table 3.5	Scattering Matrix and Characteristics of Couplers with Decoupled Symmetric NUTLs	85
Table 4.1	Scattering Matrices of Various CNU TL Folded All-pass Networks	115
Table 4.2	Phase Shifts of Various CNU TL Folded All-pass Networks	116
Table 4.3	Phase Shifts for Types IA and IB CNU TL Folded All-pass Networks with Basic Lines as Decoupled Lines	117

Table 4.4	Phase Shifts for Types IIA and IIB	
	Folded All-pass Networks with Basic	
	Lines as Decoupled Lines	118

LIST OF FIGURES

Fig. 1.1	A Pair of Lossless Coupled Lines with Common Return	5
Fig. 1.2	Various Strip Line Configurations	8
Fig. 1.3	Even and Odd Mode Circuits for a Symmetrical Coupled Line four-port	12
Fig. 2.1	A Pair of Coupled Lossless Lines and the Corresponding Decoupled Lines	22
Fig. 2.2	A Terminated Four-port Network	27
Fig. 3.1	Four-port Codirectional Coupler	33
Fig. 3.2	Four-port Contradirectional Coupler	50
Fig. 3.3	Coupling Characteristics of CNU TL Contradirectional Couplers with ELs as Decoupled Lines	67
Fig. 3.4	Coupling Characteristics of CNU TL Contradirectional Couplers with ALs as Decoupled Lines	68
Fig. 3.5	Coupling Characteristics of CNU TL Contradirectional Couplers with TLs as Decoupled Lines	69

Fig. 3.6	Coupling Characteristics of CNUTL Contradirectional Couplers with HSSLs as Decoupled Lines	70
Fig. 3.7	Coupling Characteristics of CNUTL Contradirectional Couplers with HCSLs as Decoupled Lines	71
Fig. 3.8	$S_{\beta l}^{\ell}$ Characteristics of CNUTL Contradirectional Couplers with ELs as Decoupled Lines	73
Fig. 3.9	$S_{\beta l}^{\ell}$ Characteristics of CNUTL Contradirectional Couplers with ALs as Decoupled Lines	74
Fig. 3.10	$S_{\beta l}^{\ell}$ Characteristics of CNUTL Contradirectional Couplers with TLs as Decoupled Lines	75
Fig. 3.11	$S_{\beta l}^{\ell}$ Characteristics of CNUTL Contradirectional Couplers with HSSLs as Decoupled Lines	76
Fig. 3.12	$S_{\beta l}^{\ell}$ Characteristics of CNUTL Contradirectional Couplers with HCSLs as Decoupled Lines	77

Fig. 3.13	$S_{m\ell}^e$ Characteristics of CNUTL Contradirectional Couplers with ELs as Decoupled Lines	78
Fig. 3.14	$S_{m\ell}^e$ Characteristics of CNUTL Contradirectional Couplers with ALs as Decoupled Lines	79
Fig. 3.15	$S_{m\ell}^e$ Characteristics of CNUTL Contradirectional Couplers with TLs as Decoupled Lines	80
Fig. 3.16	$S_{m\ell}^e$ Characteristics of CNUTL Contradirectional Couplers with HSSLs as Decoupled Lines	81
Fig. 3.17	$S_{m\ell}^e$ Characteristics of CNUTL Contradirectional Couplers with HCSLs as Decoupled Lines	82
Fig. 3.18	Coupling Characteristics of CNUTL Contradirectional Couplers with Symmetric ELs in Back to Back Configuration as Decoupled Lines.	87
Fig. 3.19	Coupling Characteristics of CNUTL Contradirectional Couplers with Symmetric ELs in Front to Front	

	Configuration as Decoupled Lines.	88
Fig. 3.20	Coupling Characteristics of CNU TL Contradirectional Couplers with 0° 180° Phase Shifts over a Frequency Band	92
Fig. 4.1	A Lossless Terminated Two-port Network	95
Fig. 4.2	A Coupled Line Four-port Network	98
Fig. 4.3	CNU TL Folded All-pass Networks of Types I and II	100
Fig. 4.4	CNU TL Folded All-pass Networks of Type III	110
Fig. 4.5	Phase Characteristics of Type IA CNU TL Folded All-pass Networks with ELs as Decoupled Lines	120
Fig. 4.6	Phase Characteristics of Type IA CNU TL Folded All-pass Networks with ALs as Decoupled Lines	121
Fig. 4.7	Phase Characteristics of Type IA CNU TL Folded All-pass Networks with TLs as Decoupled Lines	122
Fig. 4.8	Phase Characteristics of Type IA CNU TL Folded All-pass Networks with HSSLs as Decoupled Lines	123

Fig. 4.9	Phase Characteristics of Type IA CNUTL Folded All-pass Networks with HCSLs as Decoupled Lines	124
Fig. 4.10	Phase Characteristics of Type IB CNUTL Folded All-pass Networks with ELs as Decoupled Lines	125
Fig. 4.11	Phase Characteristics of Type IB CNUTL Folded All-pass Networks with ALs as Decoupled Lines	126
Fig. 4.12	Phase Characteristics of Type IB CNUTL Folded All-pass Networks with TLs as Decoupled Lines	127
Fig. 4.13	Phase Characteristics of Type IB CNUTL Folded All-pass Networks with HSSLs as Decoupled Lines	128
Fig. 4.14	Phase Characteristics of Type IB CNUTL Folded All-pass Networks with HCSLs as Decoupled Lines	129
Fig. 4.15	Phase Characteristics of Type IIA CNUTL Folded All-pass Networks with ELs as Decoupled Lines	130

Fig. 4.16	Phase Characteristics of Type IIA CNUTL Folded All-pass Networks with ALs as Decoupled Lines	131
Fig. 4.17	Phase Characteristics of Type IIA CNUTL Folded All-pass Networks with TLs as Decoupled Lines	132
Fig. 4.18	Phase Characteristics of Type IIA CNUTL Folded All-pass Networks with HSSLs as Decoupled Lines.	133
Fig. 4.19	Phase Characteristics of Type IIA CNUTL Folded All-pass Networks with HCSLs as Decoupled Lines	134
Fig. 4.20	Phase Characteristics of Type IIB CNUTL Folded All-pass Networks with ELs as Decoupled Lines	135
Fig. 4.21	Phase Characteristics of Type IIB CNUTL Folded All-pass Networks with ALs as Decoupled Lines	136
Fig. 4.22	Phase Characteristics of Type IIB CNUTL Folded All-pass Networks with TLs as Decoupled Lines	137

Fig. 4.23	Phase Characteristics of Type IIB CNUTL Folded All-pass Networks with HSSLs as Decoupled Lines	138
Fig. 4.24	Phase Characteristics of Type IIB CNUTL Folded All-pass Networks with HCSLs as Decoupled Lines	139
Fig. 4.25	Delay Characteristics of Type IA CNUTL Folded All-pass Networks with ELs as Decoupled Lines	142
Fig. 4.26	Delay Characteristics of Type IA CNUTL Folded All-pass Networks with ALs as Decoupled Lines	142
Fig. 4.27	Delay Characteristics of Type IA CNUTL Folded All-pass Networks with TLs as Decoupled Lines	143
Fig. 4.28	Delay Characteristics of Type IA CNUTL Folded All-pass Networks with HSSLs as Decoupled Lines.	143
Fig. 4.29	Delay Characteristics of Type IA CNUTL Folded All-pass Networks with HCSLs as Decoupled Lines	144

7

Fig. 4.30	Delay Characteristics of Type IB CNUTL Folded All-pass Networks with ELs as Decoupled Lines	145
Fig. 4.31	Delay Characteristics of Type IB CNUTL Folded All-pass Networks with ALs as Decoupled Lines	146
Fig. 4.32	Delay Characteristics of Type IB CNUTL Folded All-pass Networks with TLs as Decoupled Lines	147
Fig. 4.33	Delay Characteristics of Type IB CNUTL Folded All-pass Networks with HSSLs as Decoupled Lines	148
Fig. 4.34	Delay Characteristics of Type IB CNUTL Folded All-pass Networks with HCSLs as Decoupled Lines	149
Fig. A.1	A Terminated Four-port Network	172

LIST OF IMPORTANT ABBREVIATIONS AND SYMBOLS

AL	Algebraic Line
CNUTL	Coupled Nonuniform Transmission Line
CUTL	Coupled Uniform Transmission Line
EL	Exponential Line
HCSL	Hyperbolic Cosine Squared Line
HSSL	Hyperbolic Sine Squared Line
TL	Trigonometric Line
UTL	Uniform Transmission Line
[a]	Chain Matrix of a Four-port Network
$[a]_1$	Chain Matrix of the Decoupled Line 1 as a Two-port
$[a]_2$	Chain Matrix of the Decoupled Line 2 as a Two-port
$C_1(x)$	Capacitance per unit length of Line 1 at a distance x from the sending end
$C_2(x)$	Capacitance per unit length of Line 2 at a distance x from the sending end
$C_{11}(x)$	Self-capacitance per unit length of Line A to ground at a distance x from the sending end

$C_{22}(x)$	Self-capacitance per unit length of Line B to ground at a distance x from the sending end
$C_{12}(x)$	Mutual Capacitance per unit length between Lines A and B at a distance x from the sending end
e	Coupling of a Directional Coupler
D	Directivity of a Directional Coupler
$E_1(s,x)$	Voltage on Line 1, with respect to ground, at a distance x from the sending end
$E_2(s,x)$	Voltage on Line 2, with respect to ground, at a distance x from the sending end
$I_A(s,x)$	Current in Line A at a distance x from the sending end
$I_B(s,x)$	Current in Line B at a distance x from the sending end
$J_1(s,x)$	Current in Line 1 at a distance x from the sending end
$J_2(s,x)$	Current in Line 2 at a distance x from the sending end
l	Length of a given line.
$L_1(x)$	Self-inductance per unit length of Line 1

	at a distance x from the sending end
$L_2(x)$	Self-inductance per unit length of Line 1 at a distance x from the sending end
$L_{11}(x)$	Self-inductance per unit length of Line A at a distance x from the sending end
$L_{22}(x)$	Self-inductance per unit length of Line B at a distance x from the sending end
$L_{12}(x)$	Mutual inductance per unit length between Lines A and B at a distance x from the sending end
m	Taper per unit length of a Nonuniform Transmission Line
NUTL	Nonuniform Transmission Line
r_1, r_2, r_3, r_4	Terminating resistors
[T]	Transfer Scattering Matrix of a Four-port Network
v	Velocity of Propagation of the TEM wave
$V_A(s, x)$	Voltage on Line A, with respect to ground, at a distance x from the sending end
$V_B(s, x)$	Voltage on Line B, with respect to ground, at a distance x from the sending end
[Y]	Admittance Matrix of a Four-port Network

$[Y]_1$	Admittance Matrix of Line 1 as a Two-port
$[Y]_2$	Admittance Matrix of Line 2 as a Two-port
$[Z]$	Impedance Matrix of a Four-port Network
$[Z]_1$	Impedance Matrix of Line 1, as a Two-port
$[Z]_2$	Impedance Matrix of Line 2, as a Two-port
$Z_1(x)$	$\sqrt{L_1(x)/C_1(x)}$, "Characteristic Impedance of Line 1"
$Z_2(x)$	$\sqrt{L_2(x)/C_2(x)}$, "Characteristic Impedance of Line 2"
$\beta(x)$	$\omega\sqrt{L(x)/C(x)}$, the Phase Function of a Nonuniform Transmission Line
γ	$\beta\sqrt{1 - (m^2/\beta^2)}$
Γ	$\beta\sqrt{(m^2/4\beta^2) - 1}$
μ	$\beta\sqrt{1 + (m^2/\beta^2)}$
$\eta(x)$	$\sqrt{[Z_1(x)/Z_2(x)]}$
$\rho(x)$	$\sqrt{[L_{22}(x)/L_{11}(x)]}$
ρ_2	$\sqrt{[r_2/r_1]}$
ρ_3	$\sqrt{[r_3/r_1]}$
ρ_4	$\sqrt{[r_4/r_1]}$
τ	Group Delay of a Folded All-pass Network, using CNUILs of length ℓ

τ_o	Group Delay when TEM wave propagates through a Uniform Transmission Line of length 2ℓ
τ^*	Normalized Group Delay of a CNUTL Folded All-pass Network
ϕ_{CT}	Phase Shift between coupled and transmitted signals
ω	Angular Frequency

ACKNOWLEDGEMENTS

The author wishes to express his gratitude to Professors M.N.S.Swamy and B.B.Bhattacharyya for kindly suggesting the problem and for the continuing guidance and constructive criticism throughout the course of the investigation.

Thanks are due to Dr.V.Ramachandran and Dr.J.C.Giguere for their suggestions during the preparation of the manuscript.

Thanks are also due to Mrs.Kamala Ramachandran for kindly typing the thesis.

The author also gratefully acknowledges the patience and understanding of his wife Vibhashini and sacrifice made by his children Shakti and Dhiraj during the period of study.

This work was supported under the National Research Council of Canada, Grants Nos. A-7739 and A-7740 awarded to Professors M.N.S.Swamy and B.B.Bhattacharyya.

ABSTRACT

This thesis is concerned with an elegant method of decoupling a pair of lossless coupled nonuniform transmission lines (CNUTL), and its applications to a study of directional couplers and all-pass networks using CNUTLs.

A theory is developed whereby a pair of lossless CNUTLs (similar or dissimilar) with a common return and supporting only TEM waves, is decoupled into two lossless nonuniform transmission lines (NUTL). This theory is quite general, and is independent of the port terminations, any symmetry conditions, etc. The method directly relates the line parameters of the CNUTLs to those of the decoupled lines and vice versa; further, the matrix parameters of the CNUTLs as a four-port, are explicitly expressed in terms of those of the decoupled lines as two-ports.

The above theory is utilized to study two applications of CNUTLs, namely, as directional couplers and all-pass networks.

It is shown that for CNUTLs to behave as a codirectional coupler, each of the decoupled lines should be a proportional line, while for contradirectional coupler action, the two decoupled lines have to be duals of each other. Further, such contradirectional (codirectional) couplers have the property $S_{13} = S_{24}$ ($S_{13} = S_{24}$ and $S_{14} = S_{23}$) for their scattering parameters. The coupling response of the codirectional coupler is found to be periodic, while the phase

7

shift between coupled and transmitted signals varies linearly with frequency. Contradirectional couplers are found to exhibit different characteristics depending on the distributions of the decoupled lines. It is shown that a 90° phase shift is obtained by choosing symmetric NUTLs as decoupled lines, while 0° or 180° phase shift may be obtained by choosing one decoupled line to be the same as the other, turned around. The coupling response of various contradirectional couplers, for which the decoupled lines are "basic NUTLs with hyperbolic solutions", are studied in detail. It is shown that all these couplers have a high-pass response and that the CNUTLs with "hyperbolic cosine squared" lines as decoupled lines, have the best response of all the CNUTLs considered.

Three different types of CNUTL folded all-pass networks are studied by converting the CNUTL four-port into a two-port by proper port terminations. The requirements to be satisfied by the chain parameters of the corresponding decoupled NUTLs as two ports are derived. It is shown that these conditions are always met if dual lines are chosen as the decoupled lines for two of these types, while for the third type, the decoupled lines are, in addition, proportional. The phase and delay characteristics of the above three types are investigated, when the decoupled lines are basic lines with hyperbolic solutions. It is shown that these characteristics can be controlled by changing the taper of the lines. Further, these networks can provide delays larger than that obtainable from a single

uniform line of twice the length. Of the lines considered, the peak delay is found to be maximum when the decoupled lines are chosen to be "trigonometric" or "hyperbolic sine squared" lines.

7

CHAPTER 1

INTRODUCTION

1.1 General:

In UHF and microwave systems, the frequency is very high, causing the wavelength to become quite small (of the order of centimeters), thereby making the network elements comparable in size to the operating wavelength. This causes the elements to deviate from their low frequency characteristics, and consequently their lumped models indicating that the distributed nature of the network elements must now be considered; for example, the distributed capacitance associated with the winding of an inductor^(1,2). Thus the representation of the system by a lumped model is no longer adequate, and must be replaced by the more accurate distributed parameter model. This being the case, it is desirable to introduce distributed effects into the system systematically and by design, rather than to have them as an unavoidable consequence. Thus it is logical to construct UHF and microwave systems with distributed elements whose electrical properties can be easily and precisely predicted. Transmission lines and waveguides are some of the distributed elements which has been in use for many years in UHF and microwave systems^(2,3). Waveguide components have the advantage of high power handling capacity without radiation. However, for each waveguide, there exists a band of frequencies over which the transmission of energy takes place. This band is required to be above a cut-off frequency of the waveguide, which depends on the waveguide dimensions as well as on the mode of

propagation. On the other hand, transmission lines can support propagation of frequencies starting from zero frequency (d.c.). Further the bandwidth of transmission lines operating in TEM mode is greater than that of corresponding waveguide components. Consequently, they have found applications in wideband systems with bandwidth requirements of up to one decade ⁽⁴⁾. A more significant advantage of transmission line networks is that at low microwave frequencies, waveguide components become very large while transmission line type device remain reasonably small ^(3,5).

1.2 Lossless Transmission Lines:

The lossless lines are of particular interest since it is desirable to transmit energy from source to load with a minimum loss. It has been found, in fact, that most UHF and microwave transmission systems in existence do approximate the lossless condition. Lossless uniform transmission line (UTL) has been extensively studied and its properties are firmly established ⁽⁶⁾. These lines support TEM waves and are widely used as transformers, resonators, filters, phase equalizers and matching stubs ^(3,6-10). However, in these applications, the UTLs can be used only in a limited range of frequencies. On the other hand, many microwave communication systems require components to operate over a wide band of frequencies, so that, they can handle signals at various frequencies without degrading the system performance. In order to achieve wider bandwidths, cascaded sections of UTLs having different characteristic impedances have been employed ⁽¹¹⁻¹³⁾. Though this technique extends the frequency

band of operation to some extent, the resulting networks are larger in weight and size. To obtain superior characteristics with reduction in size and weight, attention has been given in recent years to the possibility of using lossless nonuniform transmission lines (NUTL) as various acoustics⁽¹⁴⁾ and microwave components⁽⁹⁾.

A lossless NUTL is a lossless transmission line, whose nominal characteristic impedance varies continuously along the length of the line according to a prescribed law and is described by the following distributions:

$$\begin{aligned} L(x) &= L_0 f(x) \\ C(x) &= C_0 g(x) \end{aligned} \quad 0 \leq x \leq l \quad \dots (1.1)$$

where

$L(x)$ = series inductance per unit length at a distance x from the transmitting end,

$C(x)$ = shunt capacitance per unit length at a distance x from the transmitting end,

and L_0, C_0 = arbitrary scaling factors.

Considerable work has been done on obtaining the solutions of telegrapher's equations for NUTLs as well as their properties⁽¹⁵⁻¹⁷⁾. A comprehensive bibliography on NUTLs is given by Kaufman⁽¹⁸⁾. These authors have also found various microwave applications of NUTLs as microwave components. Some of the NUTLs which have been investigated for microwave applications are Bessel⁽¹⁹⁻²¹⁾, hyperbolic⁽²²⁾, parabolic⁽²³⁾,

exponential⁽²⁴⁻²⁵⁾, Klopfenstein⁽²⁰⁾ and Chebyshev⁽²⁷⁾. Of various NUTLs, exponential line, in which $f(x)$ and $g(x)$ are inverse and exponential functions of x has received a great deal of investigation mainly because of the ease of construction and the simplicity of obtaining voltage and current solutions. This line has been extensively used as resonators, filters, transformers and other microwave components^(3,28). It has been found that these components designed with exponential lines exhibit better characteristics than those of UTLs. Nonuniform transmission lines with various other parameter distributions have also been used as pulse transformers, matching sections, filters and broad band terminations⁽²⁹⁻³³⁾.

1.3 Lossless Coupled Transmission Lines:

Applications of a pair of lossless coupled transmission lines in microwave frequencies have been investigated by many authors to obtain superior properties which are unobtainable from uncoupled lines⁽³⁵⁻³⁷⁾. Directional couplers, delay networks, impedance transformers, radiation launching devices and slow wave structures are to name but a few of such applications. A pair of lossless coupled nonuniform transmission lines (CNUTL) with common return is schematically shown in Fig.1.1, and can be described by the following distributions:

$$\begin{aligned}
 L_{11}(x) &= L_{110} f_{11}(x) \\
 L_{22}(x) &= L_{220} f_{22}(x) & 0 \leq x \leq \ell & \dots (1.2a) \\
 L_{12}(x) &= L_{21}(x) = L_{120} f_{12}(x)
 \end{aligned}$$

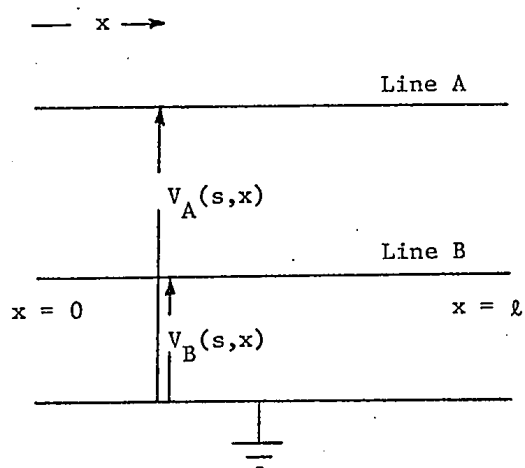


Fig. 1.1: A Pair of Lossless Coupled
Lines with Common Return

and

$$\begin{aligned}
 C_{11}(x) &= C_{110} g_{11}(x) \\
 C_{22}(x) &= C_{220} g_{22}(x) \\
 C_{12}(x) &= C_{21}(x) = C_{120} g_{12}(x)
 \end{aligned}
 \quad 0 \leq x \leq \ell \quad \dots (1.2b)$$

where the line parameters per unit length at a distance x from the transmitting end are

$$\begin{aligned}
 L_{11}(x) &= \text{self-inductance of line A,} \\
 L_{22}(x) &= \text{self-inductance of line B,} \\
 L_{12}(x) &= \text{mutual inductance between lines A and B,} \\
 C_{11}(x) &= \text{self-capacitance of line A to ground,} \\
 C_{22}(x) &= \text{self-capacitance of line B to ground,} \\
 C_{12}(x) &= \text{mutual capacitance between lines A and B.}
 \end{aligned}$$

The parameters $L_{12}(x)$ and $C_{12}(x)$ represent the distributed electro-magnetic coupling between the lines. The distributions of the line parameters are contained in $f_{ij}(x)$ and $g_{ij}(x)$, which are non-dimensional while the quantities L_{ij0} and C_{ij0} are dimensional (where $i=1,2$ and $j=1,2$). For a pair of lossless coupled uniform transmission lines (CUTL),

$$f_{ij}(x) = g_{ij}(x) = 1,$$

that is, the distributions are independent of x . Coupled uniform transmission lines become identical when in addition they also have

$$\begin{aligned}
 L_{110} &= L_{220}, \\
 C_{110} &= C_{220}
 \end{aligned}$$

In order now to distinguish clearly between various kinds of lossless CNU TLs so far investigated in microwave applications, following terms are introduced:

- (i) Identical coupled lines: Coupled lines having parameters such that

$$\begin{aligned} f_{11}(x) &= f_{22}(x) , & L_{110} &= L_{220} \\ g_{11}(x) &= g_{22}(x) , & C_{110} &= C_{220} \end{aligned} \quad 0 \leq x \leq l \quad \dots (1.3)$$

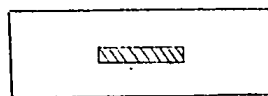
- (ii) Similar coupled lines: Coupled lines having parameters such that

$$\begin{aligned} f_{11}(x) &= f_{22}(x) , & L_{110} &\neq L_{220} \\ g_{11}(x) &= g_{22}(x) , & C_{110} &\neq C_{220} \end{aligned} \quad 0 \leq x \leq l \quad \dots (1.4)$$

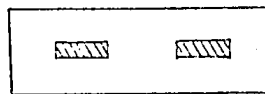
- (iii) Dissimilar coupled lines: Coupled lines having parameter distributions such that

$$\begin{aligned} f_{11}(x) &\neq f_{22}(x) \\ g_{11}(x) &\neq g_{22}(x) \end{aligned} \quad 0 \leq x \leq l \quad \dots (1.5)$$

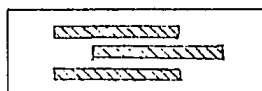
Thus dissimilar coupled lines have distributions independent of each other while the scaling constants may be same or different. There exist a number of methods to construct CUTLs, using strip lines, at microwave frequencies for various values of electromagnetic coupling⁽³⁸⁻⁵⁰⁾. Some of these configurations are shown in Fig. 1.2. Recently Arndt⁽⁵¹⁾ has shown how in some cases, these techniques can also be employed to construct CNU TLs. Oliver⁽⁵²⁾ was the first to exploit the presence of



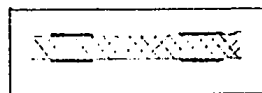
(a)



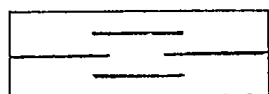
(b)



(c)



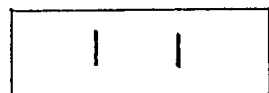
(d)



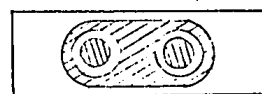
(e)



(f)



(g)



(h)

(a) Shielded Strip Line

(b) Coupled Strip Lines

(c) Interlacing Configuration

(d) Printed Dielectric Sheets

(e) Parallel Slit Coupled

(f) Perpendicular Slit Coupled

(g) Broadside Coupled

(h) Re-entrant Coaxial Lines

Fig. 1.2: Various Strip Line Configurations

electromagnetic coupling in transmission lines as directional couplers. Since then, many authors have studied identical CUTLs as directional-couplers^(34,35,53,54). It has been found that these couplers have infinite directivity with 90° phase difference between coupled and transmitted signals and require all the ports to be matched. Cristal⁽⁵⁵⁾ considered the directional couplers with similar CUTLs. These couplers demonstrate directional coupler action along with impedance transformation between certain ports. A severe limitation of CUTLs as directional couplers is their restricted bandwidth, which is often inadequate for wide band microwave systems. With a view to increasing the bandwidth, directional couplers are constructed by cascading CUTLs, with different characteristic impedances⁽⁵⁶⁻⁵⁸⁾. Using the analytical equivalence⁽⁵⁹⁾ between the directional coupler and that of stepped quarter wavelength filter, Levy⁽⁶⁰⁾ gave a general synthesis procedure for asymmetric multi-element CUTL directional couplers. While achieving a greater bandwidth, these couplers suffer from the fact that the electromagnetic coupling is discontinuous at the junction of sections, which degrades the coupler directivity and other characteristics appreciably. In order to eliminate the discontinuity effects and to further increase the coupler bandwidth, CNUTLs are used as directional couplers. These couplers are fabricated by either employing coupled NUTLs^(44,51,61,62) or are approximated by a cascade of coupled UTL segments of short lengths, whose electromagnetic coupling values match with those of the taper at one end of each of the segments^(63,64). Lossless coupled NUTLs when used as directional couplers eliminates the electromagnetic discontinuity along the line and makes it possible

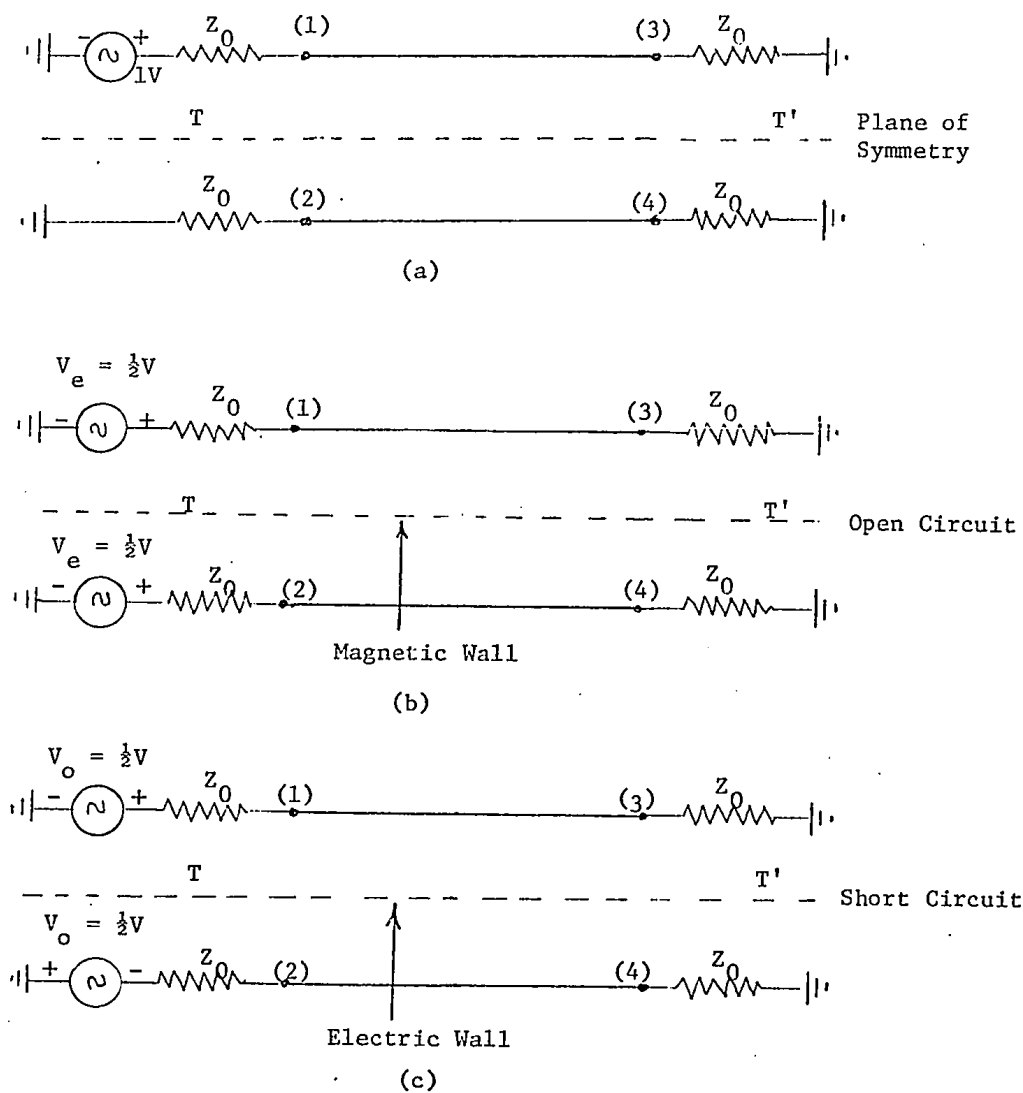
to obtain zero electromagnetic coupling at least at one of the ends of the coupled lines⁽³⁴⁾. Consequently, the smooth transition of the reactive coupling obtained at the end not only simplifies the construction of these couplers, but also provides better terminal matching conditions. In addition, these couplers possess the advantages of small size and high-pass coupling response in the frequency range of interest⁽³⁴⁾.

Another widely used application of lossless coupled UTLs is folded all-pass networks. These networks are often employed as phase or delay equalizing components in microwave systems. These are also used widely at microwave frequencies as filters^(7,9). As delay equalizers, these have been used in broad band and PCM transmission systems⁽⁶⁵⁻⁶⁷⁾. Further these networks have found applications as phase equalizers in 'Magic T'⁽⁶⁸⁻⁷¹⁾. Recently, Yamamoto et al⁽³⁴⁾ have employed coupled NUTL with exponential taper as folded all-pass networks. These tapered all-pass networks have the advantages of smaller size in addition to providing control on phase characteristics and peak time delay through their tapers. Apart from these applications, coupled transmission lines are used in microwave systems as hybrid junction⁽⁷²⁻⁷⁵⁾, balun transformers^(76,77), and resonators^(7,9,77-79).

While the lossless coupled lines have been used in a large number of applications as mentioned before, the problem of analyzing such net-

works is complicated due to the presence of distributed electromagnetic coupling terms present in their telegrapher's equations. Vlostovsky⁽⁸⁰⁾ described a method of analyzing two coupled identical uniform lines by determining characteristic roots. Amamiya⁽⁸¹⁾ has analyzed the coupled identical UTL in the time domain by using the concept of matched termination networks. Using this approach, he studied the crosstalk on transmission lines and the properties of directional couplers in time domain. Youla⁽⁸²⁾ studied various electrical properties of multiwire identical lines, while using them as synthesis building blocks in microwave systems.

A simpler approach to the problem of analyzing identical uniform coupled line networks without solving coupled line equations has been taken by several authors. The concept of even and odd mode is used for solving this problem by Jones and Bolljhan⁽⁵³⁾. The even mode is generated by applying voltage signals (V_e) of equal amplitudes ($\frac{1}{2}V$) with same phase at ports 1 and 2 respectively as shown in Fig. 1.3(b). On the other hand, the odd mode is obtained by exciting the ports 1 and 2 with voltage signals (V_o) of equal amplitudes ($\frac{1}{2}V$) but with opposite phase as shown in Fig. 1.3(c). It may be shown that the plane of symmetry TT' can be replaced by a magnetic wall (infinite impedance plane) for the even mode and by an electric wall (zero impedance plane) for the odd mode. The coupled line network of Fig. 1.3(a) can now be analyzed by superposing these two modes. However, it is necessary that the coupled line network including the terminations be absolutely symmetrical about the axis TT' . Reed and Wheeler⁽⁵⁴⁾



(a) Coupled Lines having Symmetrical terminations with port (1) excited.

(b) Even mode port conditions

(c) Odd mode port conditions

Fig. 1.3: Even and Odd Mode Circuits for a Symmetrical Coupled Line four-port.

applied this method to waveguide and co-axial networks, where apart from satisfying the symmetry condition, the size of lines has to be very small as compared to the operating wavelength. Using this method, the networks consisting of coupled identical uniform lines embedded in an inhomogeneous dielectric material (e.g. suspended, substrate, micro-strip) have also been analyzed⁽⁸³⁾. These conditions of symmetry has been modified by Ozaki and Ishi⁽⁸⁴⁾ to allow a class of non-identical uniform lines to be analyzed. Recently Yamamoto et al⁽³⁴⁾ have extended the even and odd mode principles to the analysis of tapered coupled lines. The lines, however, have got to be identical; in addition, the phase velocities of the even and odd mode signals must be equal and constant at every point along the lines. Hence this method is not applicable to lines in a suspended substrate configurations⁽⁸³⁾, where the even and odd mode signals must propagate with unequal phase velocities. Further, the coupled line networks including the terminations are required to be symmetrical about the axis. It may also be worthwhile to mention that in all the above methods, except in the case of identical uniform lines⁽⁸⁵⁾, it is not clear as to how the coupled line parameters such as self-inductance per unit length at any point on the transmission line etc. can be related to those of even and odd mode lines.

In addition to the methods cited above, Sharpe⁽⁶¹⁾ has given a technique of analyzing CNUTLs as contradirectional couplers by suitably decoupling the lines. However, his method assumes double symmetry of the scattering matrix; further, his results apply only for the case of CNUTLs having an absolutely continuous characteristic impedance matrix.

Thus it appears desirable to investigate the possibilities of developing a new method of analyzing CNUTLs. To be useful, this method should be simple to apply and be general in its scope of applications. One of the ways to approach this problem is to decouple the coupled line telegrapher's equation without any apriori assumptions.

1.4 Scope of the Thesis:

The aim of this thesis is firstly to obtain a general theory for decoupling a pair of lossless coupled lines (similar or dissimilar) with common return, and supporting TEM mode of propagation. This new theory is then employed to investigate in detail the applications of lossless CNUTLs as:

- (i) Contradirectional couplers,
- (ii) Co-directional couplers, and finally,
- (iii) Folded all-pass networks.

A theory for decoupling of the coupled lines is developed in Chapter 2. This reduces the problem of analyzing lossless CNUTLs as a four-port network to that of analyzing two 2-port networks. This theory is quite general and is independent of port terminations, symmetry conditions, etc. Further, the method is applicable to identical or non-identical, similar or dissimilar coupled lines. Another feature of this technique is that it directly relates the coupled line parameters to those of the corresponding decoupled lines and vice versa. The matrix parameters of lossless CNUTLs are also determined in this Chapter in terms of the decoupled line matrix parameters.

Chapter 3 deals with contra-directional and co-directional couplers using coupled lines with or without impedance transformation. Con-

straints on decoupled line distributions for these coupler actions are derived. The characteristics of contradirectional couplers for different decoupled lines including "Basic lines" with hyperbolic solutions are investigated. In addition, properties of codirectional couplers are also studied.

Chapter 4 presents tapered folded all-pass networks. Various folded all-pass networks are analyzed using the theory of Chapter 2, and the constraints on corresponding decoupled line distributions are obtained. Phase and delay characteristics of these networks using "Basic lines" with hyperbolic solutions as decoupled lines are investigated.

Chapter 5 summarizes the results of the thesis and makes some suggestions for further studies.

CHAPTER 2

DECOUPLING OF LOSSLESS COUPLED NON-UNIFORM TRANSMISSION LINES

2.1 Introduction:

As mentioned in Sec. 1.3, the analysis of coupled lossless lines with common return, supporting only TEM waves may be simplified by decoupling the coupled lines. In this Chapter, a simple method of decoupling a pair of coupled lossless lines into two pairs of uncoupled lines is introduced⁽⁸⁶⁾. Treating the coupled lines as a four-port network, the immittance and chain matrices are obtained in terms of the corresponding decoupled line matrices. Transfer scattering matrix of the coupled line four-port is obtained in terms of the decoupled line chain parameters.

2.2 Decoupling of Coupled Lines:

Consider a pair of lossless coupled lines with common return and supporting TEM waves as shown in Fig. 1.1. Let the per unit length parameters of these lines be

$$L_{11} = L_{110} f_{11}(x) \quad ; \quad L_{22} = L_{220} f_{22}(x) \quad \dots (2.1a)$$

$$C_{11} = C_{110} g_{11}(x) \quad , \quad C_{22} = C_{220} g_{22}(x) \quad \dots (2.1b)$$

$$L_{12} = L_{120} f_{12}(x) \quad , \quad C_{12} = C_{120} g_{12}(x) \quad \dots (2.1c)$$

where

$$L_{11}(x) = \text{Self inductance of line A,}$$

$$L_{22}(x) = \text{Self inductance of line B,}$$

$L_{12}(x)$ = Mutual inductance between lines A and B,

$C_{11}(x)$ = Self-capacitance of line A to ground,

$C_{22}(x)$ = Self-capacitance of line B to ground,

$C_{12}(x)$ = Mutual capacitance between lines A and B.

For TEM wave propagation, it is known⁽⁶¹⁾ that these coupled line parameters satisfy the relation

$$[L(x)][C(x)] = \frac{1}{v^2(x)} [U] \quad \dots (2.2)$$

where $v(x)$ is a positive function, $[U]$ is a unit matrix, and

$$[L(x)] = \begin{bmatrix} L_{11}(x) & L_{12}(x) \\ L_{12}(x) & L_{22}(x) \end{bmatrix} \quad \dots (2.3a)$$

$$[C(x)] = \begin{bmatrix} C_{11}(x) + C_{12}(x) & -C_{12}(x) \\ -C_{12}(x) & C_{22}(x) + C_{12}(x) \end{bmatrix} \quad \dots (2.3b)$$

having

$$L_{ij}(x) \geq 0, \quad L_{ii}(x) \geq L_{ij}(x), \quad C_{ij}(x) \geq 0 \quad \dots (2.3c)$$

From (2.2) and (2.3)

$$\frac{L_{12}(x)}{C_{12}(x)} = \frac{L_{11}(x)}{C_{22}(x) + C_{12}(x)} = \frac{L_{22}(x)}{C_{11}(x) + C_{12}(x)} \quad \dots (2.4)$$

and

$$v(x) = \frac{1}{\sqrt{L_{22}(x)\{C_{22}(x) + C_{12}(x)\} - L_{12}(x) C_{12}(x)}} \quad \dots (2.5)$$

Thus a pair of coupled lines supporting TEM waves have the line parameters which satisfy the requirements (2.4) and (2.5). Telegraphers equations for these lines are:

$$[V'(s, x)] = - [Z(s, x)][I(s, x)] \quad \dots (2.6a)$$

$$[I'(s, x)] = - [Y(s, x)][V(s, x)] \quad \dots (2.6b)$$

where

$$[V(s, x)] = \begin{bmatrix} V_A(s, x) \\ V_B(s, x) \end{bmatrix} ; \quad [I(s, x)] = \begin{bmatrix} I_A(s, x) \\ I_B(s, x) \end{bmatrix} \quad \dots (2.7a)$$

$$[Z(s, x)] = s[L(x)] \quad ; \quad [Y(s, x)] = s[C(x)] \quad \dots (2.7b)$$

and

s is the complex frequency.

In order to decouple the coupled lines, the following linear transformations are introduced:

$$[V(s, x)] = [Q(x)][E(s, x)] \quad \dots (2.8a)$$

$$[I(s, x)] = [M(x)][J(s, x)] \quad \dots (2.8b)$$

where

$$[Q(x)] = \begin{bmatrix} a & b \\ c & d \end{bmatrix} ; \quad [M(x)] = \begin{bmatrix} e & f \\ g & h \end{bmatrix} \quad \dots (2.9)$$

a, b, c, d, e, f, g and h are arbitrary functions of x .

Using transformations (2.8), equations (2.6) may be reduced to

$$[E'(s, x)] = -[Q^{-1}ZM][J(s, x)] = -[Z_m][J(s, x)] \quad \dots (2.10a)$$

$$[J'(s, x)] = -[M^{-1}YQ][E(s, x)] = -[Y_m][E(s, x)] \quad \dots (2.10b)$$

where

$$[Z_m] = \frac{s}{\Delta_1} \begin{bmatrix} d(L_{11}e + L_{12}g) & d(L_{11}f + L_{12}h) \\ -b(L_{12}e + L_{22}g) & -b(L_{12}f + L_{22}h) \\ a(L_{12}e + L_{22}g) & a(L_{12}f + L_{22}h) \\ -c(L_{11}e + L_{12}g) & -c(L_{11}f + L_{12}h) \end{bmatrix} \quad \dots (2.11a)$$

$$[Y_m] = \frac{s}{\Delta_2} \begin{bmatrix} h\{a(C_{11} + C_{12}) - C_{12}c\} & h\{b(C_{11} + C_{12}) - C_{12}d\} \\ -f\{c(C_{22} + C_{12}) - C_{12}a\} & -f\{d(C_{22} + C_{12}) - C_{12}b\} \\ e\{c(C_{22} + C_{12}) - C_{12}a\} & e\{d(C_{22} + C_{12}) - C_{12}b\} \\ -g\{a(C_{11} + C_{12}) - C_{12}c\} & -g\{b(C_{11} + C_{12}) - C_{12}d\} \end{bmatrix} \quad \dots (2.11b)$$

$$\Delta_1 = ad - bc \quad ; \quad \Delta_2 = eh - fg \quad \dots (2.11c)$$

In order to make the off diagonal terms in (2.11) equal to zero, it is required that,

$$d\{fL_{11} + hL_{12}\} - b\{fL_{12} + hL_{22}\} = 0 \quad \dots (2.12a)$$

$$a\{eL_{12} + gL_{22}\} - c\{eL_{11} + gL_{12}\} = 0 \quad \dots (2.12b)$$

$$b\{h(C_{11} + C_{12}) + fC_{12}\} - d\{f(C_{22} + C_{12}) + hC_{12}\} = 0 \quad \dots (2.12c)$$

$$a\{g(C_{11} + C_{12}) + eC_{12}\} - c\{e(C_{22} + C_{12}) + gC_{12}\} = 0 \quad \dots (2.12d)$$

Solving (2.12) for c, d in terms of a and b, and g, h in terms of

e and f, and substituting the requirement (2.4) for TEM wave propagation,

the matrices [Q] and [M] reduce to

$$[Q(x)] = \begin{bmatrix} 1 & 1 \\ \pm p & \mp p \end{bmatrix} \quad ; \quad [M(x)] = \begin{bmatrix} 1 & 1 \\ \pm(1/p) & \mp(1/p) \end{bmatrix} \quad \dots (2.15)$$

Substituting (2.15) in (2.11)

$$[Z_m] = s \begin{bmatrix} L_{11} \pm (L_{12}/\rho) & 0 \\ 0 & L_{11} \mp (L_{12}/\rho) \end{bmatrix} \quad \dots (2.16a)$$

and

$$[Y_m] = s \begin{bmatrix} C_{11} + (1 \mp \rho)C_{12} & 0 \\ 0 & C_{11} + (1 \pm \rho)C_{12} \end{bmatrix} \quad \dots (2.16b)$$

From (2.10) and (2.16), the transformed telegraphers equations are reduced to

$$[E'(s,x)] = -s \begin{bmatrix} L_{11} \pm (L_{12}/\rho) & 0 \\ 0 & L_{11} \mp (L_{12}/\rho) \end{bmatrix} [J(s,x)] \quad \dots (2.17a)$$

$$[J'(s,x)] = -s \begin{bmatrix} C_{11} + (1 \mp \rho)C_{12} & 0 \\ 0 & C_{11} + (1 \pm \rho)C_{12} \end{bmatrix} [E(s,x)] \quad \dots (2.17b)$$

Now the equations (2.17) may be considered as the telegraphers equations of two decoupled lines, say, line 1 and line 2. Associating the upper signs for line 1 and lower signs for line 2 in (2.17), the per unit length parameters of these lines are:

$$L_1(x) = L_{11} + (L_{12}/\rho) \quad , \quad C_1(x) = C_{11} + (1 - \rho)C_{12} \quad \dots (2.18a)$$

$$L_2(x) = L_{11} - (L_{12}/\rho) \quad , \quad C_2(x) = C_{11} + (1 + \rho)C_{12} \quad \dots (2.18b)$$

where $L_1(x)$ and $L_2(x)$ are the per unit length inductances while $C_1(x)$ and $C_2(x)$ are the per unit length capacitances of lines 1 and 2 respectively. Knowing the parameters of the decoupled lines, the coupled line parameters may be obtained as

$$L_{11} = \frac{L_1(x) + L_2(x)}{2}, \quad L_{22} = \frac{\rho^2}{2} [L_1(x) + L_2(x)] \quad \dots (2.19a)$$

$$C_{11} = \frac{1}{2\rho} [(\rho+1)C_1(x) + (\rho-1)C_2(x)], \quad C_{22} = \frac{1}{2\rho^2} [(\rho+1)C_1(x) - (\rho-1)C_2(x)] \quad \dots (2.19b)$$

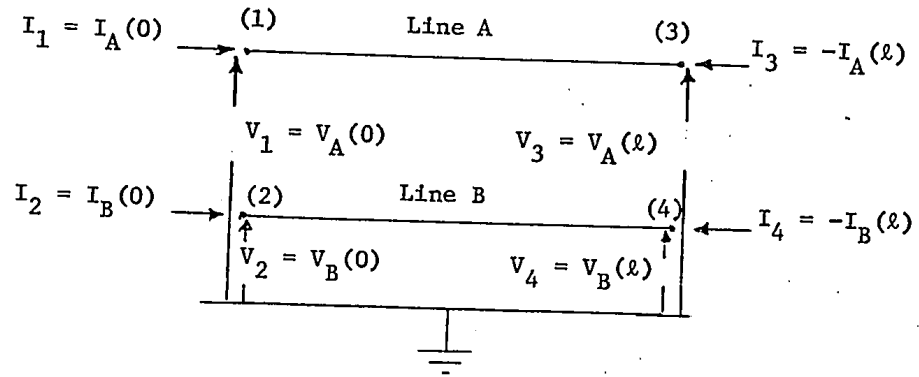
$$L_{12} = \frac{\rho}{2} [L_1(x) - L_2(x)], \quad C_{12} = \frac{C_2(x) - C_1(x)}{2\rho} \quad \dots (2.19c)$$

Thus, a pair of lossless coupled lines have been decoupled into two pairs of lossless lines, as shown in Fig. 2.1. This decoupling is independent of the port terminations and does not require the coupled lines to have any form of symmetry. It is noted that in view of the way the signs have been associated in (2.18) for lines 1 and 2, the Q and M matrices reduce to

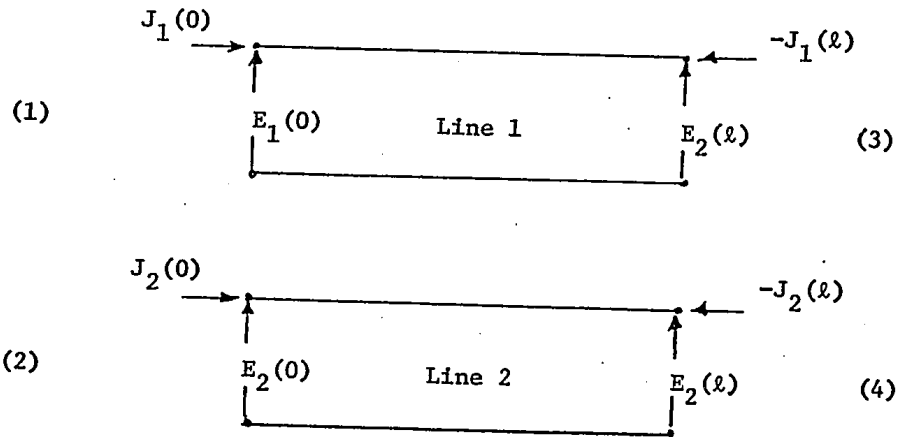
$$[Q] = \begin{bmatrix} 1 & 1 \\ \rho & -\rho \end{bmatrix}, \quad [M] = \begin{bmatrix} 1 & 1 \\ (1/\rho) & -(1/\rho) \end{bmatrix} \quad \dots (2.20)$$

2.3 Coupled Line Immittance and Chain Matrices:

Considering the coupled lines of Fig. 2.1a as a four-port network, the impedance matrix will now be obtained in terms of those of the decoupled lines. Using (2.18), the distributions of the decoupled lines may be calculated from those of the coupled lines. Once these distributions are known, the impedance matrices of the decoupled lines



(a) Coupled Lines



(b) Pair of Decoupled Lines

Fig. 2.1: A Pair of Coupled Lossless Lines and the Corresponding Decoupled Lines.

may be obtained by any of the known techniques⁽⁸⁷⁻⁸⁹⁾. Let these matrices be

$$[z]_1 = \begin{bmatrix} z_{11}^1 & z_{12}^1 \\ z_{21}^1 & z_{22}^1 \end{bmatrix}, \quad [z]_2 = \begin{bmatrix} z_{11}^2 & z_{12}^2 \\ z_{21}^2 & z_{22}^2 \end{bmatrix} \quad \dots (2.21)$$

where $[z]_1$ and $[z]_2$ are respectively the impedance matrices of the decoupled lines 1 and 2. For the four-port network formed by those decoupled lines as shown in Fig. 2.1(b), the voltages and currents at various ports are related as

$$\begin{bmatrix} E_1(0) \\ E_2(0) \\ E_1(l) \\ E_2(l) \end{bmatrix} = \begin{bmatrix} [P_{11}] & [P_{12}] \\ [P_{21}] & [P_{22}] \end{bmatrix} \begin{bmatrix} J_1(0) \\ J_2(0) \\ -J_1(l) \\ -J_2(l) \end{bmatrix} \quad \dots (2.22a)$$

where

$$[P_{ij}] = \begin{bmatrix} [z_{ij}^1] & [0] \\ [0] & [z_{ij}^2] \end{bmatrix} \quad \dots (2.22b)$$

Substituting (2.8), (2.20) and (2.21) in (2.22a)

$$\begin{bmatrix} y_A(0) \\ v_B(0) \\ v_A(l) \\ v_B(l) \end{bmatrix} = \begin{bmatrix} [Q] & [0] \\ [0] & [Q] \end{bmatrix} \begin{bmatrix} [P_{11}] & [P_{12}] \\ [P_{21}] & [P_{22}] \end{bmatrix} \begin{bmatrix} [M]^{-1} & [0] \\ [0] & [M]^{-1} \end{bmatrix} \begin{bmatrix} I_A(0) \\ I_B(0) \\ -I_A(l) \\ -I_B(l) \end{bmatrix} \quad \dots (2.23a)$$

or

$$\begin{bmatrix} V_1 \\ V_2 \\ V_3 \\ V_4 \end{bmatrix} = \begin{bmatrix} [Q] & [0] \\ [0] & [Q] \end{bmatrix} \begin{bmatrix} [P_{11}] & [P_{12}] \\ [P_{21}] & [P_{22}] \end{bmatrix} \begin{bmatrix} [M]^{-1} & [0] \\ [0] & [M]^{-1} \end{bmatrix} \begin{bmatrix} I_1 \\ I_2 \\ I_3 \\ I_4 \end{bmatrix} \quad \dots (2.23b)$$

where the V's and the I's correspond to the port voltages and currents of the coupled line four-port network in Fig. 2.1(a). From (2.23), the impedance matrix of the coupled line four-port is

$$[z] = \begin{bmatrix} (z_{11}^1 + z_{11}^2) & \rho(z_{11}^1 - z_{11}^2) & (z_{12}^1 + z_{12}^2) & \rho(z_{12}^1 - z_{12}^2) \\ \rho(z_{11}^1 - z_{11}^2) & \rho^2(z_{11}^1 + z_{11}^2) & \rho(z_{12}^1 - z_{12}^2) & \rho^2(z_{12}^1 + z_{12}^2) \\ (z_{21}^1 + z_{21}^2) & \rho(z_{21}^1 - z_{21}^2) & (z_{22}^1 + z_{22}^2) & \rho(z_{22}^1 - z_{22}^2) \\ \rho(z_{21}^1 - z_{21}^2) & \rho^2(z_{21}^1 + z_{21}^2) & \rho(z_{22}^1 - z_{22}^2) & \rho^2(z_{22}^1 + z_{22}^2) \end{bmatrix} \frac{1}{2} \quad \dots (2.24)$$

It should be pointed out that since $z_{12}^1 = z_{21}^1$, and $z_{12}^2 = z_{21}^2$, that is, the decoupled lines are reciprocal 2-ports⁽⁸⁷⁾, the impedance matrix $[z]$ given by (2.24) is symmetric and hence the coupled line four-port is reciprocal.

Similarly, the admittance and chain matrices $[y]$ and $[a]$ of the coupled line four-port may be expressed in terms of the corresponding decoupled line matrices as:

$$[y] = \frac{1}{2} \begin{bmatrix} (y_{11}^1 + y_{11}^2) & \frac{(y_{11}^1 - y_{11}^2)}{\rho} & (y_{12}^1 + y_{12}^2) & \frac{(y_{12}^1 - y_{12}^2)}{\rho} \\ \frac{(y_{11}^1 - y_{11}^2)}{\rho} & \frac{(y_{11}^1 + y_{11}^2)}{\rho^2} & \frac{(y_{12}^1 - y_{12}^2)}{\rho} & \frac{(y_{11}^1 + y_{12}^2)}{\rho^2} \\ (y_{21}^1 + y_{21}^2) & \frac{(y_{21}^1 - y_{21}^2)}{\rho} & (y_{22}^1 + y_{22}^2) & \frac{(y_{22}^1 - y_{22}^2)}{\rho} \\ \frac{(y_{21}^1 - y_{21}^2)}{\rho} & \frac{(y_{21}^1 + y_{21}^2)}{\rho^2} & \frac{(y_{22}^1 - y_{22}^2)}{\rho} & \frac{(y_{22}^1 + y_{22}^2)}{\rho^2} \end{bmatrix} \quad \dots (2.25a)$$

where

$$[y]_1 = \begin{bmatrix} y_{11}^1 & y_{12}^1 \\ y_{21}^1 & y_{22}^1 \end{bmatrix}, \quad [y]_2 = \begin{bmatrix} y_{11}^2 & y_{12}^2 \\ y_{21}^2 & y_{22}^2 \end{bmatrix} \quad \dots (2.25b)$$

are the admittance matrices of the two decoupled lines, and

$$[a] = \frac{1}{2} \begin{bmatrix} \alpha_1 & \alpha_2/\rho & \beta_1 & \beta_2\rho \\ \alpha_2\rho & \alpha_1 & \beta_2\rho & \beta_1\rho^2 \\ \gamma_1 & \gamma_2/\rho & \delta_1 & \delta_2\rho \\ \gamma_2/\rho & \gamma_1/\rho & \delta_2/\rho & \delta_1 \end{bmatrix} \quad \dots (2.26a)$$

where

$$[a]_1 = \begin{bmatrix} A_1 & B_1 \\ C_1 & D_1 \end{bmatrix}, \quad [a]_2 = \begin{bmatrix} A_2 & B_2 \\ C_2 & D_2 \end{bmatrix} \quad \dots (2.26b)$$

are the chain matrices of the two decoupled lines, and

$$\begin{aligned}
\alpha_1 &= (A_1 + A_2) \quad , \quad \alpha_2 = (A_1 - A_2) \\
\beta_1 &= (B_1 + B_2) \quad , \quad \beta_2 = (B_1 - B_2) \\
\gamma_1 &= (C_1 + C_2) \quad , \quad \gamma_2 = (C_1 - C_2) \\
\delta_1 &= (D_1 + D_2) \quad , \quad \delta_2 = (D_1 - D_2)
\end{aligned}
\quad \dots (2.26c)$$

2.4 Coupled Line Transfer Scattering Matrix:

For a four-port network with port terminations as shown in Fig.2.2, the transfer scattering matrix [T] in terms of its chain matrix [a] is (Appendix A)

$$[T] = \frac{1}{2} [X] \cdot [a] \cdot [X^*] \quad \dots (2.27a)$$

where

$$[X] = [r_i]^{-\frac{1}{2}} \begin{bmatrix} [U] & \vdots & -[z_i] \\ \cdot & \cdot & \cdot \\ [U] & \vdots & [z_i] \end{bmatrix}, \quad \dots (2.27b)$$

$$[X^*] = [r_\ell]^{-\frac{1}{2}} \begin{bmatrix} [\bar{z}_\ell] & \vdots & [z_\ell] \\ \cdot & \cdot & \cdot \\ -[U] & \vdots & [U] \end{bmatrix} \quad \dots (2.27c)$$

$$[z_i] = \text{dia } [z_1, z_2] \quad , \quad [z_\ell] = \text{dia } [z_3, z_4] \quad \dots (2.27d)$$

$$[r_i] = \text{Re } [z_i] \quad , \quad [r_\ell] = \text{Re } [z_\ell] \quad \dots (2.27e)$$

\bar{z} = Complex conjugate of z

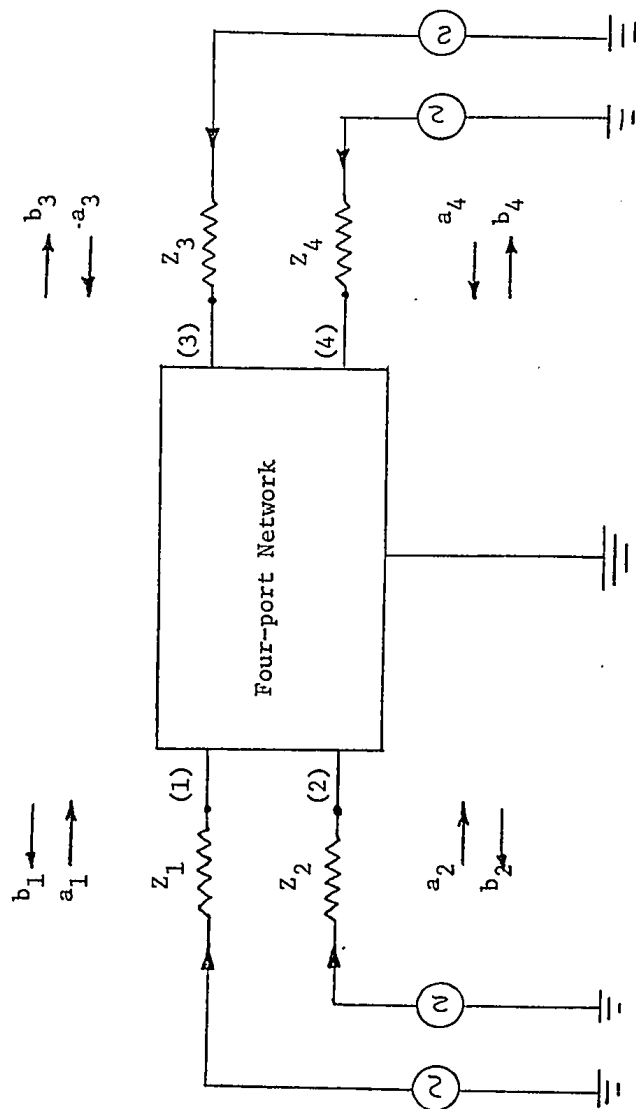


Fig. 2.2: A Terminated Four-port Network

7

$$\begin{bmatrix} b_{in} \\ a_{in} \end{bmatrix} = [T] \begin{bmatrix} a_{out} \\ b_{out} \end{bmatrix} \quad \dots (2.27f)$$

$$a_{in} = \begin{bmatrix} a_1 \\ a_2 \end{bmatrix}, \quad a_{out} = \begin{bmatrix} a_3 \\ a_4 \end{bmatrix} \quad \dots (2.27g)$$

$$b_{in} = \begin{bmatrix} b_1 \\ b_2 \end{bmatrix}, \quad b_{out} = \begin{bmatrix} b_3 \\ b_4 \end{bmatrix} \quad \dots (2.27h)$$

Substituting the coupled line chain matrix $[a]$ given by (2.26) in (2.27), the coupled line transfer scattering matrix may be expressed in terms of the decoupled line chain parameters in the form

$$[T] = \frac{1}{4} \begin{bmatrix} \frac{1}{\sqrt{r_1}} & 0 & \frac{\bar{z}_1}{\sqrt{r_1}} & 0 \\ 0 & \frac{1}{\sqrt{r_2}} & 0 & \frac{\bar{z}_2}{\sqrt{r_2}} \\ \frac{1}{\sqrt{r_1}} & 0 & \frac{z_1}{\sqrt{r_1}} & 0 \\ 0 & \frac{1}{\sqrt{r_2}} & 0 & \frac{z_2}{\sqrt{r_2}} \end{bmatrix} \begin{bmatrix} \alpha_1 & \frac{\alpha_2}{\rho} & \beta_1 & \beta_2 \rho \\ \alpha_2 \rho & \alpha_1 & \beta_2 \rho & \beta_1 \rho^2 \\ \gamma_1 & \frac{\gamma_2}{\rho} & \delta_1 & \delta_2 \rho \\ \frac{\gamma_2}{\rho} & \frac{\gamma_1}{\rho^2} & \frac{\delta_2}{\rho} & \delta_1 \end{bmatrix} \begin{bmatrix} \frac{\bar{z}_3}{\sqrt{r_3}} & 0 & \frac{z_3}{\sqrt{r_3}} & 0 \\ 0 & \frac{\bar{z}_4}{\sqrt{r_4}} & 0 & \frac{z_4}{\sqrt{r_4}} \\ -\frac{1}{\sqrt{r_3}} & 0 & \frac{1}{\sqrt{r_3}} & 0 \\ 0 & -\frac{1}{\sqrt{r_4}} & 0 & \frac{1}{\sqrt{r_4}} \end{bmatrix}$$

This becomes

$$\begin{aligned}
&= \frac{1}{4} \left[\begin{array}{cccc}
\frac{\{\alpha_1 z_3 - \beta_1 - \gamma_1 z_1 z_3 + \delta_1 z_1\}}{\sqrt{r_1 r_3}} & \frac{\{\alpha_2 z_4 - \beta_2 \rho^2 - \gamma_2 z_1 z_4 + \delta_2 z_1 \rho^2\}}{\rho \sqrt{r_1 r_4}} & \frac{\{\alpha_1 z_3 + \beta_1 - \gamma_1 z_1 z_3 - \delta_1 z_1\}}{\sqrt{r_1 r_3}} & \frac{\{\alpha_2 z_4 + \beta_2 \rho^2 - \gamma_2 z_1 z_4 - \delta_2 z_1 \rho^2\}}{\rho \sqrt{r_1 r_4}} \\
\frac{\{\alpha_2 \rho^2 z_3 - \beta_2 \rho^2 - \gamma_2 z_1 z_3 + \delta_2 z_1\}}{\rho \sqrt{r_2 r_3}} & \frac{\{\alpha_1 z_4 \rho^2 - \beta_1 \rho^4 - \gamma_1 z_1 z_4 + \delta_1 z_1 \rho^2\}}{\rho^2 \sqrt{r_2 r_4}} & \frac{\{\alpha_2 \rho^2 z_3 + \beta_2 \rho^2 - \gamma_2 z_1 z_3 - \delta_2 z_1\}}{\rho \sqrt{r_2 r_3}} & \frac{\{\alpha_1 z_4 \rho^2 + \beta_1 \rho^4 - \gamma_1 z_1 z_4 - \delta_1 z_1 \rho^2\}}{\rho^2 \sqrt{r_2 r_4}} \\
\frac{\{\alpha_1 z_3 - \beta_1 + \gamma_1 z_1 z_3 - \delta_1 z_1\}}{\sqrt{r_1 r_3}} & \frac{\{\alpha_2 z_4 - \beta_2 \rho^2 + \gamma_2 z_1 z_4 - \delta_2 z_1 \rho^2\}}{\rho \sqrt{r_1 r_4}} & \frac{\{\alpha_1 z_3 + \beta_1 + \gamma_1 z_1 z_3 + \delta_1 z_1\}}{\sqrt{r_1 r_3}} & \frac{\{\alpha_2 z_4 + \beta_2 \rho^2 + \gamma_2 z_1 z_4 + \delta_2 z_1 \rho^2\}}{\rho \sqrt{r_1 r_4}} \\
\frac{\{\alpha_2 \rho^2 z_3 - \beta_2 \rho^2 + \gamma_2 z_1 z_3 - \delta_2 z_1\}}{\rho \sqrt{r_2 r_3}} & \frac{\{\alpha_1 z_4 \rho^2 - \beta_1 \rho^4 + \gamma_1 z_1 z_4 - \delta_1 z_1 \rho^2\}}{\rho^2 \sqrt{r_2 r_4}} & \frac{\{\alpha_2 \rho^2 z_3 + \beta_2 \rho^2 + \gamma_2 z_1 z_3 + \delta_2 z_1\}}{\rho \sqrt{r_2 r_3}} & \frac{\{\alpha_1 z_4 \rho^2 + \beta_1 \rho^4 + \gamma_1 z_1 z_4 + \delta_1 z_1 \rho^2\}}{\rho^2 \sqrt{r_2 r_4}}
\end{array} \right]
\end{aligned}$$

.. (2.28)

For resistive port terminations ($z_j = r_j$), the above transfer scattering matrix is reduced to

$$\begin{aligned}
& \left[\begin{array}{ll}
\{\alpha_1 \rho_3 - \beta_1 / (\rho_3 x_1)\} & \{\alpha_2 \rho_4 / \rho_2 - \beta_2 \rho / (\rho_4 x_1)\} \\
-\gamma_1 \rho_3 x_1 + \delta_1 / \rho_3\} & -\gamma_2 \rho_4 x_1 / \rho_2 + \delta_2 \rho / \rho_4\} \\
\{\alpha_2 \rho \rho_3 / \rho_2 - \beta_2 \rho / (\rho_2 \rho_3 x_1)\} & \{\alpha_1 \rho_4 / \rho_2 - \beta_1 \rho^2 / (\rho_2 \rho_4 x_1)\} \\
-\gamma_2 \rho_2 \rho_3 x_1 / \rho_2 + \delta_2 \rho_2 / \rho \rho_3\} & -\gamma_1 \rho_2 \rho_4 x_1 / \rho_2 - \delta_1 \rho_2 / \rho_4\} \\
\{\alpha_1 \rho_3 - \beta_1 / (\rho_3 x_1)\} & \{\alpha_2 \rho_4 / \rho_2 - \beta_2 \rho / (\rho_4 x_1)\} \\
+\gamma_1 \rho_3 x_1 - \delta_1 / \rho_3\} & +\gamma_2 \rho_4 x_1 / \rho_2 + \delta_2 \rho / \rho_4\} \\
\{\alpha_2 \rho \rho_3 / \rho_2 - \beta_2 \rho / (\rho_2 \rho_3 x_1)\} & \{\alpha_1 \rho_4 / \rho_2 - \beta_1 \rho^2 / (\rho_2 \rho_4 x_1)\} \\
+\gamma_2 \rho_2 \rho_3 x_1 / \rho_2 - \delta_2 \rho_2 / \rho \rho_3\} & +\gamma_1 \rho_2 \rho_4 x_1 / \rho_2 + \delta_1 \rho_2 / \rho_4\}
\end{array} \right] \\
& = [T]
\end{aligned}$$

.. (2.29)

where

$$\rho_2 = \sqrt{\frac{x_2}{x_1}} \quad , \quad \rho_3 = \sqrt{\frac{x_3}{x_1}} \quad \text{and} \quad \rho_4 = \sqrt{\frac{x_4}{x_1}} \quad \text{.. (2.30)}$$

2.7 Conclusions:

A simple method of decoupling a pair of similar or dissimilar coupled transmission lines with common return and supporting only TEM waves into two pairs of decoupled lines has been introduced in this Chapter. This method does not require any symmetry conditions to be satisfied by the coupled system nor does it depend on the port terminations. In fact, the method is quite general since the coupled telegrapher's equations are directly decoupled without any assumption. This method also enables us to obtain the parameters of the coupled lines as well as the matrix parameters of the coupled pair as a four-port from those of the two decoupled lines.

For identical coupled lines, $\rho = 1$. In this case, the relations between the voltages and currents of the coupled and of the decoupled lines, are the same as those between the coupled lines and the even and odd mode lines⁽⁵³⁾. For non-identical coupled lines, the method in this Chapter gives two decoupled lines as compared to four uncoupled lines in the even and odd mode method⁽⁸⁴⁾. Further, the method described in this Chapter, contains as a special case that given by Dvorak⁽⁸⁵⁾, for identical CUTLs.

This theory of decoupling is applied in the next Chapter to study the codirectional and contradirectional couplers with or without impedance transformation.

CHAPTER 3

COUPLED NONUNIFORM TRANSMISSION LINE DIRECTIONAL COUPLERS

3.1 Introduction:

The theory described in Chapter 2 will now be applied to investigate the behaviour of a pair of lossless coupled lines as codirectional and contradirectional couplers without or with impedance transformation and having an infinite directivity. Starting with the scattering matrices of the directional couplers, the corresponding conditions to be satisfied by the elements of the transfer scattering matrices are first obtained. These conditions are then used to obtain the relations between the matrix parameters of the two decoupled lines, so that, the given coupled line may behave as a codirectional or a contradirectional coupler; the corresponding distributions of the decoupled lines are also obtained. The characteristics of codirectional and contradirectional couplers using various coupled NUTLs are investigated⁽⁸⁶⁾.

3.2 A Four-Port Codirectional Coupler:

Consider a lossless reciprocal four-port with terminating resistors as shown in Fig. 3.1. This four-port will behave as a codirectional coupler if, when terminated in prescribed resistances, it is matched at all ports with (1) and (2), and (3) and (4) mutually isolated⁽⁴⁷⁾. There may or may not be impedance transformation depending upon the values of the terminating resistors. The scattering matrix of this codirectional coupler is

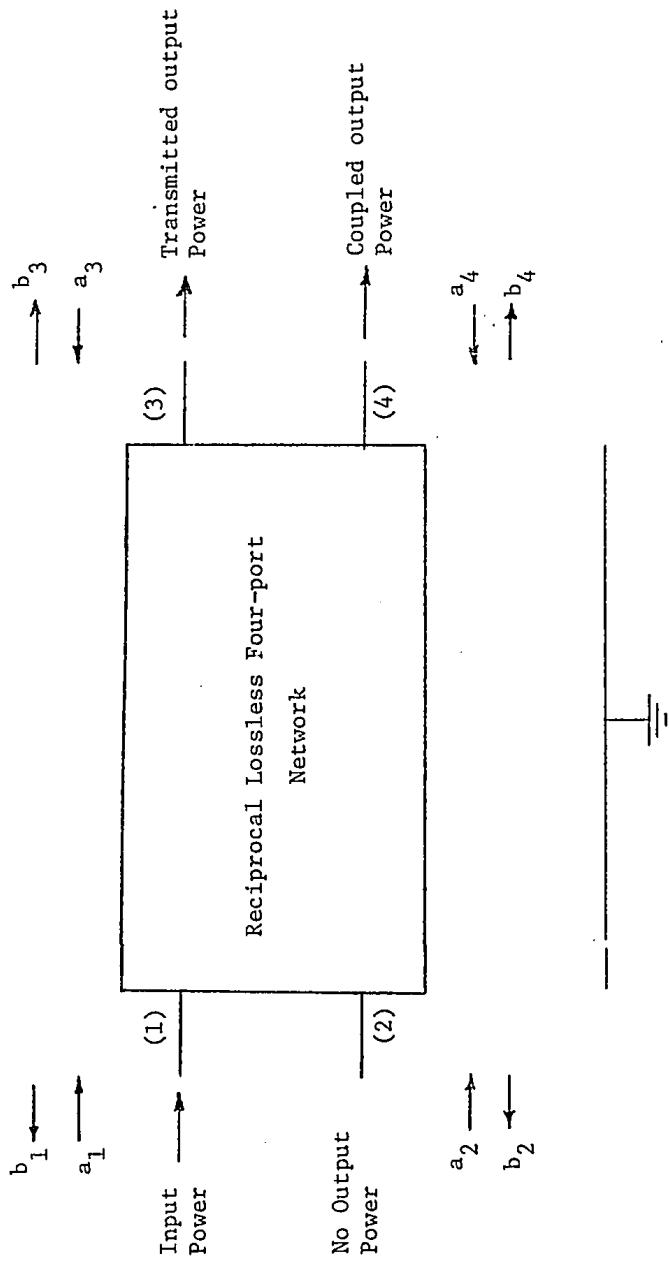


Fig. 3.1: Four-port Codirectional Coupler

$$[S] = \begin{bmatrix} 0 & 0 & S_{13} & S_{14} \\ 0 & 0 & S_{23} & S_{24} \\ S_{13} & S_{23} & 0 & 0 \\ S_{14} & S_{24} & 0 & 0 \end{bmatrix} \quad \dots (3.1)$$

Now the corresponding conditions to be satisfied by the elements of transfer scattering matrix of the reciprocal lossless four-port will be obtained. The scattering matrix of any four-port, in terms of its transfer scattering matrix, may be obtained as (See Appendix B)

$$[S] = \frac{1}{\Delta} \begin{bmatrix} \begin{bmatrix} t_{13}t_{44} \\ -t_{14}t_{43} \end{bmatrix} \begin{bmatrix} t_{14}t_{33} \\ -t_{13}t_{34} \end{bmatrix} \Delta t_{11} - \begin{bmatrix} t_{31}(t_{13}t_{44} - t_{14}t_{43}) \\ +t_{41}(t_{14}t_{33} - t_{13}t_{34}) \end{bmatrix} \Delta t_{12} - \begin{bmatrix} t_{32}(t_{13}t_{44} - t_{14}t_{43}) \\ +t_{42}(t_{14}t_{33} - t_{13}t_{34}) \end{bmatrix} \\ \begin{bmatrix} t_{23}t_{44} \\ -t_{24}t_{43} \end{bmatrix} \begin{bmatrix} t_{24}t_{33} \\ -t_{23}t_{34} \end{bmatrix} \Delta t_{21} - \begin{bmatrix} t_{31}(t_{23}t_{44} - t_{24}t_{43}) \\ +t_{41}(t_{24}t_{33} - t_{23}t_{34}) \end{bmatrix} \Delta t_{22} - \begin{bmatrix} t_{32}(t_{23}t_{44} - t_{24}t_{43}) \\ +t_{42}(t_{24}t_{33} - t_{23}t_{34}) \end{bmatrix} \\ t_{44} \quad -t_{34} \quad (t_{41}t_{34} - t_{44}t_{31}) \quad (t_{34}t_{42} - t_{44}t_{32}) \\ -t_{43} \quad t_{33} \quad (t_{43}t_{31} - t_{33}t_{41}) \quad (t_{43}t_{32} - t_{33}t_{42}) \end{bmatrix} \quad \dots (3.2a)$$

where t_{ij} are elements of transfer scattering matrix and

$$\Delta = (t_{33}t_{44} - t_{34}t_{43}) \quad \dots (3.2b)$$

From (3.1) and (3.2), the conditions to be satisfied by the elements of the transfer scattering matrix are:

$$t_{44} = \Delta t_{11} - t_{31}(t_{13}t_{44} - t_{14}t_{43}) - t_{41}(t_{14}t_{33} - t_{13}t_{34}) \quad \dots (3.3a)$$

$$t_{43} = -\Delta t_{12} + t_{32}(t_{13}t_{44} - t_{14}t_{43}) + t_{42}(t_{14}t_{33} - t_{13}t_{34}) \quad \dots (3.3b)$$

$$t_{34} = -\Delta t_{21} + t_{31}(t_{23}t_{44} - t_{24}t_{43}) + t_{41}(t_{24}t_{33} - t_{23}t_{34}) \quad \dots (3.3c)$$

$$t_{33} = \Delta t_{22} - t_{32}(t_{23}t_{44} - t_{24}t_{43}) - t_{42}(t_{24}t_{33} - t_{23}t_{34}) \quad \dots (3.3d)$$

due to the symmetry requirements in (3.1), and

$$(t_{13}t_{44} - t_{14}t_{43}) = 0 \quad \dots (3.4a)$$

$$(t_{24}t_{33} - t_{23}t_{34}) = 0 \quad \dots (3.4b)$$

$$(t_{41}t_{34} - t_{44}t_{31}) = 0 \quad \dots (3.4c)$$

$$(t_{43}t_{32} - t_{33}t_{42}) = 0 \quad \dots (3.4d)$$

$$(t_{14}t_{33} - t_{13}t_{34}) = 0 \quad \dots (3.4e)$$

$$(t_{23}t_{44} - t_{24}t_{43}) = 0 \quad \dots (3.4f)$$

$$(t_{34}t_{42} - t_{44}t_{32}) = 0 \quad \dots (3.4g)$$

$$(t_{43}t_{31} - t_{33}t_{41}) = 0 \quad \dots (3.4h)$$

due to the zero terms in (3.1). From (3.2a), it is required that

$$t_{33} \neq 0, \quad t_{44} \neq 0, \quad t_{34} \neq 0, \quad t_{43} \neq 0 \quad \dots (3.5a)$$

$$\Delta = (t_{33}t_{44} - t_{34}t_{43}) \neq 0 \quad \dots (3.5b)$$

Equations (3.4) are satisfied if

$$t_{13} = t_{31} = t_{14} = t_{41} = t_{23} = t_{32} = t_{24} = t_{42} = 0 \quad \dots (3.6)$$

Substituting (3.4a), (3.4b), (3.4e) and (3.4f) in (3.3)

$$t_{44} = \Delta t_{11}, \quad t_{43} = -\Delta t_{12}, \quad t_{34} = -\Delta t_{21}, \quad t_{33} = \Delta t_{22} \quad \dots (3.7)$$

From (3.5) and (3.7), the transfer scattering matrix also has

$$t_{11} \neq 0, \quad t_{12} \neq 0, \quad t_{21} \neq 0, \quad t_{22} \neq 0 \quad \dots (3.8)$$

Thus, from (3.5), (3.6) and (3.8), the transfer scattering matrix should have

$$t_{13} = t_{31} = t_{14} = t_{41} = t_{23} = t_{32} = t_{24} = t_{42} = 0 \quad \dots (3.9a)$$

$$t_{11} \neq 0, \quad t_{22} \neq 0, \quad t_{33} \neq 0, \quad t_{44} \neq 0, \quad t_{33}t_{44} \neq t_{34}t_{43} \quad \dots (3.9b)$$

$$t_{12} \neq 0, \quad t_{21} \neq 0, \quad t_{34} \neq 0, \quad t_{43} \neq 0 \quad \dots (3.9c)$$

and should satisfy the equality conditions in (3.3). Substituting (3.9) in (3.2), the scattering matrix of the codirectional coupler in terms of its transfer scattering matrix is

$$[S] = \begin{bmatrix} 0 & 0 & t_{11} & t_{12} \\ 0 & 0 & t_{21} & t_{22} \\ \frac{t_{44}}{\Delta} & -\frac{t_{34}}{\Delta} & 0 & 0 \\ -\frac{t_{43}}{\Delta} & \frac{t_{33}}{\Delta} & 0 & 0 \end{bmatrix} \quad \dots (3.10a)$$

with

$$\Delta = \frac{t_{44}}{t_{11}} = \frac{t_{33}}{t_{22}} = -\frac{t_{43}}{t_{12}} = -\frac{t_{34}}{t_{21}} = \frac{t_{33}}{t_{22}} = (t_{33}t_{44} - t_{34}t_{43}) \neq 0 \quad \dots (3.10b)$$

3.3 Coupled Lines as Codirectional Coupler:

Consider the four-port network of Fig. 3.1. to be that of lossless coupled lines shown in Fig. 1.1. Using the theory of Chapter 2, the

transfer scattering matrix of the coupled line four-port, in terms of the corresponding decoupled line chain parameters, may be obtained as in (2.29). Using (2.29) and (3.9a), it is required that

$$\begin{aligned}
 (A_1+A_2)\rho_3 - \frac{(D_1+D_2)}{\rho_3} + \frac{(B_1+B_2)}{\rho_3 r_1} - (C_1+C_2)\rho_3 r_1 &= 0 \\
 (A_1+A_2)\rho_3 - \frac{(D_1+D_2)}{\rho_3} - \frac{(B_1+B_2)}{\rho_3 r_1} + (C_1+C_2)\rho_3 r_1 &= 0 \\
 \frac{(A_1-A_2)\rho_4}{\rho} - \frac{(D_1-D_2)\rho}{\rho_4} + \frac{(B_1-B_2)\rho}{\rho_4 r_1} - \frac{(C_1-C_2)\rho_4 r_1}{\rho} &= 0 \\
 \frac{(A_1-A_2)\rho\rho_3}{\rho_2} - \frac{(D_1-D_2)\rho_2}{\rho\rho_3} - \frac{(B_1-B_2)\rho}{\rho_3\rho_2 r_1} + \frac{(C_1-C_2)\rho_2\rho_3 r_1}{\rho} &= 0 \quad \dots (3.11) \\
 \frac{(A_1-A_2)\rho_3\rho}{\rho_2} - \frac{(D_1-D_2)\rho_2}{\rho\rho_3} + \frac{(B_1-B_2)\rho}{\rho_2\rho_3 r_1} - \frac{(C_1-C_2)\rho_2\rho_3 r_1}{\rho} &= 0 \\
 \frac{(A_1-A_2)\rho_4}{\rho} - \frac{(D_1-D_2)\rho}{\rho_4} - \frac{(B_1-B_2)\rho}{\rho_4 r_1} + \frac{(C_1-C_2)\rho_4 r_1}{\rho} &= 0 \\
 \frac{(A_1+A_2)\rho_4}{\rho_2} - \frac{(D_1+D_2)\rho_2}{\rho_4} + \frac{(B_1+B_2)\rho^2}{\rho_2\rho_4 r_1} - \frac{(C_1+C_2)\rho_2\rho_4 r_1}{\rho^2} &= 0 \\
 \frac{(A_1+A_2)\rho_4}{\rho_2} - \frac{(D_1+D_2)\rho_2}{\rho_4} - \frac{(B_1+B_2)\rho^2}{\rho_2\rho_4 r_1} + \frac{(C_1+C_2)\rho_2\rho_4 r_1}{\rho^2} &= 0
 \end{aligned}$$

or

$$\begin{aligned}
r_1[\rho_3^2(A_1+A_2) - (D_1+D_2)] + [(B_1+B_2) - (C_1+C_2)\rho_3^2r_1^2] &= 0 \\
r_1[\rho_3^2(A_1+A_2) - (D_1+D_2)] - [(B_1+B_2) - (C_1+C_2)\rho_3^2r_1^2] &= 0 \\
r_1[\rho_4^2(A_1-A_2) - \rho_2^2(D_1-D_2)] + [\rho^2(B_1-B_2) - \rho_4^2r_1^2(C_1-C_2)] &= 0 \\
r_1[\rho_3^2\rho_3^2(A_1-A_2) - \rho_2^2(D_1-D_2)] - [\rho^2(B_1-B_2) - \rho_3^2\rho_2^2r_1^2(C_1-C_2)] &= 0 \\
r_1[\rho_3^2\rho_3^2(A_1-A_2) - \rho_2^2(D_1-D_2)] + [\rho^2(B_1-B_2) - \rho_3^2\rho_2^2r_1^2(C_1-C_2)] &= 0 \quad \dots (3.12) \\
r_1[\rho_4^4(A_1-A_2) - \rho^2(D_1-D_2)] - [\rho^2(B_1-B_2) - \rho_4^2r_1^2(C_1-C_2)] &= 0 \\
r_1[\rho_4^2(A_1+A_2) - \rho_2^2(D_1+D_2)] + [\rho^4(B_1+B_2) - \rho_2^2\rho_4^2r_1^2(C_1+C_2)] &= 0 \\
r_1[\rho_4^2(A_1+A_2) - \rho_2^2(D_1+D_2)] - [\rho^4(B_1+B_2) - \rho_2^2\rho_4^2r_1^2(C_1+C_2)] &= 0
\end{aligned}$$

It is known that for lossless lines, the A and D parameters are real, while the B and C parameters are imaginary for $s = j\omega$ (87,88). Noting these properties for decoupled lines, the real and imaginary parts of (3.12) may be separated as:

$$\begin{aligned}
\rho_3^2(A_1+A_2) - (D_1+D_2) &= 0 \\
\rho_4^2(A_1-A_2) - \rho_2^2(D_1-D_2) &= 0 \\
\rho_3^2\rho_3^2(A_1-A_2) - \rho_2^2(D_1-D_2) &= 0 \\
\rho_4^2(A_1+A_2) - \rho_2^2(D_1+D_2) &= 0
\end{aligned} \quad \dots (3.13)$$

and

$$\begin{aligned}
(B_1+B_2) - \rho_3^2 r_1^2 (C_1+C_2) &= 0 \\
\rho^2 (B_1-B_2) - \rho_4^2 r_1^2 (C_1-C_2) &= 0 \\
\rho^2 (B_1-B_2) - \rho_3^2 \rho_2^2 r_1^2 (C_1-C_2) &= 0 \quad \dots (3.14) \\
\rho^4 (B_1+B_2) - \rho_2^2 \rho_4^2 r_1^2 (C_1+C_2) &= 0
\end{aligned}$$

From (3.13)

$$\frac{A_1+A_2}{D_1+D_2} = \frac{1}{\rho_3^2} = \frac{\rho_2^2}{\rho_4^2} \quad \dots (3.15a)$$

$$\frac{A_1-A_2}{D_1-D_2} = \frac{\rho^2}{\rho_4^2} = \frac{\rho_2^2}{\rho^2 \rho_3^2} \quad \dots (3.15b)$$

From (3.14)

$$\frac{r_1^2 (C_1+C_2)}{(B_1+B_2)} = \frac{1}{\rho_3^2} = \frac{\rho^4}{\rho_2^2 \rho_4^2} \quad \dots (3.16a)$$

$$\frac{r_1^2 (C_1-C_2)}{(B_1-B_2)} = \frac{\rho^2}{\rho_4^2} = \frac{\rho^2}{\rho_2^2 \rho_3^2} \quad \dots (3.16b)$$

Equations (3.15) and (3.16) may be combined as

$$\frac{(A_1+A_2)}{(D_1+D_2)} = \frac{r_1^2 (C_1+C_2)}{(B_1+B_2)} = \frac{1}{\rho_3^2} = \frac{\rho_2^2}{\rho_4^2} = \frac{\rho^4}{\rho_2^2 \rho_4^2} \quad \dots (3.17a)$$

$$\frac{(A_1 - A_2)}{(D_1 - D_2)} = \frac{r_1^2 (C_1 - C_2)}{(B_1 - B_2)} = \frac{\rho_2^2}{\rho_4^2} = \frac{\rho_2^2}{\rho^2 \rho_3^2} = \frac{\rho_2^2}{\rho_2^2 \rho_3^2} \quad \dots (3.17b)$$

From (3.17a)

$$\rho_4^2 = \rho_2^2 \rho_3^2 \quad \dots (3.18a)$$

$$\rho_4^2 \rho_2^2 = \rho_3^2 \rho^4 \quad \dots (3.18b)$$

Solving (3.18)

$$\rho_2^2 = \rho^2 \quad ; \quad \rho_3^2 = \frac{\rho_4^2}{\rho^2} \quad \dots (3.19)$$

$$\text{or} \quad r_2 = \rho^2 r_1 \quad ; \quad r_4 = \rho^2 r_3 \quad \dots (3.20)$$

Substituting (3.19) in (3.17)

$$\rho_3^2 (A_1 + A_2) = (D_1 + D_2) \quad \dots (3.21a)$$

$$\rho_3^2 (A_1 - A_2) = (D_1 - D_2) \quad \dots (3.21b)$$

Solving (3.21)

$$\rho_3^2 = \frac{D_1}{A_1} \quad \dots (3.22)$$

As $\rho_3^2 = (r_3/r_1)$ is a ratio of two resistances, it is independent of frequency and hence may be evaluated at $s = 0$. For lossless lines, the values of D_1 and A_1 are unity at $s = 0$. Thus,

$$\rho_3^2 = 1 \quad \dots (3.23a)$$

$$r_1 = r_3 \quad ; \quad r_2 = r_4 = \rho^2 r_1 \quad \dots (3.23b)$$

Thus, the terminating resistances and the taper of the coupled lines

A and B are constrained by (3.23) for a codirectional coupler action.

Now, from (2.14), $\rho^2 = [L_{22}(x)/L_{11}(x)]$. However, ρ should be independent of x from (3.23b). Hence the lines A and B must be similar (that is, have the same taper). Substituting (3.23) in (3.17) and solving, the chain parameters of the two decoupled lines are found to be related as

$$A_1 = D_1, \quad B_1 = r_1^2 C_1 \quad \dots (3.24a)$$

$$A_2 = D_2, \quad B_2 = r_1^2 C_2 \quad \dots (3.24b)$$

where r_1 is independent of frequency. Substituting (3.23) and (3.24) in (2.29), the transfer scattering matrix is

$$[T] = \frac{1}{2} \begin{bmatrix} (A_1+A_2) - \frac{(B_1+B_2)}{r_1} & (A_1-A_2) - \frac{(B_1-B_2)}{r_1} & 0 & 0 \\ (A_1-A_2) - \frac{(B_1-B_2)}{r_1} & (A_1+A_2) - \frac{(B_1+B_2)}{r_1} & 0 & 0 \\ 0 & 0 & (A_1+A_2) + \frac{(B_1+B_2)}{r_1} & (A_1-A_2) + \frac{(B_1-B_2)}{r_1} \\ 0 & 0 & (A_1-A_2) + \frac{(B_1-B_2)}{r_1} & (A_1+A_2) + \frac{(B_1+B_2)}{r_1} \end{bmatrix} \quad \dots (3.25a)$$

with

$$\Delta = (t_{33}t_{44} - t_{34}t_{43}) = (A_1 + \frac{B_1}{r_1})(A_2 + \frac{B_2}{r_1}) \quad \dots (3.25b)$$

Since the decoupled lines as two-ports are reciprocal,

$$(A_1 D_1 - B_1 C_1) = 1, \quad (A_2 D_2 - B_2 C_2) = 1 \quad \dots (3.26)$$

Using (3.24), (3.25b) and (3.26), it may be shown that the equality

conditions in (3.10b) are also satisfied by the various elements of the transfer scattering matrix (3.25a). Thus, the transfer scattering matrix (3.25) satisfies all the required conditions for the coupled line four-port to behave as a codirectional coupler. Substituting (3.25) and (3.26) in (3.2) and simplifying, the scattering matrix of the coupled line four-port may be expressed as

$$[S] = \frac{1}{2} \begin{bmatrix} 0 & 0 & (A_1 + A_2) - \frac{(B_1 + B_2)}{r_1} & (A_1 - A_2) - \frac{(B_1 - B_2)}{r_1} \\ 0 & 0 & (A_1 - A_2) - \frac{(B_1 - B_2)}{r_1} & (A_1 + A_2) - \frac{(B_1 + B_2)}{r_1} \\ (A_1 + A_2) - \frac{(B_1 + B_2)}{r_1} & (A_1 - A_2) - \frac{(B_1 - B_2)}{r_1} & 0 & 0 \\ (A_1 - A_2) - \frac{(B_1 - B_2)}{r_1} & (A_1 + A_2) - \frac{(B_1 + B_2)}{r_1} & 0 & 0 \end{bmatrix} \quad \dots (3.27a)$$

It is noted from (3.27a) that $S_{13} = S_{24}$, $S_{14} = S_{23}$. Hence, codirectional couplers formed from a pair of lossless coupled lines always have the property that

$$S_{13} = S_{24} \quad , \quad S_{14} = S_{23} \quad \dots (3.27b)$$

Thus, a lossless reciprocal four-port using coupled lines with $r_1 = r_3$ and $r_2 = r_4 = \rho^2 r_1$, will behave as a codirectional coupler, if the corresponding decoupled line chain parameters satisfy (3.24).

The expressions for the various characteristics of the codirectional coupler from the scattering matrix (3.27) are⁽⁷⁾:

$$\mathcal{D} = \infty \quad \dots (3.28a)$$

$$\mathcal{C} = 20 \log_{10} \left| \frac{2}{\left(A_1 - \frac{B_1}{r_1}\right) - \left(A_2 - \frac{B_2}{r_1}\right)} \right| \quad \dots (3.28b)$$

$$\phi_{CT} = \tan^{-1} \frac{(B_2 - B_1)}{jr_1(A_1 - A_2)} - \tan^{-1} \frac{-(B_1 + B_2)}{jr_1(A_1 + A_2)} \quad \dots (3.28c)$$

where

$$\mathcal{D} = \text{Coupler directivity} = 20 \log_{10} \left| \frac{S_{41}}{S_{21}} \right| \quad \dots (3.29a)$$

$$\mathcal{C} = \text{Coupling of the coupler} = 20 \log_{10} \left| \frac{1}{S_{41}} \right| \quad \dots (3.29b)$$

$$\phi_{CT} = \text{Phase shift between coupled and transmitted} = \angle \frac{S_{41}}{S_{31}}$$

It is shown in Appendix C that a lossless line whose parameters are related as

$$A = D, \quad B = r^2 C \quad \dots (3.30)$$

with r independent of s and x , should have proportional distributions, that is,

$$L = L_0 F(x), \quad C = C_0 F(x) \quad \dots (3.31a)$$

$$\text{with} \quad r = \sqrt{L_0/C_0} \quad \dots (3.31b)$$

Using this result and the conditions (3.24) to be satisfied by the two decoupled lines, it is seen that for a codirectional coupler, the distributions of corresponding decoupled lines 1 and 2 are required to be of the form

$$L_1 = L_{10} F(x) \quad , \quad C_1 = C_{10} F(x) \quad \dots (3.32a)$$

$$\text{and} \quad L_2 = L_{20} G(x) \quad , \quad C_2 = C_{20} G(x) \quad \dots (3.32b)$$

where

$$r_1 = \sqrt{(L_{10}/C_{10})} = \sqrt{(L_{20}/C_{20})} \quad , \quad L_1 C_1 \neq L_2 C_2 \quad \dots (3.33)$$

From (2.19), (3.32) and (3.33), the coupled line parameters are:

$$L_{11} = \frac{L_{10} F(x) + L_{20} G(x)}{2} \quad , \quad L_{22} = \rho^2 L_{11} \quad \dots (3.34a)$$

$$C_{11} = \frac{C_{10}(\rho+1) F(x) + C_{20}(\rho-1) G(x)}{2\rho} \quad , \quad C_{22} = \frac{C_{10}(\rho+1) F(x) - C_{20}(\rho-1) G(x)}{2\rho^2} \quad \dots (3.34b)$$

$$L_{12} = \frac{\rho}{2} [L_{10} F(x) - L_{20} G(x)] \quad , \quad C_{12} = \frac{1}{2\rho} [C_{20} G(x) - C_{10} F(x)] \quad \dots (3.34c)$$

$$r_1 = r_3 = \sqrt{(L_{10}/C_{10})} = \sqrt{(L_{20}/C_{20})} \quad , \quad r_2 = r_4 = \rho^2 r_1 \quad \dots (3.34d)$$

From (3.34c), it is noted that for these lines, smooth transition in the electromagnetic coupling at $x = 0$ may be obtained by making $L_{12}(0)$ and $C_{12}(0)$ equal to zero, that is,

$$L_{10} F(0) = L_{20} G(0) \quad \dots (3.35)$$

3.4 Codirectional Coupler Characteristics:

For the codirectional coupler, the decoupled line distributions are as described in (3.32) and (3.33). From these distributions, the chain parameters may be obtained from well known techniques⁽⁸⁷⁻⁹¹⁾ as

$$A_1 = D_1 = \cos \theta_1 \quad ; \quad B_1 = j z_{10}(0) \sin \theta_1 \quad ; \quad C_1 = \frac{j \sin \theta_1}{z_{10}(0)} \quad \dots (3.37a)$$

$$A_2 = D_2 = \cos K\theta_1 \quad ; \quad B_2 = jz_{20}(0)\sin K\theta_1 \quad ; \quad C_2 = \frac{j\sin K\theta_1}{z_{20}(0)} \quad \dots (3.37b)$$

where A_1, B_1, C_1, D_1 and A_2, B_2, C_2, D_2 are respectively the chain parameters of decoupled lines 1 and 2, and

$$\theta_1 = \omega \sqrt{L_{10}C_{10}} \int_0^{\ell} F(x)dx \quad \dots (3.37c)$$

$$r_1 = z_{10}(0) = z_{20}(0) = \sqrt{\frac{L_{10}}{C_{10}}} \quad , \quad K = \sqrt{\frac{L_{20}C_{20}}{L_{10}C_{10}}} \frac{\int_0^{\ell} G(x)dx}{\int_0^{\ell} F(x)dx} \quad \dots (3.37d)$$

It is assumed that $K \neq 1$, since otherwise the lines given by (3.35) are no longer coupled. Substituting (3.37) in (3.33), the coupling of codirectional coupler is

$$\begin{aligned} \mathcal{C} &= 20 \log_{10} \left| \frac{2}{(\cos\theta_1 - \cos K\theta_1) - j(\sin\theta_1 - \sin K\theta_1)} \right| \\ &= 10 \log_{10} \left| \frac{1}{\{1 - \cos(K-1)\theta_1\}} \right| \quad \dots (3.38) \end{aligned}$$

From (3.38), it is found that the variation of coupling of codirectional coupler, with frequency, is periodic. Substituting (3.37) in (3.28c), the phase shift produced between coupled and transmitted signals is

$$\phi_{CT} = \frac{\pi}{2} + (K+1)\theta_1 \quad \dots (3.39)$$

From (3.39), it is noted that the phase difference between coupled and transmitted signals varies linearly with frequency, because K is independent of frequency. Thus, for lossless coupled line codirectional coupler, the coupling response is periodic with frequency, while,

the phase shift between coupled and transmitted signals varies linearly with frequency.

For identical coupled lines, $\rho = \sqrt{L_{22}/L_{11}}$ is unity, showing that the codirectional coupler ports must be terminated in equal resistances, thereby exhibiting codirectional action without any impedance transformation. When the coupled lines are non-identical, ρ is not equal to unity and an impedance transformation of ρ^2 between ports (1) and (2), and between (3) and (4), may be obtained as the port resistances $r_2 = r_4 = \rho^2 r_1$. Hence, for a codirectional coupler with impedance transformation, the port pair (1,3) should be terminated with equal resistances, with a similar statement holding for the port pairs (2,4), while, an impedance transformation between the port pairs (1,3) and (2,4) may be achieved. It is further noted from (3.33) that the expression for codirectional coupler directivity, coupling and phase shift, do not depend on the impedance transformation ratio ρ . Thus the various coupler characteristics \mathcal{C} , \mathcal{D} and ϕ_{CT} remain unchanged when non-identical coupled lines are used to have an impedance transformation along with the codirectional coupler action.

3.5 A Four-Port Contradirectional Coupler:

Consider a lossless reciprocal four-port with terminating resistors as shown in Fig.3.2. This four-port will behave as a contradirectional coupler if, when terminated in prescribed resistances, it is matched at all ports with ports (1) and (4), and (2) and (3) mutually isolated⁽³⁾. There may or may not be impedance transformation depending on the values

of the terminating resistors. The scattering matrix of this contra-directional coupler is

$$[S] = \begin{bmatrix} 0 & S_{12} & S_{13} & 0 \\ S_{12} & 0 & 0 & S_{24} \\ S_{13} & 0 & 0 & S_{34} \\ 0 & S_{24} & S_{34} & 0 \end{bmatrix} \quad \dots (3.40)$$

The scattering matrix of any four-port network in terms of its transfer scattering matrix is given by (3.2).

Now the corresponding conditions to be satisfied by the elements of the transfer scattering matrix of the lossless reciprocal four-port will be obtained. Comparing (3.40) and (3.2), it is required that

$$(t_{14}t_{33} - t_{13}t_{34}) = (t_{23}t_{44} - t_{24}t_{43}) \quad \dots (3.41a)$$

$$(t_{34}t_{42} - t_{44}t_{32}) = (t_{43}t_{31} - t_{33}t_{41}) \quad \dots (3.41b)$$

$$t_{44} = \Delta t_{11} - t_{31}(t_{13}t_{44} - t_{14}t_{43}) - t_{41}(t_{14}t_{33} - t_{13}t_{34}) \quad \dots (3.42a)$$

$$t_{33} = \Delta t_{22} - t_{32}(t_{23}t_{44} - t_{24}t_{43}) - t_{42}(t_{24}t_{33} - t_{23}t_{24}) \quad \dots (3.42b)$$

$$(t_{13}t_{44} - t_{14}t_{43}) = 0 \quad \dots (3.43a)$$

$$(t_{24}t_{33} - t_{23}t_{34}) = 0 \quad \dots (3.43b)$$

$$(t_{41}t_{34} - t_{44}t_{31}) = 0 \quad \dots (3.43c)$$

$$(t_{43}t_{32} - t_{33}t_{42}) = 0 \quad \dots (3.43d)$$

$$t_{43} = t_{34} = 0 \quad \dots (3.44a)$$

$$\Delta t_{21} - [t_{31}(t_{23}t_{44} - t_{24}t_{43}) + t_{41}(t_{24}t_{33} - t_{23}t_{34})] = 0 \quad \dots (3.44b)$$

$$\Delta t_{12} - [t_{32}(t_{13}t_{44} - t_{14}t_{43}) + t_{42}(t_{14}t_{33} - t_{13}t_{34})] = 0 \quad \dots (3.44c)$$

$$\Delta = (t_{33}t_{44} - t_{34}t_{43}) \neq 0 \quad \dots (3.44d)$$

From (3.44a) and (3.44d)

$$t_{44} \neq 0, \quad t_{33} \neq 0, \quad \Delta = t_{33}t_{44} \neq 0 \quad \dots (3.45)$$

Substituting (3.44a) in (3.43)

$$t_{13}t_{44} = t_{24}t_{34} = t_{44}t_{31} = t_{33}t_{42} = 0 \quad \dots (3.46a)$$

From (3.43), (3.45) and (3.46)

$$t_{13} = t_{31} = t_{24} = t_{42} = 0 \quad \dots (3.46b)$$

Substituting (3.44a) and (3.46a) in (3.44b) and (3.44c)

$$t_{33}t_{44}t_{21} = 0; \quad t_{33}t_{44}t_{12} = 0 \quad \dots (3.47)$$

Equation (3.47) requires from (3.45) that $t_{21} = t_{12} = 0$. Thus the contradirectional transfer scattering matrix elements should be such that

$$t_{12} = t_{21} = t_{13} = t_{31} = t_{24} = t_{42} = t_{34} = t_{43} = 0 \quad \dots (3.48a)$$

$$t_{23} \neq 0, \quad t_{32} \neq 0, \quad t_{14} \neq 0, \quad t_{41} \neq 0, \quad t_{33} \neq 0, \quad t_{44} \neq 0 \quad \dots (3.48b)$$

$$t_{11} \neq 0, \quad t_{22} \neq 0, \quad t_{44}t_{11} \neq t_{41}t_{14}, \quad t_{33}t_{22} \neq t_{32}t_{23} \quad \dots (3.48c)$$

Substituting (3.48) in (3.41) and (3.42), the scattering matrix of the contradirectional coupler is

$$[S] = \begin{bmatrix} 0 & \frac{t_{14}}{t_{44}} & (t_{11} - \frac{t_{41}t_{14}}{t_{44}}) & 0 \\ \frac{t_{23}}{t_{33}} & 0 & 0 & (t_{22} - \frac{t_{32}t_{23}}{t_{33}}) \\ \frac{1}{t_{33}} & 0 & 0 & -\frac{t_{32}}{t_{33}} \\ 0 & \frac{1}{t_{44}} & -\frac{t_{41}}{t_{44}} & 0 \end{bmatrix} \quad \dots (3.49)$$

with

$$\frac{t_{33}}{t_{44}} = \frac{t_{23}}{t_{14}} = \frac{t_{32}}{t_{41}} = \frac{1}{(t_{11}t_{44} - t_{14}t_{41})} = (t_{22}t_{33} - t_{32}t_{23}) \quad \dots (3.50)$$

3.6 Coupled Lines as Contradirectional Coupler:

Consider the four-port network of Fig.3.2 to be that of lossless coupled lines shown in Fig.2.1. Using the theory of Chapter 2, the transfer scattering matrix of the coupled line four-port in terms of the corresponding decoupled line chain parameters may be obtained as in (2.29). Using (2.29) and (3.49), it is required that

$$\begin{aligned} \frac{(A_1 - A_2)\rho_4}{\rho} + \frac{(D_1 - D_2)\rho}{\rho_4} - \frac{(B_1 - B_2)\rho}{\rho_4 r_1} - \frac{(C_1 - C_2)\rho_4 \rho_1}{\rho} &= 0 \\ \frac{(A_1 - A_2)\rho \rho_3}{\rho_2} + \frac{(D_1 - D_2)\rho_2}{\rho \rho_3} - \frac{(B_1 - B_2)\rho}{\rho_2 \rho_3 r_1} - \frac{(C_1 - C_2)\rho_2 \rho_3 r_1}{\rho} &= 0 \\ (A_1 + A_2)\rho_3 - \frac{(D_1 + D_2)}{\rho_3} - \frac{(B_1 + B_2)}{\rho_3 r_1} - (C_1 + C_2)\rho_3 r_1 &= 0 \end{aligned}$$

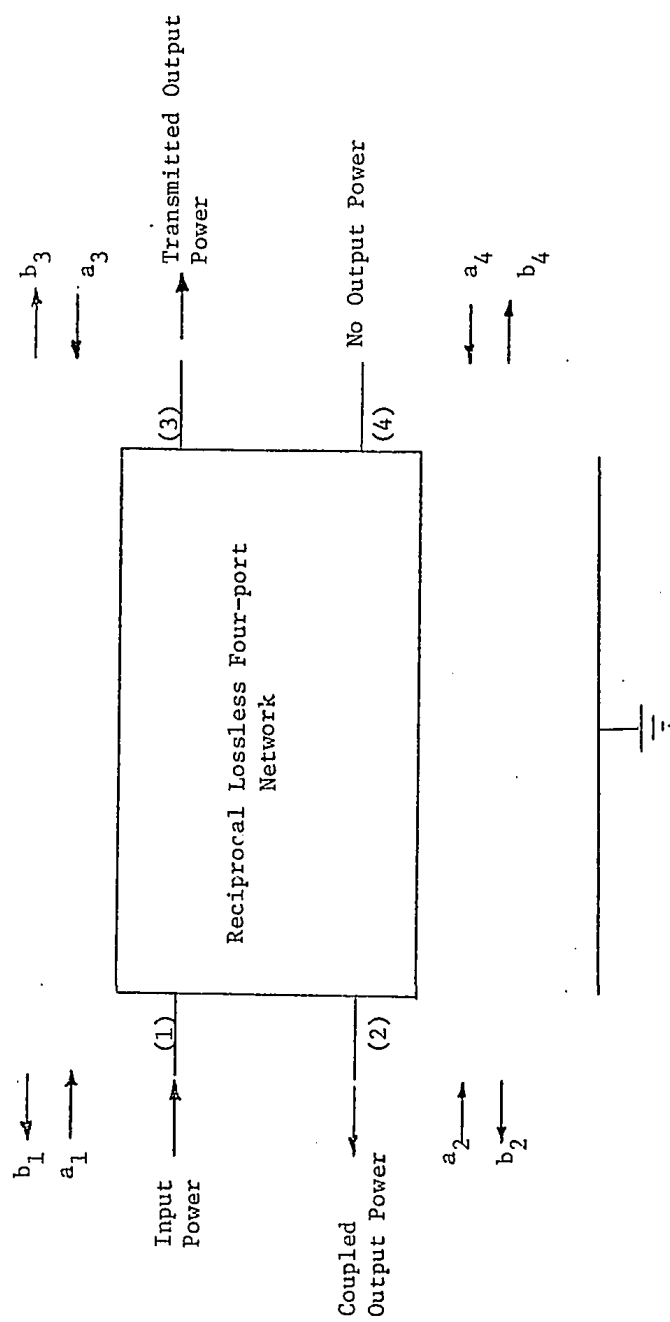


Fig. 3.2: Four-port Contradiirectional Coupler

$$(A_1+A_2)\rho_3 - \frac{(D_1+D_2)}{\rho_3} - \frac{(B_1+B_2)}{\rho_3 r_1} + (C_1+C_2)\rho_3 r_1 = 0$$

$$\frac{(A_1+A_2)\rho_4}{\rho_2} - \frac{(D_1+D_2)\rho_2}{\rho_4} + \frac{(B_1+B_2)\rho^2}{\rho_2 \rho_4 r_1} - \frac{(C_1+C_2)\rho_2 \rho_4 r_1}{\rho^2} = 0$$

$$\frac{(A_1+A_2)\rho_4}{\rho_2} - \frac{(D_1+D_2)\rho_2}{\rho_4} - \frac{(B_1+B_2)\rho^2}{\rho_2 \rho_4 r_1} + \frac{(C_1+C_2)\rho_2 \rho_4 r_1}{\rho^2} = 0 \quad \dots (3.51)$$

$$\frac{(A_1-A_2)\rho_4}{\rho} + \frac{(D_1-D_2)\rho}{\rho_4} + \frac{(B_1-B_2)\rho}{\rho_4 r_1} + \frac{(C_1-C_2)\rho_4 r_1}{\rho} = 0$$

$$\frac{(A_1-A_2)\rho \rho_3}{\rho_2} + \frac{(D_1-D_2)\rho_2}{\rho \rho_3} + \frac{(B_1-B_2)\rho}{\rho_2 \rho_3 r_1} + \frac{(C_1-C_2)\rho_2 \rho_3 r_1}{\rho} = 0$$

or

$$r_1[\rho_4^2(A_1-A_2) + \rho^2(D_1-D_2)] - [\rho^2(B_1-B_2) + \rho_4^2 r_1(C_1-C_2)] = 0$$

$$r_1[\rho^2 \rho_3^2(A_1-A_2) + \rho_2^2(D_1-D_2)] - [\rho^2(B_1-B_2) + \rho_2^2 \rho_3^2 r_1^2(C_1-C_2)] = 0$$

$$r_1[\rho_3^2(A_1+A_2) - (D_1+D_2)] + [(B_1+B_2) - \rho_3^2 r_1^2(C_1+C_2)] = 0$$

$$r_1[\rho_3^2(A_1+A_2) - (D_1+D_2)] - [(B_1+B_2) - \rho_3^2 r_1^2(C_1+C_2)] = 0$$

$$\rho^2 r_1[\rho_4^2(A_1+A_2) - \rho_2^2(D_1+D_2)] + [\rho^4(B_1+B_2) - \rho_2^2 \rho_4^2 r_1^2(C_1+C_2)] = 0$$

$$\rho^2 r_1[\rho_4^2(A_1+A_2) - \rho_2^2(D_1+D_2)] - [\rho^4(B_1+B_2) - \rho_2^2 \rho_4^2 r_1^2(C_1+C_2)] = 0$$

$$r_1[\rho_4^2(A_1-A_2) + \rho^2(D_1-D_2)] + [\rho^2(B_1-B_2) + \rho_4^2 r_1^2(C_1-C_2)] = 0$$

$$r_1[\rho_3^2 \rho^2(A_1-A_2) + \rho_2^2(D_1-D_2)] + [\rho^2(B_1-B_2) + \rho_2^2 \rho_3^2 r_1^2(C_1-C_2)] = 0 \quad \dots (3.52)$$

For lossless lines, it is known that A_1 , D_1 , A_2 and D_2 are real, while B_1 , C_1 , B_2 and C_2 are imaginary for $s = j\omega$ ^(87,88). Using these properties for decoupled line chain parameters in (3.52) and separating real and imaginary parts respectively

$$\begin{aligned}
 \rho_4^2 (A_1 - A_2) + \rho^2 (D_1 - D_2) &= 0 \\
 \rho^2 \rho_3^2 (A_1 - A_2) + \rho_2^2 (D_1 - D_2) &= 0 \\
 \rho_3^2 (A_1 + A_2) - (D_1 + D_2) &= 0 \\
 \rho_4^2 (A_1 + A_2) - \rho_2^2 (D_1 + D_2) &= 0
 \end{aligned}
 \quad \dots (3.53)$$

and

$$\begin{aligned}
 \rho^2 (B_1 - B_2) + \rho_4^2 r_1^2 (C_1 - C_2) &= 0 \\
 \rho^2 (B_1 - B_2) + \rho_2^2 \rho_3^2 r_1^2 (C_1 - C_2) &= 0 \\
 (B_1 + B_2) - \rho_3^2 r_1^2 (C_1 + C_2) &= 0 \\
 \rho^4 (B_1 + B_2) - \rho_2^2 \rho_4^2 r_1^2 (C_1 + C_2) &= 0
 \end{aligned}
 \quad \dots (3.54)$$

From (3.53)

$$\frac{A_1 + A_2}{D_1 + D_2} = \frac{1}{\rho_3^2} = \frac{\rho_2^2}{\rho_4^2} \quad \dots (3.55a)$$

$$\frac{A_2 - A_1}{D_1 - D_2} = \frac{\rho_2^2}{\rho_4^2} = \frac{\rho_2^2}{\rho_2^2 \rho_3^2} \quad \dots (3.55b)$$

$$\frac{r_1^2 (C_1 + C_2)}{(B_1 + B_2)} = \frac{1}{\rho_3^2} = \frac{\rho_4^4}{\rho_2^2 \rho_4^2} \quad \dots (3.56a)$$

$$\frac{r_1^2 (C_2 - C_1)}{(B_1 - B_2)} = \frac{\rho_2^2}{\rho_4^2} = \frac{\rho_2^2}{\rho_2^2 \rho_3^2} \quad \dots (3.56b)$$

Equations (3.55) and (3.56) may be combined as

$$\frac{(A_1 + A_2)}{(D_1 + D_2)} = \frac{r_1^2 (C_1 + C_2)}{(B_1 + B_2)} = \frac{1}{\rho_3^2} = \frac{\rho_2^2}{\rho_4^2} = \frac{\rho_4^4}{\rho_2^2 \rho_4^2} \quad \dots (3.57a)$$

$$\frac{(A_2 - A_1)}{(D_1 - D_2)} = \frac{r_1^2 (C_2 - C_1)}{(B_1 - B_2)} = \frac{\rho_2^2}{\rho_4^2} = \frac{\rho_2^2}{\rho_2^2 \rho_3^2} = \frac{\rho_2^2}{\rho_2^2 \rho_3^2} \quad \dots (3.57b)$$

From (3.56)

$$\rho_4^2 = \rho_2^2 \rho_3^2 \quad \dots (3.58a)$$

$$\rho_4^2 \rho_2^2 = \rho_3^2 \rho_4^4 \quad \dots (3.58b)$$

Solving (3.58)

$$\rho_2^2 = \rho^2 \quad ; \quad \rho_3^2 = \frac{\rho_4^2}{\rho^2} \quad \dots (3.59a)$$

or

$$r_2 = \rho^2 r_1 \quad ; \quad r_4 = \rho^2 r_3 \quad \dots (3.59b)$$

Substituting (3.59) in (3.56)

$$\rho_3^2 (A_1 + A_2) = (D_1 + D_2) \quad \dots (3.60a)$$

$$\rho_3^2 (A_2 - A_1) = (D_1 - D_2) \quad \dots (3.60b)$$

Solving (3.60)

$$\rho_3^2 = \frac{D_1}{A_2} \quad \dots (3.61)$$

Since $\rho_3^2 = (r_3/r_1)$ is a ratio of two resistances, it is independent of frequency, and hence, may be evaluated at $s = 0$. For lossless lines, values of D_1 and A_2 are unity at $s = 0$. Thus

$$\rho_3^2 = 1 \quad \dots (3.62a)$$

$$r_1 = r_3 \quad ; \quad r_2 = r_4 = \rho^2 r_1 \quad \dots (3.62b)$$

Equation (3.62) puts constraints on the terminating resistances as well as on the taper of coupled lines A and B. Since $\rho^2 = [L_{22}(x)/L_{11}(x)]$ is now required to be constant, the lines A and B have got to be similar (that is, have the same taper). Substituting (3.62) in (3.57) and solving for decoupled line chain parameters

$$A_1 = D_2 \quad , \quad D_1 = A_2 \quad \dots (3.63a)$$

$$B_1 = r_1^2 C_2 \quad , \quad C_1 = \frac{B_2}{r_1} \quad \dots (3.63b)$$

where r_1 is independent of frequency.

Substituting (3.62) and (3.63) in (2.29), the transfer scattering matrix reduces to

$$[T] = \frac{1}{2} \begin{bmatrix} (A_1 + D_1) - \left(\frac{B_1}{r_1} + C_1 r_1\right) & 0 & 0 & (A_1 - D_1) + \left(\frac{B_1}{r_1} - C_1 r_1\right) \\ 0 & (A_1 + D_1) - \left(\frac{B_1}{r_1} + C_1 r_1\right) & (A_1 - D_1) + \left(\frac{B_1}{r_1} - C_1 r_1\right) & 0 \\ 0 & (A_1 - D_1) - \left(\frac{B_1}{r_1} - C_1 r_1\right) & (A_1 + D_1) + \left(\frac{B_1}{r_1} + C_1 r_1\right) & 0 \\ (A_1 - D_1) - \left(\frac{B_1}{r_1} - C_1 r_1\right) & 0 & 0 & (A_1 + D_1) + \left(\frac{B_1}{r_1} + C_1 r_1\right) \end{bmatrix} \quad \dots (3.64)$$

From (3.64), it is found that the elements of this transfer scattering matrix satisfies the conditions (3.48). Using the fact that the decoupled lines as two-ports are reciprocal, that is,

$$(A_1 D_1 - B_1 C_1) = 1 \quad , \quad (A_2 D_2 - B_2 C_2) = 1 \quad \dots (3.65)$$

it may be shown that the equality conditions in (3.50) are also satisfied by the various elements of the transfer scattering matrix (3.64). Thus, all the required conditions for the four-port contra-directional coupler are satisfied by the transfer scattering matrix (3.64).

Substituting (3.64) and (3.65) in (3.49) and simplifying, the four-port scattering matrix may be expressed as:

$$[S] = \frac{1}{2} \begin{bmatrix} 0 & (A_1 - D_1) + \frac{B_1}{r_1} - C_1 r_1 & 2 & 0 \\ (A_1 - D_1) + \frac{B_1}{r_1} - C_1 r_1 & 0 & 0 & 2 \\ 2 & 0 & 0 & (A_1 - D_1) - \frac{B_1}{r_1} - C_1 r_1 \\ 0 & 2 & (A_1 - D_1) - \frac{B_1}{r_1} - C_1 r_1 & 0 \end{bmatrix} \frac{1}{\{(A_1 + D_1) + (\frac{B_1}{r_1} + C_1 r_1)\}}$$

.. (3.66)

It is noted from (3.66) that $S_{13} = S_{24}$. Hence, contradirectional coupler formed by a pair of lossless reciprocal coupled lines always have the property that $S_{13} = S_{24}$. Thus, the conditions $S_{13} = S_{24}$, as well as the interrelations (3.63) between the matrix parameters of the two decoupled lines, apply to a more general case of coupled line contradirectional coupler than that considered by Sharp⁽⁶¹⁾, since his results apply only for the case of CNU TLs having an absolutely continuous characteristic impedance matrix.

Thus a lossless reciprocal four-port using coupled lines, with $r_1 = r_3$ and $r_2 = r_4 = \rho^2 r_1$, will behave as a contradirectional coupler if the corresponding decoupled line chain parameters satisfy the

requirements (3.63). The various characteristics of the contra-directional coupler, from the scattering matrix (3.66), are⁽⁷⁾:

$$\mathcal{D} = \infty \quad \dots (3.67a)$$

$$\mathcal{C} = 20 \log_{10} \left| \frac{(A_1 + D_1) + \left(\frac{B_1}{r_1} + C_1 r_1\right)}{(A_1 - D_1) + \left(\frac{B_1}{r_1} - C_1 r_1\right)} \right| \quad \dots (3.67b)$$

$$\phi_{CT} = \tan^{-1} \frac{\left(\frac{B_1}{r_1} - C_1 r_1\right)}{j(A_1 - D_1)} \quad \dots (3.68)$$

where

$$\mathcal{D} = \text{Coupler directivity} = 20 \log_{10} \left| \frac{S_{21}}{S_{41}} \right| \quad \dots (3.69a)$$

$$\mathcal{C} = \text{Coupling of contradirectional coupler} = 20 \log_{10} \left| \frac{1}{S_{21}} \right| \quad \dots (3.69b)$$

$$\begin{aligned} \phi_{CT} &= \text{Phase shift between coupled and transmitted signals} \\ &= \angle \frac{S_{21}}{S_{31}} \end{aligned} \quad \dots (3.69c)$$

It is shown in Appendix C that two lossless lines, whose parameters are related as in (3.63), should have dual distributions, that is, if line 1 has distributions

$$L_1 = L_{10} F(x) \quad , \quad C_1 = C_{10} G(x) \quad 0 \leq x \leq \ell \quad \dots (3.70)$$

then line 2 will have for its distributions

$$L_2 = L_{20} G(x) \quad , \quad C_2 = C_{20} F(x) \quad 0 \leq x \leq \ell \quad \dots (3.71)$$

where

$$r_1 = \sqrt{(L_{10}/C_{20})} = \sqrt{(L_{20}/C_{10})} \quad \dots (3.72)$$

Thus, for a coupled line four-port to behave as a contradirectional coupler, the corresponding decoupled lines should be dual lines with distributions as given in (3.70)-(3.72). Also from (2.19), (3.70), (3.71) and (3.72), the coupled line parameters are

$$L_{11} = \frac{1}{2} [L_{10}F(x) + L_{20}G(x)] \quad , \quad L_{22} = \rho^2 L_{11} \quad \dots (3.73a)$$

$$C_{11} = \frac{1}{2\rho} [C_{10}(\rho+1)G(x) + C_{20}(\rho-1)F(x)] \quad , \quad C_{22} = \frac{1}{2\rho^2} [(\rho+1)G(x) - (\rho-1)C_{20}F(x)] \quad \dots (3.73b)$$

$$L_{12} = \frac{\rho}{2} [L_{10}F(x) - L_{20}G(x)] \quad , \quad C_{12} = \frac{1}{2\rho} [C_{20}F(x) - C_{10}G(x)] \quad \dots (3.73c)$$

$$r_1 = r_3 = \sqrt{(L_{10}/C_{20})} = \sqrt{(L_{20}/C_{10})} \quad , \quad r_2 = r_4 = \rho^2 r_1 \quad \dots (3.73d)$$

From (3.72), it is seen that for identical coupled lines, $\rho = \sqrt{(L_{22}/L_{11})}$ is unity, which makes all the terminating resistances equal. Under this condition, the coupled line four-port exhibits contradirectional characteristics without impedance transformation. When the coupled lines are identical, ρ is not equal to unity and impedance transformation of ρ^2 between ports (1) and (2), and between (3) and (4) may be achieved by using non-identical lines. Thus, if a contradirectional coupler is designed using coupled lines, the port pairs (1,3) should be terminated with equal resistances, with a similar statement holding for the port pairs (2,4), while there may be

an impedance transformation between the port pairs (1,3) and (2,4). From (3.67), it is observed that the characteristics of the contradirectional coupler are independent of the transformation ratio ρ . Thus the characteristics \mathcal{D} , \mathcal{C} and ϕ_{CT} are unchanged when non-identical coupled lines are used to have an impedance transformation along with the contradirectional coupler action.

From (3.72c), it is observed that for these couplers, smooth transition in the electromagnetic coupling at $x = 0$, may be obtained by making $L_{12}(0)$ and $C_{12}(0)$ equal to zero, that is,

$$L_{10} F(0) = L_{20} G(0) \quad \dots (3.74a)$$

$$C_{10} G(0) = C_{20} F(0) \quad \dots (3.74b)$$

Now, since B_1 and C_1 have units of impedance and admittance respectively, the coupler characteristics (3.67) are unaffected with a change in r_1 ; hence the terminating resistances may be normalized with respect to $r_1 = 1$ ohm. For this condition, from (3.73d), the decoupled line parameters should have

$$L_{10} = C_{20} \quad , \quad L_{20} = C_{10} \quad \dots (3.75)$$

that is

$$L_1 = L_{10} F(x) \quad , \quad C_1 = C_{10} G(x) \quad \dots (3.76a)$$

$$L_2 = C_{10} G(x) \quad , \quad C_2 = L_{10} F(x) \quad \dots (3.76b)$$

For a coupler with terminations normalized to one ohm and having smooth transition at $x = 0$, it is required from (3.74) and (3.75) that

$$L_{10} = C_{10} = L_{20} = C_{20} \quad , \quad F(0) = G(0) \quad \dots (3.77)$$

From (3.76) and (3.77), the decoupled line distributions become

$$L_1 = L_{10} F(x) \quad , \quad C_1 = C_{10} G(x) \quad , \quad F(0) = G(0) \quad \dots (3.78a)$$

$$L_2 = L_{10} G(x) \quad , \quad C_2 = C_{10} F(x) \quad , \quad L_{10} = C_{10} \quad \dots (3.78b)$$

Also, when the terminations are normalized to one ohm, the coupler characteristics \mathcal{C} and ϕ_{CT} given by (3.67) reduce to

$$\mathcal{C} = 20 \log_{10} \left| \frac{(A_1 + D_1) + (B_1 + C_1)}{(A_1 - D_1) + (B_1 - C_1)} \right| \quad \dots (3.79a)$$

$$\phi_{CT} = \tan^{-1} \left[\frac{(B_1 - C_1)}{j(A_1 - D_1)} \right] \quad \dots (3.80)$$

In the next section, characteristics of such contradirectional couplers for which the decoupled lines are different, "basic lines with hyperbolic solutions" are investigated.

3.7 Coupled Line Contradirectional Couplers with Decoupled Basic Lines:

Swamy et al⁽⁹²⁾ have shown that all nonuniform lines having hyperbolic solutions are contained in five classes of lines and their duals. They have also shown that for any given class of NUTLs, there exists always an electrically equivalent "inverse line", for which the distributions of $L(x)$ and $C(x)$ are inversely proportional⁽⁹²⁾. Thus the study of networks containing NUTLs with hyperbolic solutions may be carried out in terms of their inverse lines, which they have called as the basic lines of the different classes of NUTLs. In

this section, the characteristics of contradirectional couplers for which the decoupled lines are different, basic lines with hyperbolic solutions will be investigated.

The chain parameters for the basic lines and their duals for the five classes, which have hyperbolic solutions, are known^(33,90). Tables 3.1 and 3.2 list the chain parameters of these lines with the basic lines and their duals as decoupled lines 1 and 2 respectively. Using these chain parameters in (3.79), the coupling \mathcal{C} for the different contradirectional couplers having basic lines with hyperbolic solutions as decoupled lines may be obtained. These are tabulated in Table 3.3. In order to determine the taper of the decoupled lines for a required value of coupling \mathcal{C} , the limiting value of \mathcal{C} , as $\beta l \rightarrow \infty$ is obtained from (3.80), and these are also tabulated in Table 3.3. Using these limiting values, the decoupled line tapers for various commonly used coupling values are calculated for the different contradirectional couplers and are given in Table 3.4. The coupling response of these couplers, with normalized frequency, are calculated and plotted by using digital computer CDC 3300. These plots are shown in Fig.3.3 to Fig.3.7. On examination of these plots, it is found that all these contradirectional couplers have high-pass coupling response; this is in conformity with the results of Yamamoto et al⁽³⁴⁾ for exponential lines. Further, to determine the couplers having best coupling response, the sensitivity of the coupling \mathcal{C} with respect to normalized frequency βl is calculated using

TABLE 3.1

CHAIN MATRICES OF THE BASIC LINES

Line Type and distributions	Chain Parameters
Exponential $L_1(x) = L_{10} e^{mx}$ $C_1(x) = C_{10} e^{-mx}$	$\frac{e^{-(m\ell/2)} [\cosh \gamma \ell + \frac{m}{2\gamma} \sinh \gamma \ell]}{Z_{10}(0) \Gamma} \sinh \gamma \ell$ $\frac{j Z_{10}(0) \beta e^{(m\ell/2)}}{e^{(m\ell/2)} [\cosh \gamma \ell - \frac{m}{2\gamma} \sinh \gamma \ell]}$
Algebraic $L_1 = L_{10} (1+mx)^{-2}$ $C_1 = C_{10} (1+mx)^2$	$\frac{j Z_{10}(0)}{(1+m\ell)} \frac{\sin \beta \ell}{[\cos \beta \ell + \frac{m}{\beta} \sin \beta \ell]}$
Trigonometric $L_1 = L_{10} \cos^{-2}(mx)$ $C_1 = C_{10} \cos^{+2}(mx)$	$\frac{j \cos m\ell \frac{\mu}{\beta} \sin \mu \ell + \cos \mu \ell}{Z_{10}(0) [\frac{\mu}{\beta} \sin \mu \ell - \frac{m}{\beta} \tan m\ell \cos \mu \ell]}$
Hyperbolic Sine Squared $L_1 = L_{10} \sinh^{-2}(mx)$ $C_1 = C_{10} \sinh^2(mx)$	$\frac{\sinh(m\ell+n) [\cos \gamma \ell - \frac{m}{\gamma} \coth(m\ell+n) \sin \gamma \ell]}{j \sinh n \sinh(m\ell+n) [\{\frac{\gamma}{\beta} + \frac{m^2}{\gamma \beta} \coth n \coth(m\ell+n)\} \sin \gamma \ell + \frac{m}{\beta} \cos \gamma \ell \{\coth(m\ell+n) - \coth n\}]}$
Hyperbolic Cosine Squared $L_1 = L_{10} \cosh^{-2}(mx)$ $C_1 = C_{10} \cosh^2(mx)$	$\frac{j \cosh m\ell [\cos \gamma \ell - \frac{m}{\gamma} \tanh m\ell \sin \gamma \ell]}{Z_{10}(0) [\frac{\gamma}{\beta} \sin \gamma \ell + \frac{m}{\beta} \cos \gamma \ell \tanh m\ell]}$

$$\gamma = \beta \sqrt{1 - (m^2/\beta^2)}, \quad \mu = \beta \sqrt{1 + (m^2/\beta^2)}, \quad \Gamma = \beta \sqrt{(m^2/4\beta^2) - 1}, \quad \beta = \omega \sqrt{L_{10} C_{10}}, \quad Z_{10}(0) = \sqrt{L_{10}(0) F(0)/C_{10}(0) G(0)}$$

$$n = 0.881$$

TABLE 3.2

CHAIN MATRIX OF DUAL OF BASIC LINES IN TABLE 3.1

Dual Line Type and distributions	Chain Parameters
Exponential $L_2 = L_{20} e^{-mx}$ $C_2 = C_{20} e^{mx}$	$\frac{j\beta Z_{20}(0) e^{-\frac{m\ell}{2}} \sinh \frac{\ell}{2}}{e^{-\frac{m\ell}{2}} \left[\cosh \frac{\ell}{2} + \frac{m}{2\Gamma} \sinh \frac{\ell}{2} \right]}$
Algebraic $L_2 = L_{20} (1+mx)^2$ $C_2 = C_{20} (1+mx)^{-2}$	$\frac{j\beta Z_{20}(0) \left[(1+m\ell + \frac{m^2}{\beta^2}) \sin \beta \ell - \frac{m^2 \ell}{\beta} \cos \beta \ell \right]}{(1+m\ell) \cos \beta \ell - \frac{m}{\beta} \sin \beta \ell}$
Trigonometric $L_2 = L_{20} \cos^2 mx$ $C_2 = C_{20} \cos^{-2} mx$	$\frac{j\beta Z_{20}(0) \cos m\ell \left[\frac{\mu}{\beta} \sin \mu \ell - \frac{m}{\beta} \tan m\ell \cos \mu \ell \right]}{\cos m\ell \left[\frac{m}{\mu} \tan m\ell \sin \mu \ell + \cos \mu \ell \right]}$
Hyperbolic Sine Squared $L_2 = L_{20} \sinh^2 (mx+n)$ $C_2 = C_{20} \sinh^{-2} (mx+n)$	$\frac{j\beta Z_{20}(0) \sinh n \sinh (m\ell+n) \left[\frac{\gamma}{\beta} + \frac{m^2}{\beta^2} \coth n \coth (m\ell+n) \sinh \gamma \ell + \frac{m}{\beta} \cosh \gamma \ell \{ \coth (m\ell+n) - \coth n \} \right]}{\sinh n \left[\cosh \gamma \ell - \frac{m}{\gamma} \coth (m\ell+n) \sinh \gamma \ell \right]}$
Hyperbolic cosine Squared $L_2 = L_{20} \cosh^2 mx$ $C_2 = C_{20} \cosh^{-2} mx$	$\frac{j\beta Z_{20}(0) \cosh m\ell \left[\frac{\gamma}{\beta} \sinh \gamma \ell + \frac{m}{\beta} \cosh \gamma \ell \tanh m\ell \right]}{\cosh m\ell \left[\cosh \gamma \ell - \frac{m}{\gamma} \tanh m\ell \sinh \gamma \ell \right]}$

$$Z_{20}(0) = \sqrt{L_{20} G(0) / C_{20} F(0)}$$

TABLE 3.3

Decoupled lines	e	Limiting value of e
Exponential	$20 \log_{10} \left \frac{j\beta \tanh \Gamma \ell - \frac{m}{2\Gamma} \tanh \frac{m\ell}{2} \tanh \Gamma \ell + 1}{j\beta \tanh \Gamma \ell \tanh \frac{m\ell}{2} - \tanh \frac{m\ell}{2} + \frac{m}{2\Gamma}} \right $	$20 \log_{10} \left \coth \frac{m\ell}{2} \right $
Algebraic	$20 \log_{10} \left \frac{1 + (1+m\ell)^2 + j \tanh \beta \ell \left[1 + (1+m\ell + \frac{m}{\beta^2})(1+m\ell) - \frac{m^2 \ell (1+m\ell)}{\beta \tanh \beta \ell} \right]}{1 - (1+m\ell)^2 + j \tanh \beta \ell \left[1 - (1+m\ell + \frac{m}{\beta^2})(1+m\ell) + \frac{m^2 \ell (1+m\ell)}{\beta \tanh \beta \ell} \right]} \right $	$20 \log_{10} \left \frac{1+(1+m\ell)^2}{1-(1+m\ell)^2} \right $
Trigonometric	$20 \log_{10} \left \frac{\frac{m}{\mu} + \frac{\cot m\ell}{\tan \mu \ell} + \frac{1}{\tan \mu \ell \sin m\ell \cos m\ell} + j \left[\frac{\beta}{\mu \cos m\ell \sin m\ell} + \frac{\mu \cot m\ell}{\beta} - \frac{m}{\beta \tan \mu \ell} \right]}{\frac{m}{\mu} + \frac{\cot m\ell}{\tan \mu \ell} - \frac{1}{\tan \mu \ell \sin m\ell \cos m\ell} + j \left[\frac{\beta}{\mu \cos m\ell \sin m\ell} - \frac{\mu \cot m\ell}{\beta} + \frac{m}{\beta \tan \mu \ell} \right]} \right $	$20 \log_{10} \left \frac{1+\cos^2 \frac{m\ell}{2}}{1-\cos^2 \frac{m\ell}{2}} \right $

(Cont'd)

Hyperbolic Sine Squared	$20 \log_{10} \left \frac{[1 + \sinh^2(m\ell + .881)] - \frac{m \tan \gamma \ell}{\tanh(m\ell + .881)} + j \left[\frac{\beta \tan \gamma \ell}{\gamma \sinh^2(m\ell + .881)} + \frac{\gamma \tanh \ell}{\beta} + \frac{m}{\beta} \coth(m\ell + .881) \right]}{[1 - \sinh^2(m\ell + .881)] - \frac{m \tan \gamma \ell}{\tanh(m\ell + .881)} + j \left[\frac{\beta \tanh \ell}{\gamma \sinh^2(m\ell + .881)} + \frac{\gamma \tanh \ell}{\beta} + \frac{m}{\beta} \coth(m\ell + .881) \right]} \right $	$20 \log_{10} \left \frac{1 + \sinh^2(m\ell + .881)}{1 - \sinh^2(m\ell + .881)} \right $
Hyperbolic Cosine Squared	$20 \log_{10} \left \frac{\coth \gamma \ell - \frac{m}{\gamma} \tanh \ell + \frac{\cot \gamma \ell}{\cosh^2 m \ell} + j \left[\frac{\beta}{\gamma \cosh^2 m \ell} + \frac{\gamma}{\beta} + \frac{m \tanh m \ell}{\beta \tan \gamma \ell} \right]}{\coth \gamma \ell - \frac{m}{\gamma} \tanh m \ell - \frac{\cot \gamma \ell}{\cosh^2 m \ell} + j \left[\frac{\beta}{\gamma \cosh^2 m \ell} - \frac{\gamma}{\beta} - \frac{m \tanh m \ell}{\beta \tan \gamma \ell} \right]} \right $	$20 \log_{10} \left \frac{1 + \cosh^2 m \ell}{1 - \cosh^2 m \ell} \right $

TABLE 3.4
DECOUPLED LINE TAPERS FOR VARIOUS COUPLINGS

Coupling	Taper mλ			
	Exponential	Algebraic	Trigonometric	Hyperbolic Sine Squared
20 db	0.21	-0.096	0.44	-0.07
10 db	0.6551	-0.028	0.77	-0.212
6 db	1.111	-0.424	0.955	-0.333
3 db	1.760	-0.578	1.145	-0.481
				0.455
				0.854
				1.148
				1.529

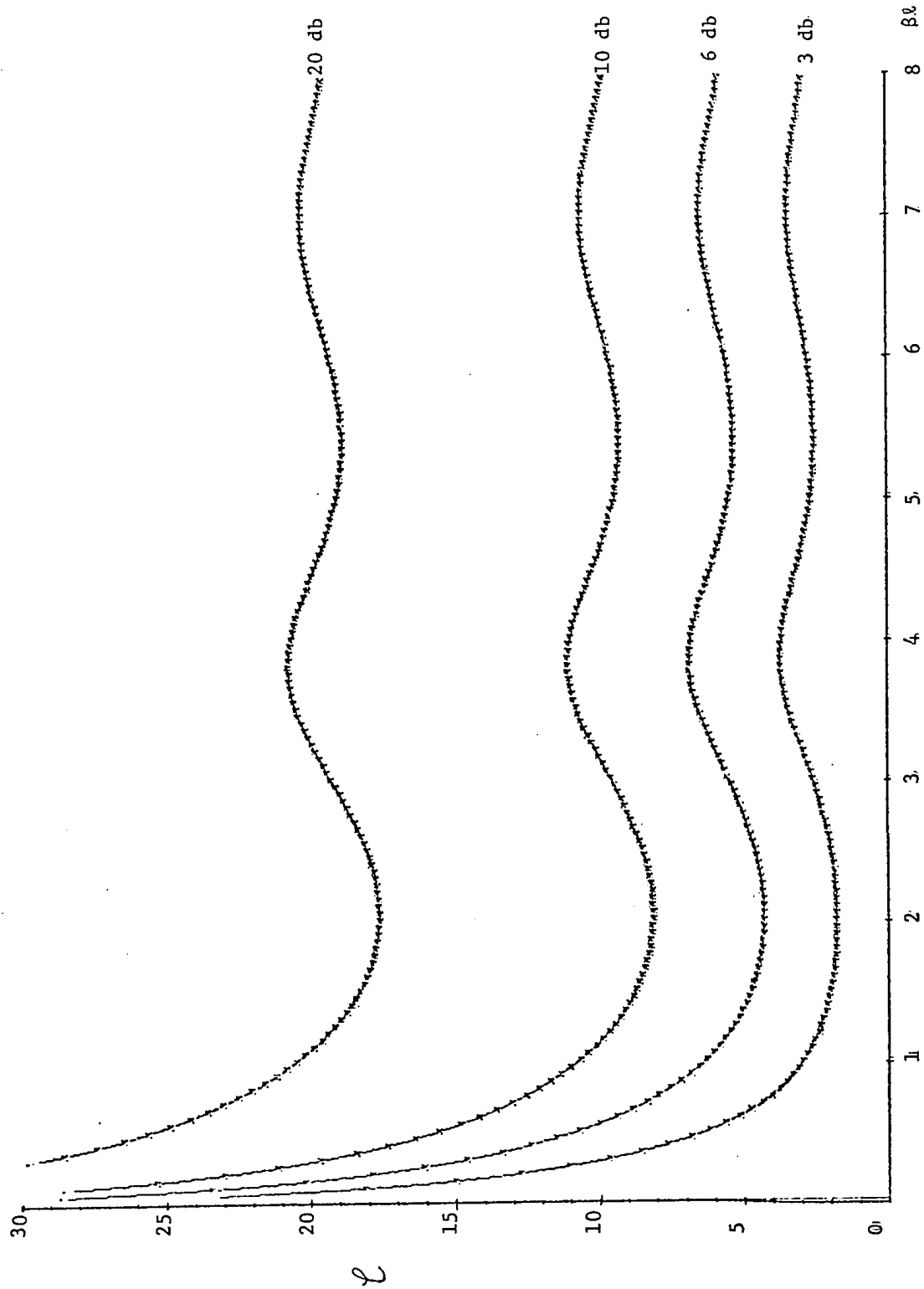


Fig. 3.3: Coupling Characteristics of CNUTL Contradirectional Couplers with ELs as Decoupled Lines

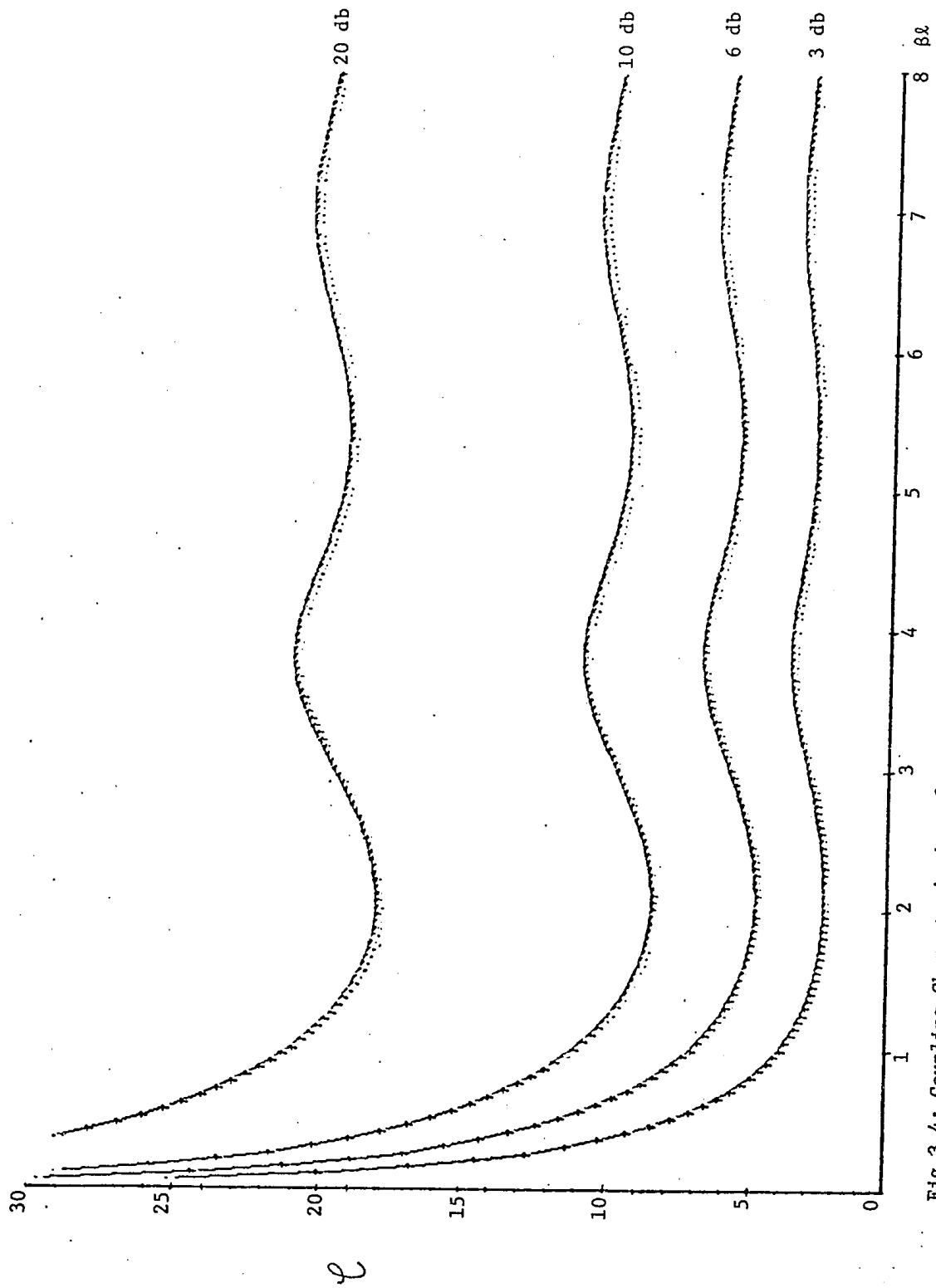


Fig.3.4: Coupling Characteristics of CNUYL Contradirectional Couplers with ALs as Decoupled Lines.

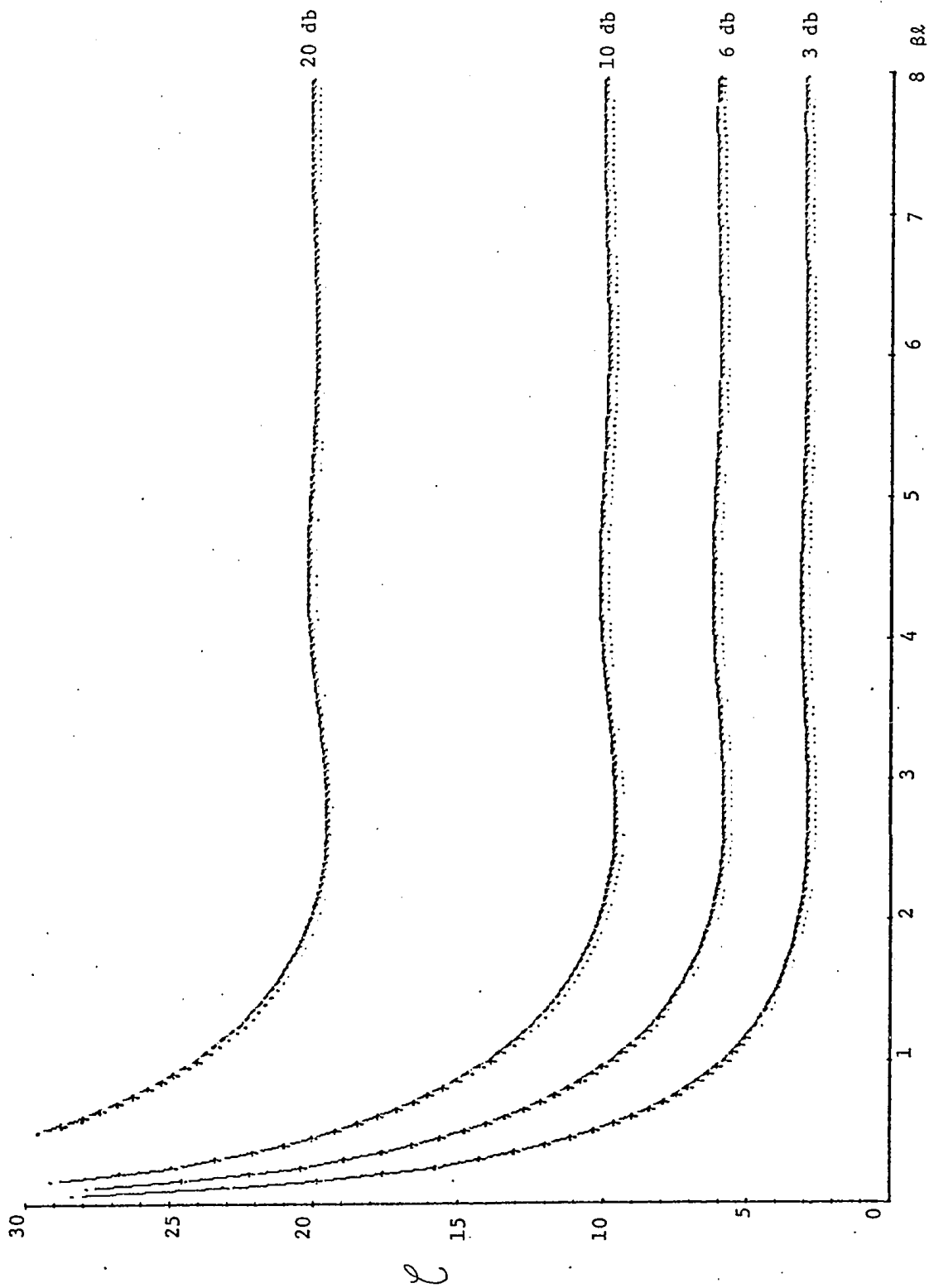


Fig. 3.5: Coupling Characteristics of CNUTL Contradirectional Couplers with TLs as Decoupled Lines

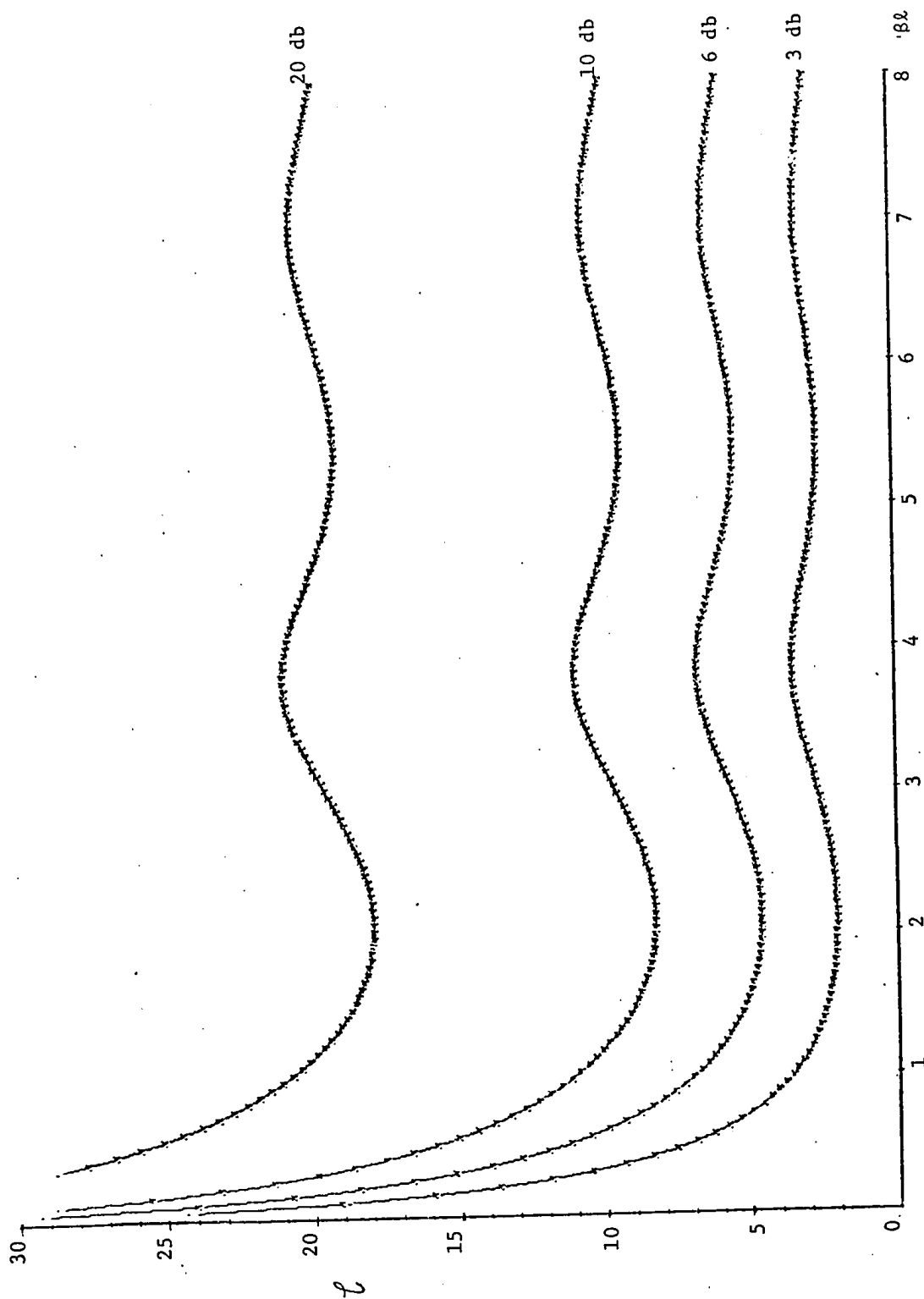


Fig. 3.6: Coupling Characteristics of CNUTL Contradirectional Couplers with HSSLs as Decoupled Lines

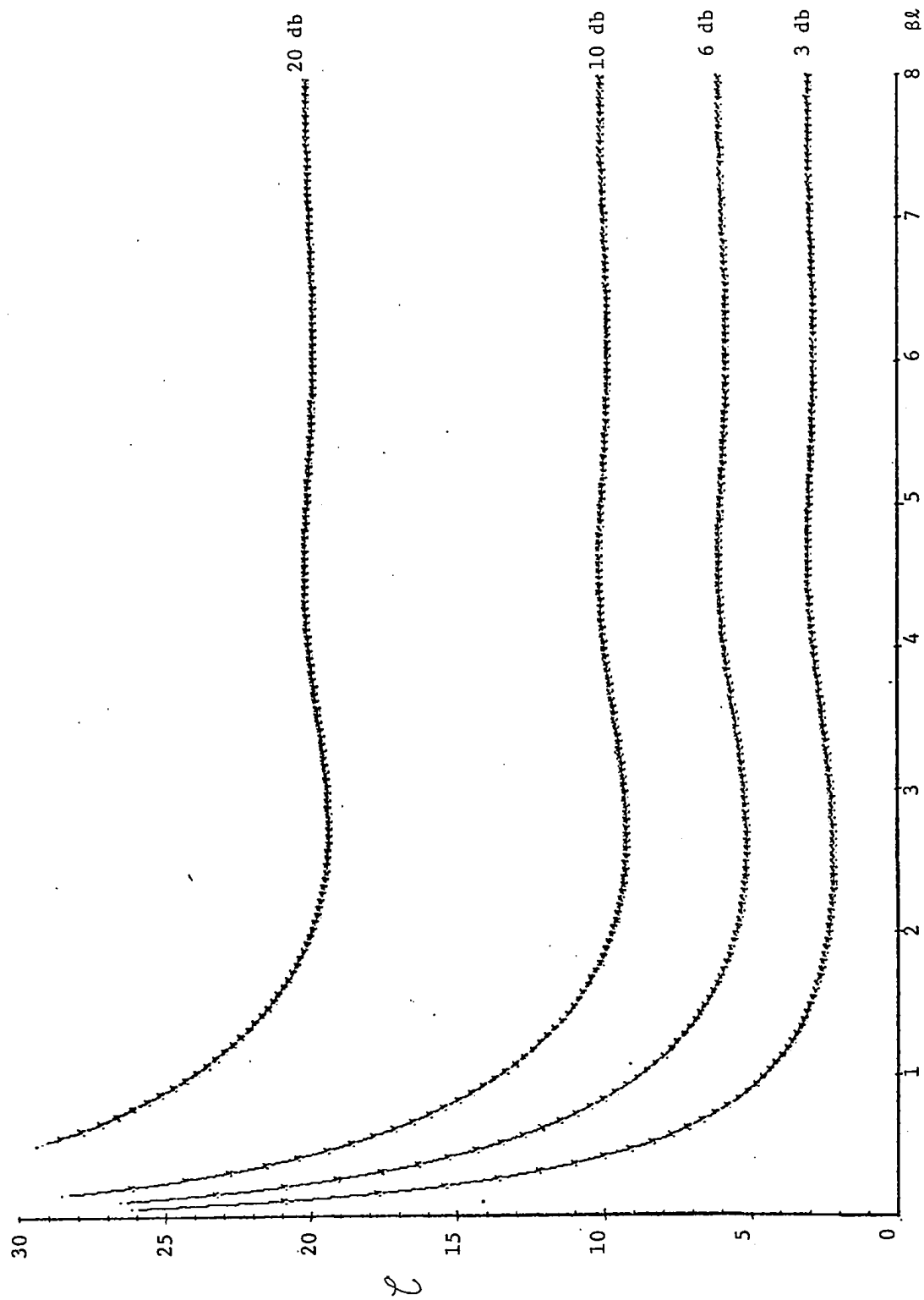


Fig. 3.7: Coupling Characteristics of CNUTL Contradirectional Couplers with HCSSLs as Decoupled Lines

$$S_{\beta\ell}^{\mathcal{C}} = \frac{\partial \mathcal{C}}{\partial \beta\ell} \cdot \frac{\beta\ell}{\mathcal{C}} \quad \dots (3.81)$$

The variation of sensitivity for different couplers are obtained as shown in Fig.3.8 to Fig.3.12. It is noticed from these Figures that for couplers with 'Trigonometric' or 'Hyperbolic cosine squared' lines as decoupled lines, the peak value of the sensitivity $S_{\beta\ell}^{\mathcal{C}}$ reduces with frequency. Thus the best coupling response is exhibited by the contradirectional coupler, for which the decoupled lines are trigonometric or hyperbolic cosine squared lines.

As the coupling responses of these couplers are functions of the taper $m\ell$, a variation in the taper due to fabrication or otherwise may affect the coupling \mathcal{C} . Hence, to investigate the effect of a variation in taper on the coupling, the sensitivity of coupling \mathcal{C} with respect to taper is obtained for each coupler using

$$S_{m\ell}^{\mathcal{C}} = \frac{\partial \mathcal{C}}{\partial m\ell} \cdot \frac{m\ell}{\mathcal{C}} \quad \dots (3.82)$$

Fig.3.13 to Fig.3.17 show the sensitivity $S_{m\ell}^{\mathcal{C}}$ as a function of the normalized frequency for the various contradirectional couplers. On an examination of these curves, it is found that for the coupler for which the hyperbolic cosine squared lines are decoupled lines, the coupling \mathcal{C} is less affected by variation in taper as compared to that of the coupler for which trigonometric lines are decoupled lines. Thus, the contradirectional coupler with hyperbolic cosine squared lines as decoupled lines have the best coupling response and is less affected due to taper variations. Even though the variation

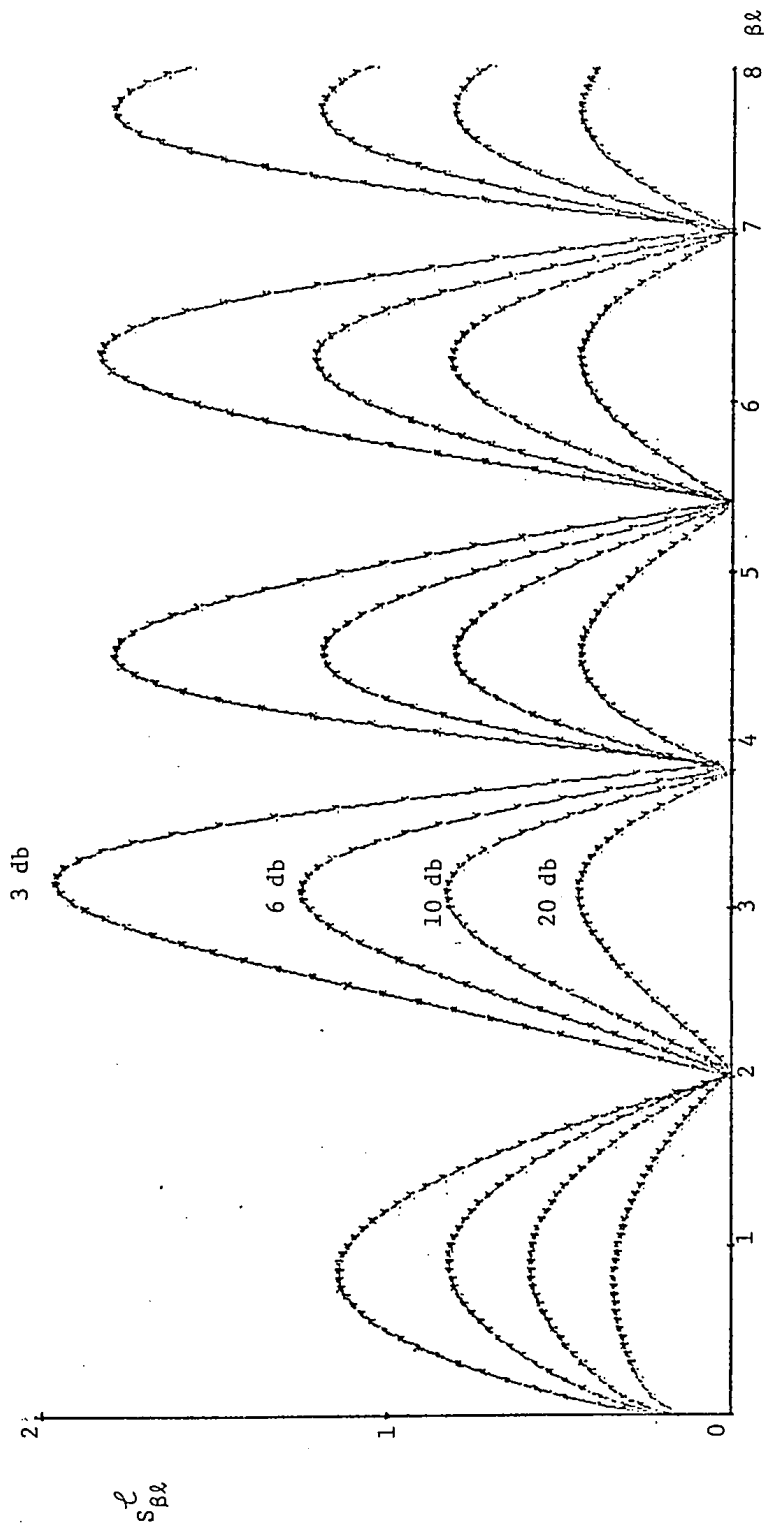


Fig. 3.8: $S_{\beta\alpha}^{\mathcal{L}}$ Characteristics of CNUTL Contradirectional Couplers with ELs as Decoupled Lines

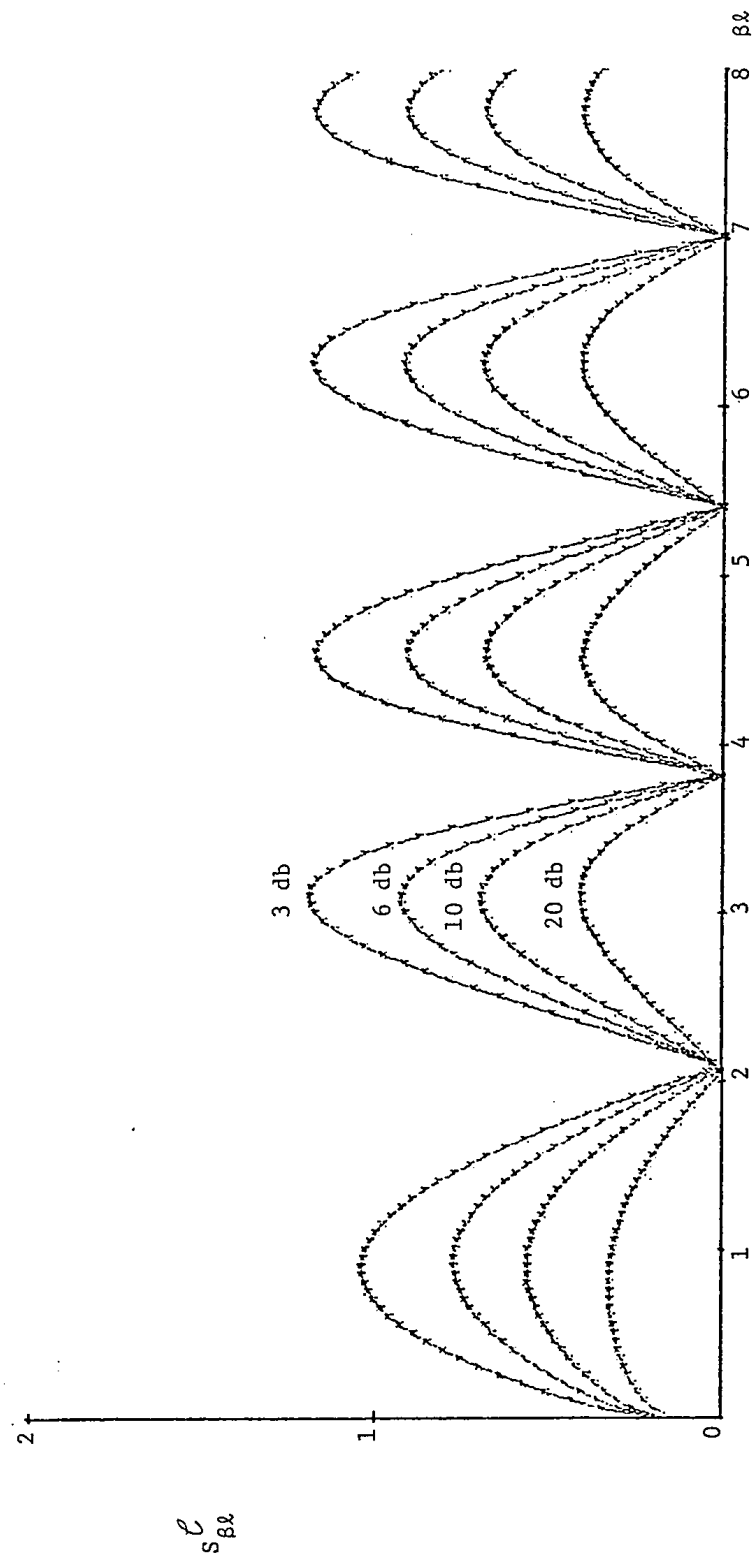


Fig. 3.9: $S_{\beta\lambda}$ Characteristics of CNUTL Contradirectional Couplers with ALs as Decoupled Lines

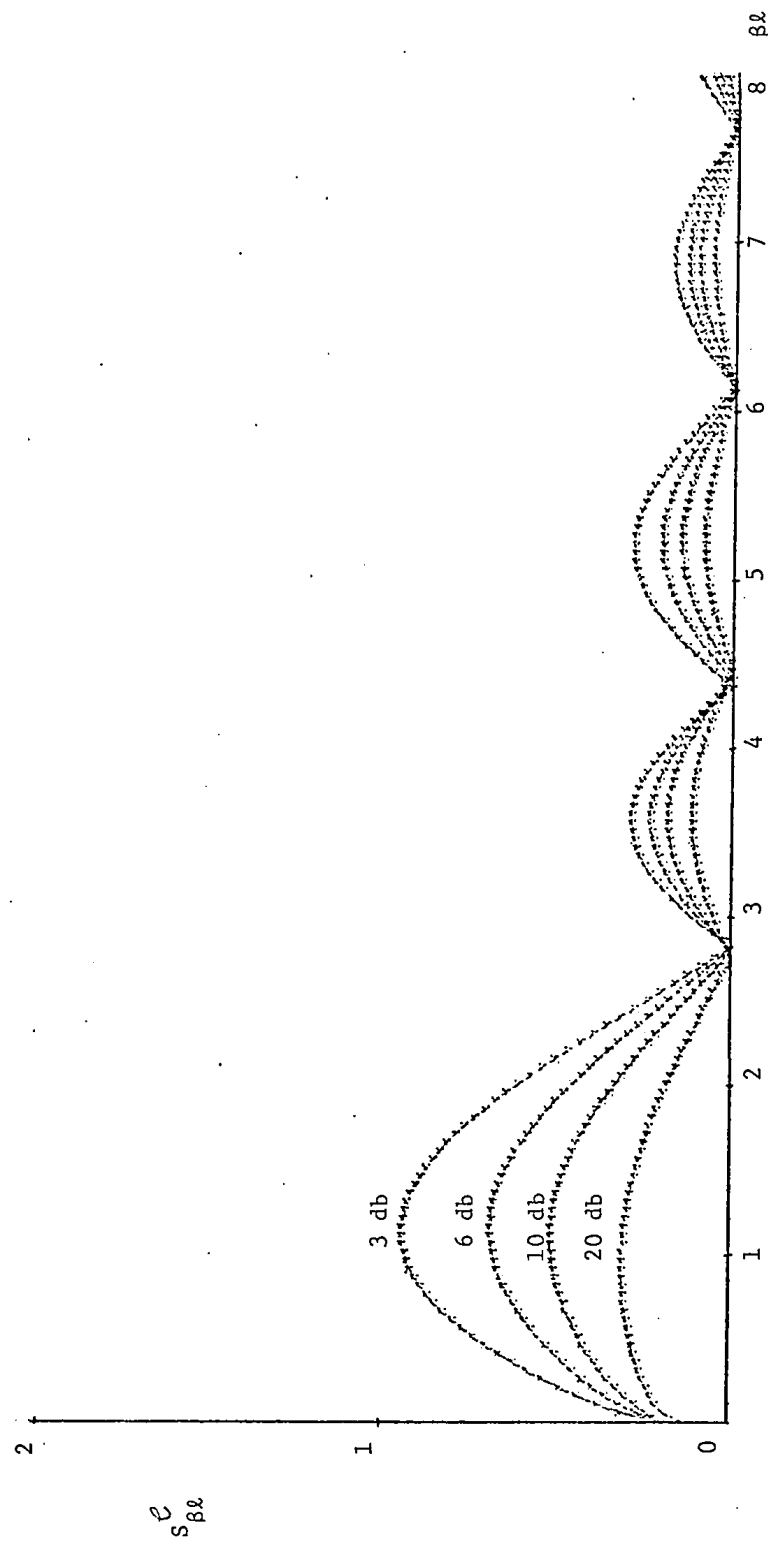


Fig. 3.10: $S_{\beta\ell}$ Characteristics of CNUTL Contradirectional Couplers with TLs as Decoupled Lines

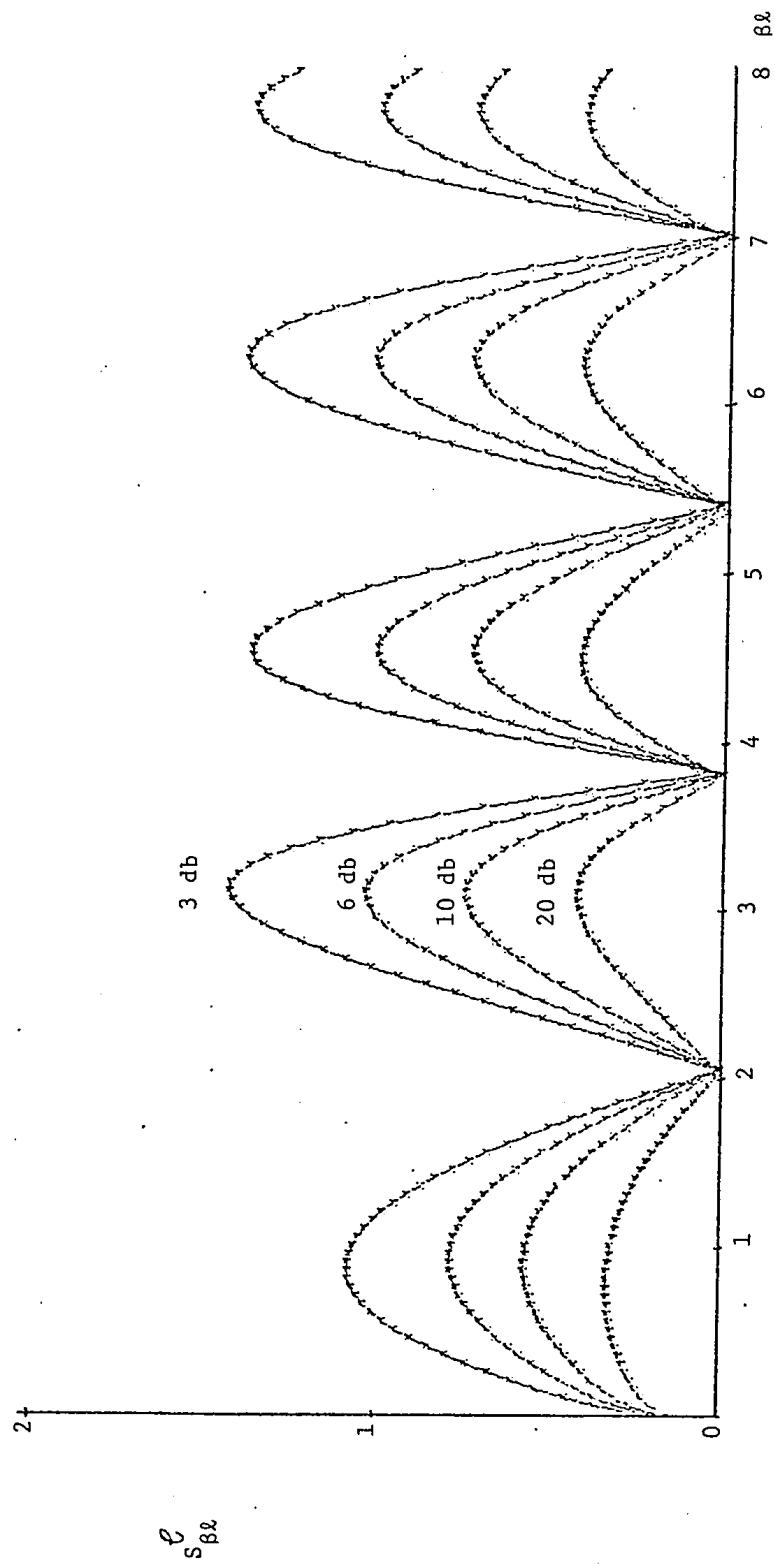


Fig. 3.11.5 $_{\beta\lambda}$ Characteristics of CNUTL Contradirectional Couplers with HSSLs as Decoupled Lines

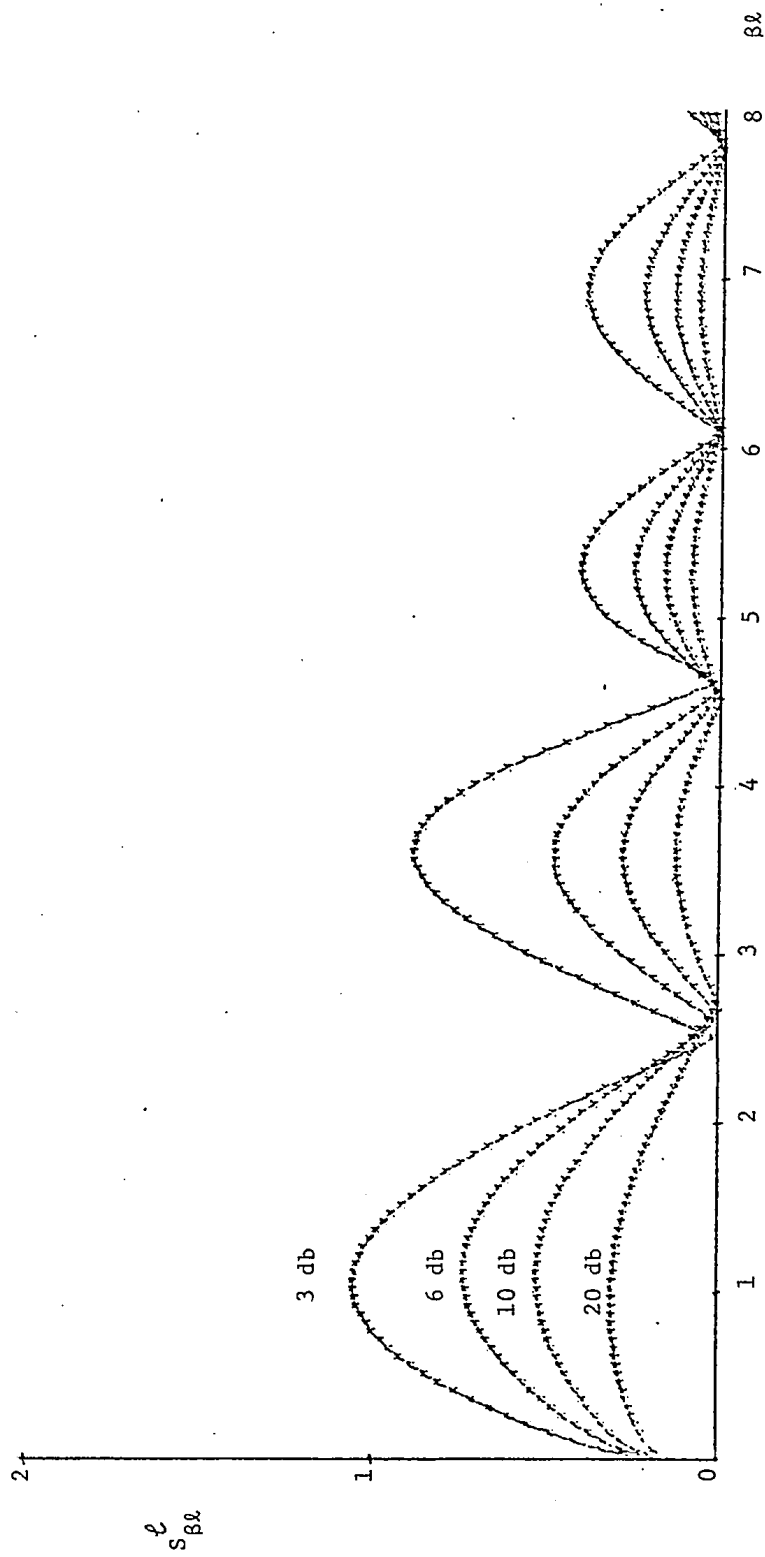


Fig. 3.12: $S_{\beta\lambda}^{\ell}$ Characteristics of CNUTL Contradirectional Couplers with HCSLs as Decoupled Lines

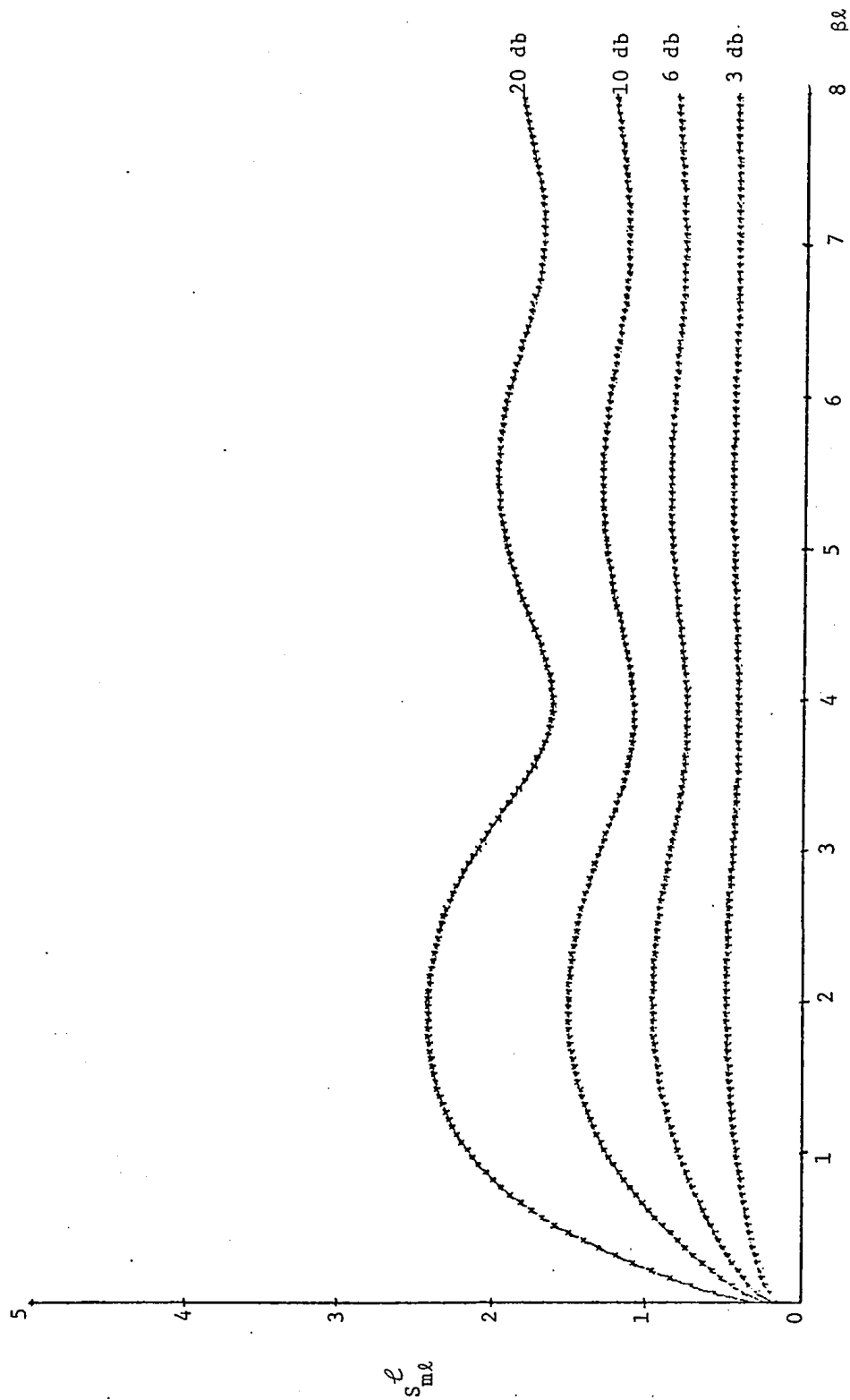


Fig. 3.13: $S_{m\lambda}^{\mathcal{L}}$ Characteristics of CNUIL Contradirectional Couplers with ELs as Decoupled Lines

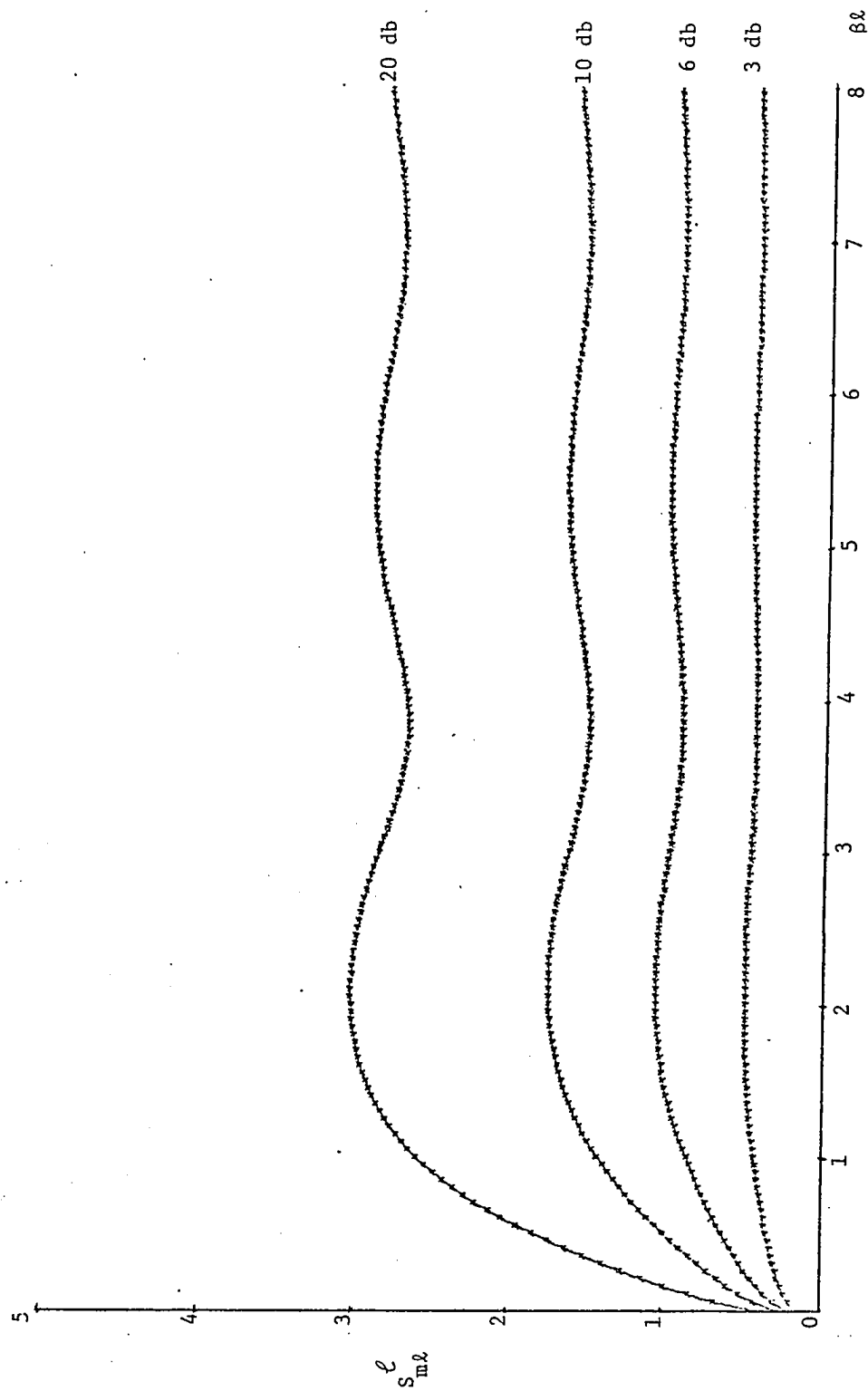


Fig. 3.14: $S_{m\ell}$ Characteristics of CNUTL Contradirectional Couplers with ALs as Decoupled Lines

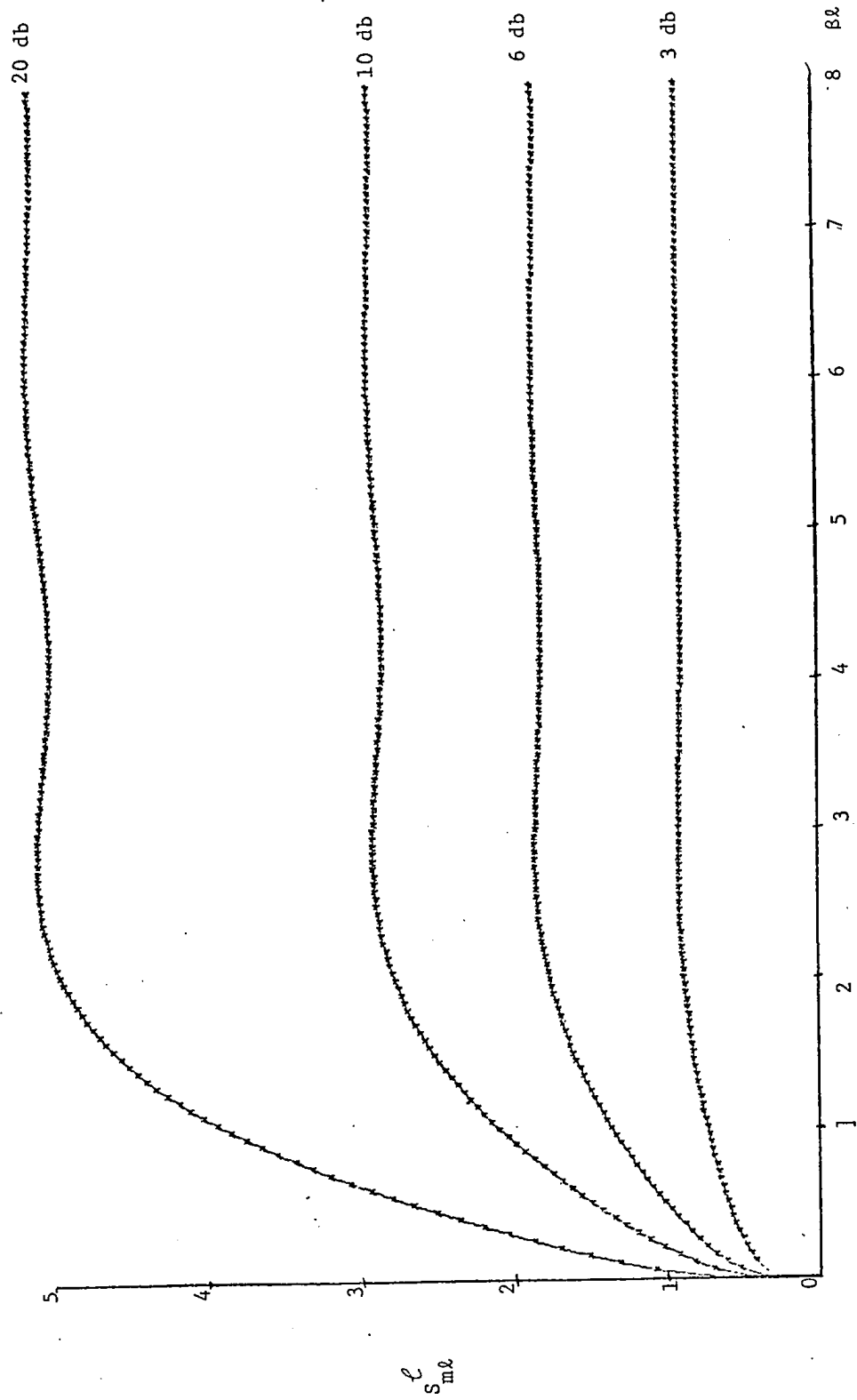


Fig. 3.15: $|S_{m\ell}|$ Characteristics of CNUTL Contradirectional Couplers with TLs as Decoupled Lines

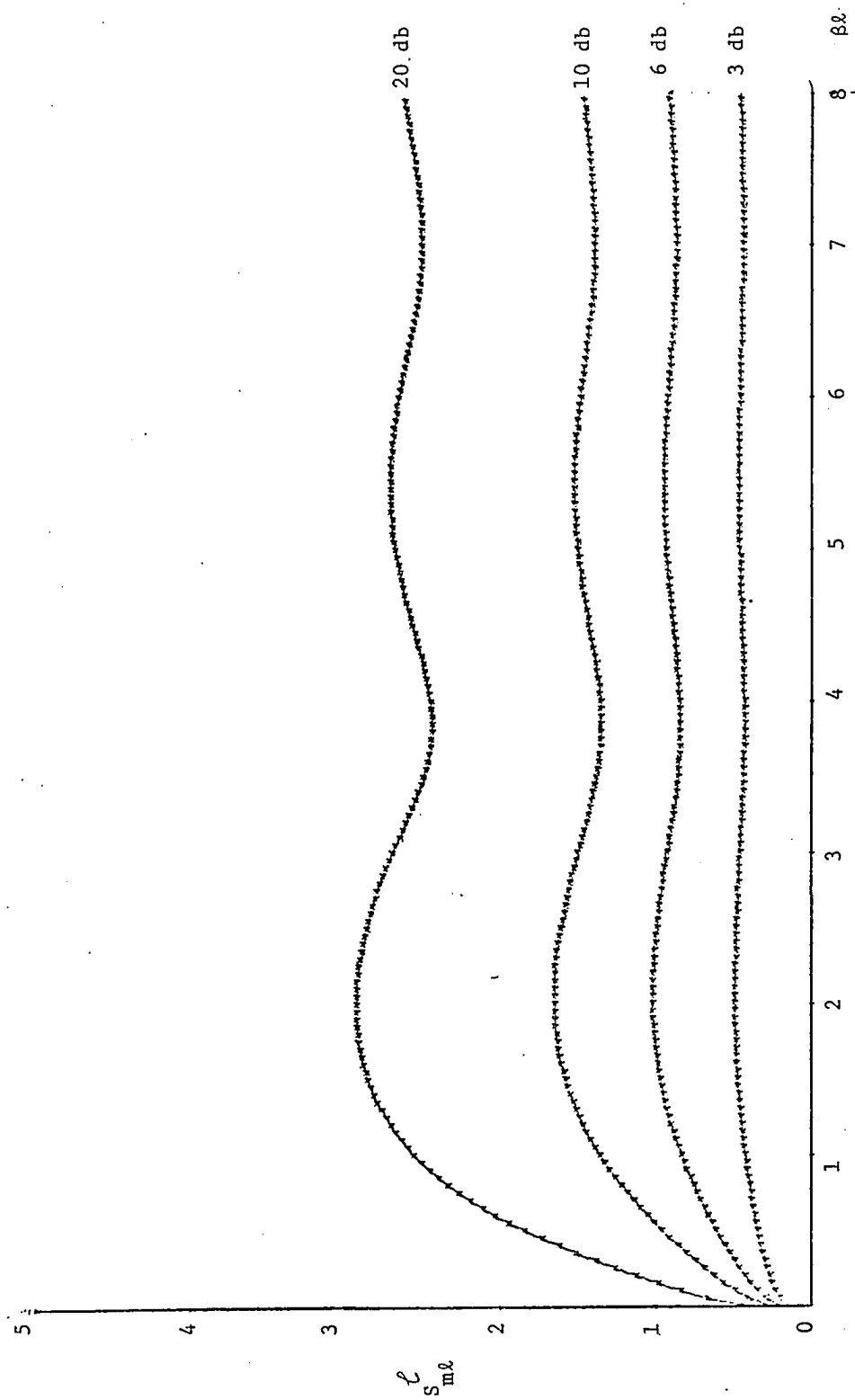


Fig. 3.16: $S_{m\ell}$ Characteristics of CNUTL Contradirectional Couplers with HSSLs as Decoupled Lines

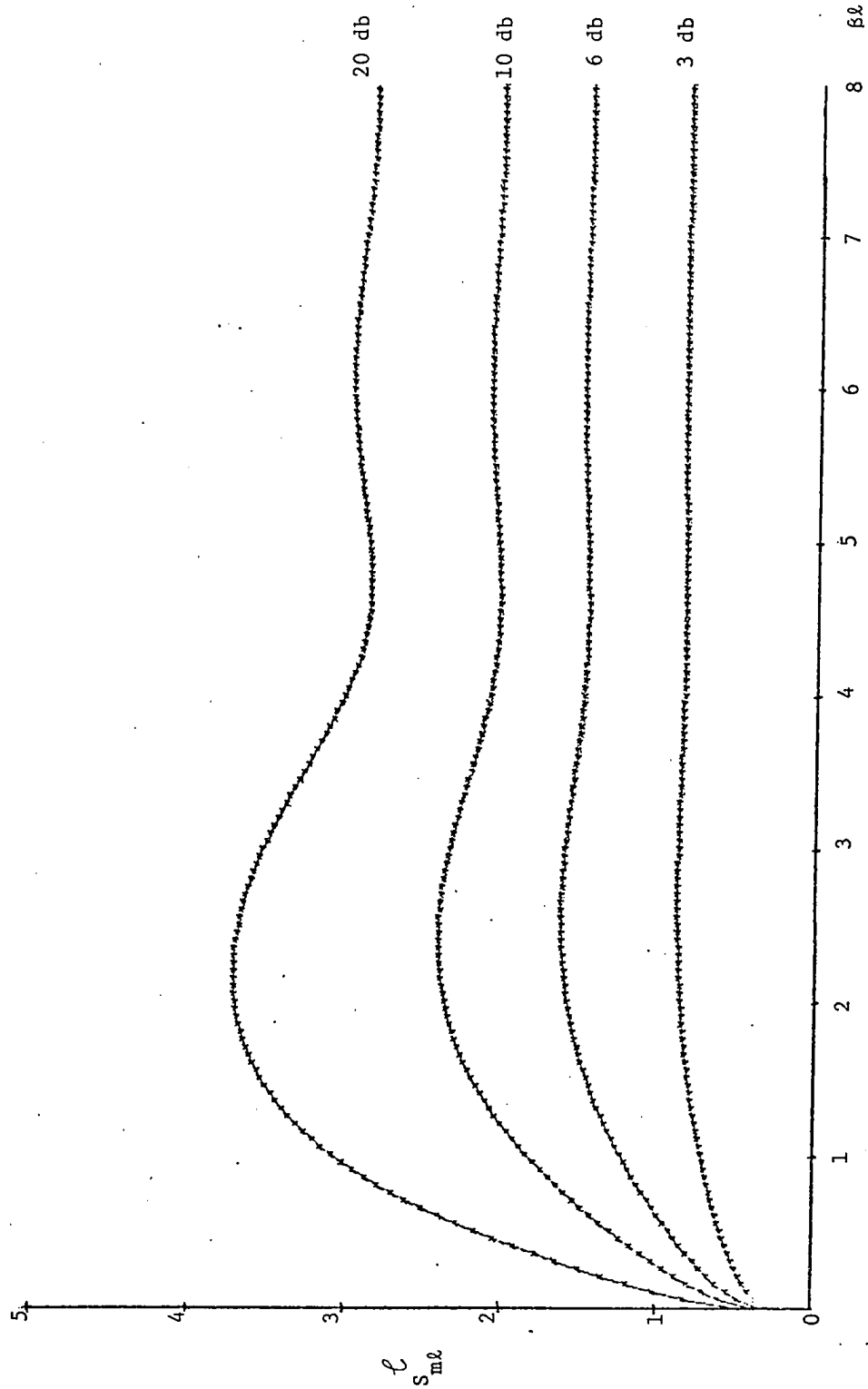


Fig. 3.17: S_{ml} Characteristics of CNUTL Contradirectional Couplers with HCSLs as Decoupled Lines

of the sensitivity $S_{m\ell}^e$ with frequency is least for the coupler with exponential decoupled lines, as shown in Fig.3.13, it suffers from the disadvantage of having a coupling response which is not smooth with respect to frequency.

From (3.68), it is observed that for all these couplers, the phase shift between coupled and transmitted signals changes with frequency, and hence cannot be maintained at a constant value at all frequencies. However, it is possible to obtain a phase shift of 0° , 90° or 180° over a band of frequencies, from coupled line contradirectional couplers by choosing properly the decoupled line distributions. Such couplers are considered in the following section.

3.8 Coupled Line Contradirectional Couplers with 0, 90 or 180 degrees phase shift:

The phase shift between the coupled and transmitted signals of the tapered line contradirectional coupler may be made with either 90° , or zero or 180° over a band of frequencies. These two couplers are considered next.

Case A:

Consider the contradirectional coupler for which the decoupled lines are symmetric lossless lines formed out of lossless NUTLs with back to back or front to front connections⁽³³⁾. For the case when the decoupled lines are the symmetric lines with back to back connection and its dual, the distributions are of the form

$$L_1 = L_{10} F(x) \quad , \quad C_1 = C_{10} G(x) \quad 0 \leq x \leq \ell \quad \dots (3.83a)$$

$$L_1 = L_{10} F(2\ell-x) \quad , \quad C_1 = C_{10} G(2\ell-x) \quad 0 \leq x \leq 2\ell \quad \dots (3.83b)$$

and

$$L_2 = L_{20} G(x) \quad , \quad C_2 = C_{20} F(x) \quad 0 \leq x \leq \ell \quad \dots (3.83c)$$

$$L_2 = L_{20} G(2\ell-x) \quad , \quad C_2 = C_{20} F(2\ell-x) \quad \ell \leq x \leq 2\ell \quad \dots (2.83d)$$

For the case when the decoupled lines are the symmetric lines with front to front connection and its dual, the distributions are of the form

$$L_1 = L_{10} F(\ell-x) \quad , \quad C_1 = C_{10} G(\ell-x) \quad 0 \leq x \leq \ell \quad \dots (3.84a)$$

$$L_1 = L_{10} F(x-\ell) \quad , \quad C_1 = C_{10} G(x-\ell) \quad \ell \leq x \leq 2\ell \quad \dots (3.84b)$$

and

$$L_2 = L_{20} G(\ell-x) \quad , \quad C_2 = C_{20} F(\ell-x) \quad 0 \leq x \leq \ell \quad \dots (3.84c)$$

$$L_2 = L_{20} G(x-\ell) \quad , \quad C_2 = C_{20} F(x-\ell) \quad \ell \leq x \leq 2\ell \quad \dots (3.84d)$$

The coupled line parameters of these couplers may be obtained from (2.19), (2.83) and (2.84).

For the above decoupled lines, the chain parameters may be expressed in terms of those of the nonuniform transmission line given by (3.83a), and then used to obtain the scattering matrix of the corresponding contradirectional couplers. These are tabulated in Table 3.5, where \hat{A} , \hat{B} , \hat{C} and \hat{D} refer to the chain parameters of NUTL (3.8a). The characteristics \mathcal{D} , \mathcal{C} and ϕ_{CT} may now be obtained using scattering matrix and (3.69); these are also shown in Table 3.5. It is noted

TABLE 3.5
SCATTERING MATRIX AND CHARACTERISTICS OF COUPLERS WITH DECOUPLED SYMMETRIC NUTLS

Connection	Scattering Matrix	Characteristics
Back to back configuration	$\frac{1}{\begin{bmatrix} \hat{A}\hat{D}+\hat{B}\hat{C}+ \\ \hat{A}\hat{B}+\hat{C}\hat{D}r_1 \end{bmatrix} r_1} \begin{bmatrix} 0 & \frac{\hat{A}\hat{B}}{r_1} - \hat{C}\hat{D}r_1 & 1 & 0 \\ \frac{\hat{A}\hat{B}}{r_1} - \hat{C}\hat{D}r_1 & 0 & 0 & 1 \\ 1 & 0 & \hat{C}\hat{D}r_1 - \frac{\hat{A}\hat{B}}{r_1} & 0 \\ 0 & 1 & \hat{C}\hat{D}r_1 - \frac{\hat{A}\hat{B}}{r_1} & 0 \end{bmatrix}$	$\mathcal{P} = \infty$ $\mathcal{L} = 20 \log_{10} \left \frac{\frac{\hat{A}\hat{B}}{r_1} + \hat{C}\hat{D}r_1 + \hat{A}\hat{D} + \hat{B}\hat{C}}{\frac{\hat{A}\hat{B}}{r_1} + \hat{C}\hat{D}r_1} \right $ $\phi_{CT} = \pm 90^\circ$
Front to front configuration	$\frac{1}{\begin{bmatrix} \hat{A}\hat{D}+\hat{B}\hat{C}+ \\ \hat{B}\hat{D}+\hat{A}\hat{C}r_1 \end{bmatrix} r_1} \begin{bmatrix} 0 & \frac{\hat{B}\hat{D}}{r_1} - \hat{A}\hat{C}r_1 & 1 & 0 \\ \frac{\hat{B}\hat{D}}{r_1} - \hat{A}\hat{C}r_1 & 0 & 0 & 1 \\ 1 & 0 & \hat{A}\hat{C}r_1 - \frac{\hat{B}\hat{D}}{r_1} & 0 \\ 0 & 1 & \hat{A}\hat{C}r_1 - \frac{\hat{B}\hat{D}}{r_1} & 0 \end{bmatrix}$	$\mathcal{P} = \infty$ $\mathcal{L} = 20 \log_{10} \left \frac{\frac{\hat{B}\hat{D}}{r_1} + \hat{A}\hat{C}r_1 + \hat{A}\hat{D} + \hat{B}\hat{C}}{\frac{\hat{B}\hat{D}}{r_1} - \hat{A}\hat{C}r_1} \right $ $\phi = \pm 90^\circ$

from this Table that these couplers have a phase shift of 90° between coupled and transmitted signals at all frequencies. It may be shown that these couplers provide smooth transition in electromagnetic coupling at both the ends, when the decoupled line distributions are such that

$$L_1(0) = L_2(0) \quad , \quad C_1(0) = C_2(0) \quad \dots (3.85)$$

The coupling responses with frequency for these two types of contradirectional couplers, when the line (3.83a) is an exponential line $[F(x) = e^{mx}]$, are obtained as shown in Figs. 3.18 and 3.19.

It is noticed from these plots that both the couplers have band pass coupling responses.

Case B:

Consider two nonuniform transmission lines for which the distributions are of the form

$$L_1 = L_{10} F(x) \quad , \quad C_1 = C_{10} G(x) \quad \dots (3.86a)$$

and

$$L_2 = L_{10} F(\ell-x) \quad , \quad C_2 = C_{10} G(\ell-x) \quad \dots (3.86b)$$

with

$$F(x) = G(\ell-x) \quad \dots (3.86c)$$

It is noted that line 2 is nothing but line 1 seen from the other end. For these lines, it may be shown that their chain parameters are related as

$$A_1 = D_2 \quad , \quad D_1 = A_2 \quad , \quad B_1 = B_2 \quad , \quad C_1 = C_2 \quad \dots (3.87)$$

Also, if the lines 1 and 2 correspond to the decoupled lines of a contra-

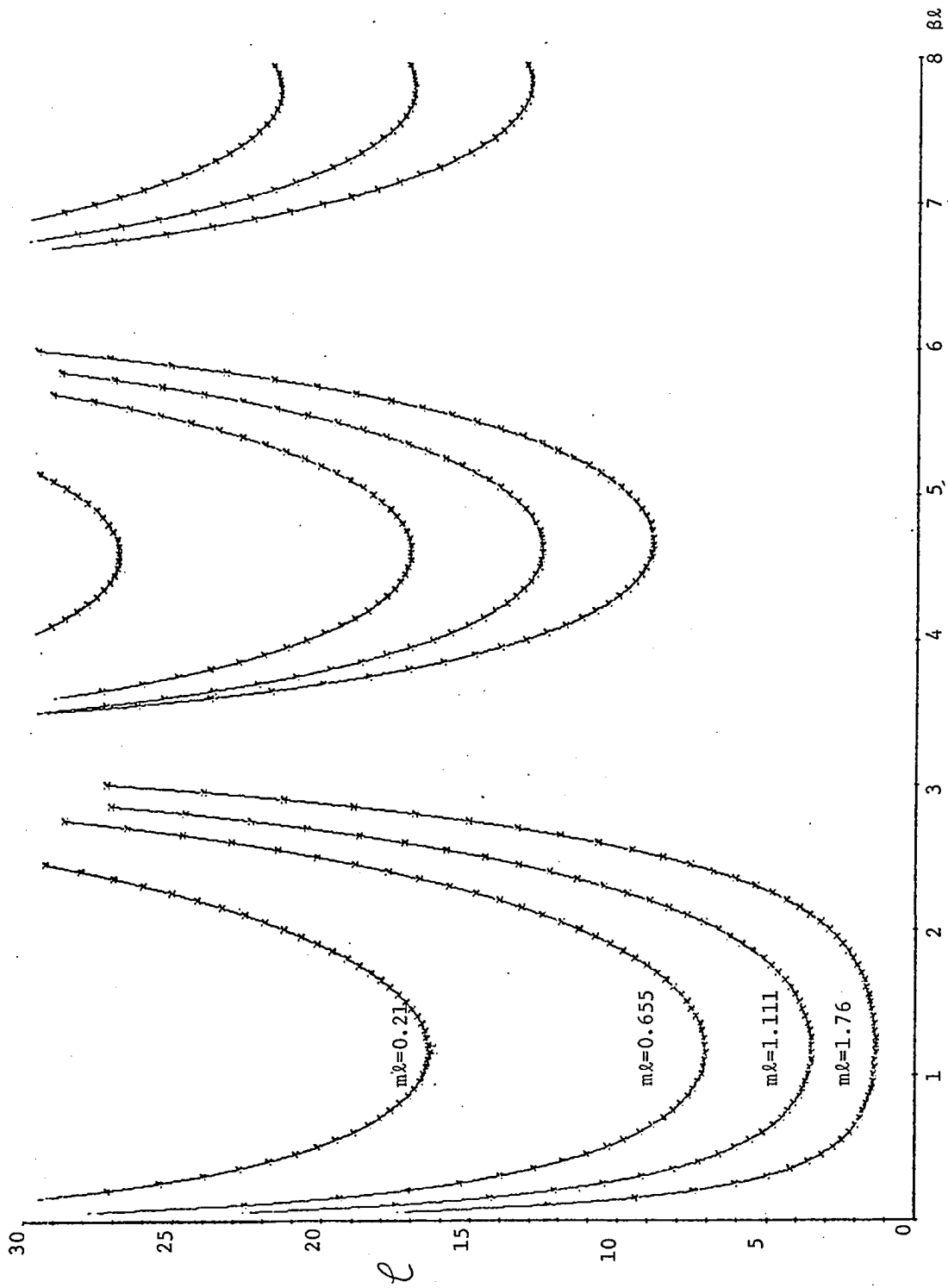


Fig. 3.18: Coupling Characteristics of CNUTL Contradirectional Couplers with Symmetric ELs in Back to Back Configuration as Decoupled Lines.

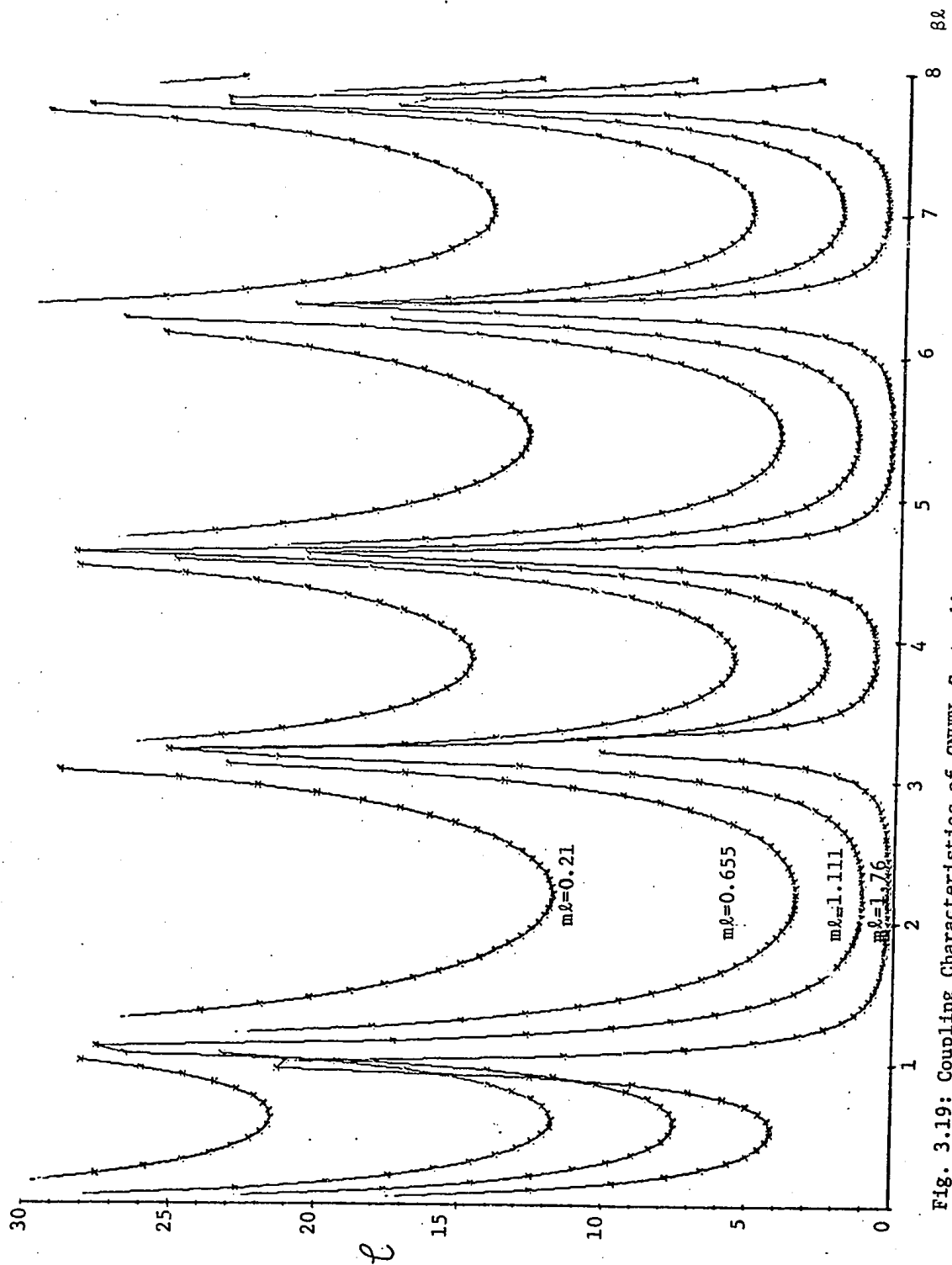


Fig. 3.19: Coupling Characteristics of CNUTL Contradirectional Couplers with Symmetric ELs in Front to Front Configuration as Decoupled Lines

directional coupler, then from (3.63)

$$A_1 = D_2, \quad D_1 = A_2, \quad B_1 = r_1^2 C_2, \quad B_2 = r_1^2 C_1 \quad \dots (3.88)$$

where r_1 is independent of frequency. Thus, if a contradirectional coupler is to be obtained using (3.86) as decoupled lines, then these lines should have their B and C parameters such that

$$r_1 = \sqrt{(B_1/C_1)} = \sqrt{(B_2/C_2)} \quad \dots (3.89)$$

is independent of frequency. For such a contradirectional coupler, the scattering matrix may be obtained using (3.66) and (3.87) as

$$[S] = \frac{1}{(A_1 + D_1) + \frac{2B_1}{r_1}} \begin{bmatrix} 0 & (A_1 - D_1) & 2 & 0 \\ (A_1 - D_1) & 0 & 0 & 2 \\ 2 & 0 & 0 & (D_1 - A_1) \\ 0 & 2 & (D_1 - A_1) & 0 \end{bmatrix} \quad \dots (3.90)$$

Also the coupler characteristics from (3.90) are

$$\mathcal{D} = \infty \quad \dots (3.91a)$$

$$\mathcal{L} = 20 \log_{10} \left| \frac{(A_1 + D_1) + \frac{2B_1}{r_1}}{(A_1 - D_1)} \right| \quad \dots (3.91b)$$

$$\phi_{CT} = 0^\circ \text{ or } 180^\circ \quad \dots (3.91c)$$

where

$$\mathcal{D} = \text{Coupler directivity} = 20 \log_{10} \left| \frac{S_{21}}{S_{41}} \right| \quad \dots (3.92a)$$

$$\mathcal{C} = \text{Coupling of coupler} = 20 \log_{10} \left| \frac{1}{S_{21}} \right| \quad \dots (3.92b)$$

ϕ_{CT} = Phase shift between coupled and transmitted signals

$$= \angle \frac{S_{21}}{S_{31}} \quad \dots (3.92c)$$

From (2.19) and (3.86), the parameters of the coupler are

$$L_{11} = \frac{L_{10}}{2}[F(x) + F(\ell-x)] \quad , \quad L_{22} = \rho^2 L_{11} \quad \dots (3.93a)$$

$$C_{11} = \frac{C_{10}}{2\rho}[(\rho+1)F(\ell-x) + (\rho-1)F(x)] \quad , \quad C_{22} = \frac{C_{10}}{2\rho}[(\rho+1)F(\ell-x) - (\rho-1)F(x)] \quad \dots (3.93b)$$

$$L_{12} = \frac{L_{10}\rho}{2}[F(x) - F(\ell-x)] \quad , \quad C_{12} = \frac{C_{10}}{2\rho}[F(x) - F(\ell-x)] \quad \dots (3.93c)$$

$$r_1 = r_3 = \sqrt{(B_1/C_1)} \quad , \quad r_2 = r_4 = \rho^2 r_1 \quad \dots (3.93d)$$

where r_1 is independent of frequency. From (3.91), it is found that these couplers have a phase difference of 0° or 180° between the coupled and transmitted signals at all frequencies. Further, the coupler characteristics \mathcal{D} , \mathcal{C} and ϕ_{CT} are independent of ρ , hence are same for couplers using identical or non-identical coupled lines. Again, in this case, it is possible to obtain smooth transition in electromagnetic coupling at $x = 0$ if the decoupled line distributions have

$$F(0) = F(\ell) \quad \dots (3.94)$$

An example of a coupler with a 0° or 180° phase difference, is

the one which has exponential decoupled lines, that is, have distributions:

$$L_1 = L_{10} e^{mx}, \quad C_1 = C_{10} e^{-m(\ell-x)} = C_{10}' e^{-mx} \quad \dots (3.95a)$$

$$L_2 = L_{10} e^{m(\ell-x)}, \quad C_2 = C_{10} e^{mx} = C_{10}' e^{-m(\ell-x)} \quad \dots (3.95b)$$

with

$$r_1 = \sqrt{L_{10}/C_{10}} e^{\frac{m\ell}{2}} = \sqrt{L_{10}/C_{10}'} \quad \dots (3.95c)$$

The coupling response of this coupler is shown in Fig.3.20, where the terminations are normalized to one ohm. It should be pointed out, however, that this coupler cannot have smooth transition, since (3.94) is not satisfied.

3.9 Conclusions:

Using the theory developed in Chapter 2, the tapered coupled line codirectional and contradirectional couplers with and without impedance transformation have been analyzed. It is shown that a coupled line four-port behaves as a codirectional coupler if each of the corresponding decoupled lines are 'Proportional lines', while it behaves as contradirectional coupler when the decoupled lines are 'Dual lines'. The conditions required to be satisfied by the decoupled lines for obtaining smooth electromagnetic transition at one of the ends of a codirectional or contradirectional coupler are obtained. Using non-identical coupled lines, it is possible to obtain codirectional and contradirectional coupler action along with an impedance transformation

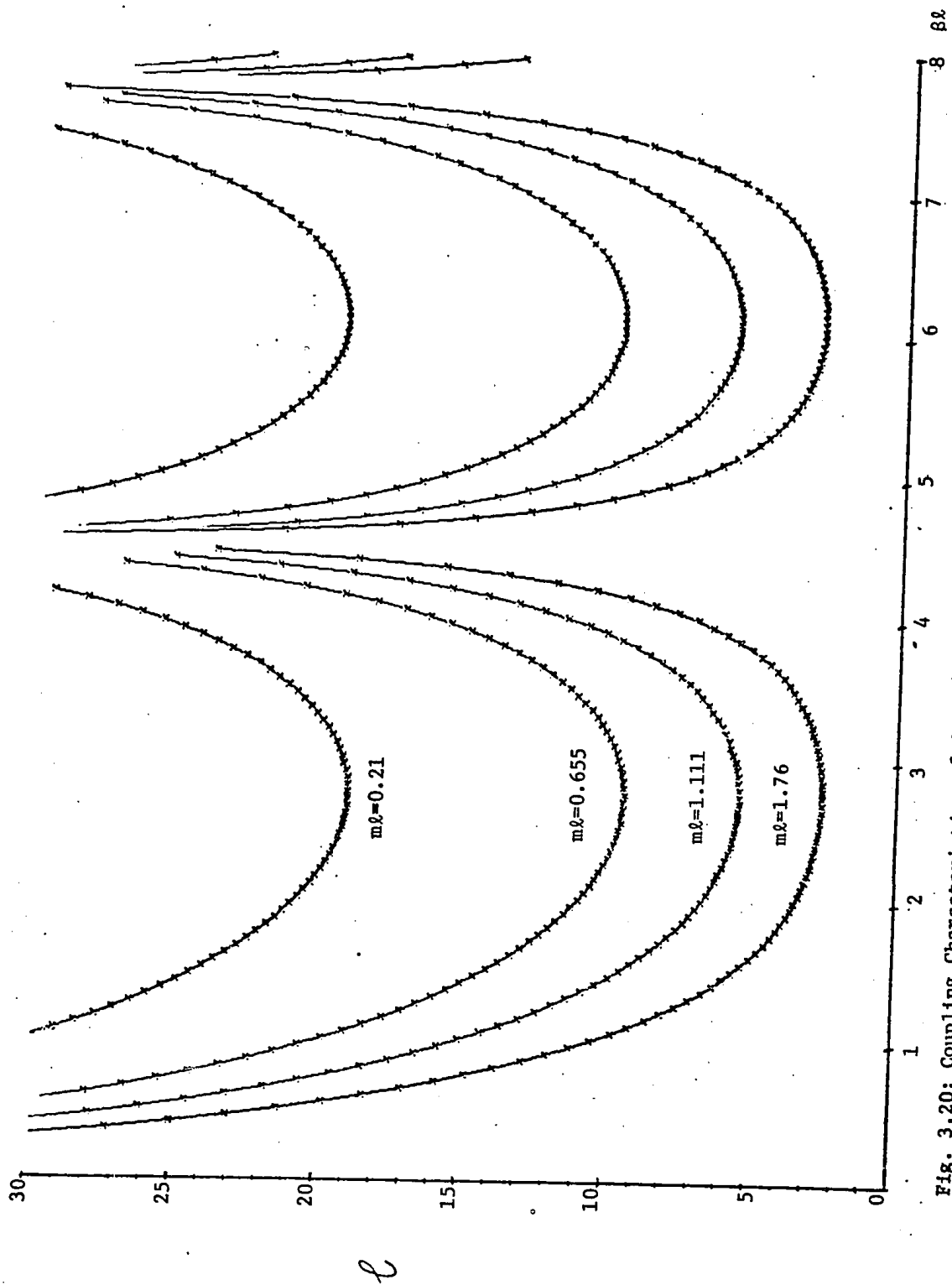


Fig. 3.20: Coupling Characteristics of CNUTL Contradirectional Couplers with 0° or 180° Phase Shifts over a Frequency Band

between certain ports. It is found that the coupling response of codirectional coupler is periodic in nature with frequency, while the phase shift between coupled and transmitted signals changes linearly with frequency. Coupling characteristics for contradirectional couplers using 'Basic lines' with hyperbolic solutions as decoupled lines, are investigated. Further, the sensitivities of coupling for these couplers with taper are obtained to study the effect of variation in taper on coupling. It has been found that contradirectional couplers, with hyperbolic cosine squared lines as decoupled lines, have the best coupling response which is least affected due to taper variations. Finally, tapered coupled line contradirectional couplers with a zero, or 90° or 180° phase shift between coupled and transmitted signals, are obtained.

CHAPTER 4

COUPLED NONUNIFORM TRANSMISSION LINE FOLDED ALL-PASS NETWORKS

4.1 Introduction:

As mentioned in Chapter 1, lossless CUTLs have been used as folded all-pass networks. These networks are often employed as phase or delay components in microwave systems. Recently, Yamamoto⁽³⁴⁾ et al have employed CNUTLs with exponential taper as folded all-pass networks. These have advantages of small size, in addition to providing control on phase characteristics and peak time delay through their tapers.

In this Chapter, CNUTLs are considered as two-port networks and various folded all-pass networks are analyzed using the theory of Chapter 2.. The decoupled line distributions for these networks to exhibit all-pass action are determined. The phase and delay characteristics of different CNUTL folded all-pass networks are investigated, when the decoupled lines are basic lines with hyperbolic solutions.

4.2 Lossless All-pass Two-Port Networks:

Consider a lossless two-port network shown in Fig. 4.1. If this network is matched at both ports (1) and (2), then

$$S_{11} = S_{22} = 0 \quad \dots (4.1)$$

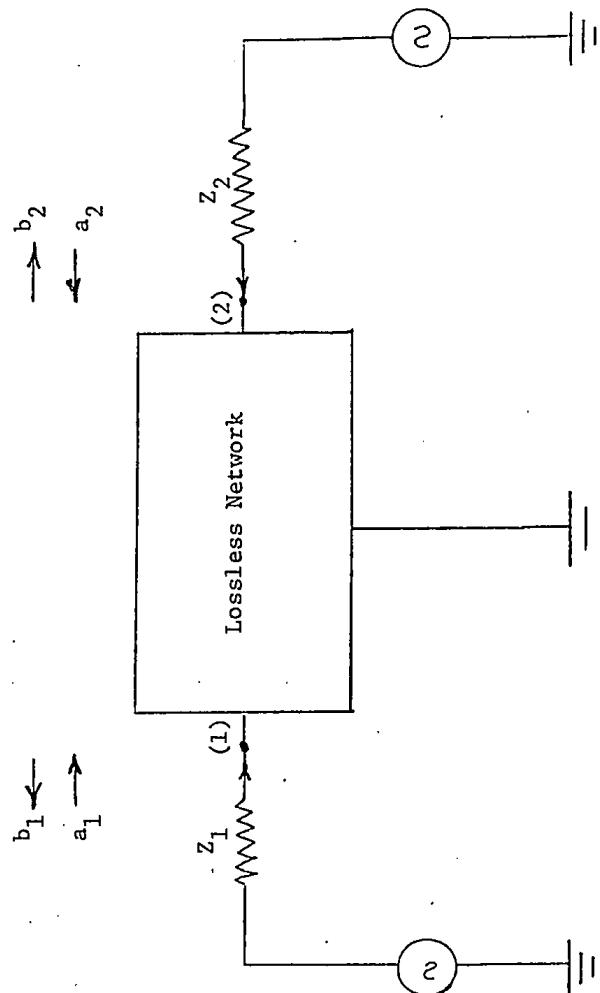


Fig. 4.1: A Lossless Terminated Two-port Network

However, for two-port lossless networks

$$\sum_{k=1}^2 |S_{ik}(j\omega)|^2 = 1, \quad i = 1, 2 \quad \dots (4.2)$$

Thus, from (4.1) and (4.2), whether the network is reciprocal or not

$$|S_{12}(j\omega)| = |S_{21}(j\omega)| = 1 \quad \dots (4.3)$$

which are the conditions for an all-pass network. Thus, if a lossless two-port network is matched at all frequencies at both the ports, then it exhibits all-pass action.

It is known that a two-port network with chain parameters A, B, C and D, may be matched at its two-ports, if the terminating impedances are⁽⁹⁴⁾

$$Z_1 = \sqrt{AB/CD}, \quad Z_2 = \sqrt{BD/AC} \quad \dots (4.4)$$

at all frequencies. With these terminations, the scattering matrix of the two-port may be written as

$$[S] = \begin{bmatrix} 0 & \sqrt{AD} - \sqrt{BC} \\ \frac{1}{\sqrt{AD} + \sqrt{BC}} & 0 \end{bmatrix} \quad \dots (4.5a)$$

$$\text{where} \quad |\sqrt{AD} - \sqrt{BC}| = |\sqrt{AD} + \sqrt{BC}| = 1 \quad \dots (4.5b)$$

from Eq. (4.2).

If the network is reciprocal, Eqs. (4.5a) and (4.5b) reduce to

$$[S] = \begin{bmatrix} 0 & \sqrt{AD} - \sqrt{BC} \\ \sqrt{AD} - \sqrt{BC} & 0 \end{bmatrix} \quad \dots (4.6a)$$

with

$$|\sqrt{AD} - \sqrt{BC}| = 1 \quad \dots (4.6b)$$

If the network is in addition symmetric, then it behaves as an all-pass network, when the terminating impedances are

$$Z_1 = Z_2 = \sqrt{B/C} \quad \dots (4.7a)$$

at all frequencies; further, its scattering matrix is

$$[S] = \begin{bmatrix} 0 & A - \sqrt{A^2 - 1} \\ A - \sqrt{A^2 - 1} & 0 \end{bmatrix} \quad \dots (4.7b)$$

with

$$|A - \sqrt{A^2 - 1}| = 1 \quad \dots (4.7c)$$

4.3 Coupled Lines as Folded All-pass Networks:

The four-port network formed by a pair of coupled lines may be converted into a two-port network by properly terminating the ports. Some of these two-ports may be used as folded all-pass networks, which exhibit different phase and delay characteristics depending upon the terminating conditions. Analysis of these networks will be performed by applying the decoupling theory described in Chapter II. Consider the four-port network of Fig.4.2 to be consisting of a pair of identical coupled lossless lines of length l . From (2.31), the voltages and

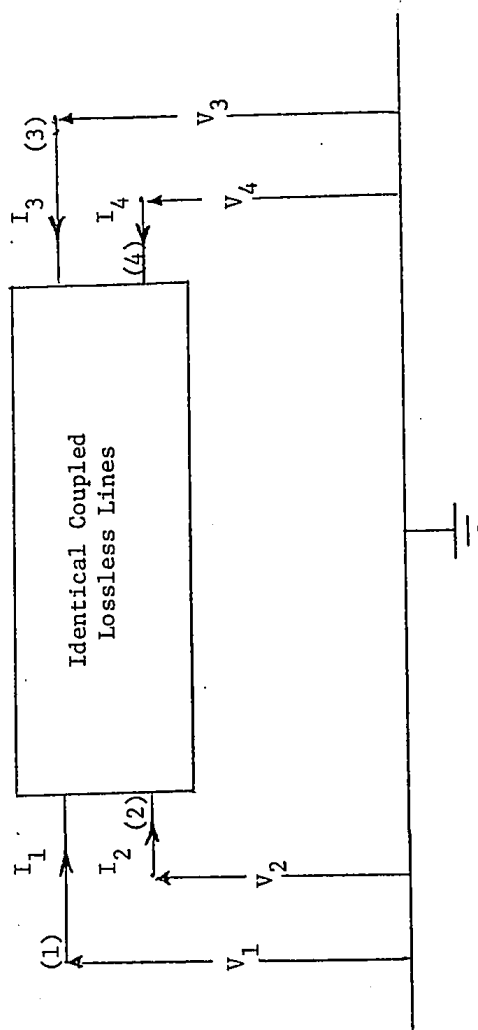


Fig. 4.2: A Coupled Line Four-port Network

currents at various ports of the coupled line four-port network are related through the decoupled line chain parameters as

$$\begin{bmatrix} V_1 \\ V_2 \\ I_1 \\ I_2 \end{bmatrix} = \frac{1}{2} \begin{bmatrix} A_1 + A_2 & A_1 - A_2 & B_1 + B_2 & B_1 - B_2 \\ A_1 - A_2 & A_1 + A_2 & B_1 - B_2 & B_1 + B_2 \\ C_1 + C_2 & C_1 - C_2 & D_1 + D_2 & D_1 - D_2 \\ C_1 - C_2 & C_1 + C_2 & D_1 - D_2 & D_1 + D_2 \end{bmatrix} \begin{bmatrix} V_3 \\ V_4 \\ -I_3 \\ -I_4 \end{bmatrix} \quad \dots (4.8)$$

where A_1, B_1, C_1, D_1 and A_2, B_2, C_2, D_2 are respectively the chain parameters of the decoupled lines 1 and 2. Different folded all-pass networks are next obtained by converting the coupled line network into a two-port network.

Type I: The four-port network of Fig.4.2 is first converted into a two-port network either by shorting ports (3) and (4) or Ports (1) and (2); these will be considered as Types IA and IB respectively as shown in Fig.4.3. For these networks, the voltage at the shorting ports are equal and in phase, while the currents are equal in magnitude but opposite in phase.

Type IA: The network is excited at port (1) with the output taken at port (2), and the shorted port voltages and currents are related as

$$V_3 = V_4, \quad I_3 = -I_4 \quad \dots (4.9)$$

Substituting (4.9) in (4.8),

$$V_1 = A_1 V_3 - B_2 I_3 \quad \dots (4.10a)$$

$$V_2 = A_1 V_3 + B_2 I_3 \quad \dots (4.10b)$$

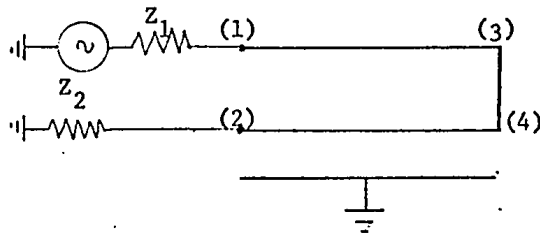
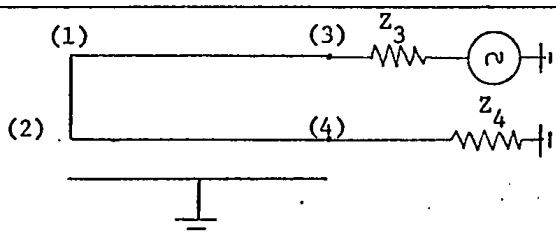
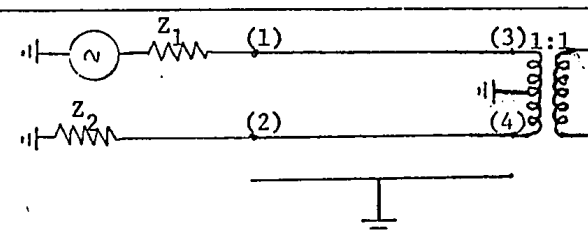
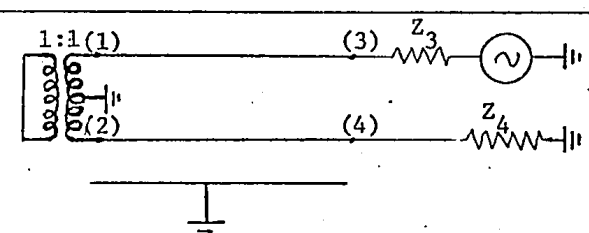
Type	Folded All-pass Network
IA	 $Z_1 = Z_2, \quad V_3 = V_4, \quad I_3 = -I_4$
IB	 $V_1 = V_2, \quad I_1 = -I_2, \quad Z_3 = Z_4$
IIA	 $V_3 = -V_4, \quad I_3 = I_4, \quad Z_1 = Z_2$
IIB	 $Z_3 = Z_4, \quad V_1 = -V_2, \quad I_1 = I_2$

Fig. 4.3: CNU TL Folded All-pass Networks of Types I and II

$$I_1 = C_1 V_3 - D_2 I_3 \quad \dots (4.10c)$$

$$I_2 = C_1 V_3 + D_2 I_3 \quad \dots (4.10d)$$

Eliminating V_3 and I_3 from the above equations,

$$\begin{bmatrix} V_1 \\ I_1 \end{bmatrix} = \frac{1}{A_1 D_2 - B_2 C_1} \begin{bmatrix} A_1 D_2 + B_2 C_1 & 2A_1 B_2 \\ 2C_1 D_2 & A_1 D_2 + B_2 C_1 \end{bmatrix} \begin{bmatrix} V_2 \\ -I_2 \end{bmatrix} \quad \dots (4.11)$$

Hence, the chain matrix parameters of this transformed two-port in terms of the decoupled line chain parameters are

$$A = D = \frac{A_1 D_2 + B_2 C_1}{(A_1 D_2 - B_2 C_1)}, \quad \dots (4.12a)$$

$$B = \frac{2A_1 B_2}{(A_1 D_2 - B_2 C_1)}, \quad C = \frac{2C_1 D_2}{(A_1 D_2 - B_2 C_1)} \quad \dots (4.12b)$$

From (4.12), it may be noted that this two-port is reciprocal and symmetric. Hence, from (4.7), this network will exhibit all-pass action provided

$$Z_1 = Z_2 = \sqrt{A_1 B_2 / C_1 D_2} \quad \dots (4.13)$$

at all frequencies; further, its scattering matrix will be

$$[S] = \begin{bmatrix} 0 & \frac{\sqrt{A_1 D_2} - \sqrt{B_2 C_1}}{\sqrt{A_1 D_2} + \sqrt{B_2 C_1}} \\ \frac{\sqrt{A_1 D_2} - \sqrt{B_2 C_1}}{\sqrt{A_1 D_2} + \sqrt{B_2 C_1}} & 0 \end{bmatrix} \quad \dots (4.14a)$$

$$\text{where } \left| \frac{\sqrt{A_1 D_2} - \sqrt{B_2 C_1}}{\sqrt{A_1 D_2} + \sqrt{B_2 C_1}} \right| = 1 \quad \dots (4.14b)$$

Also, the phase shift between the output and input ports is

$$\phi_{21} = \angle \left[\frac{\sqrt{A_1 D_2} - \sqrt{B_2 C_1}}{\sqrt{A_1 D_2} + \sqrt{B_2 C_1}} \right] \quad \dots (4.15)$$

It is to be noted that since the network is reciprocal and symmetric, the characteristics of this network are unchanged when the excitation is changed from port (1) to (2); that is $\phi_{21} = \phi_{12}$.

It can be shown (See Appendix C, Theorem 2) that for the lossless lines having dual distributions

$$L_1 = L_{10} F(x) \quad \dots (4.16a)$$

$$C_1 = C_{10} G(x) \quad 0 \leq x \leq \ell \quad \dots (4.16b)$$

and

$$L_2 = L_{20} G(x) \quad \dots (4.16c)$$

$$C_2 = C_{20} F(x) \quad 0 \leq x \leq \ell \quad \dots (4.16d)$$

with

$$L_{10} C_{10} = L_{20} C_{20} \quad \dots (4.16e)$$

the chain parameters are related as

$$A_1 = D_2, \quad D_1 = A_2 \quad \dots (4.17a)$$

$$B_1 = r^2 C_2, \quad C_1 = B_2 / r^2 \quad \dots (4.17b)$$

where

$$r = \sqrt{L_{10}/C_{20}} = \sqrt{L_{20}/C_{10}} \quad \dots (4.17c)$$

If the two decoupled lines for Type IA network are chosen to be the dual lines given by (4.16), then it is clear from (4.13) and (4.17) that Type IA network will behave as an all-pass network provided

$$Z_1 = Z_2 = \sqrt{L_{10}/C_{20}} \quad \dots (4.18)$$

Thus the Type IA network having dual lines as decoupled lines will behave as an all-pass network provided the the two terminating impedances Z_1 and Z_2 are purely resistive, say r_1 and r_2 , and

$$r_1 = r_2 = \sqrt{L_{10}/C_{20}} = \sqrt{L_{20}/C_{10}} \quad \dots (4.19)$$

Furhter, from (4.7) and (4.12), its scattering matrix is

$$[S] = \begin{bmatrix} 0 & \frac{A_1 - C_1 r_1}{A_1 + C_1 r_1} \\ \frac{A_1 - C_1 r_1}{A_1 + C_1 r_1} & 0 \end{bmatrix} \quad \dots (4.20)$$

It is seen that in (4.20) $|S_{21}(j\omega)| = 1$ is automatically satisfied, since A_1 is real and C_1 is imaginary for $s = j\omega$.

Also, from (4.15) and (4.17), the phase shift

$$\phi_{21} = 2 \tan^{-1} (C_1 r_1 / jA_1) \quad \dots (4.21)$$

Type IB: In this case, the network is excited at port (3) with the output taken at port (4), while the shorted port voltages and currents are related as

$$V_1 = V_2, \quad I_1 = -I_2 \quad \dots (4.22)$$

Substituting (4.22) in (4.8),

$$A_2(V_3 - V_4) - B_2(I_3 - I_4) = 0 \quad \dots (4.23a)$$

$$C_1(V_3 + V_4) - D_1(I_3 + I_4) = 0 \quad \dots (4.23b)$$

or

$$\begin{bmatrix} V_3 \\ I_3 \end{bmatrix} = \frac{1}{(A_2 D_1 - B_2 C_1)} \begin{bmatrix} A_2 D_1 + B_2 C_1 & 2B_2 D_1 \\ 2A_2 C_1 & A_2 D_1 + B_2 C_1 \end{bmatrix} \begin{bmatrix} V_4 \\ -I_4 \end{bmatrix} \quad \dots (4.24)$$

Hence, from (4.22), the chain matrix parameters of this transformed two-port in terms of the decoupled line chain parameters are

$$A = D = \frac{A_2 D_1 + B_2 C_1}{A_2 D_1 - B_2 C_1} \quad \dots (4.25a)$$

$$B = \frac{2B_2 D_1}{(A_2 D_1 - B_2 C_1)} \quad C = \frac{2A_2 C_1}{(A_2 D_1 - B_2 C_1)} \quad \dots (4.25b)$$

From (4.25a) it is seen that this two-port network is also reciprocal and symmetric. Hence, from (4.7a) and (4.25), Type IB network will exhibit all-pass action provided

$$Z_3 = Z_4 = \sqrt{B_2 D_1 / A_2 C_1} \quad \dots (4.26)$$

at all frequencies; further, the scattering matrix is

$$[S] = \begin{bmatrix} 0 & \frac{\sqrt{A_2 D_1} - \sqrt{B_2 C_1}}{\sqrt{A_2 D_1} + \sqrt{B_2 C_1}} \\ \frac{\sqrt{A_2 D_1} - \sqrt{B_2 C_1}}{\sqrt{A_2 D_1} + \sqrt{B_2 C_1}} & 0 \end{bmatrix} \quad \dots (4.27a)$$

$$\text{with} \quad \left| \frac{\sqrt{A_2 D_1} - \sqrt{B_2 C_1}}{\sqrt{A_2 D_1} + \sqrt{B_2 C_1}} \right| = 1 \quad \dots (4.27b)$$

Also, the phase shift between ports (4) and (3) is

$$\phi_{43} = \frac{\sqrt{A_2 D_1} - \sqrt{B_2 C_1}}{\sqrt{A_2 D_1} + \sqrt{B_2 C_1}} \quad \dots (4.28)$$

Again $\phi_{43} = \phi_{34}$ since the network is reciprocal and symmetric.

Following the procedure used in the case of Type IA network, it can be shown that Type IB network, having dual lines given by (4.16) as decoupled lines, will exhibit all-pass action provided Z_3 and Z_4 are real, say r_3 and r_4 such that

$$r_3 = r_4 = \sqrt{L_{10}/C_{20}} = \sqrt{L_{20}/C_{10}} \quad \dots (4.29)$$

The corresponding scattering matrix and the phase shift are tabulated in Tables 4.1 and 4.2 respectively.

From (4.19) and (4.29), it is noted that if dual lines are used as decoupled lines, then the corresponding CNUIL will behave as an all-pass network in both Type IA and Type IB configuration, provided the terminating resistances are each equal to $\sqrt{L_{10}/C_{20}}$; however, the phase characteristics will, in general, be different.

Type II: The folded all-pass networks considered in this type are obtained by converting the coupled line four-port network of Fig.4.2 into a two-port network, such that the currents at the shorting ports are equal and in phase, while the voltages are equal in amplitude but opposite in phase. These configurations require ideal transformers, as shown in Fig.4.3. The shorting of ports (3) with (4) and (1) with (2) are considered as Types IIA and IIB respectively.

Type IIA: The four-port network is excited at port (1) with the output taken at port (2), while shorted port voltages and currents as:

$$V_3 = -V_4, \quad I_3 = I_4 \quad \dots (4.30)$$

Substituting (4.30) in (4.8)

$$V_1 = A_2 V_3 - B_1 I_3 \quad \dots (4.31a)$$

$$V_2 = -A_2 V_3 - B_1 I_3 \quad \dots (4.31b)$$

$$I_1 = C_2 V_3 - D_1 I_3 \quad \dots (4.31c)$$

$$I_2 = -C_2 V_3 - D_1 I_3 \quad \dots (4.31d)$$

Eliminating V_3 and I_3 in (4.31)

$$\begin{bmatrix} V_1 \\ I_1 \end{bmatrix} = \frac{1}{B_1 C_2 - A_2 D_1} \begin{bmatrix} A_2 D_1 + B_1 C_2 & 2B_1 A_2 \\ 2C_2 D_1 & A_2 D_1 + B_1 C_2 \end{bmatrix} \begin{bmatrix} V_2 \\ -I_2 \end{bmatrix} \quad \dots (4.32)$$

Hence the chain parameters of this transformed two-port in terms of decoupled line chain parameters, from (4.32), are

$$A = D = \frac{A_2 D_1 + B_1 C_2}{B_1 C_2 - A_2 D_1} \quad \dots (4.33a)$$

$$B = \frac{2A_2 B_1}{B_1 C_2 - A_2 D_1} \quad C = \frac{2C_2 D_1}{B_1 C_2 - A_2 D_1} \quad \dots (4.33b)$$

From (4.33a), it is observed that this two-port network is also reciprocal and symmetric. Hence, from (4.7) and (4.33), this network will exhibit all-pass action provided

$$Z_1 = Z_2 = \sqrt{A_2 B_1 / C_2 D_1} \quad \dots (4.34)$$

at all frequencies; further the scattering matrix is

$$[S] = \begin{bmatrix} 0 & \frac{\sqrt{B_1 C_2} - \sqrt{A_2 D_1}}{\sqrt{B_1 C_2} + \sqrt{A_2 D_1}} \\ \frac{\sqrt{B_1 C_2} - \sqrt{A_2 D_1}}{\sqrt{B_1 C_2} + \sqrt{A_2 D_1}} & 0 \end{bmatrix} \quad \dots (4.35a)$$

with $\left| \frac{\sqrt{B_1 C_2} - \sqrt{A_2 D_1}}{\sqrt{B_1 C_2} + \sqrt{A_2 D_1}} \right| = 1 \quad \dots (4.35b)$

Also, the phase shift between ports (2) and (1) is

$$\phi_{21} = \angle \left[\frac{\sqrt{B_1 C_2} - \sqrt{A_2 D_1}}{\sqrt{B_1 C_2} + \sqrt{A_2 D_1}} \right] \quad \dots (4.36)$$

Again, $\phi_{21} = \phi_{12}$, since the network is reciprocal and symmetric.

Following the procedure used in the case of Type IA network, it can be shown that Type IIA network, having dual lines given by (4.16) as decoupled lines, will exhibit all-pass action provided Z_1 and Z_2 are real, namely r_1 and r_2 such that

$$r_1 = r_2 = \sqrt{L_{10}/C_{20}} = \sqrt{L_{20}/C_{10}} \quad \dots (4.37)$$

The corresponding scattering matrix and the phase shift are tabulated in Tables 4.1 and 4.2 respectively.

Type IIB: Now the network is excited at port (3) with output at port (4), while the shorted port voltages and currents are related

as

$$V_1 = -V_2, \quad I_1 = I_2 \quad \dots (4.38)$$

Substituting (4.38) in (4.7) and simplifying

$$\begin{bmatrix} V_3 \\ I_3 \end{bmatrix} = \frac{1}{B_1 C_2 - A_1 D_2} \begin{bmatrix} A_1 D_2 + B_1 C_2 & 2B_1 D_2 \\ 2A_1 C_2 & A_1 D_2 + B_1 C_2 \end{bmatrix} \begin{bmatrix} V_4 \\ -I_4 \end{bmatrix} \quad \dots (4.39)$$

Hence, from (4.39), the chain parameters of this transformed two-port in terms of decoupled line chain parameters are

$$A = D = \frac{A_1 D_2 + B_1 C_2}{B_1 C_2 - A_1 D_2} \quad \dots (4.40a)$$

$$B = \frac{2B_1 D_2}{B_1 C_2 - A_1 D_2} \quad C = \frac{2A_1 C_2}{A_1 D_2 - B_2 C_1} \quad \dots (4.40b)$$

Again from (4.40a), it is noted that this two-port is also reciprocal and symmetric. Hence, from (4.7) and (4.40), this network will exhibit all-pass action provided

$$Z_3 = Z_4 = \sqrt{B_1 D_2 / A_1 C_2} \quad \dots (4.4)$$

at all frequencies; further the scattering matrix is

$$[S] = \begin{bmatrix} 0 & \frac{\sqrt{B_1 C_2} - \sqrt{A_1 D_2}}{\sqrt{B_1 C_2} + \sqrt{A_1 D_2}} \\ \frac{\sqrt{B_1 C_2} - \sqrt{A_1 D_2}}{\sqrt{B_1 C_2} + \sqrt{A_1 D_2}} & 0 \end{bmatrix} \quad \dots (4.42a)$$

with

$$\left| \frac{\sqrt{B_1 C_2} - \sqrt{A_1 D_2}}{\sqrt{B_1 C_2} + \sqrt{A_1 D_2}} \right| = 1 \quad \dots (4.42b)$$

Also the phase shift between ports (4) and (3) is

$$\phi_{43} = \angle \left[\frac{\sqrt{B_1 C_2} - \sqrt{A_1 D_2}}{\sqrt{B_1 C_2} + \sqrt{A_1 D_2}} \right] \quad \dots (4.43)$$

Since the network is reciprocal and symmetric, $\phi_{43} = \phi_{34}$.

Again, following the procedure used in the case of Type IA network, it can be shown that Type IIB network, having dual lines given by (4.16) as decoupled lines, will exhibit all-pass action provided Z_3 and Z_4 are real, namely r_3 and r_4 , such that

$$r_3 = r_4 = \sqrt{L_{10}/C_{20}} = \sqrt{L_{20}/C_{10}} \quad \dots (4.44)$$

The corresponding scattering matrix and the phase shift are given in Table 4.1.

From (4.37) and (4.44), it is noted that if dual lines are used as decoupled lines, then the corresponding CNU TL will behave as an all-pass network in both Type IIA and Type IIB configurations, provided the terminating resistances are each equal to $\sqrt{L_{10}/C_{20}}$; however, the phase characteristics will, in general, be different.

Type III: The folded all-pass networks considered in this type are obtained from the coupled line four-port by grounding or open-circuiting the two ports of the same line as shown in Fig.4.4; the

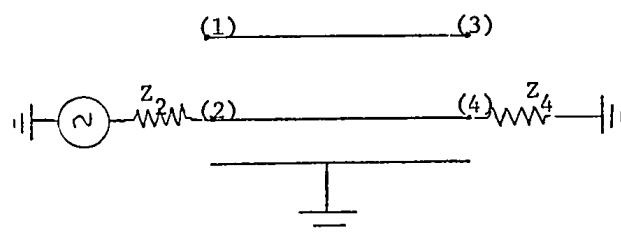
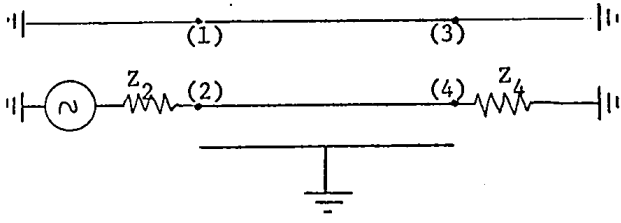
Type	Folded All-Pass Network
IIIA	 <p data-bbox="617 987 941 1039">$I_1 = I_3 = 0, \quad Z_2 = Z_4$</p>
IIIB	 <p data-bbox="617 1396 941 1449">$V_1 = V_3 = 0, \quad Z_2 = Z_4$</p>

Fig. 4.4: CNUFL Folded All-pass Networks of Type III.

former will be referred to as Type IIIA, while the latter as Type IIIB network.

Type IIIA: The network in this case is excited at port (2) with the output at port (4), while ports (1) and (3) have

$$I_1 = I_3 = 0 \quad \dots (4.45)$$

Substituting (4.45) in (4.7) and eliminating V_3

$$\begin{bmatrix} V_2 \\ I_2 \end{bmatrix} = \frac{1}{C_1 + C_2} \begin{bmatrix} A_1 C_2 + A_2 C_1 & [(B_1 + B_2)(C_1 + C_2) - (A_1 - A_2)(D_1 - D_2)] \frac{1}{2} \\ 2C_1 C_2 & C_1 D_2 + D_1 C_2 \end{bmatrix} \begin{bmatrix} V_4 \\ -I_4 \end{bmatrix} \quad \dots (4.46)$$

Hence, the chain parameters of this transformed two-port in terms of decoupled line chain parameters from (4.46) are

$$A = \frac{A_1 C_2 + A_2 C_1}{(C_1 + C_2)} \quad \dots (4.47a)$$

$$B = \frac{(B_1 + B_2)(C_1 + C_2) - (A_1 - A_2)(D_1 - D_2)}{2(C_1 + C_2)} \quad \dots (4.47b)$$

$$C = \frac{2C_1 C_2}{C_1 + C_2} \quad \dots (4.47c)$$

$$D = \frac{C_1 D_2 + D_1 C_2}{(C_1 + C_2)} \quad \dots (4.47d)$$

From (4.47), it is seen that the network is reciprocal, but non-symmetric. Hence, from (4.4) and (4.47), this network will

exhibit all-pass action provided

$$Z_1 = \sqrt{\left[\frac{(A_1 C_2 + A_2 C_1) \{ (B_1 + B_2) (C_1 + C_2) - (A_1 - A_2) (D_1 - D_2) \}}{4 C_1 C_2 (C_1 D_2 + D_1 C_2)} \right]} \quad \dots (4.48a)$$

and

$$Z_2 = \sqrt{\left[\frac{(C_1 D_2 + D_1 C_2) \{ (B_1 + B_2) (C_1 + C_2) - (A_1 - A_2) (D_1 - D_2) \}}{4 C_1 C_2 (A_1 C_2 + A_2 C_1)} \right]} \quad \dots (4.48b)$$

at all frequencies. From (4.6) and (4.47), the scattering matrix and the phase shift for this network may be obtained; these are tabulated in Tables 4.1 and 4.2 respectively.

In general, it is not possible to synthesize the NUTL, which satisfies the requirements (4.48). However, these conditions are satisfied when proportional lines distributions ,

$$L_1 = L_{10} F(x) \quad , \quad C_1 = C_{10} F(x) \quad 0 \leq x \leq \ell \quad \dots (4.49a)$$

and

$$L_2 = L_{20} F(x) \quad , \quad C_2 = C_{20} F(x) \quad 0 \leq x \leq \ell \quad \dots (4.49b)$$

with

$$L_{10} C_{10} = L_{20} C_{20} \quad , \quad \frac{L_{10}}{C_{10}} \neq \frac{L_{20}}{C_{20}} \quad \dots (4.49c)$$

are chosen as the two decoupled lines. In this case, from (4.49), it is seen that the corresponding CNUTL is also a proportional line. Using the result that a proportional CNUTL is nothing but a CUTL of a different length⁽⁹²⁾, it is seen that this folded all-pass network exhibit the same characteristics as obtained by Jones and Bolljahan⁽⁵³⁾

for CUTL folded all-pass networks.

Type IIIB: The coupled line four-port in this case is excited at port (2) with output at port (4) while voltages and currents have

$$V_1 = V_3 = 0 \quad \dots (4.50)$$

Following the procedure used in the case of Type IIIA, it can be shown from (4.50) and (4.7) that the chain parameters of this transformed two-port network, in terms of decoupled line chain parameters, are

$$A = \frac{A_1 B_2 + A_2 B_1}{B_1 + B_2} \quad \dots (4.51a)$$

$$B = \frac{2B_1 B_2}{B_1 + B_2} \quad \dots (4.51b)$$

$$C = \frac{(B_1 + B_2)(C_1 + C_2) - (A_1 - A_2)(D_1 - D_2)}{2(B_1 + B_2)} \quad \dots (4.51c)$$

$$D = \frac{B_1 D_2 + B_2 D_1}{(B_1 + B_2)} \quad \dots (4.51d)$$

From (4.51), it is seen that this network is also reciprocal but non-symmetric. Hence, from (4.4) and (4.51), this network will exhibit all-pass action provided

$$Z_3 = \sqrt{\frac{4B_1 B_2 (A_1 B_2 + A_2 B_1)}{(B_1 D_2 + B_2 D_1) \{ (B_1 + B_2)(C_1 + C_2) - (A_1 - A_2)(D_1 - D_2) \}}} \quad \dots (4.52a)$$

and

$$Z_4 = \sqrt{\frac{4B_1 B_2 (B_1 D_2 + B_2 D_1)}{(A_1 B_2 + A_2 B_1) \{ (B_1 + B_2)(C_1 + C_2) - (A_1 - A_2)(D_1 - D_2) \}}} \quad \dots (4.52b)$$

at all frequencies. From (4.6) and (4.51), the scattering matrix and the phase shift for this network may be obtained, and these are tabulated in Tables 4.1 and 4.2 respectively. Again, in general, it is not possible to synthesize NUTLs satisfying the requirements (4.52). However, these are satisfied by the chain parameters of proportional decoupled lines described in (4.49). In this case, as in case of Type IIIA network, the folded all-pass network consists of a CUTL, and hence exhibits characteristics similar to that obtained by Jones and Bolljahan⁽⁵³⁾.

4.4 Folded All-Pass Network with Basic Decoupled Lines:

In the previous Section, it was shown that if dual lines are chosen as decoupled lines, then the corresponding CNUTLs will exhibit all-pass characteristics in both Type I and Type II configurations, provided the ports are suitably terminated. In the following two subsections, the characteristics of such all-pass networks are studied in detail using basic lines with hyperbolic solutions as the decoupled lines.

4.4.1 Phase Characteristics:

The chain parameters of the basic lines with hyperbolic solutions are given in Tables 3.1 and 3.2. Using these parameters and Tables 4.1 and 4.2, the phase shifts of folded all-pass networks of Type I and Type II are obtained and are shown in Tables 4.3 and 4.4, where

TABLE 4.1
SCATTERING MATRIX OF VARIOUS FOLDED ALL-PASS NETWORKS

Type	Scattering Matrix
IA	$\begin{array}{cc} 0 & \{(A_1 - C_1 r_1)/(A_1 + C_1 r_1)\} \\ \{(A_1 - C_1 r_1)/(A_1 + C_1 r_1)\} & 0 \end{array}$
IB	$\begin{array}{cc} 0 & \{(D_1 - C_1 r_1)/(D_1 + C_1 r_1)\} \\ \{(D_1 - C_1 r_1)/(D_1 + C_1 r_1)\} & 0 \end{array}$
IIA	$\begin{array}{cc} 0 & \{(B_1 - r_1 D_1)/(B_1 + r_1 D_1)\} \\ \{(B_1 - D_1 r_1)/(B_1 + D_1 r_1)\} & 0 \end{array}$
IIB	$\begin{array}{cc} 0 & \{(B_1 - A_1 r_1)/(B_1 + A_1 r_1)\} \\ \{(B_1 - A_1 r_1)/(B_1 + A_1 r_1)\} & 0 \end{array}$
IIIA	$\begin{array}{cc} 0 & \frac{\sqrt{[(A_1 C_2 + A_2 C_1)(C_1 D_2 + D_1 C_2)] - \sqrt{[C_1 C_2 \{(B_1 + B_2)(C_1 + C_2) - (A_1 - A_2)(D_1 - D_2)\}]}}}{(C_1 + C_2)} \\ \frac{\sqrt{[(A_1 C_2 + A_2 C_1)(C_1 D_2 + D_1 C_2)] + \sqrt{[C_1 C_2 \{(B_1 + B_2)(C_1 + C_2) - (A_1 - A_2)(D_1 - D_2)\}]}}}{(C_1 + C_2)} & 0 \end{array}$
IIIB	$\begin{array}{cc} 0 & \frac{\sqrt{[(A_1 B_2 + A_2 B_1)(B_1 D_2 + B_2 D_1)] - \sqrt{[B_1 B_2 \{(B_1 + B_2)(C_1 + C_2) - (A_1 - A_2)(D_1 - D_2)\}]}}}{(B_1 + B_2)} \\ \frac{\sqrt{[(A_1 B_2 + A_2 B_1)(B_1 D_2 + B_2 D_1)] + \sqrt{[B_1 B_2 \{(B_1 + B_2)(C_1 + C_2) - (A_1 - A_2)(D_1 - D_2)\}]}}}{(B_1 + B_2)} & 0 \end{array}$

TABLE 4.2

PHASE SHIFT FOR VARIOUS FOLDED ALL-PASS NETWORKS

Type	Phase Shift
IA	$\phi_{21} = \phi_{12} = -2 \tan^{-1} [C_1 r_1 / jA_1]$
IB	$\phi_{21} = \phi_{12} = -2 \tan^{-1} [C_1 r_1 / jD_1]$
IIA	$\phi_{21} = \phi_{12} = \pi - 2 \tan^{-1} [B_1 / jD_1 r_1]$
IIB	$\phi_{21} = \phi_{12} = \pi - 2 \tan^{-1} [B_1 / jA_1 r_1]$
IIIA	$\phi_{42} = \angle \left[\frac{\sqrt{[(A_1 C_2 + A_2 C_1)(C_1 D_2 + D_1 C_2)]} - \sqrt{[C_1 C_2 \{(B_1 + B_2)(C_1 + C_2) - (A_1 - A_2)(D_1 - D_2)\}]}}{(C_1 + C_2)} \right]$
	$\phi_{24} = \angle \left[\frac{\sqrt{[(A_1 C_2 + A_2 C_1)(C_1 D_2 + D_1 C_2)]} - \sqrt{[C_1 C_2 \{(B_1 + B_2)(C_1 + C_2) - (A_1 - A_2)(D_1 - D_2)\}]}}{(C_1 + C_2)} \right]$
IIIB	$\phi_{42} = \angle \left[\frac{\sqrt{[(A_1 B_2 + A_2 B_1)(B_1 D_2 + B_2 D_1)]} - \sqrt{[B_1 B_2 \{(B_1 + B_2)(C_1 + C_2) - (A_1 - A_2)(D_1 - D_2)\}]}}{(B_1 + B_2)} \right]$
	$\phi_{24} = \angle \left[\frac{\sqrt{[(A_1 B_2 + A_2 B_1)(B_1 D_2 + B_2 D_1)]} - \sqrt{[B_1 B_2 \{(B_1 + B_2)(C_1 + C_2) - (A_1 - A_2)(D_1 - D_2)\}]}}{(B_1 + B_2)} \right]$

TABLE 4.3

PHASE SHIFT FOR NONUNIFORM LINE FOLDED ALL-PASS NETWORKS TO TYPE IA AND IB

	IA	IB
Decoupled Line	$\phi_{12} = -2 \tan^{-1} \psi$	$\phi_{12} = -2 \tan^{-1} \psi$
	$\psi = [C_1 r_1 / j A_1]$	$\psi = [C_1 r_1 / j D_1]$
Exponential	$\frac{\beta}{n(0)} \cdot \frac{1}{[\Gamma \coth \Gamma \ell + (m/2)]}$	$\frac{\beta}{n(0)} \cdot \frac{e^{-m\ell}}{[\Gamma \coth \Gamma \ell - (m/2)]}$
Algebraic	$(1 + m\ell + \frac{m^2}{2}) - \frac{m^2 \ell}{\beta} \cot \beta \ell$ $n(0) [(1+m\ell) \cos \beta \ell - \frac{m}{\beta} \sin \beta \ell]$	$(1 + m\ell + \frac{m^2}{2}) - \frac{m^2 \ell}{\beta} \cot \beta \ell$ $n(0) [\cos \beta \ell + \frac{m}{\beta} \sin \beta \ell]$
Trigonometric	$\frac{\mu}{n(0)} \cdot \frac{\mu \tan \mu \ell - m \tan m \ell}{\mu + m \tan m \ell \tan \mu \ell}$	$\frac{\cos^2 m \ell}{n(0) \beta} [\mu \tan \mu \ell - m \tan m \ell]$
Hyperbolic Sine Squared	$\frac{\sinh^2 n}{\beta n(0)} \cdot \frac{[\{\gamma^2 + m^2 \coth n \coth (m\ell+1)\} \tan \gamma \ell + m \{\coth (m\ell+1) - \coth n\}]}{[\gamma - m \coth (m\ell+n) \tan \gamma \ell]}$	$\frac{\sinh^2 (m\ell+n)}{\beta n(0)} \cdot \frac{[\{\gamma^2 + m^2 \coth n \coth (m\ell+n)\} \tan \gamma \ell + m \{\coth (m\ell+n) - \coth n\}]}{[\gamma + m \coth n \tan \gamma \ell]}$
Hyperbolic Cosine Squared	$\frac{\gamma}{\beta n(0)} \cdot \frac{[\gamma \tan \gamma \ell + m \tanh m \ell]}{[\gamma - m \tanh m \ell \sin \gamma \ell]}$	$\frac{\cosh^2 m \ell}{\beta n(0)} [\gamma \tan \gamma \ell + m \tanh m \ell]$

$$n = 0.881$$

TABLE 4.4

PHASE SHIFT FOR NONUNIFORM LINE FOLDED ALL-PASS NETWORKS OF TYPE IIA AND IIB

	IIA	IIB
Decoupled Lines	$\phi_{34} = \pi - 2 \tan^{-1} \psi$ $\psi = \{B_1 / j r_1 D_1\}$	$\phi_{34} = \pi - 2 \tan^{-1} \psi$ $\psi = \{B_1 / j A_1 r_1\}$
Exponential	$\eta(0) \cdot \frac{1}{[\Gamma \coth \Gamma l - \frac{m}{2}]}$	$\eta(0) \beta \cdot \frac{e^{m l}}{[\Gamma \coth \Gamma l + \frac{m}{2}]}$
Algebraic	$\frac{\eta(0) \beta}{[\beta \cot \beta l + m]}$	$\frac{\eta(0) \beta}{(1+m l) [\beta (1+m l) \cot \beta l - m]}$
Trigonometric	$\frac{\eta(0) \beta \cdot \tan \beta l}{\mu}$	$\frac{\eta(0) \beta}{\cos^2 m l [m \tan m l + \mu \cot \mu l]}$
Hyperbolic Sine Squared	$\frac{\eta(0) \beta}{\sinh^2 n [\gamma \cot \gamma l + m \coth n]}$	$\frac{\eta(0) \beta}{\sinh^2 (m l + n) [\gamma \cot \gamma l - m \coth (m l + n)]}$
Hyperbolic Cosine Squared	$\frac{\eta(0) \beta \tan \gamma l}{\gamma}$	$\frac{\eta(0) \beta}{\cosh^2 m l [\gamma \cot \gamma l - m \tanh m l]}$

$$\eta(0) = \sqrt{\frac{Z_{10}(0)}{Z_{20}(0)}} \quad \dots (4.53)$$

$\eta(0)$ being the square root of the ratio of characteristic impedances of lines 1 and 2 at $x = 0$. These phase shifts are plotted with frequency for various values of taper $m\lambda$ and $\eta(0)$ and are shown in Figs. 4.5 to 4.24. On examination of the phase characteristics for Type IA and IB, it is found that:

- (i) The frequency at which the phase shift is 180° may be controlled by varying the taper, while the variation of $\eta(0)$ controls the phase shift at other frequencies. Hence, when these networks are used for phase compensation, the frequency at which a phase shift of 180° is required may be controlled by the taper, while the phase shifts at other frequencies may be adjusted by changing $\eta(0)$. It may be mentioned that in order to obtain the same property with CUTLs, cascaded networks are employed. However, these are larger in size with a consequent degraded performance⁽⁹⁵⁾.

- (ii) The phase shift is fairly constant over a band of frequencies, when 'Trigonometric' or 'Hyperbolic Sine Squared' lines are employed as decoupled lines in Type IB configurations. The required amount of phase shift can be obtained by properly adjusting the values of $m\lambda$ and $\eta(0)$. Thus, these networks can provide

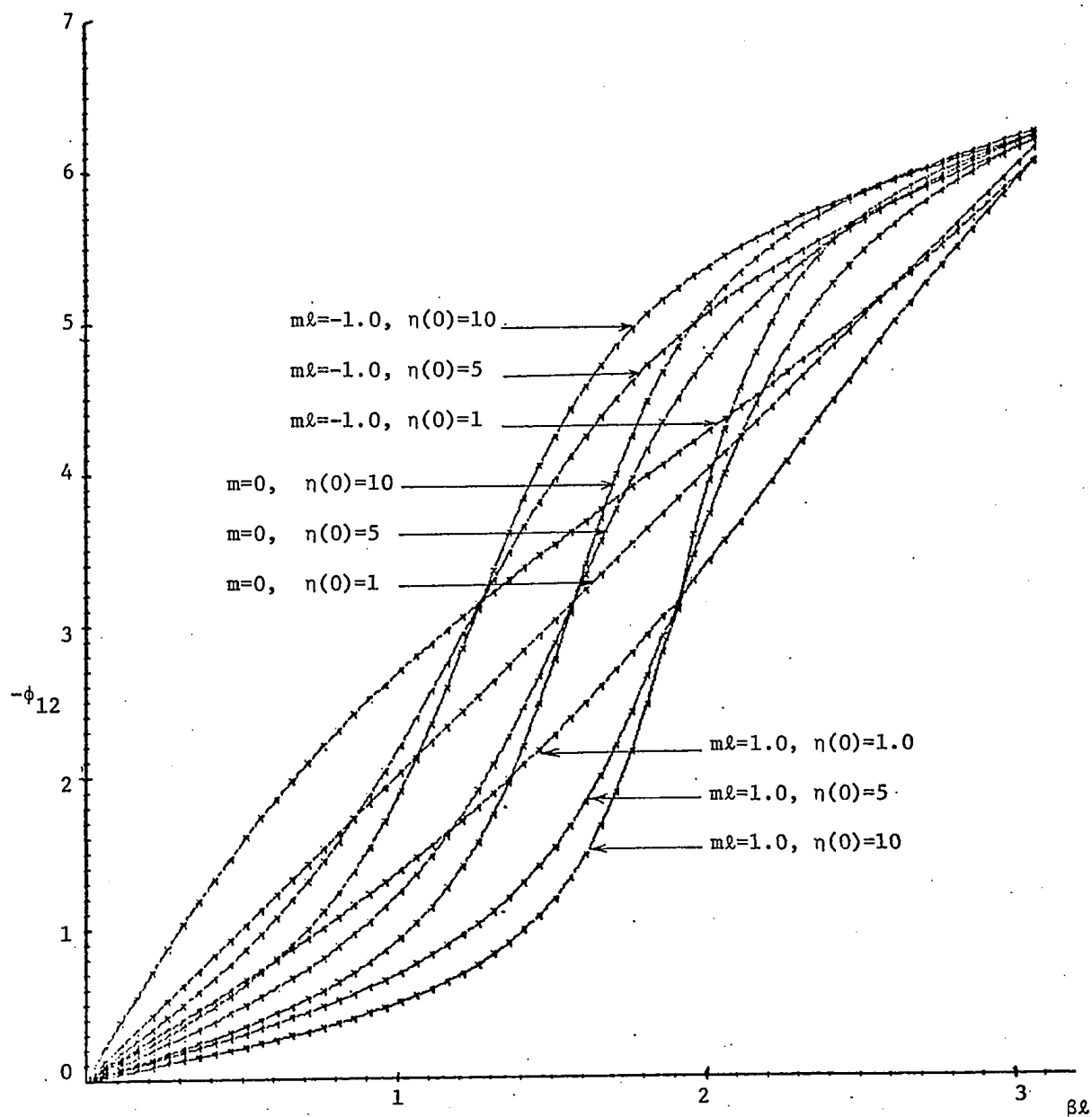


Fig. 4.5: Phase Characteristics of Type IA CNUTL Folded All-pass Networks
with ELs as Decoupled Lines

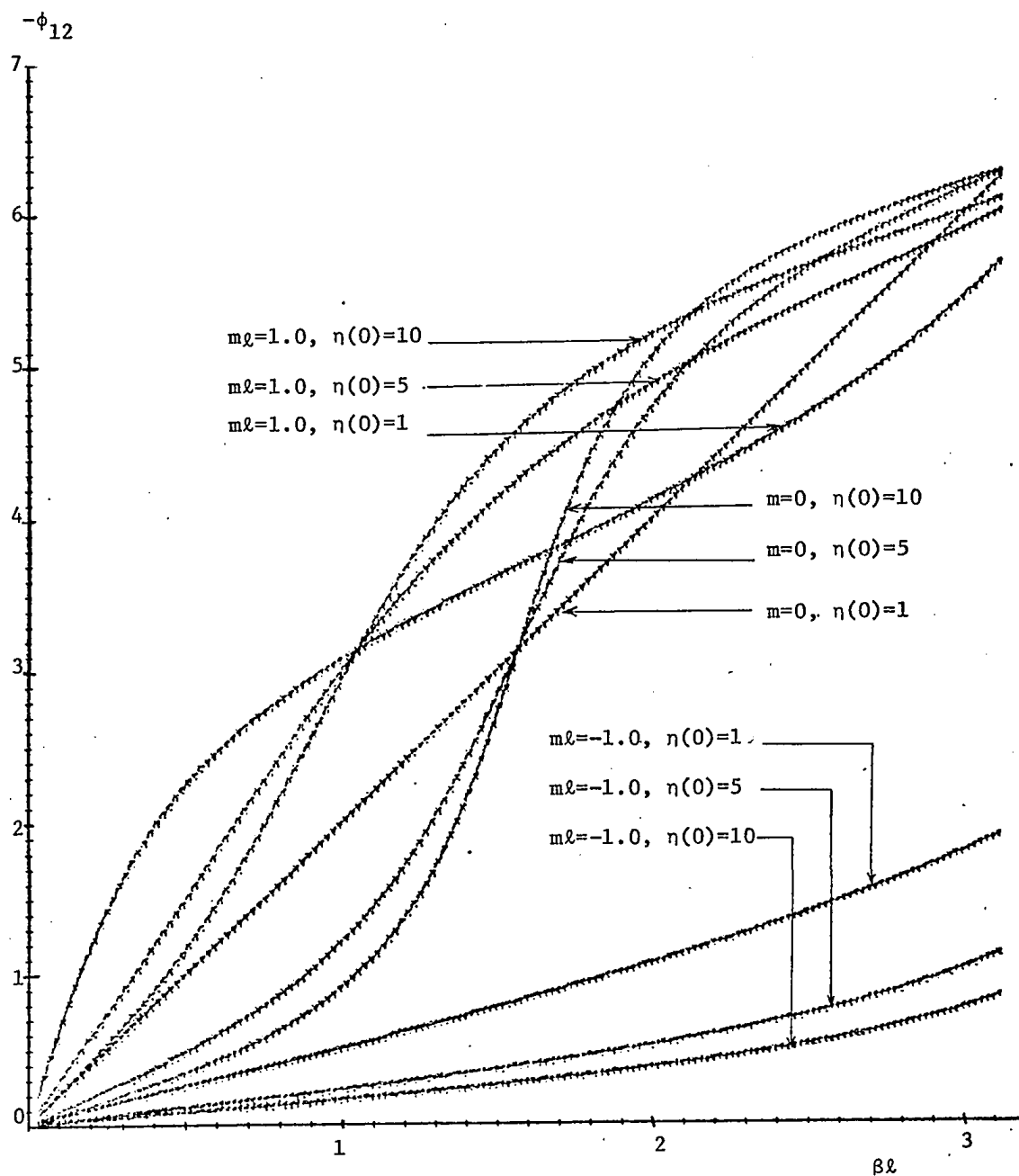


Fig. 4.6: Phase Characteristics of Type IA CNUTL Folded All-pass Networks
with ALs as Decoupled Lines

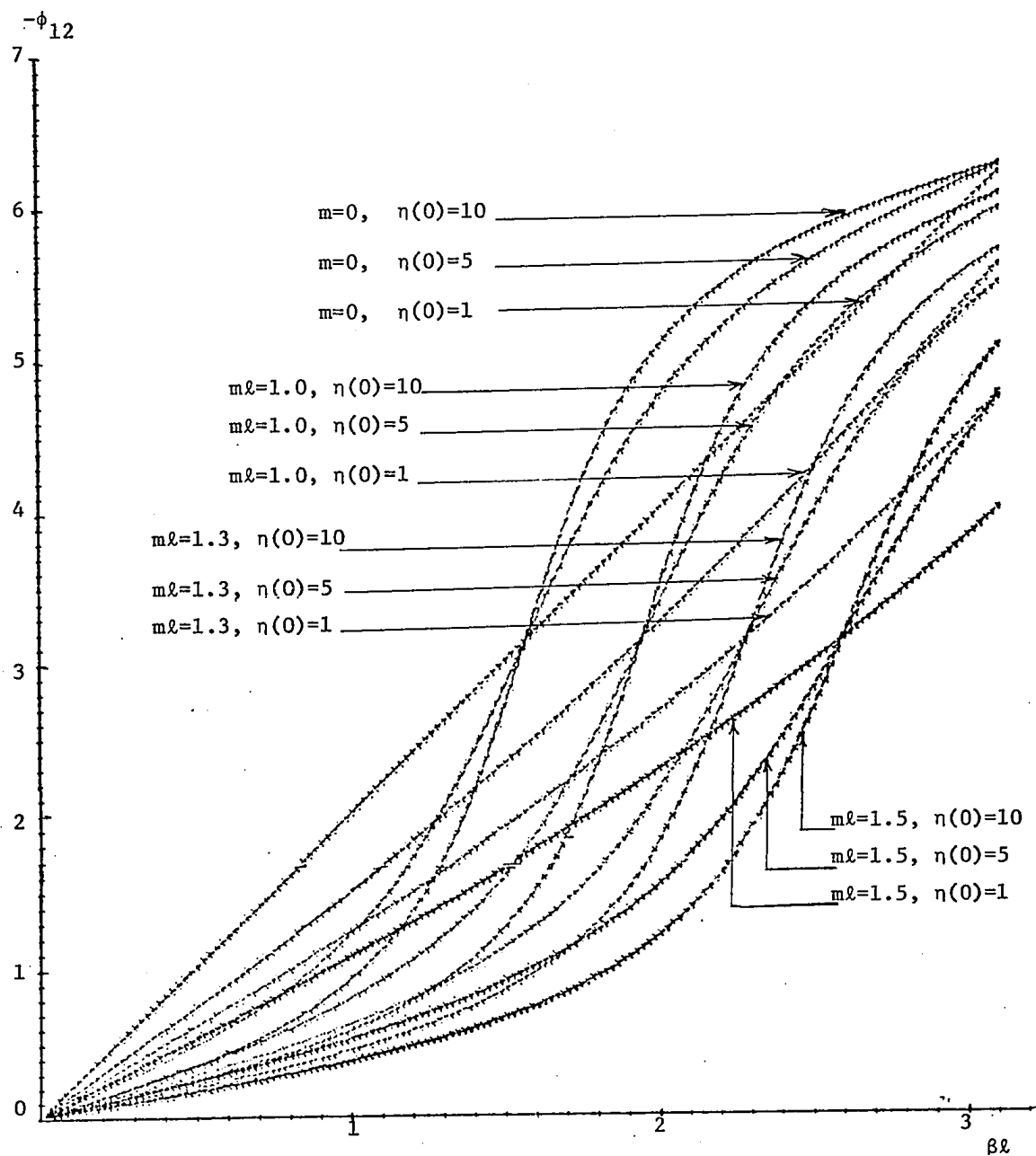


Fig. 4.7: Phase Characteristics of Type IA CNU TL Folded All-pass Networks
with TLs as Decoupled Lines

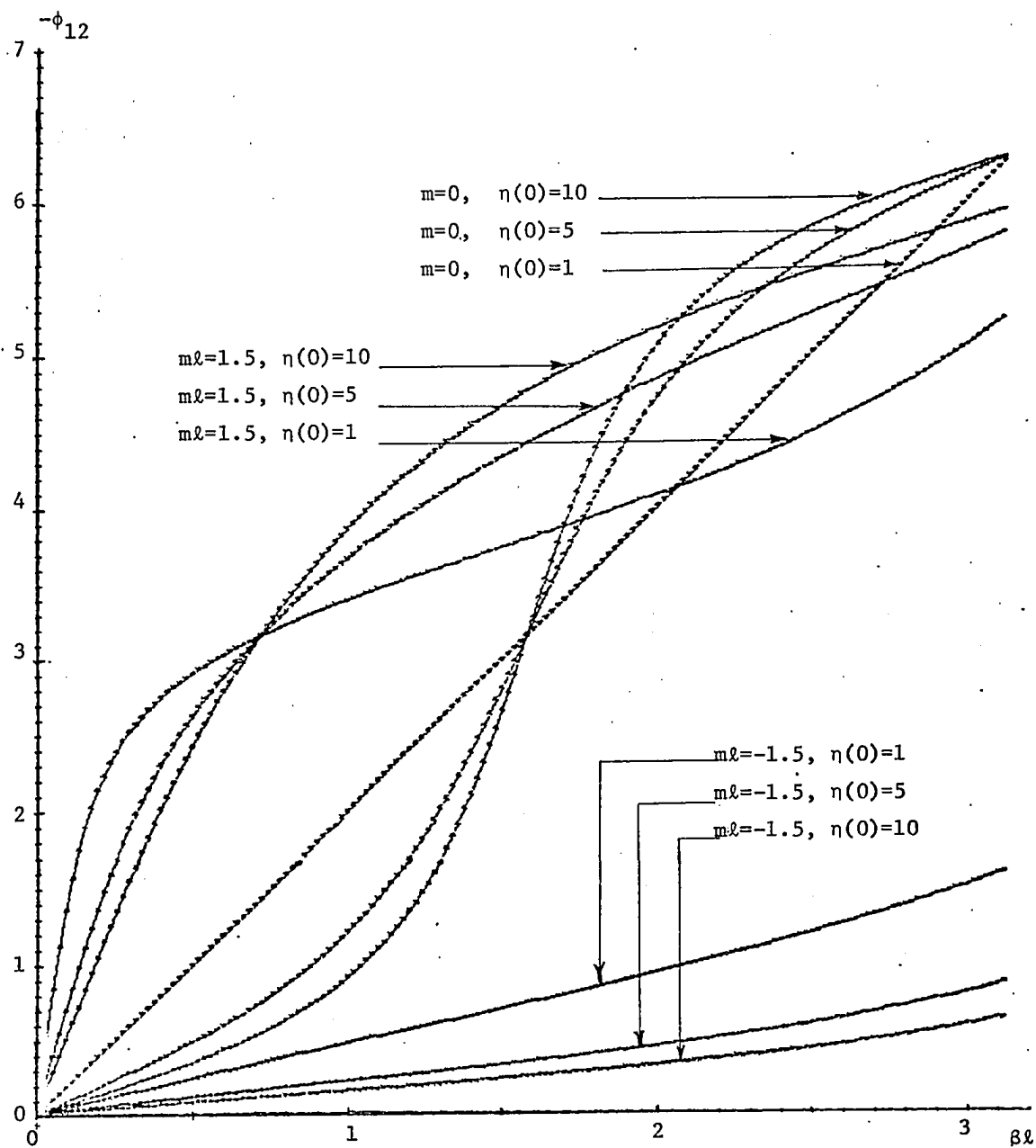


Fig. 4.8: Phase Characteristics of Type IA CNU TL Folded All-pass Networks
with HSSLs as Decoupled Lines

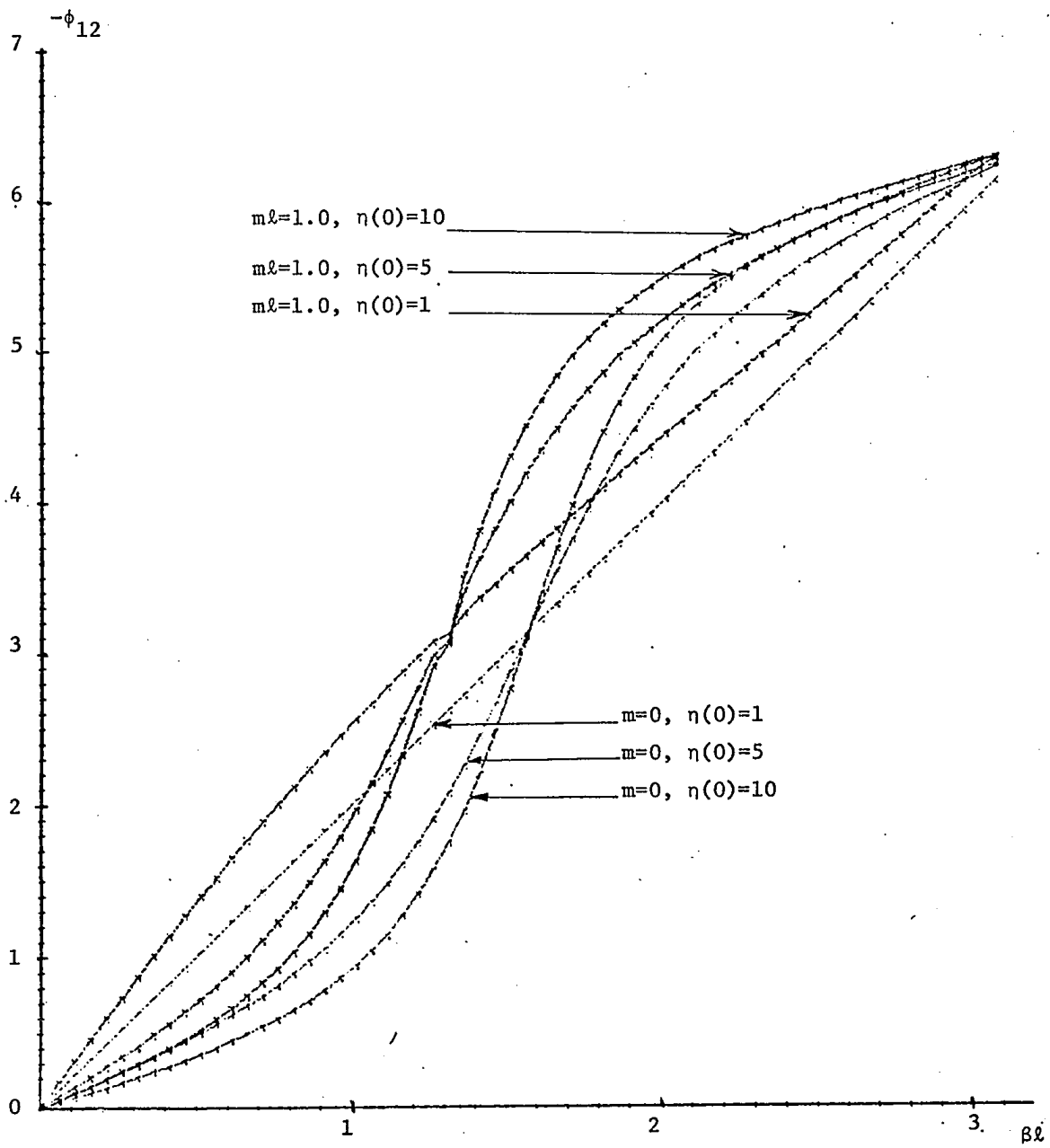


Fig. 4.9: Phase Characteristics of Type IA CNUTL Folded All-pass Networks
with HCSLs as Decoupled Lines

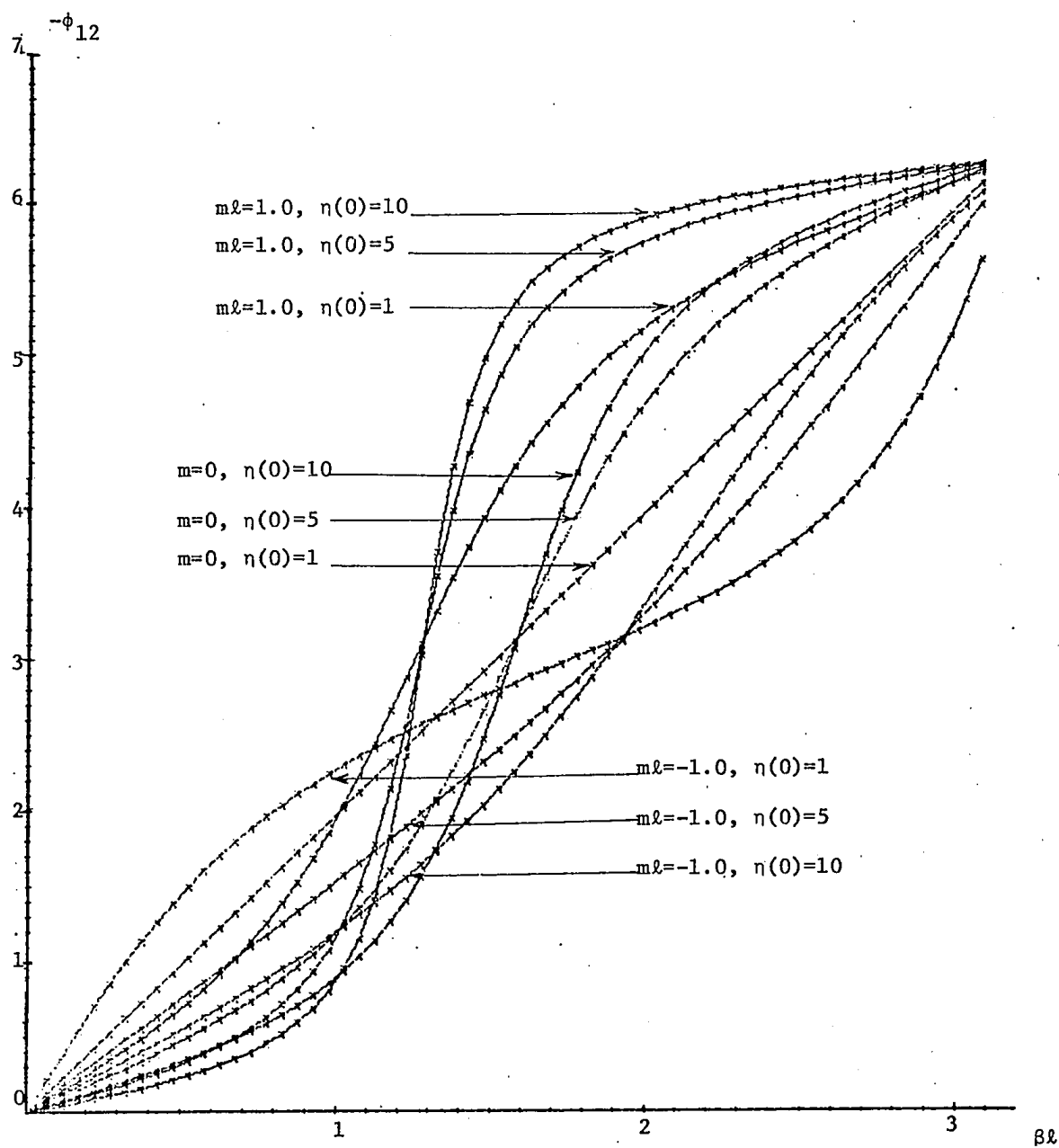


Fig. 4.10: Phase Characteristics of Type IB CNUTL Folded All-pass Networks
with ELs as Decoupled Lines

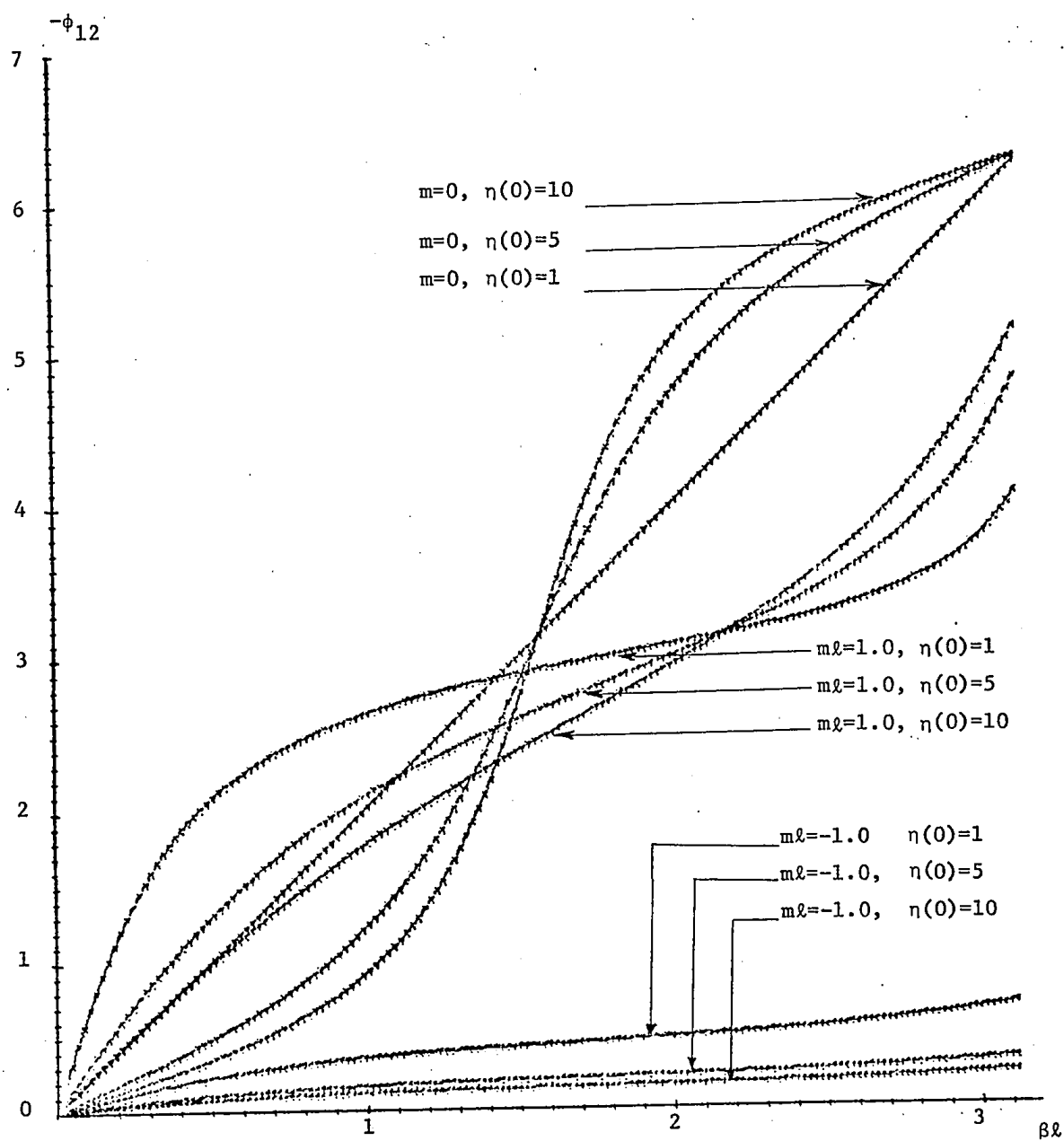


Fig. 4.11: Phase Characteristics of Type IB CNUTL Folded All-pass Networks
with ALs as Decoupled Lines

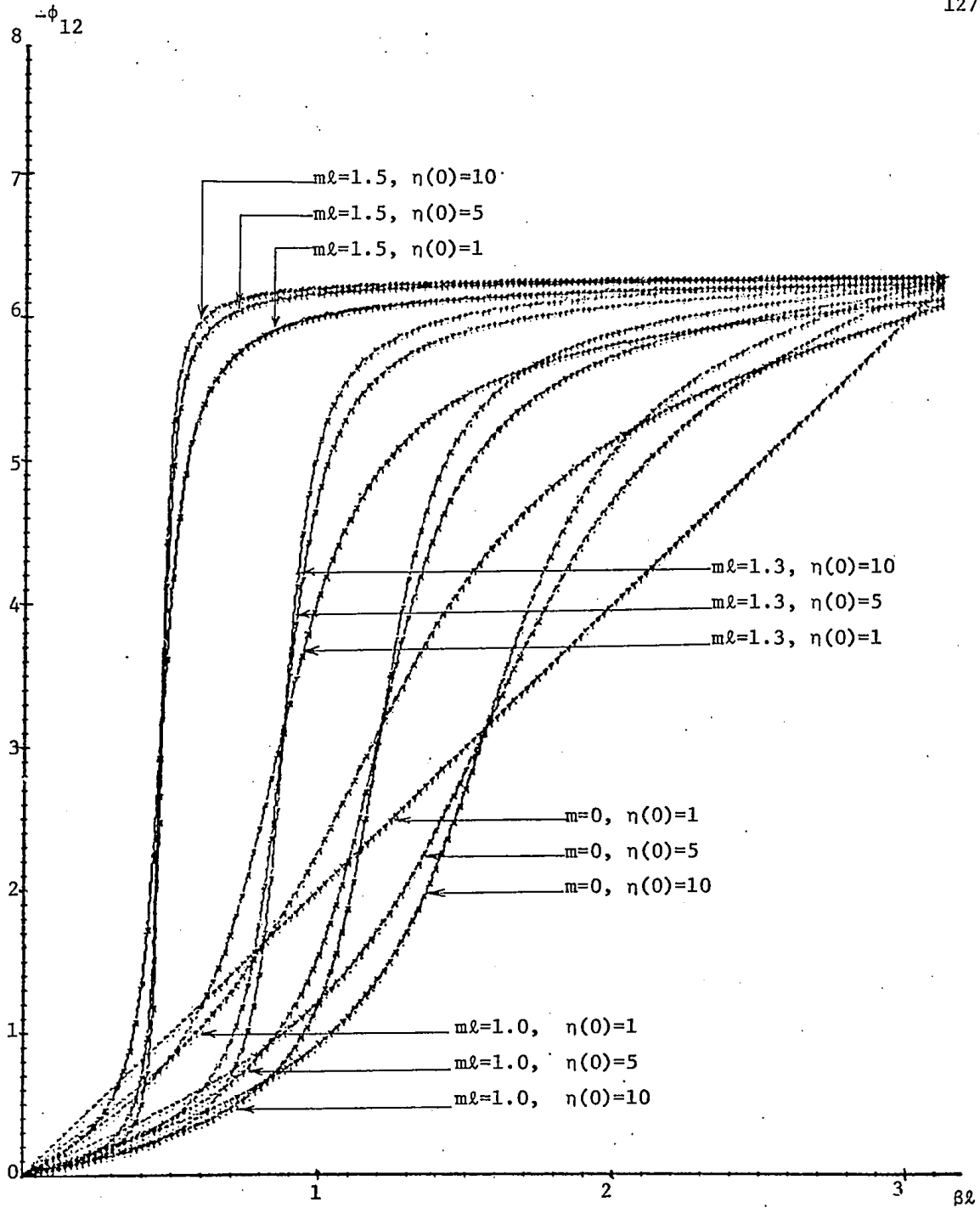


Fig. 4.12: Phase Characteristics of Type IB CNU TL Folded All-pass Networks
with TLs as Decoupled Lines

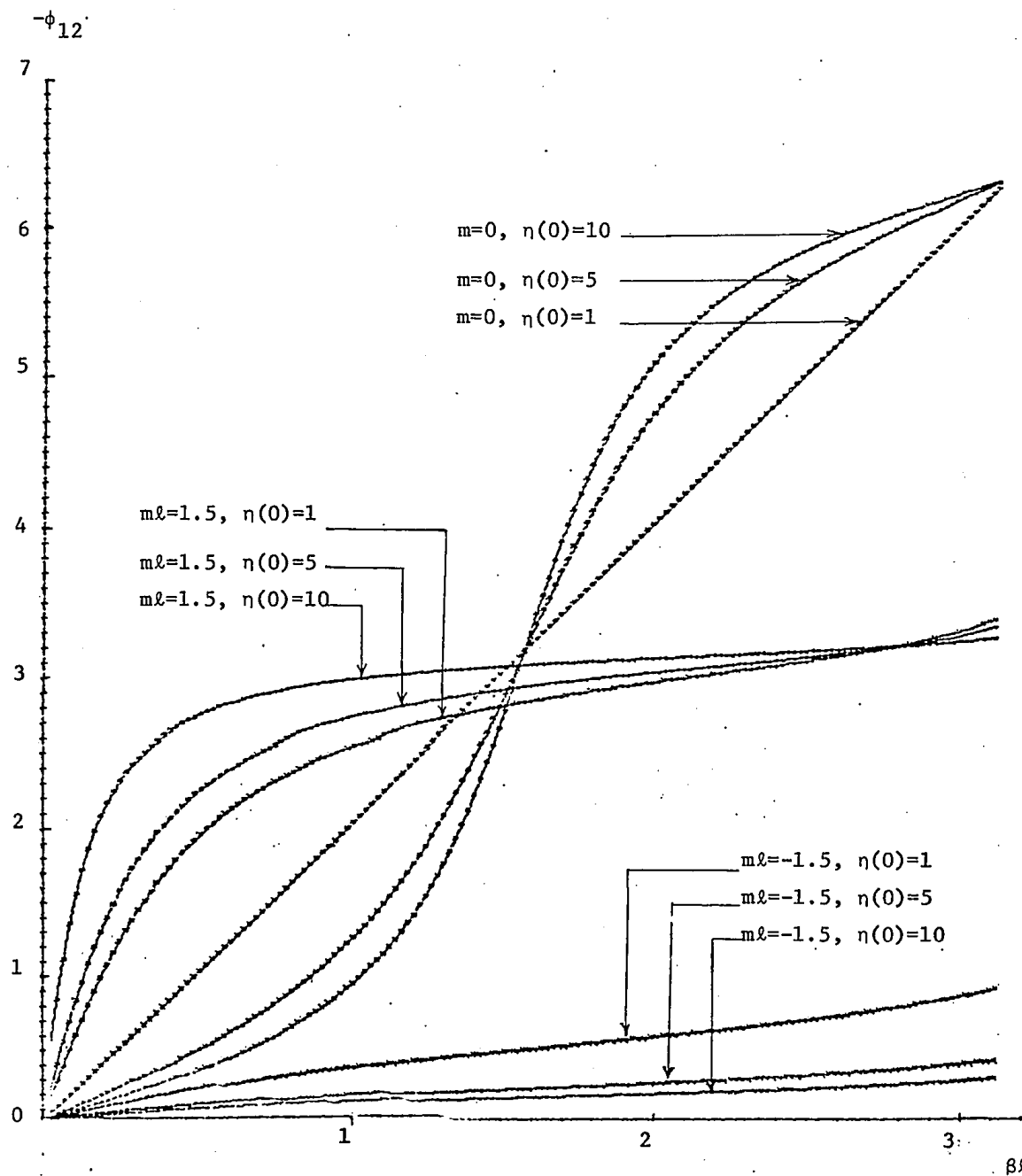


Fig. 4.13: Phase Characteristics of Type IB CNU TL Followed All-pass Networks
with HSSLs as Decoupled Lines

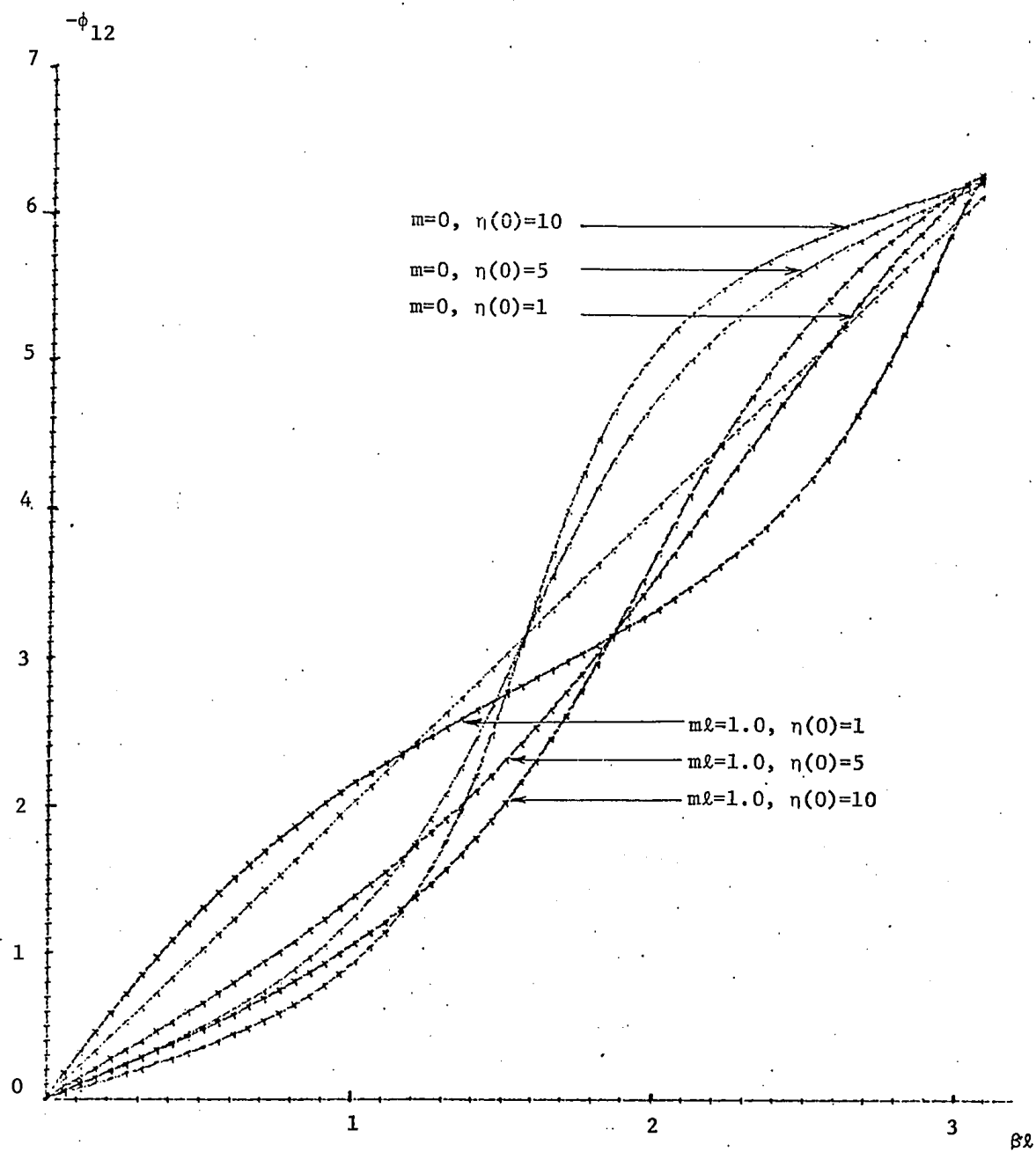


Fig. 4.14: Phase Characteristics of Type IB CNUTL Folded All-pass Networks
with HCSLs as Decoupled Lines

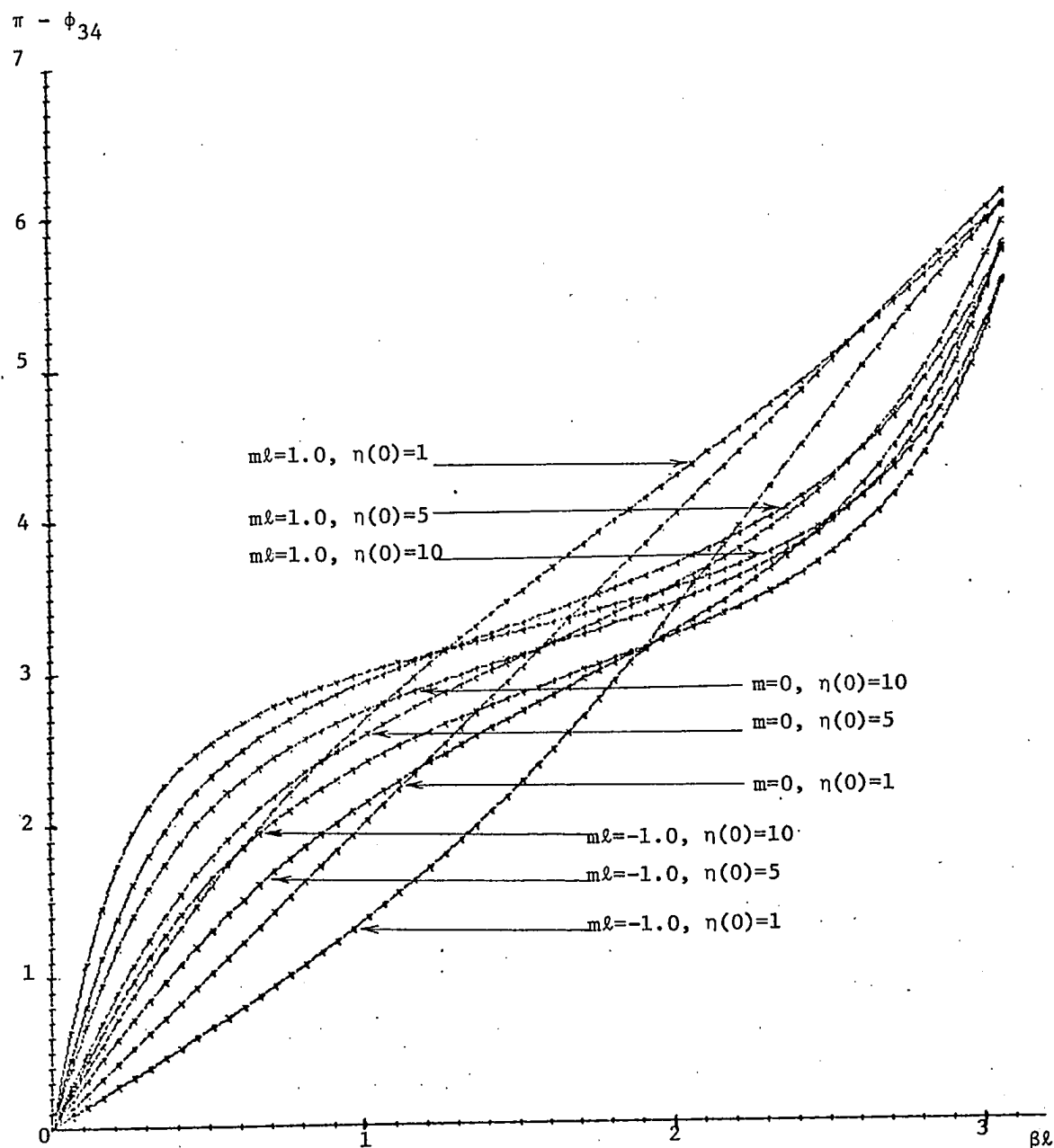


Fig. 4.15: Phase Characteristics of Type IIA CNUTL Folded All-pass Networks
with ELs as Decoupled Lines

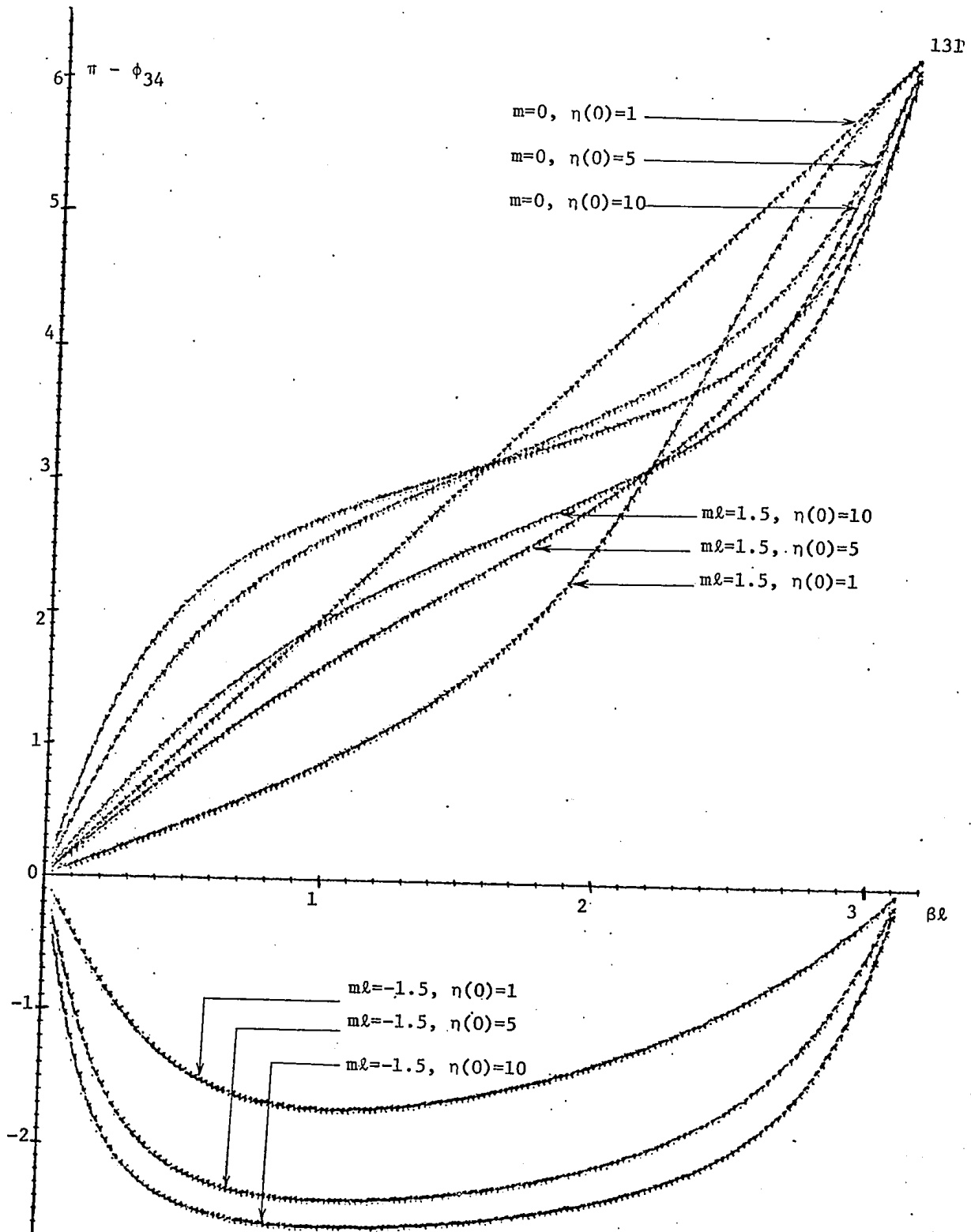


Fig. 4.16: Phase Characteristics of Type IIA CNUTL Folded All-pass Networks with ALs as Decoupled Lines

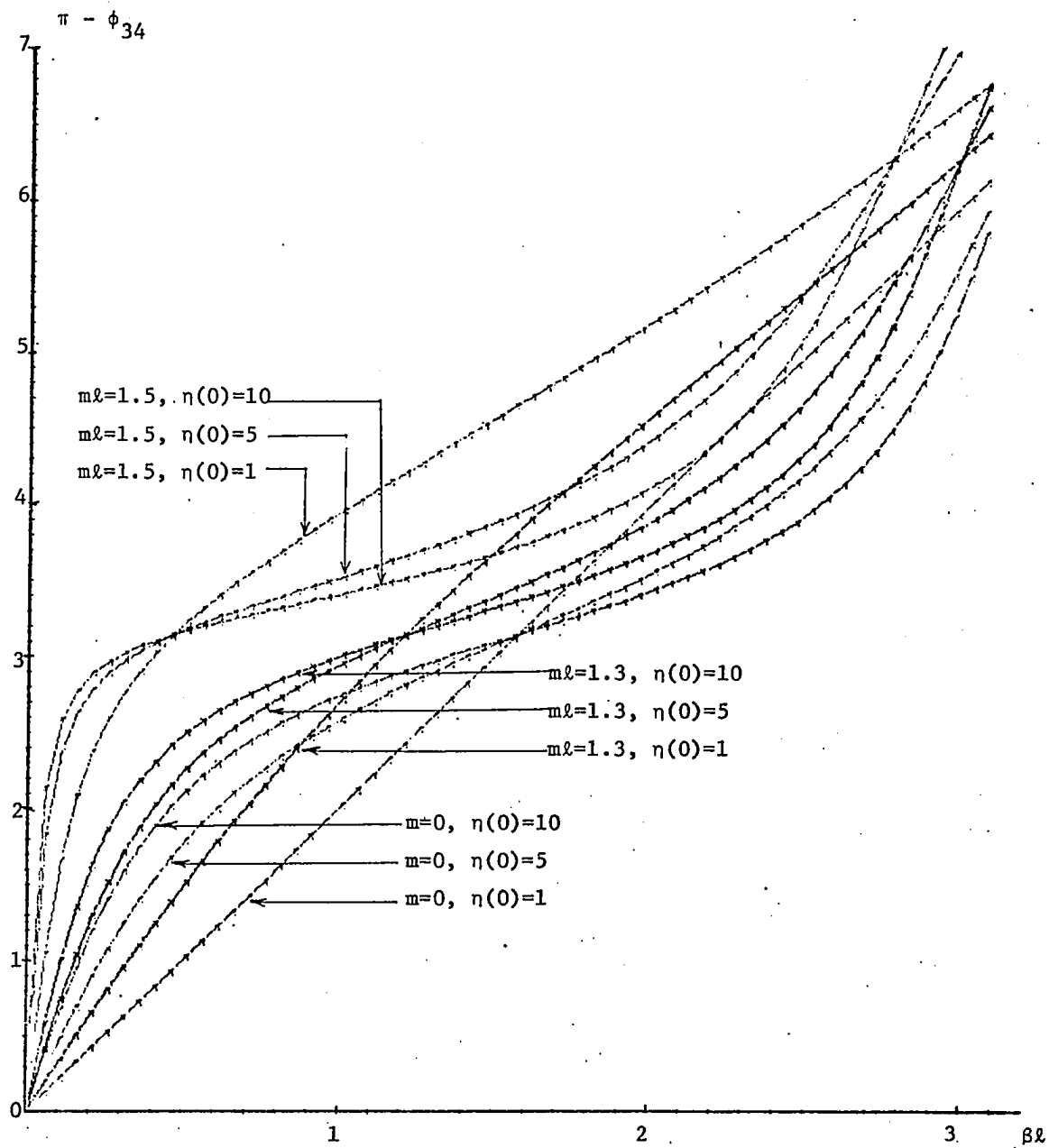


Fig. 4.17: Phase Characteristics of Type IIA CNUTL Folded All-pass Networks
with TLs as Decoupled Lines

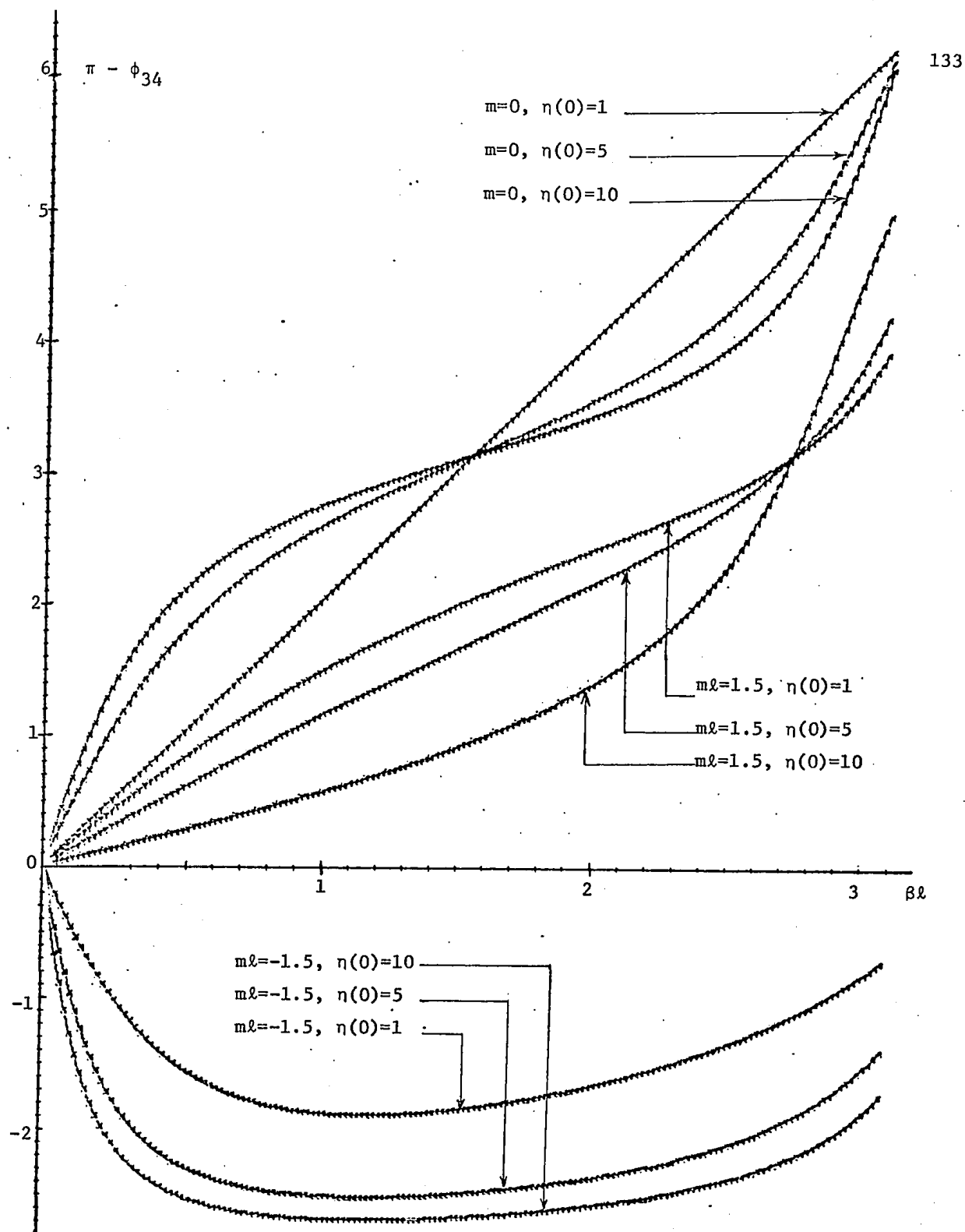


Fig. 4.18: Phase Characteristics of Type IIA CNUTL Folded All-pass Networks
with HSSLs as Decoupled Lines

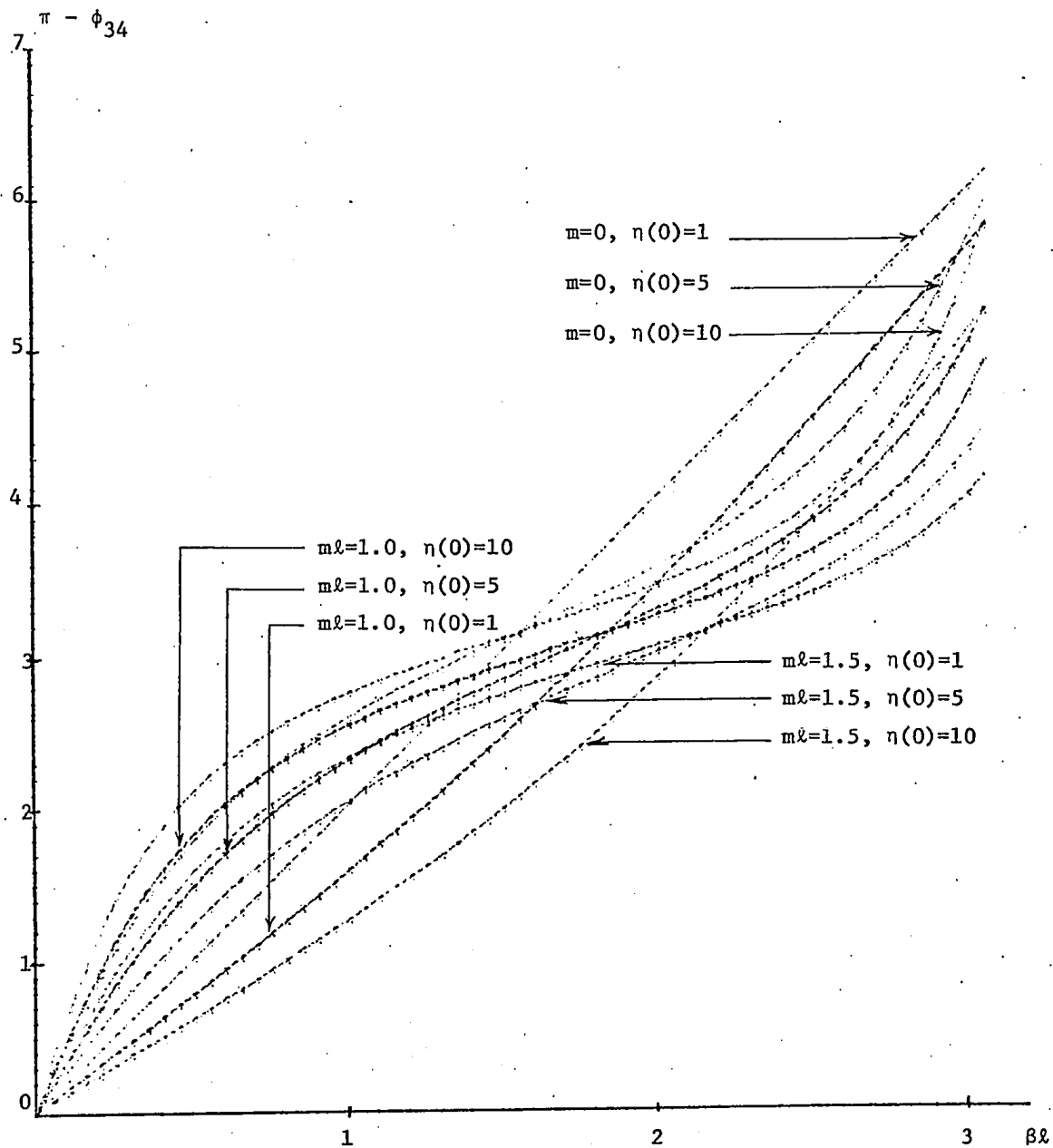


Fig. 4.19: Phase Characteristics of Type IIA CNUTL Folded All-pass Networks
with HCSLs as Decoupled Lines

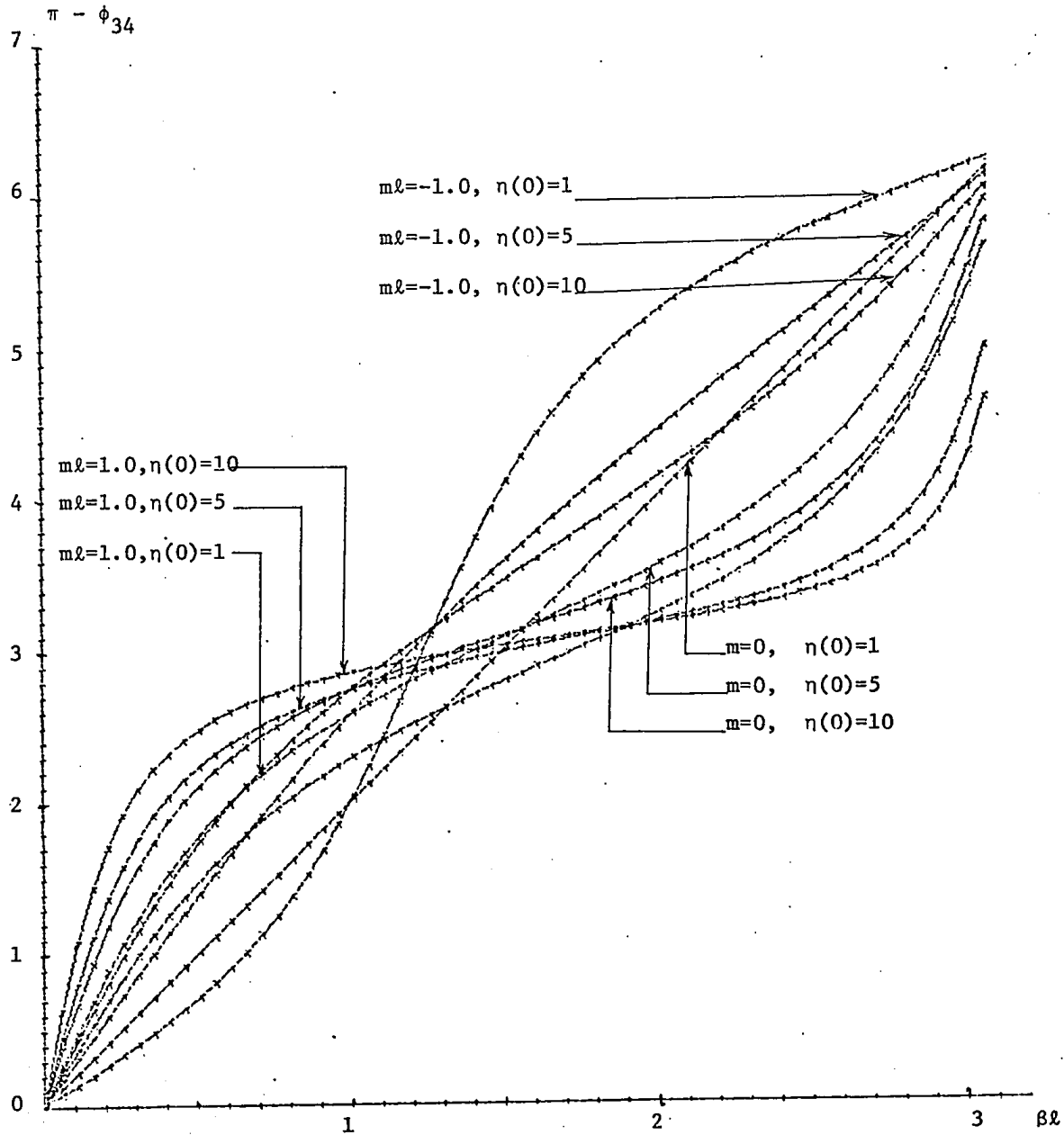


Fig. 4.20: Phase Characteristics of Type IIB CNUTL Folded All-pass Networks
with ELs as Decoupled Lines

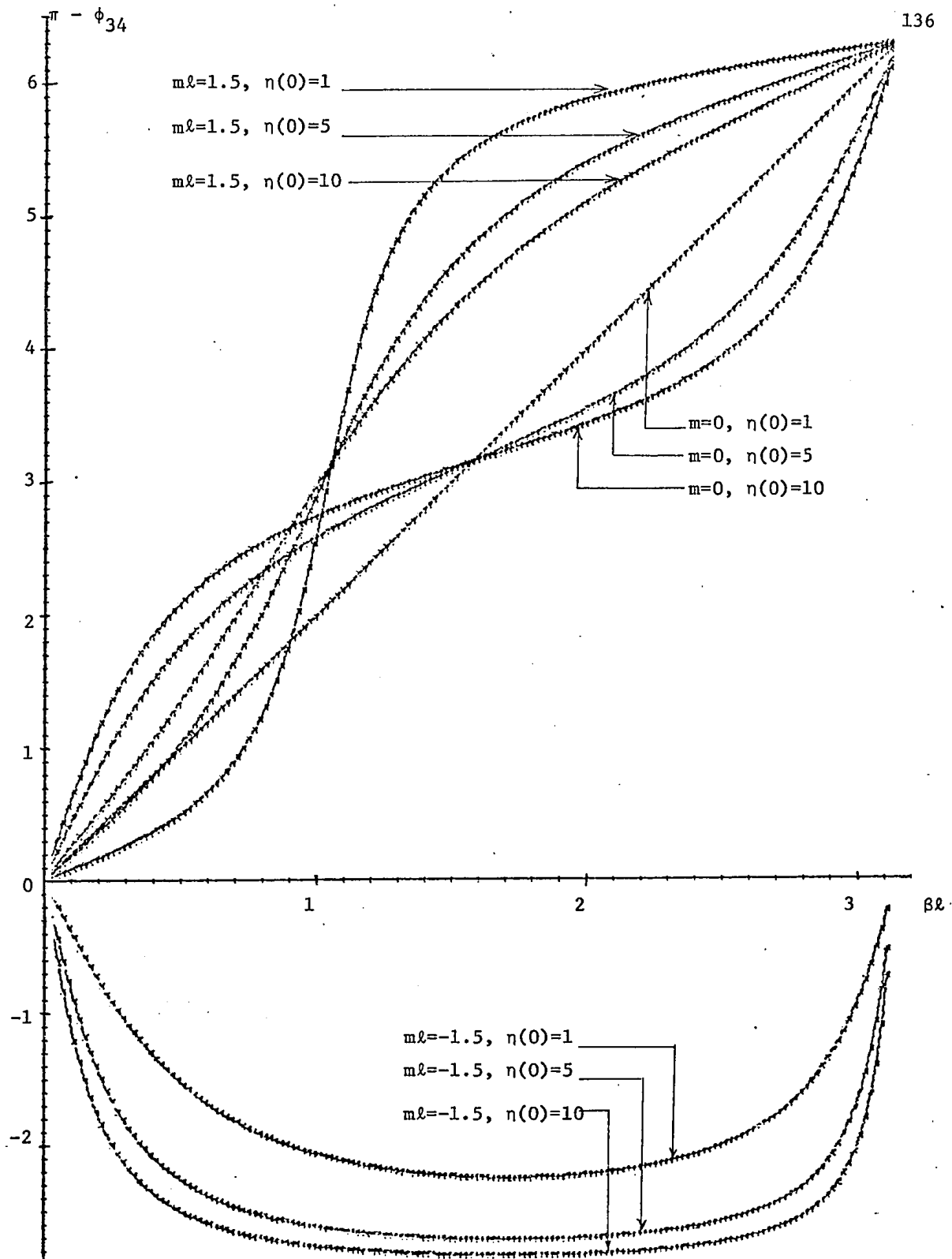


Fig. 4.21: Phase Characteristics of Type IIB CNUTL Folded All-pass Networks with Als as Decoupled Lines

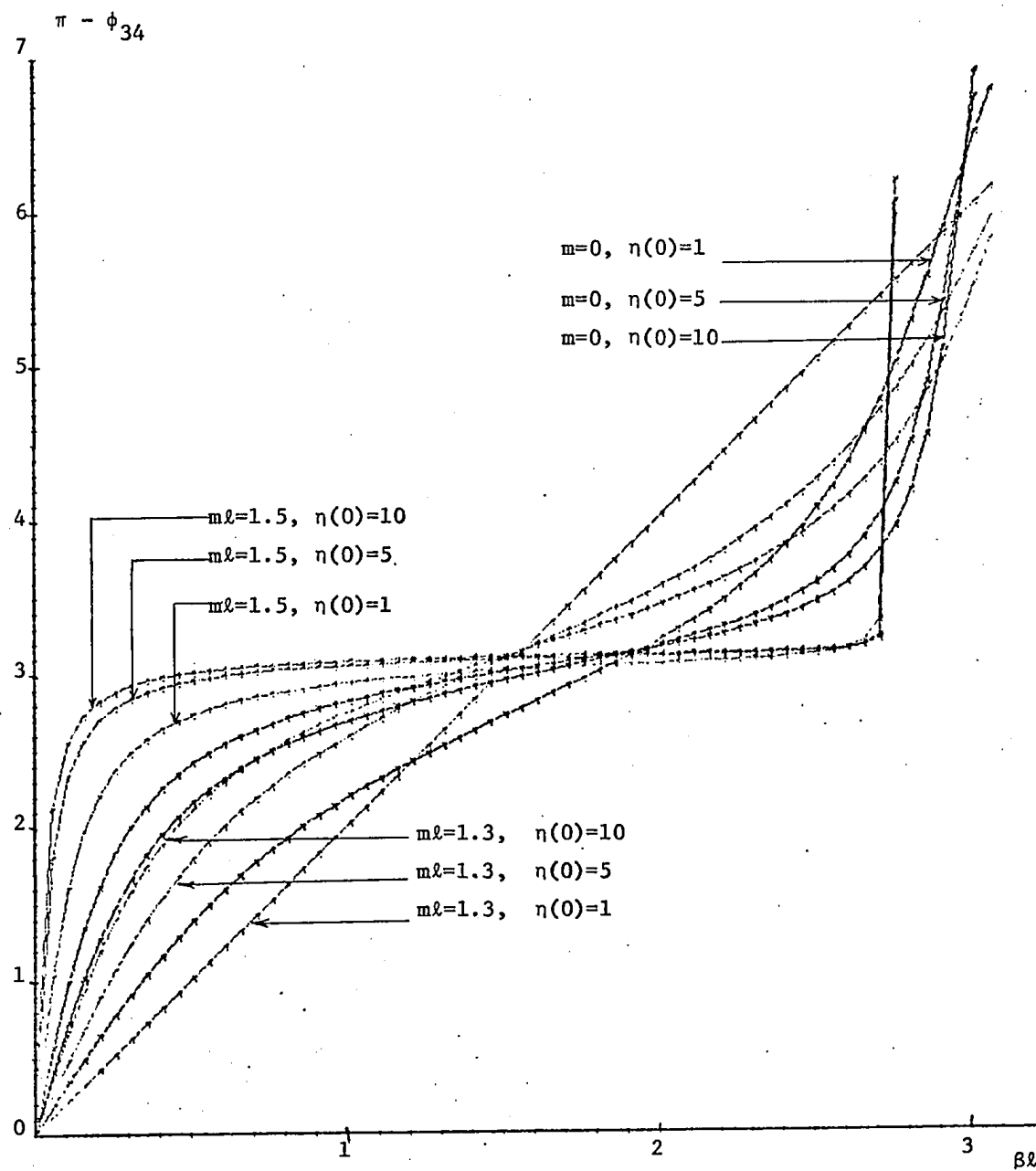


Fig. 4.22: Phase Characteristics of Type IIB CNUTL Folded All-pass Networks
with TLs as Decoupled Lines

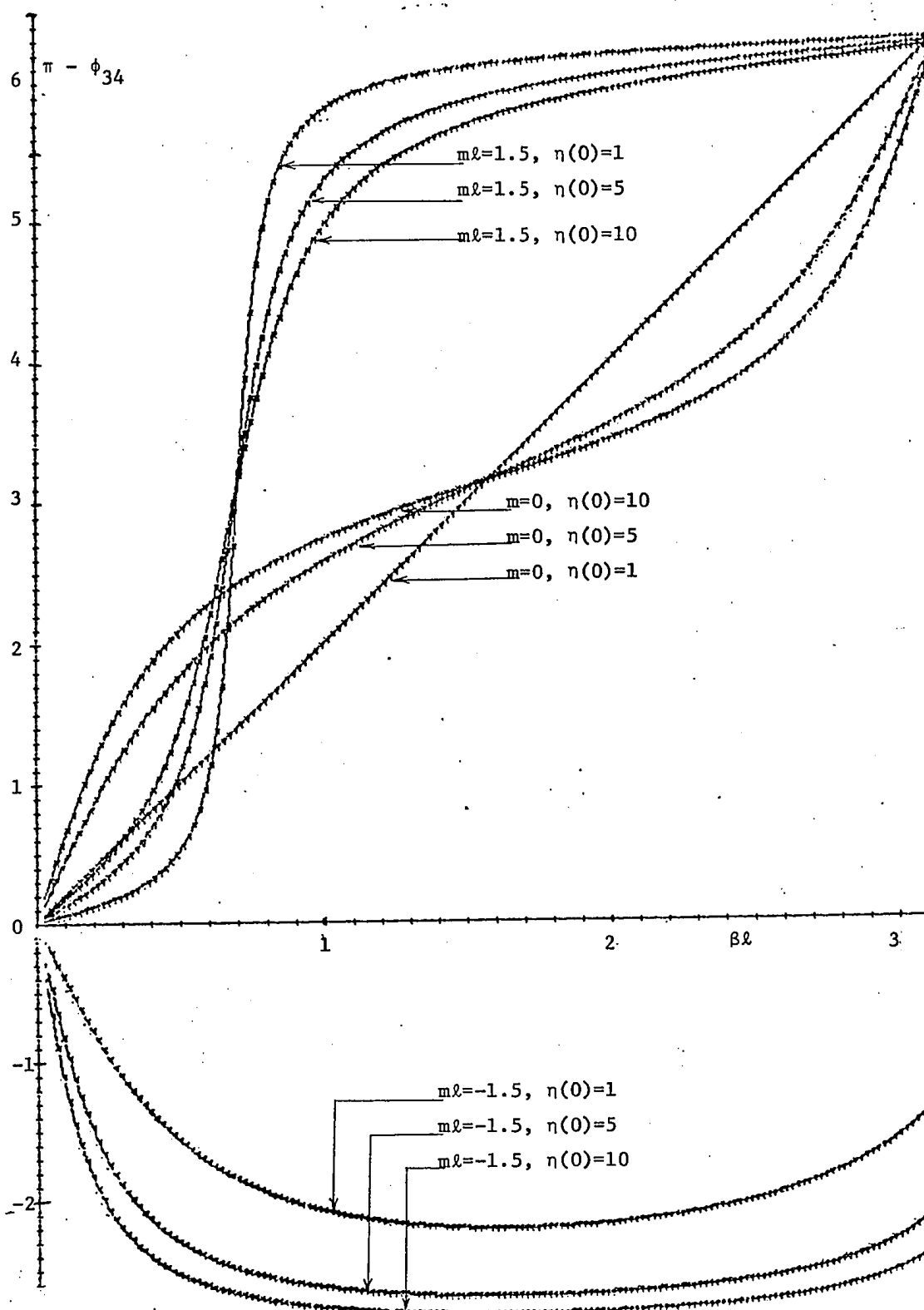


Fig. 4.23: Phase Characteristics of Type IIB CNU TL Folded All-pass Networks with HSSLs as Decoupled Lines

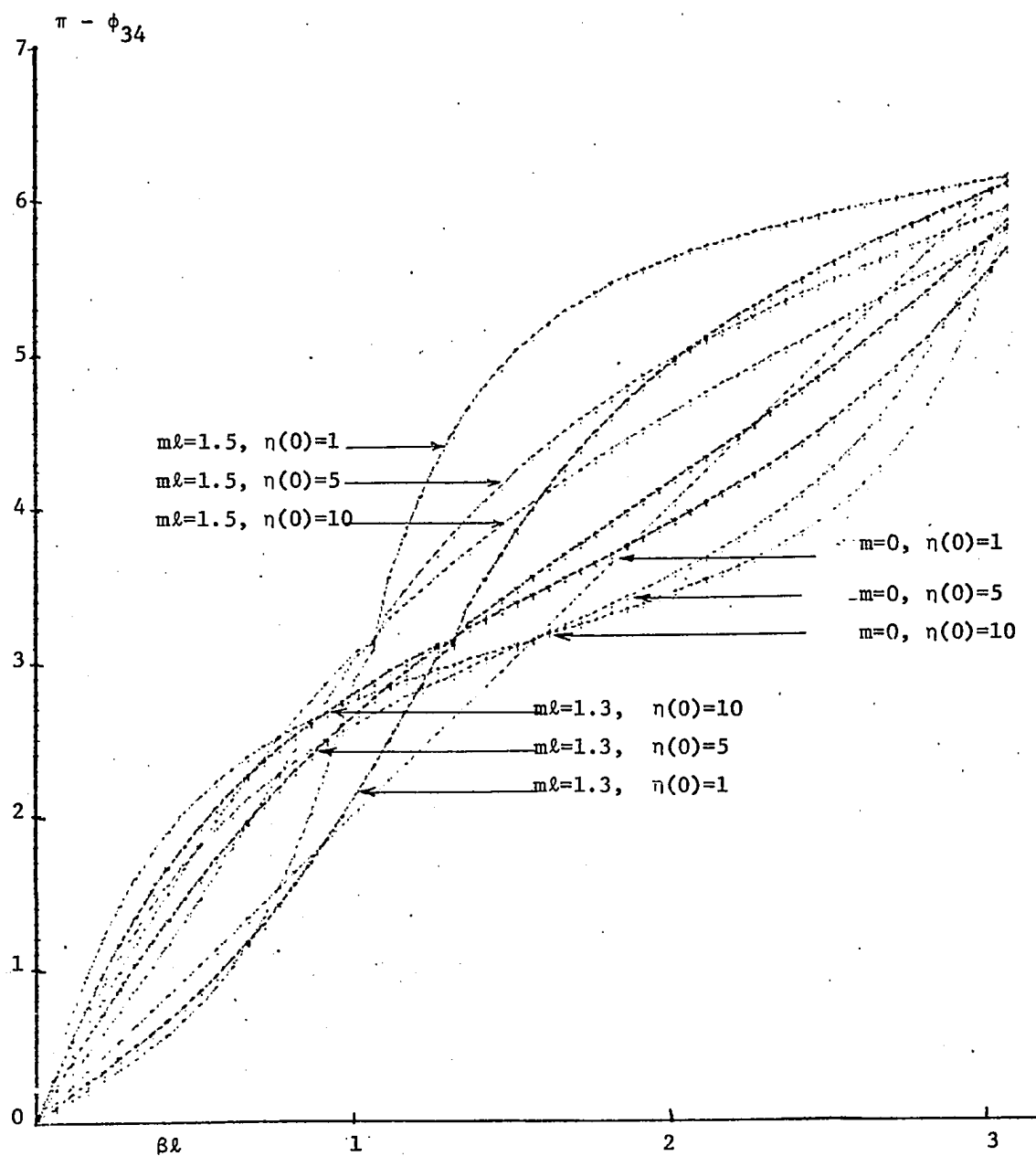


Fig. 4.24: Phase Characteristics of Type IIB CNUTL Folded All-pass Networks
with HCSLs as Decoupled Lines

constant phase shift compensation over a band of frequencies.

It is also noted from these plots that for Types IB and IIA networks with 'Trigonometric' lines as decoupled lines, as well as for Type IA and IIB network with 'Hyperbolic Cosine Squared' lines as decoupled lines, the frequencies at which the phase shift of 180° and 0° respectively occurs is always less than that for a CUTL network. However, for Types IA and IIB networks with 'Trigonometric' lines as decoupled lines, as well as for Type IB and IIA with 'Hyperbolic Cosine Squared' lines as decoupled lines, the frequencies at which the phase shift of 180° and 0° respectively occurs, is always larger than that for a CUTL Network. In particular, constant phase shift over a band of frequencies can be obtained by using 'Algebraic', 'Trigonometric' or 'Hyperbolic Sine Squared' lines as decoupled lines in Type II networks. However, as mentioned earlier, the practical realization of Type II networks require the realization of ideal transformers, which are difficult to build.

4.4.2 Delay Characteristics:

The delay characteristics of CNUTL folded all-pass networks will now be considered. The delay versus frequency function is, by definition⁽³⁴⁾

$$\tau = \frac{d\phi}{d\omega}$$

where ω and ϕ are respectively the angular frequency and phase shift. Let the normalized delay function τ^* be defined as

$$\tau^* = \frac{\tau}{\tau_0} \quad \dots (4.55)$$

where τ_0 is the delay produced when TEM wave propagates along a single uniform transmission line of length 2ℓ (twice the length of the folded network), and is given by

$$\tau_0 = \frac{2\ell}{v} \quad \dots (4.56)$$

v being the velocity of propagation of the TEM wave. From (4.54)-(4.56), the delay τ^* may be expressed as

$$\tau^* = \frac{1}{2} \frac{d\phi}{d(\beta\ell)} \quad \dots (4.57)$$

For the various Type I folded all-pass networks, the normalized delay with frequency are obtained as shown in Figs. 4.25 to 4.34. From these plots, it is found that all these networks provide a larger delay around the frequencies at which the peak delay occurs, than is obtainable with a single uniform delay line of twice the length. The variation in peak height may be accomplished by varying $\eta(0)$, and the position of peak delay by changing the taper. Further, it is found that the folded all-pass Type IB networks provide larger peak delay than that of Type IA. It is also found that Type IB networks with 'Trigonometric' or 'Hyperbolic Sine Squared' lines as decoupled lines provide a larger peak delay than the ones which use other basic lines as decoupled lines. It may also be shown that the delay produced by the Type II networks can easily be obtained by the networks of Type I which do not require ideal transformers

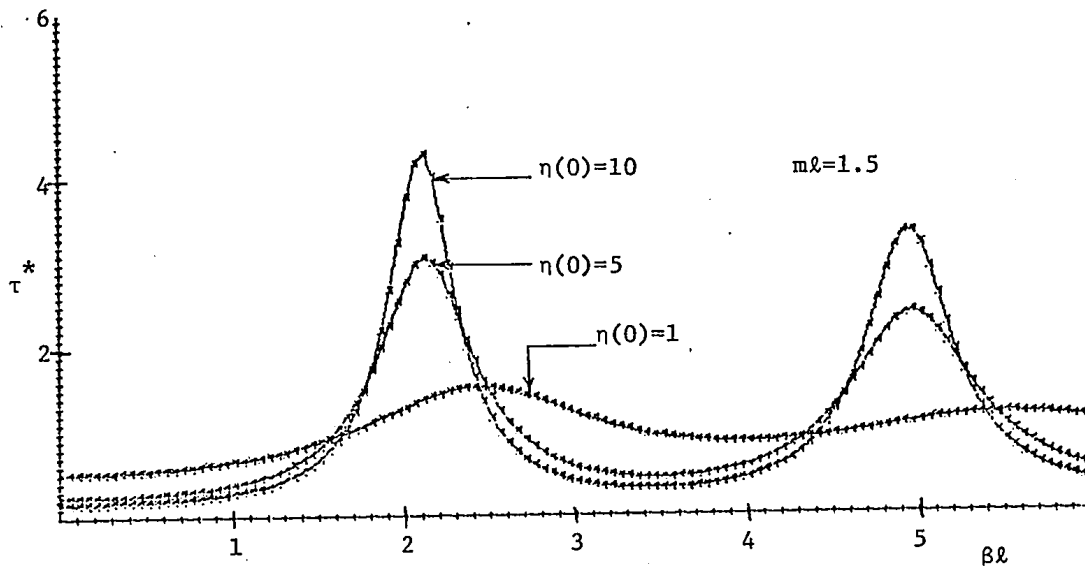


Fig. 4.25: Delay Characteristics of Type IA CNUTL Folded All-pass Networks
with ELs as Decoupled Lines

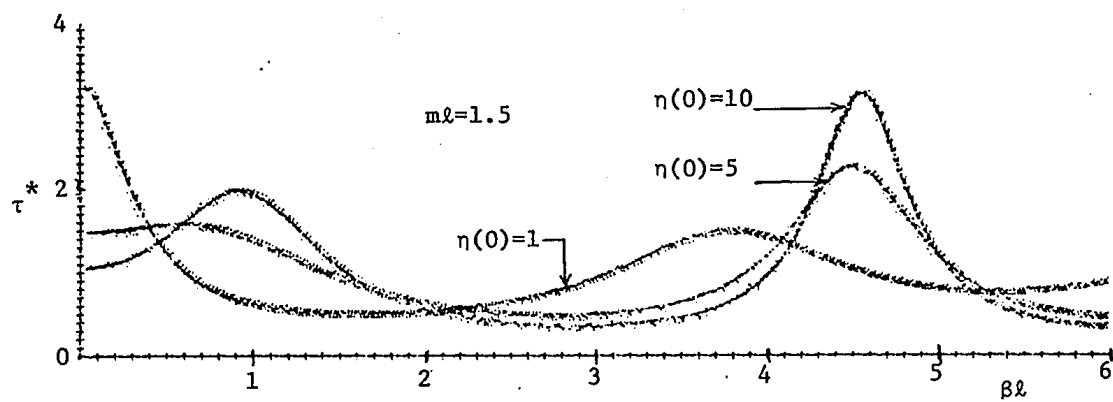


Fig. 4.26: Delay Characteristics of Type IA CNUTL Folded All-pass Networks
with ALs as Coupled Lines

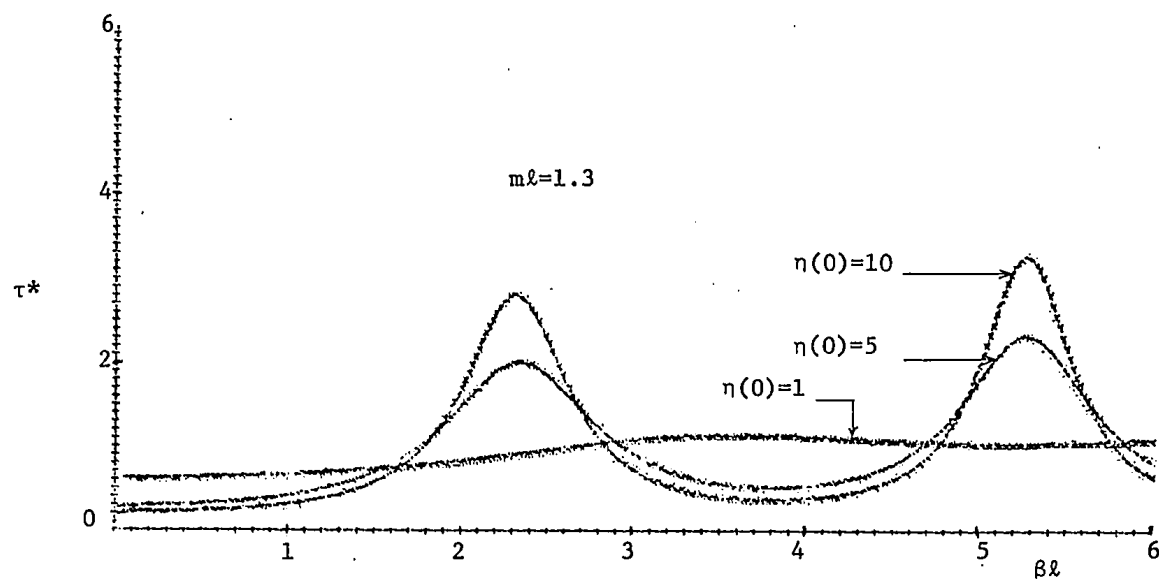


Fig. 4.27: Delay Characteristics of Type IA CNU TL Folded All-pass Networks with TLs as Decoupled Lines

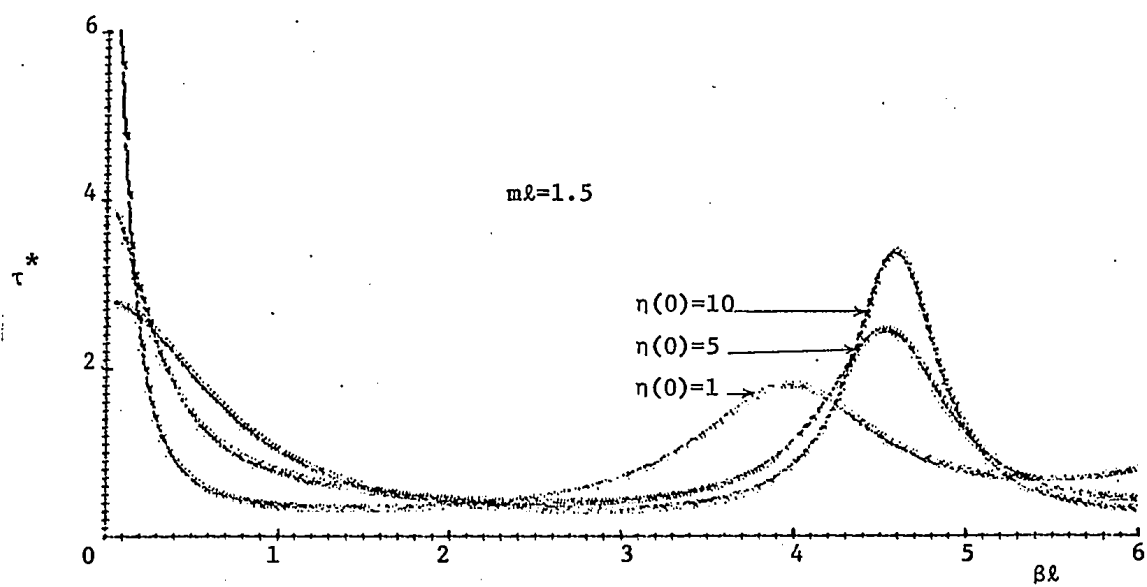


Fig. 4.28: Delay Characteristics of Type IA CNU TL Folded All-pass Networks with HSSLs as Decoupled Lines

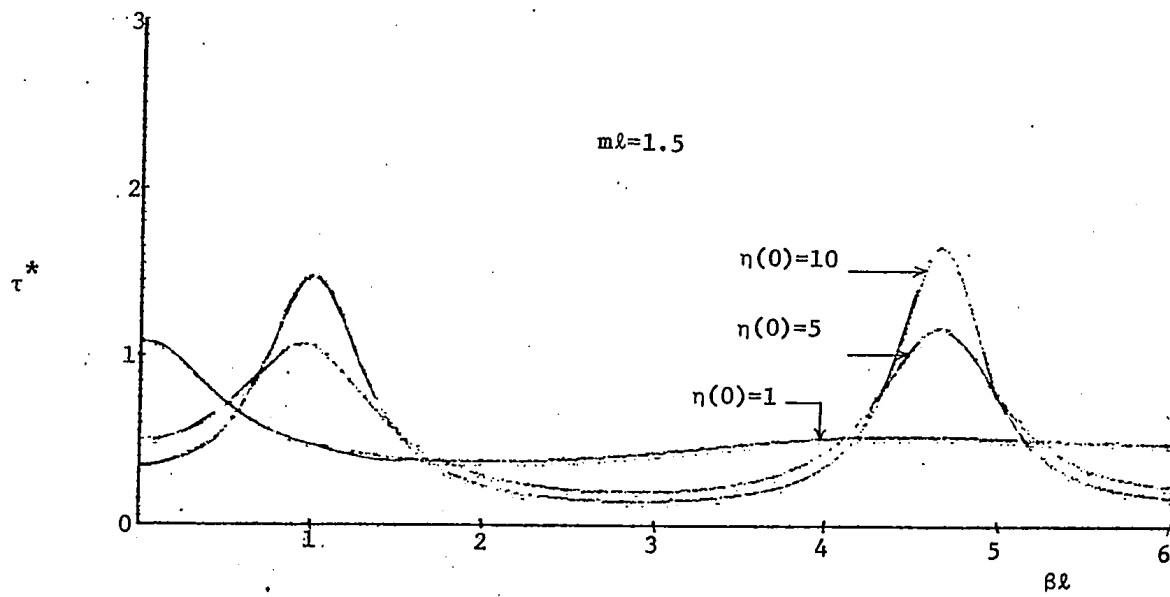


Fig. 4.29: Delay Characteristics of Type IA CNU TL Folded All-pass Networks with HCSLs as Decoupled Lines

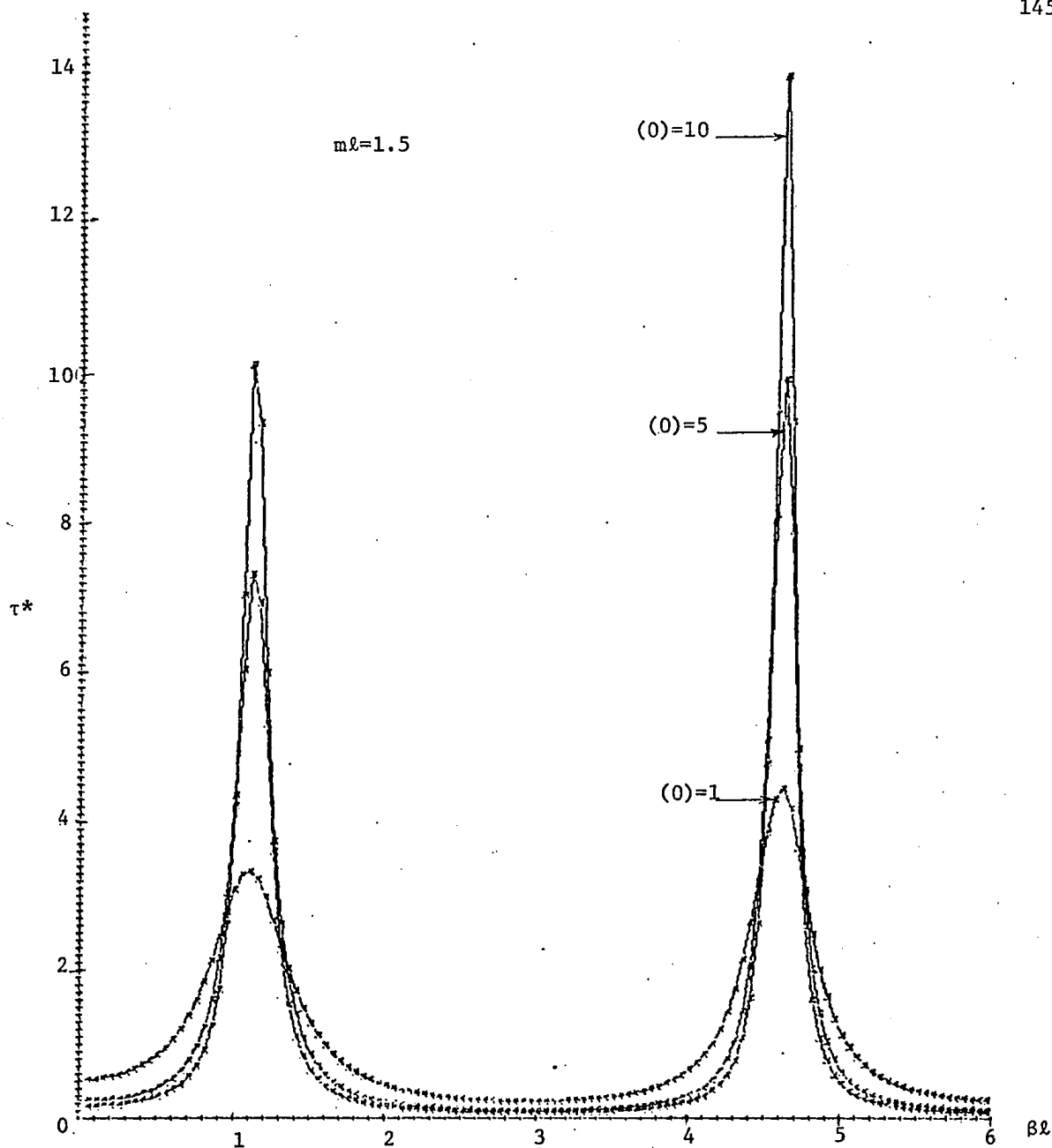


Fig. 4.30: Delay Characteristics of Type IB CNUTL Folded All-pass Networks
with ELs as Decoupled Lines

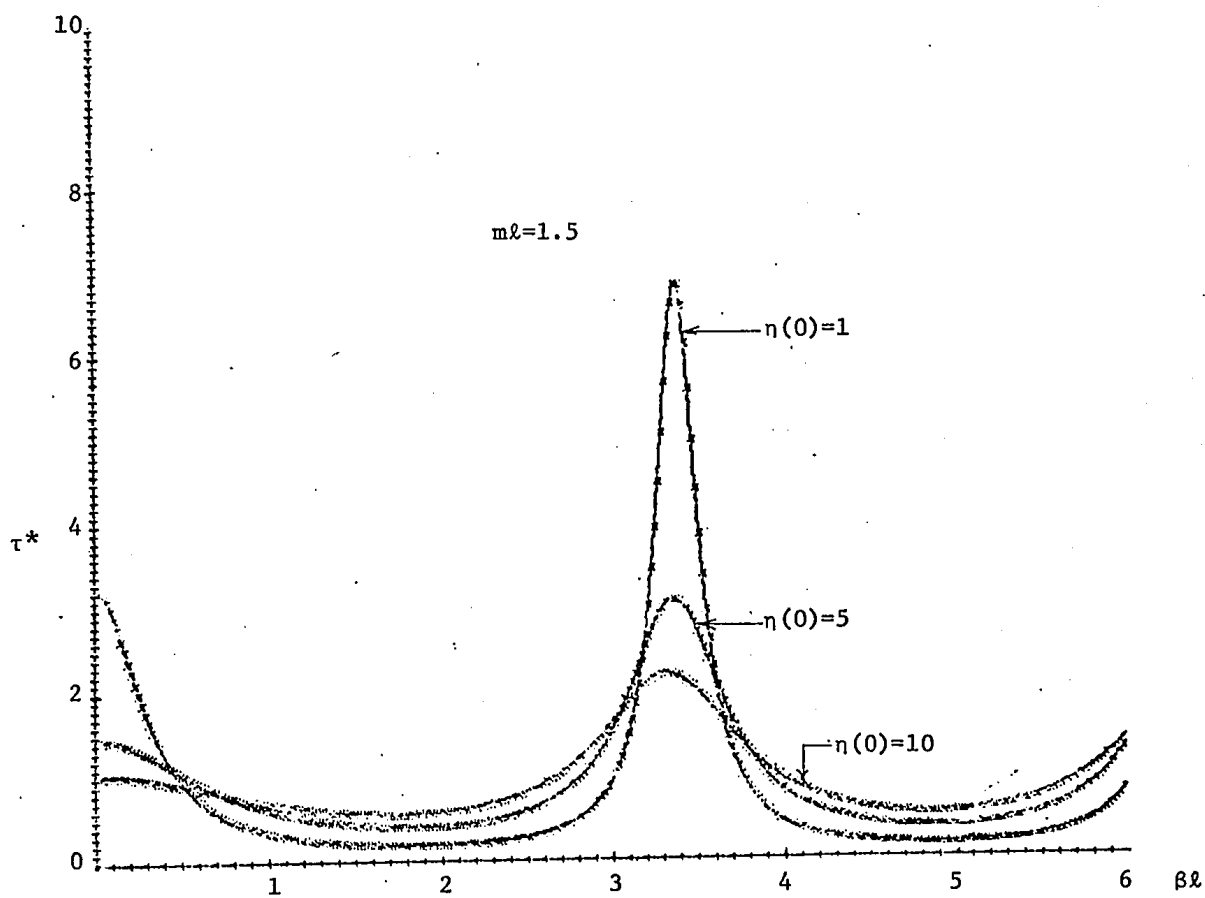


Fig. 4.31: Delay Characteristics of Type IB CNU TL Folded All-pass Networks
with ALs as Decoupled Lines

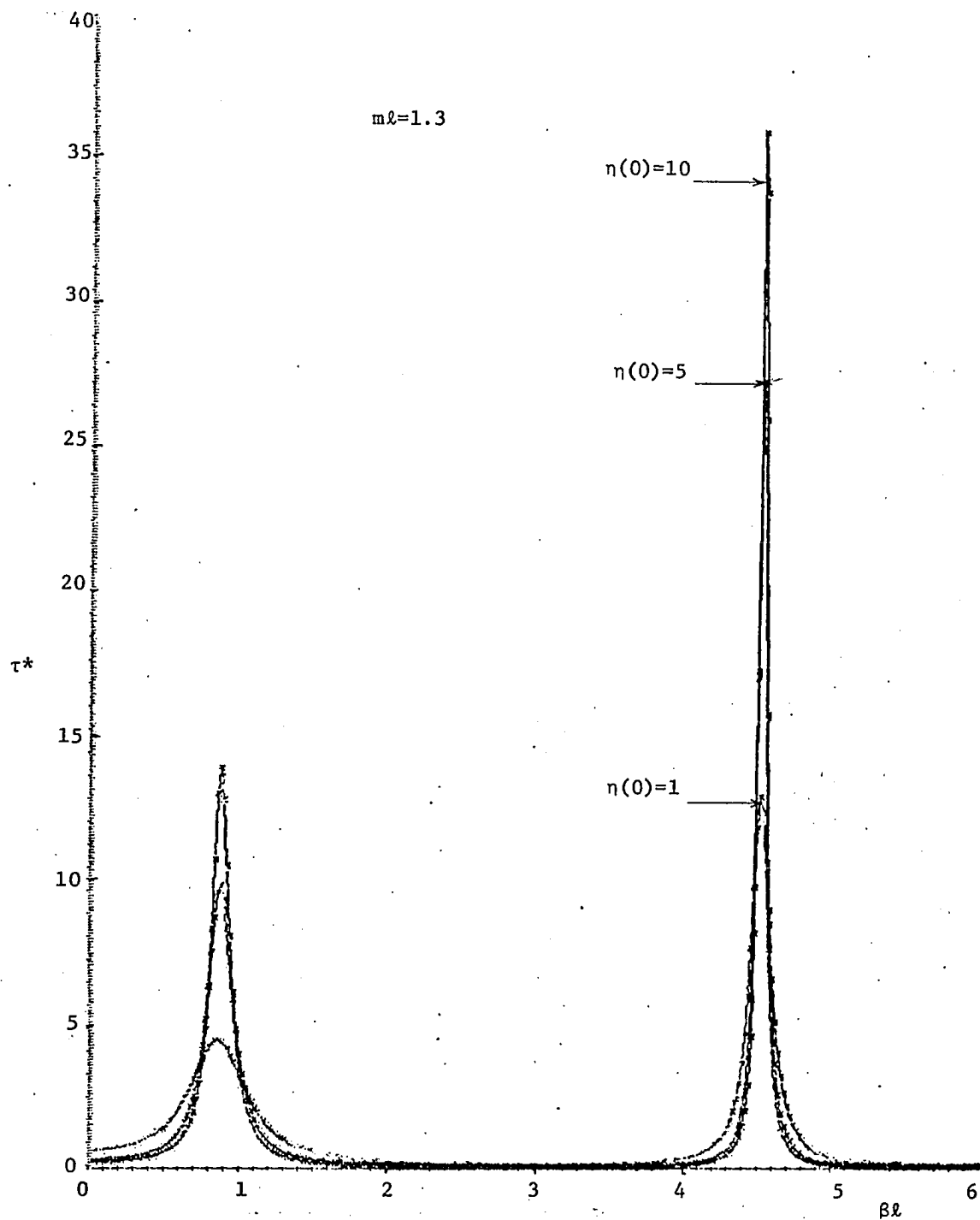


Fig. 4.32: Delay Characteristics of Type IB CNUTL Folded All-pass Networks
with TLs as Decoupled Lines

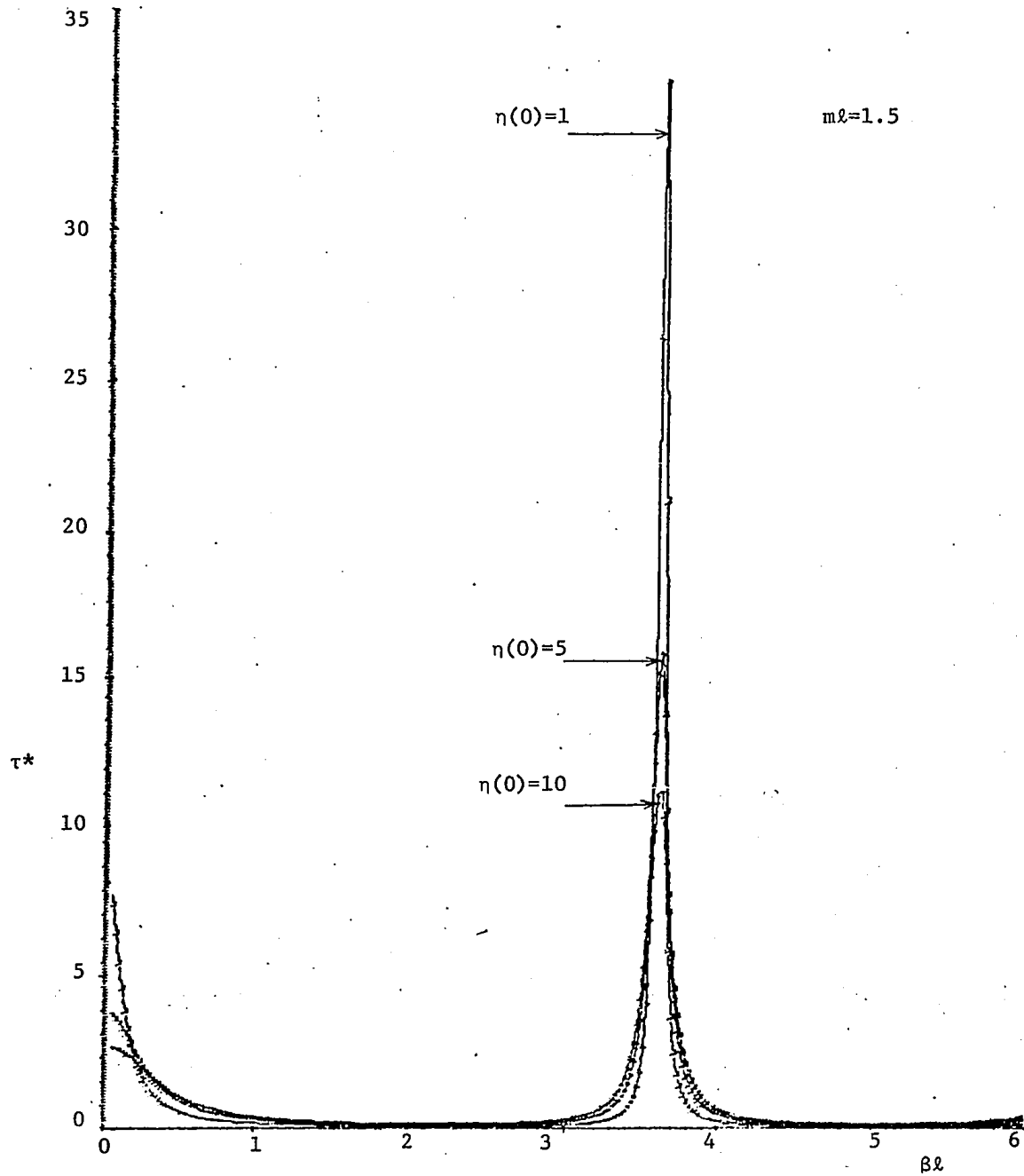


Fig. 4.33: Delay Characteristics of Type IB CNUTL Folded All-pass Networks
with HSSLs as Decoupled Lines

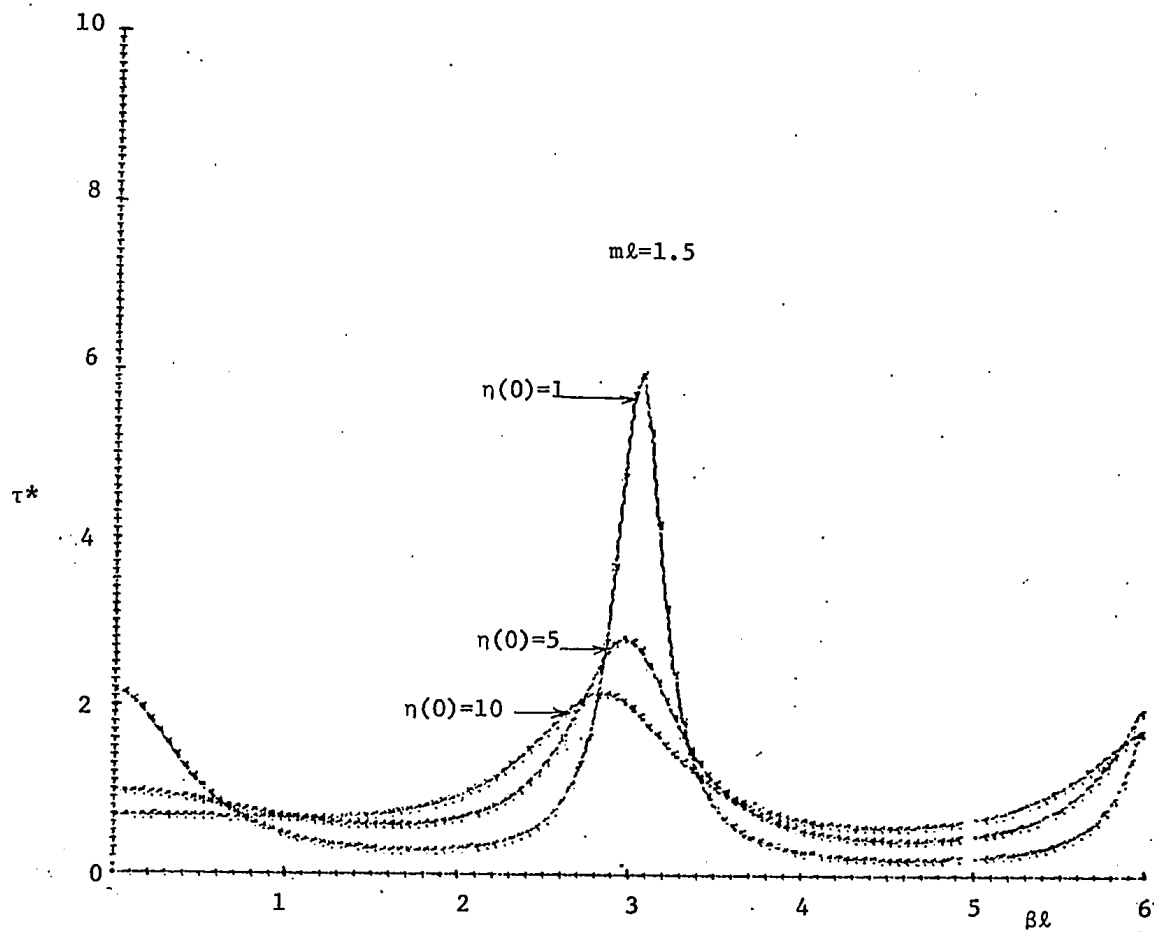


Fig. 4.34: Delay Characteristics of Type IB CNUTL Folded All-pass Networks with HCSLs as Decoupled Lines

and hence their delay characteristics are not included.

Thus, by properly selecting $\eta(0)$ and $m\ell$, CNUTL folded all-pass networks can be effectively used as delay equalizers, which are extremely compact.

4.5 Conclusions:

Various folded all-pass networks have been obtained from a pair of identical lossless CNUTLs by converting them into a two-port network. For these folded all-pass networks, the required conditions to be satisfied by the corresponding decoupled lines have been determined. It has been found that the requirements for Type III networks may be satisfied by using proportional decoupled lines; however, the phase characteristics exhibited by such networks are similar to those of CUTL folded all-pass networks as obtained by Jones and Bolljahan⁽⁵³⁾. It is shown that if dual lines are chosen as decoupled lines, then the corresponding CNUTLs will exhibit all-pass characteristics in both Type I and Type II configurations, provided the ports are suitably terminated. The phase and delay characteristics of such all-pass networks are studied in detail using basic lines with hyperbolic solutions as the decoupled lines. The phase characteristics of Types I and II networks have the following properties:

- (i) The frequency at which the phase shift is 180° may be controlled by changing the taper, while the

phase at other frequencies, by changing $\eta(0)$.

- (ii) The phase shift is fairly constant over a band of frequencies, when Type IB network has 'Trigonometric' or 'Hyperbolic Sine Squared' lines as decoupled lines. Fairly constant phase shift over a band of frequencies may also be obtained from Type II networks by using 'Algebraic' 'Trigonometric' or 'Hyperbolic Sine Squared' lines as decoupled lines. The amount of phase shift can be adjusted by properly selecting the taper and $\eta(0)$.

Further, it has been found that all these networks provide a larger delay around the frequencies at which the peak delay occurs, than is obtainable with a single uniform delay line of twice the length. The height of peak delay may be controlled by varying $\eta(0)$ while the position of peak delay, by changing the taper. The networks with 'Trigonometric' or 'Hyperbolic Sine Squared' lines as decoupled lines in Type IB configuration provide the maximum amount of peak delay.

CHAPTER 5

CONCLUSIONS

A general theory for decoupling a pair of lossless CNUTLs and supporting TEM mode of propagation has been developed. This theory has been applied to study the applications of CNUTLs as directional couplers and folded all-pass networks.

The theory that has been developed reduces the problem of analyzing lossless CNUTLs as a four-port network to that of analyzing two two-port networks. This theory is quite general and is independent of the port terminations, the ratio of wavelength to line size, any symmetry conditions etc. Further, the method is applicable to identical or nonidentical, similar or dissimilar coupled lines. This method also directly relates the line parameters of CNUTLs to those of decoupled lines and vice versa; further the matrix parameters of CNUTLs as a four-port, are explicitly expressed in terms of those of the decoupled lines as two-ports.

Utilizing this theory, CNUTL codirectional and contradirectional couplers with and without impedance transformations have been studied. It has been shown that for CNUTLs to behave as a codirectional coupler, each of the decoupled lines should be proportional line, while for contradirectional coupler action, the two decoupled lines have to be duals of each other. Further, such codirectional (contradirectional) couplers have the property $S_{13} = S_{24}$ ($S_{13} = S_{24}$ and $S_{14} = S_{23}$). It has been found that the coupled line four-port using nonidentical

lossless CNUTLs exhibits an impedance transformation between certain ports along with the directional coupler action. Further, the conditions to be satisfied by the decoupled lines for obtaining smooth electromagnetic transition at one of the ends of a codirectional or contradirectional coupler have been obtained.

The coupling response of codirectional coupler is found to be periodic, while the phase shift between coupled and transmitted signals varies linearly with frequency. Contradirectional couplers are found to exhibit different characteristics depending on the distributions of the decoupled lines. It is shown that a 90° phase shift is obtained by choosing symmetric NUTLs as decoupled lines, while 0° or 180° phase shift may be obtained by choosing one decoupled line to be the same as the other, turned around. These couplers with exponential decoupled lines exhibit band pass coupling response. The coupling response of various contradirectional couplers with smooth transition at one end, for which the decoupled lines are 'basic NUTLs with hyperbolic solutions' have also been studied in detail. It is shown that all these couplers have a high pass response and that the CNUTLs with 'hyperbolic cosine squared' lines as decoupled lines have the best response of all the CNUTLs considered.

Three different types of CNUTL folded all-pass networks have been studied by converting the CNUTL four-port into a two-port by

proper port terminations. The requirements to be satisfied by the chain parameters of the corresponding decoupled NUTLs as two-ports have been derived. It is shown that these conditions may always be met for the first two types, if dual lines are chosen as the decoupled lines, while, for the third type, the decoupled lines are, in addition, proportional. The phase and delay characteristics of these three types have been investigated, when the decoupled lines are basic lines with hyperbolic solutions. It is found that, in Types I and II networks, the frequency at which the phase shift is 180° may be controlled by changing $\eta(0)$. Further, these networks can provide delays larger than that obtainable from a single uniform line of twice the length. Of all the lines considered, the peak delay is found to be maximum when the decoupled lines are chosen to be 'trigonometric' or 'hyperbolic sine squared' lines.

As has been pointed out above, it was possible to obtain only a partial solution regarding the decoupled line distributions, for the corresponding CNUTL to behave as an all-pass network. It should be interesting to see if a general solution should be obtained for the same. The author also feels that further worthwhile investigations could be carried out in the area of coupled nonuniform transmission line networks. The coupling response of CNUTL contradirectional couplers with exponential symmetric lines has recently been obtained⁽³⁴⁾. The coupling response of other CNUTL contradirectional couplers having 'basic symmetric NUTLs' with hyperbolic solutions as decoupled

lines should be investigated in an attempt to find the response which yields optimum results. It is also worthwhile to study the phase and delay characteristics of folded all-pass networks with other symmetric NUTLs as decoupled lines. It should be worthwhile to investigate the possibility of using CNUTLs as other TEM components such as Magic-T, filters, hybrid networks, etc. Finally, it should be possible to extend the decoupling theory described in the thesis for a pair of CNUTLs, to n-pairs of CNUTLs and consider its applications to multiport TEM networks.

REFERENCES

1. C.G. Montgomery, R.H. Dicke and E.M. Purcell, Principles of Microwave Circuits, Radiation Laboratory Series, Vol. 8, McGraw-Hill Book Co., 1948.
2. A. Alford, Coupled Networks in Radio Frequency Circuits, Proc. IRE, Vol. 29, No. 2, pp. 55-70, February, 1941.
3. R.N. Ghose, Microwave Circuit Theory and Applications, McGraw-Hill Book Co., 1963.
4. R.H. Duhamel and D.E. Isbell, Broadband Logarithmically Periodic Antenna Structures, IRE National Convention Record, Part. 5, pp. 119, 1957.
5. R. Levy, Transmission Line Directional Couplers for Very Broadband Operation, Proc. IEE, Vol. 112, No. 3, pp. 469-476, March, 1965.
6. J.D. Ryder, Networks, Lines and Fields, Prentice-Hall Inc., 1955.
7. G.L. Matthaei, L. Young and E.M. Jones, Microwave Filters, Impedance Matching Networks and Coupling Structures, McGraw-Hill Book Co., 1963.
8. H. Ozaki and J. Ishi, Synthesis of Transmission Line Networks and the Design of UHF Filters, IRE Trans. on Circuit Theory,

- Vol. CT-2, No. 4, pp. 325-356, December, 1955.
9. A. Matasumoto, Microwave Filters and Circuits, Academic Press, 1970.
 10. A.I.Grayzel, A Synthesis Procedure for Transmission Line Networks, IRE Trans. on Circuit Theory, Vol. CT-5, No. 4, pp. 172-181, September, 1958.
 11. B.K. Kinariwala, Theory of Cascaded Transmission Lines, Proc. Polytechnic Institute of Brooklyn Symposium on Generalized Networks, Vol. XVI, pp. 345-352, 1966.
 12. G.L.Matthaei, Short Step Chebyshev Impedance Transformer, IEEE Trans. on Microwave Theory and Techniques, Vol. MTT-14, No. 8, pp 372-383, August, 1966.
 13. C.S. Gledhill and M.H. Issa, Exact Solutions of Stepped Impedance Transformer having Maximally Flat and Chebyshev Characteristics, IRE Trans. on Microwave Theory and Techniques, Vol. MTT-17, No. 7, pp. 379-386, July, 1969.
 14. J.E. Holte and R.F. Lambert, Synthesis of Stepped Acoustic Transmission Systems, Journal of Acoustical Society of America, Vol. 34, No. 5, pp. 289-301, March, 1961.
 15. B.B. Bhattacharyya, Some General Properties and Solutions of Nonuniform Transmission Lines, Ph. D Thesis, Nova Scotia

Technical College, 1968..

16. E.N. Protonotarios and O. Wing, Analysis and Intrinsic Properties of the General Nonuniform Line, IEEE Trans. on Microwave Theory and Techniques, Vol. MTT-15, No. 3, pp. 142-150, March, 1967.
17. D.C. Youla, Analysis and Synthesis of Arbitrarily Terminated Lossless Nonuniform Lines, IEEE Trans. on Circuit Theory, Vol. CT-11, No. 4, pp. 363-372, September, 1964.
18. H. Kaufman, Bibliography of Nonuniform Transmission Lines, IRE Trans. on Antenna and Propagation, Vol. AP-3, No. 10, pp. 218-220, October, 1955.
19. S. Ballantine, Nonuniform Lumped Electrical Lines, Journal of Franklin Institute, Vol. 203, No. 4, pp. 561-582, April, 1927.
20. J.W. Arnold and R.F. Bechberger, Sinusoidal Currents in Linearly Tapered Loaded Transmission Lines, Proc. IRE, Vol. 19, No. 2, pp. 304-310, February, 1931.
21. G.N. Tsandoulas, The Linearly Tapered Lines as a Matching Section - High and Low Frequency Behaviour, Proc. IEEE, Vol. 55, No. 9, pp. 1958-1959, September, 1967.
22. H.J. Scott, The Hyperbolic Transmission Line as Matching Section, Proc. IRE, Vol. 41, No. 11, pp. 1654-1657, November, 1953.

23. R.F.H. Young, Parabolic Transmission Line, Proc. IRE, Vol. 43, No. 8, pp. 1010, August, 1955.
24. C.R. Burrows, The Exponential Transmission Lines, Bell System Technical Journal, Vol. 17, No. 10, pp. 555-573, October, 1938.
25. V. Ramachandran, Some Studies on Exponential Transmission Lines, Ph. D Thesis, Indian Institute of Science, Bangalore, 1964.
26. R.W. Klopfenstein, A Transmission Line of Improved Design, Proc. IRE, Vol. 44, No. 1, pp. 31-35, January, 1956.
27. R.E. Collin, The Optimum Tapered Transmission Line Matching Section, Proc. IRE, Vol. 44, No. 4, pp. 534-548, April, 1956.
28. C.P. Womack, The Use of Exponential Transmission Lines in Microwave Components, IRE Trans. on Microwave Theory and Techniques, Vol. MTT-11, No. 3, pp. 124-132, March, 1962.
29. D.B. Large, Synthesis of a Transmission Line Resonator with a Specified Frequency Spectrum, Proc. IEEE, Vol. 52, No. 5, pp. 633-634, May, 1964.
30. L. Gruner, Synthesis of a Transmission Line Resonator with a Specified Frequency Spectrum, Proc. IEEE, Vol. 53, No. 5, pp. 502-503, May, 1965.

31. S. Yamamoto, Equivalent Nonuniform Transmission Line Type Pulser, Proc. IEEE, Vol. 56, No. 9, pp. 1640-1641, September, 1968.
32. I. Jacobs, The Nonuniform Transmission Line as a Broadband Termination, Bell System Technical Journal, Vol. 37, No. 4, pp. 913-924, April, 1958.
33. R.T. Pederson, A Study of Basic Lossless Symmetric Lines with Hyperbolic Solutions, M.S.Thesis, University of Calgary, 1970.
34. S. Yamamoto, T. Azakami and K. Itakura, Coupled Nonuniform Transmission Lines and its Applications, IEEE Trans. on Microwave Theory and Techniques, Vol. MTT-15, No. 4, pp. 220-231, April, 1967.
35. G.D. Monteath, Coupled Transmission Lines as Symmetrical Directional Couplers, Proc. IEE, Vol. 43, No. 3, pp. 383-392, May, 1955.
36. S.O. Scanlan and J.D. Rhodes, Microwave All-pass Networks, Part I, IEEE Trans. on Microwave Theory and Techniques, Vol. MTT-16, No. 2, pp. 62-72, February, 1968.
37. S.O. Scanlan and J.D. Rhodes, Microwave All-pass Networks, Part II, IEEE Trans. on Microwave Theory and Techniques, Vol. MTT-16, No. 2, pp. 72-79, February, 1968.

38. S.B. Cohn, Characteristic Impedance of the Shielded Strip Transmission Lines, IRE Trans. on Microwave Theory and Techniques, Vol. MTT-2, No. 7, pp. 52-57, July, 1954.
39. S.B. Cohn, Shielded Coupled Strip Transmission Line, IRE Trans. on Microwave Theory and Techniques, Vol. MTT-3, No. 10, pp. 29-38, October, 1955.
40. S.B. Cohn, Thickness Correction for Capacitive Obstacle and Strip Conductors, IRE Trans. on Microwave Theory and Techniques, Vol. MTT-8, No. 11, pp. 638-644, November, 1960.
41. W.J. Getsinger, Coupled Rectangular Bars between Parallel Plates, IRE Trans. on Microwave Theory and Techniques, Vol. MTT-10, No. 1, pp. 65-72, January, 1962.
42. J.D. Horgan, Coupled Strip Transmission Lines with Rectangular Inner Conductors, IRE Trans. on Microwave Theory and Techniques, Vol. MTT-5, No. 4, pp. 92-99, April, 1957.
43. W.J. Getsinger, A Coupled Stripline Configuration using Printed Circuit Construction that allows Very Close Coupling, IRE Trans. on Microwave Theory and Techniques, Vol. MTT-9, No. 11, pp. 542-553, November, 1961.
44. S. Yamamoto, T. Azakami and K. Itakura, Slit Coupled Transmission Lines, IRE Trans. on Microwave Theory and Techniques, Vol. MTT-14, No. 11, pp. 542-553, November, 1966.

45. E.G. Cristal, Coupled Circular Cylindrical Rods between Parallel Ground Planes, IRE Trans. on Microwave Theory and Techniques, Vol. MTT-12, No. 7, pp. 428-439, July, 1964.
46. S.B. Cohn, Characteristic Impedance of Broadside Coupled Strip Transmission Lines, IRE Trans. on Microwave Theory and Techniques, Vol. MTT-8, No. 11, pp. 633-637, November, 1960.
47. L. Young, Advances in Microwaves, Vol. 4, Academic Press, 1966.
48. H.A. Wheeler, Transmission Line Properties of Parallel Strips separated by a Dielectric Sheet, IEEE Trans. on Microwave Theory and Techniques, Vol. MTT-13, No. 3, pp. 172-185, March, 1965.
49. J.I. Smith, The Even and Odd Mode Capacitance Parameters for Coupled Lines in Suspended Substrate, presented at the G. MTT International Microwave Symposium, Dallas, Texas, 1969.
50. F. Arndt, Ultra-broadband Transmission Line 90° Directional Couplers, Electronics Letters, Vol. 6, No. 13, pp. 418-419, June, 1970.
51. F. Arndt, High Pass Transmission Line Directional Coupler,

- IEEE Trans. on Microwave Theory and Techniques, Vol. MTT-16,
No. 5, pp. 310-311, May, 1968.
52. B.M. Oliver, Directional Electromagnetic Coupler, Proc.
IRE, Vol. 42, No. 11, pp. 1686-1692, November, 1954
53. E.M.T. Jones and J.T. Bolljahan, Coupled Stripline Filters
and Directional Couplers, IEEE Trans. on Microwave Theory
and Techniques, Vol. MTT-4, No. 4, pp. 75-81, April, 1956.
54. J. Reed and G.J. Wheeler, A Method of Analysis of Symmetrical
4-port Networks, IEEE Trans. on Microwave Theory and Techni-
ques, Vol. MTT-4, No. 4, pp. 246-255, October, 1956.
55. E.G. Cristal, Coupled Transmission Line Directional Couplers
with Coupled Lines of Unequal Characteristic Impedances,
IEEE Trans. on Microwave Theory and Techniques, Vol. MTT-14,
No. 7, pp. 337-346, July, 1966.
56. J.K. Shimizu and E.M.T. Jones, Coupled Transmission Line
Directional Couplers, IEEE Trans. on Microwave Theory and
Techniques, Vol. MTT-6, No. 11, pp. 405-410, October, 1958.
57. P.P. Toullos and A.C. Todd, Synthesis of Symmetrical TEM
Mode Directional Couplers, IEEE Trans. on Microwave Theory
and Techniques, Vol. MTT-13, No. 9, pp. 536-544, September,
1965.
58. E.G. Cristal and L. Young, Theory and Tables of Optimum

- Symmetrical TEM Mode Coupled Transmission Line Directional Couplers, IEEE Trans. on Microwave Theory and Techniques, Vol. MTT-13, No. 5, pp. 544-553, September, 1965.
59. L. Young, The Analytical Equivalence of TEM Mode Directional Couplers and Transmission Line Stripped Impedance Filters, Proc. IEE, Vol. 110, No. 2, pp. 275-289, February, 1963.
60. R. Levy, General Synthesis of Asymmetric Multielement Coupled Transmission Line Directional Couplers, IEEE Trans. on Microwave Theory and Techniques, Vol. MTT-11, No. 7, pp. 226-237, July, 1963.
61. C.B. Sharp, An Equivalence Principle for Nonuniform Transmission Line Directional Couplers, IEEE Trans. on Microwave Theory and Techniques, Vol. MTT-15, No. 7, pp. 398-405, July, 1967.
62. J.E. Dalley, A Strip Line Directional Coupler Utilizing a Non-Homogeneous Dielectric Medium, IEEE Trans. on Microwave Theory and Techniques, Vol. MTT-17, No. 9, pp. 706-712, September, 1969.
63. C.P. Tresselt, The Design and Construction of Broadband High Directivity 90° Couplers using Nonuniform Line Techniques, IEEE Trans. on Microwave Theory and Techniques, Vol. MTT-14, No. 12, pp. 647-656, December, 1966.
64. C.P. Tresselt, Design and Computed Theoretical Performance

- of Three Classes of Equiripple Nonuniform Line Couplers,
IEEE Trans. on Microwave Theory and Techniques, Vol. MTT-17,
No. 4, pp. 218-230, April, 1969.
65. H.E. Kallmann, Equalized Delay Lines, Proc. IRE, Vol. 34,
No. 9, pp. 646-657, September, 1950.
66. R.A. Erickson and H. Somner, The Compensation of Delay
Distortion in Video Delay Lines, Proc. IRE, Vol. 38, No. 9,
pp. 1036-1040, September, 1950.
67. W.J.D. Steenart, The Synthesis of Coupled Transmission Line
All-pass Networks in Cascade of 1 to n, IEEE Trans. on
Microwave Theory and Techniques, Vol. MTT-11, No. 1,
pp 23-29, January, 1962.
68. D.I. Karker, Asymmetric Coupled Transmission Line Magic T,
IEEE Trans. on Microwave Theory and Techniques, Vol. MTT-12,
No. 6, pp. 595-599, November, 1964.
69. E.M.T. Jones, Wideband Stripline Magic T, IEEE Trans. on
Microwave Theory and Techniques, Vol. MTT-8, No. 3, pp.
March, 1960.
70. B.M. Shifman, A New Class of Broadband Microwave 90°
Phase Shifters, IRE Trans. on Microwave Theory and
Techniques, Vol. MTT-6, No. 4, pp. 232-237, April, 1958.
71. R.H. Duhamel and M.E. Armstrong, A Wideband Monopulse

Antenna utilizing the Tapered Line Magic T, Report of Hughes Aircraft Company Ground System Corporation, Fullerton, California, 1965.

72. H.G. Pascalar, Stripline Hybrid Junctions, IRE Trans. on Microwave Theory and Techniques, Vol. MTT-5, No. 1, pp. 23-30, January 1957.
73. N. Nagai and A. Matsumoto, Application of Multiwire Networks to a Distributed Hybrid Network, Journal of Inst. Elect. and Commn. Engg. Japan, Vol. 51, No. 3, pp. 11-19, March, 1968.
74. R.B. Eking, A New Method of Synthesizing Matched Broadband TEM Mode Three-ports, IEEE Trans. on Microwave Theory and Techniques, Vol. MTT-19, No. 1, pp. 81-88, January, 1971.
75. R.P. Tetarenko, Broadband Properties of a Class of TEM Mode Hybrids, M.Sc. Thesis, Dept. of Elec. Engg., University of Alberta, Edmonton, 1970.
76. W.K. Roberts, A New Wideband Balun, Proc. IRE, Vol. 50, No. 12, pp. 1628-1631, December, 1957.
77. N. Nagai, and A. Matsumoto, Application of Distributed Constant Network Theory to Balun Transformers, Journal of Inst. Elect. and Commn. Engg., Japan, Vol. 50, No. 5, pp. 114-121, May, 1967.

78. S.B. Cohn, Parallel Coupled Transmission Line Resonator Filters, IRE Trans. on Microwave Theory and Techniques, Vol. MTT-6, No. 4, pp. 223-231, April, 1958.
79. S.B. Cohn, Direct Coupled Resonator Filters, Proc. IRE, Vol. 50, No. 2, pp. 187-196, February, 1957.
80. E.G. Vlostovskiy, Theory of Coupled Transmission Lines, Telecommunication and Radio Engg., Vol. 18, No. 4, pp. 595-599, April, 1964.
81. H. Anemiy, Time Domain Analysis of Multiple Parallel Transmission Lines, RCA Review, Vol. 28, No. 2, pp. 241-276, June, 1967.
82. D.C. Youla, An Introduction to Coupled Line Network Theory - Part I, PIBMRI Memorandum No. 54, October, 1961.
83. G.I. Zysman and A.K. Johnson, Coupled Transmission Line Networks in an Homogeneous Medium, IEEE Trans. on Microwave Theory and Techniques, Vol. MTT-17, No. 10, pp. 753-759, October, 1969.
84. H. Ozaki and J. Ishi, Synthesis of a Class of Stripline Filters, IRE Trans. on Circuit Theory, Vol. CT-5, No. 2, pp. 104-109, June, 1958.
85. Vaclav Dvorak, Numerical Solution of the Transient Response of a Distributed Parameter Transformer, IEEE Trans. on

Circuit Theory, Vol. CT-17, No. 2, pp. 270-273, May, 1970.

86. M.N.S. Swamy, B.B. Bhattacharyya and S.N. Verma, A General Theory for the Decoupling of Coupled Tapered Lines and Its Applications to Directional Couplers, Proc. of the 15th Midwest Symposium on Circuit Theory, University of Missouri, Rolla, pp. XIV.6.1 to XIV.6.10, May, 1972.
87. E.N. Protonotarios and O. Wing, Delay and Rise Time of Arbitrary Tapered RC Transmission Lines, IEEE International Convention Record, Part 7, pp. 1-7, 1965.
88. M.N.S. Swamy, Matrix Parameters of an Arbitrary Tapered RC Lines, Proc. of Mid-American Electronic Conference, pp. 72-82, 1965.
89. S.C. Dutta Roy, Matrix Parameters of Nonuniform Transmission Lines, IEEE Trans. on Circuit Theory, Vol. CT-12, No. 1, pp. 142-143, March, 1965.
90. M.N.S. Swamy and B.B. Bhattacharyya, On Nonuniform RCG Lines, IEE Conference Publication, No. 23, pp. 228-243, September, 1966.
91. B.B. Bhattacharyya and M.N.S. Swamy, Interrelationships among the Chain Matrix Parameters of a Nonuniform Transmission Line, Proc. IEEE, Vol. 54, No. 10, pp. 1763-1764, October, 1967.

92. M.N.S. Swamy, J. Walsh, J.C. Giguere and B.B. Bhattacharyya, Basic Nonuniform Lines, Proc. IEE, Vol. 116, No. 5, pp. 710-712, May, 1969.
93. N. Balabanian and T.E. Bickart, Electrical Network Theory, John Wiley and Sons, 1969.
94. F.M. Reza and S. Seely, Modern Network Analysis, McGraw-Hill Book Co., 1959.
95. E.G. Cristal, Analysis and Exact Synthesis of Cascaded Commensurate Transmission Line C Section All-pass Networks, IEEE Trans. on Microwave Theory and Techniques, Vol. MTT-14, No. 6, pp. 285-291, June, 1966.
96. D.C. Youla, Solution to the Problem of Complex Normalization, Microwave Research Institute, Polytechnic Inst. of Brooklyn, Memo 48, January, 1961.
97. R.W. Beatty and D.M. Kerns, Relationships between Different Kinds of Network Parameters, not assuming Reciprocity or Equality of the Waveguide or Transmission Line Characteristic Impedances, Proc. IEEE, Vol. 51, No. 1, pp. 84, January, 1963.
98. H.J. Carlin and A.B. Giordano, Network Theory, An Introduction to Reciprocal and Non-Reciprocal Circuits, Prentice-Hall Inc., 1964.

99. H.J. Helstrom, Symmetrical RC Distributed Networks, Proc. IRE,
Vol. 50, No. 1, pp. 97-98, January, 1962.

APPENDIX A
DETERMINATION OF SCATTERING MATRIX FROM THE
CHAIN MATRIX FOR A FOUR-PORT

Consider the four-port network of Fig.A.1, where Z_j , V_j , I_j , a_j and b_j are respectively the terminating impedance, voltage, current, incident and reflected wave amplitudes at the j th port. The equation relating the voltages and currents of input ports (1) and (2) with that of voltages and currents at the output ports (3) and (4) is

$$\begin{bmatrix} \underline{V}_{in} \\ \underline{I}_{in} \end{bmatrix} = [a] \begin{bmatrix} \underline{V}_{out} \\ -\underline{I}_{out} \end{bmatrix} \quad \dots (A.1a)$$

where $[a]$ is the chain matrix of the 4-port and

$$\underline{V}_{in} = \begin{bmatrix} V_1 \\ V_2 \end{bmatrix} ; \quad \underline{V}_{out} = \begin{bmatrix} V_3 \\ V_4 \end{bmatrix} \quad \dots (A.1b)$$

$$\underline{I}_{in} = \begin{bmatrix} I_1 \\ I_2 \end{bmatrix} ; \quad \underline{I}_{out} = \begin{bmatrix} I_3 \\ I_4 \end{bmatrix} \quad \dots (A.1c)$$

Using complex normalization⁽⁹⁶⁾, the incident and reflected wave amplitudes are related with the voltage and current at that port as

$$a_j = \frac{1}{2/r_j} (V_j + Z_j I_j) \quad \dots (A.2a)$$

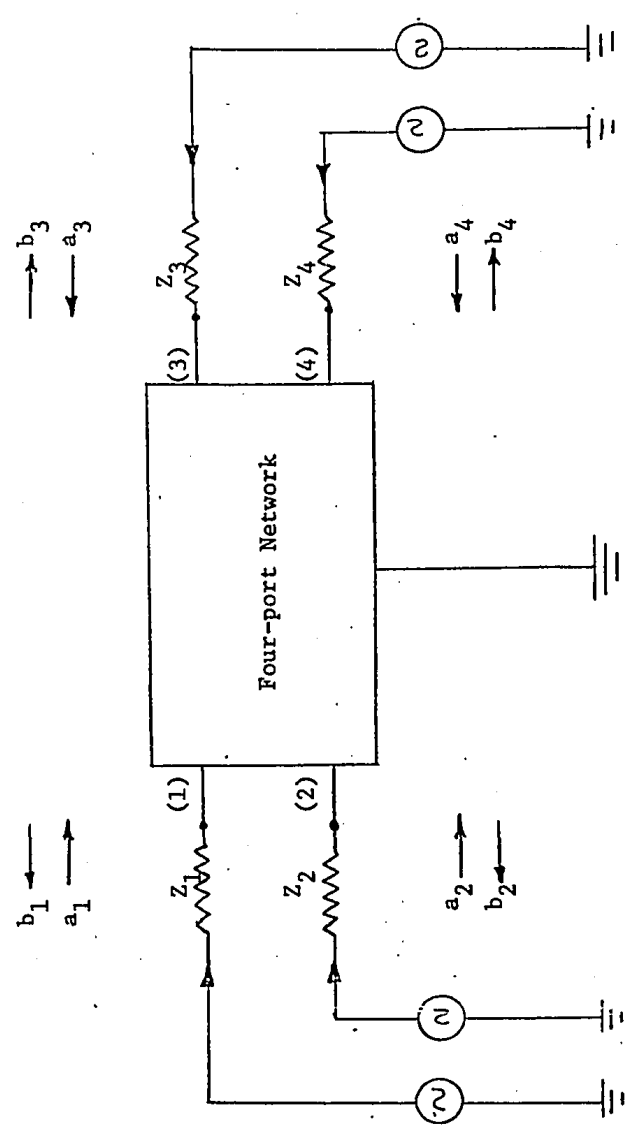


Fig. A.1: A Terminated Four-port Network

$$b_j = \frac{1}{2\sqrt{r_j}} (V_j - \bar{Z}_j I_j) \quad \dots (A.2b)$$

where

$$\operatorname{Re} Z_j = r_j > 0$$

Writing (A.2) for this four-port in the matrix form

$$\begin{bmatrix} a_{in} \\ \dots \\ b_{in} \end{bmatrix} = [N_i] \begin{bmatrix} V_{in} \\ \dots \\ I_{in} \end{bmatrix} \quad \dots (A.3a)$$

$$\begin{bmatrix} a_{out} \\ \dots \\ b_{out} \end{bmatrix} = [N_\ell] \begin{bmatrix} V_{out} \\ \dots \\ I_{out} \end{bmatrix} \quad \dots (A.3b)$$

where

$$[N_i] = \frac{1}{2}[r_i]^{-1/2} \begin{bmatrix} [U] : [Z_i] \\ \dots : \dots \\ [U] : -[\bar{Z}_i] \end{bmatrix} \quad \dots (A.3c)$$

$$[N_\ell] = \frac{1}{2}[r_\ell]^{-1/2} \begin{bmatrix} [U] : [Z_\ell] \\ \dots : \dots \\ [U] : -[\bar{Z}_\ell] \end{bmatrix} \quad \dots (A.3d)$$

$$[Z_i] = \operatorname{diag} (Z_1, Z_2) \quad , \quad [r_i] = \operatorname{Re} [Z_i] = \operatorname{diag} (r_1, r_2) \quad \dots (A.3e)$$

$$[Z_\ell] = \operatorname{diag} (Z_3, Z_4) \quad , \quad [r_\ell] = \operatorname{Re} [Z_\ell] = \operatorname{diag} (r_3, r_4) \quad \dots (A.3f)$$

$$a_{in} = \begin{bmatrix} a_1 \\ a_2 \end{bmatrix} \quad , \quad a_{out} = \begin{bmatrix} a_3 \\ a_4 \end{bmatrix} \quad \dots (A.3g)$$

$$b_{in} = \begin{bmatrix} b_1 \\ b_2 \end{bmatrix} \quad , \quad b_{out} = \begin{bmatrix} b_3 \\ b_4 \end{bmatrix} \quad \dots (A.3h)$$

From (A.3a) and (A.1a)

$$\begin{bmatrix} \tilde{a}_{in} \\ \dots \\ \tilde{b}_{in} \end{bmatrix} = [N_i][a] \begin{bmatrix} \tilde{v}_{out} \\ \dots \\ -\tilde{I}_{out} \end{bmatrix} \quad \dots (A.4)$$

The above equation may also be written as

$$\begin{bmatrix} \tilde{a}_{in} \\ \dots \\ \tilde{b}_{in} \end{bmatrix} = [N_i][a] \begin{bmatrix} [U] : [0] \\ \dots \\ [0] : -[U] \end{bmatrix} [N_\ell]^{-1} \begin{bmatrix} \tilde{a}_{out} \\ \dots \\ \tilde{b}_{out} \end{bmatrix}$$

or

$$\begin{bmatrix} \tilde{b}_{in} \\ \dots \\ \tilde{a}_{in} \end{bmatrix} = \begin{bmatrix} [0] : [U] \\ \dots \\ [U] : [0] \end{bmatrix} [N_i][a] \begin{bmatrix} [U] : [0] \\ \dots \\ [0] : -[U] \end{bmatrix} [N_\ell]^{-1} \begin{bmatrix} \tilde{a}_{out} \\ \dots \\ \tilde{b}_{out} \end{bmatrix} \quad \dots (A.5)$$

The transfer scattering matrix of this network is defined by

$$\begin{bmatrix} \tilde{b}_{in} \\ \dots \\ \tilde{a}_{in} \end{bmatrix} = [T] \begin{bmatrix} \tilde{a}_{out} \\ \dots \\ \tilde{b}_{out} \end{bmatrix} \quad \dots (A.6a)$$

where

$$[T] = \begin{bmatrix} [T_{11}] : [T_{12}] \\ \dots \\ [T_{21}] : [T_{22}] \end{bmatrix} = \begin{bmatrix} t_{11} & t_{12} & t_{13} & t_{14} \\ t_{21} & t_{22} & t_{23} & t_{24} \\ \dots & \dots & \dots & \dots \\ t_{31} & t_{32} & t_{33} & t_{34} \\ t_{41} & t_{42} & t_{43} & t_{44} \end{bmatrix} \quad \dots (A.6b)$$

From (A.5) and (A.6), the transfer scattering matrix is expressed as

$$[T] = \begin{bmatrix} [0] : [U] \\ \dots \\ [U] : [0] \end{bmatrix} [N_i][a] \begin{bmatrix} [U] : [0] \\ \dots \\ [0] : -[U] \end{bmatrix} [N_\ell]^{-1} \quad \dots (A.7)$$

From (A.3)

$$\tilde{a}_{out} = \frac{1}{2} [r_\ell]^{-1} \{ \tilde{v}_{out} + [Z_\ell] \tilde{I}_{out} \} \quad \dots (A.8a)$$

$$b_{out} = \frac{1}{2}[r_\ell]^{-\frac{1}{2}}\{v_{out} - [\bar{Z}_\ell] i_{out}\} \quad \dots (A.8b)$$

By subtracting and adding (A.8b) with (A.8a), and simplifying

$$i_{out} = [r_\ell]^{-\frac{1}{2}}\{a_{out} - b_{out}\}$$

$$v_{out} = [r_\ell]^{-\frac{1}{2}}\{[\bar{Z}_\ell] a_{out} + [Z_\ell] b_{out}\}$$

or

$$\begin{bmatrix} v_{out} \\ \dots \\ i_{out} \end{bmatrix} = [r_\ell]^{-\frac{1}{2}} \begin{bmatrix} [\bar{Z}_\ell] : [Z_\ell] \\ \dots \\ [U] : -[U] \end{bmatrix} \begin{bmatrix} a_{out} \\ \dots \\ b_{out} \end{bmatrix} \quad \dots (A.9)$$

Hence, from (A.3b) and (A.9)

$$[N_\ell]^{-1} = [r_\ell]^{-\frac{1}{2}} \begin{bmatrix} [\bar{Z}_\ell] : [Z_\ell] \\ \dots \\ [U] : -[U] \end{bmatrix} \quad \dots (A.10)$$

Substituting (A.10) in (A.7), the transfer scattering matrix in terms of four-port chain matrix [a] is obtained as

$$[T] = \frac{1}{2}[X][a][X^*] \quad \dots (A.11a)$$

where

$$[X] = [r_1]^{-\frac{1}{2}} \begin{bmatrix} [U] : -[\bar{Z}_1] \\ \dots \\ [U] : [Z_1] \end{bmatrix} \quad \dots (A.11b)$$

and

$$[X^*] = [r_\ell]^{-\frac{1}{2}} \begin{bmatrix} [\bar{Z}_\ell] : [Z_\ell] \\ \dots \\ -[U] : [U] \end{bmatrix} \quad \dots (A.11c)$$

APPENDIX B

SCATTERING MATRIX FOR A FOUR-PORT IN TERMS OF THE TRANSFER
SCATTERING MATRIX PARAMETERS

Consider the four-port network of Fig.A.1. The scattering matrix of this four-port is defined as

$$\begin{bmatrix} \tilde{b}_{in} \\ \dots \\ \tilde{b}_{out} \end{bmatrix} = [S] \begin{bmatrix} \tilde{a}_{in} \\ \dots \\ \tilde{a}_{out} \end{bmatrix} \quad \dots (B.1)$$

where the scattering variable vectors \tilde{a}_{in} , \tilde{b}_{in} , \tilde{a}_{out} and \tilde{b}_{out} are defined by (A.3). The transfer scattering matrix of the four-port is described in (A.6). From (A.6) and (B.1), the scattering matrix in terms of transfer scattering matrix is obtained as⁽⁹⁷⁾

$$[S] = \begin{bmatrix} [T_{12}] [T_{22}]^{-1} & : & [T_{11}] - [T_{22}]^{-1} [T_{21}] \\ \dots & & \dots \\ [T_{22}]^{-1} & : & -[T_{22}]^{-1} [T_{21}] \end{bmatrix} \quad \dots (B.2)$$

Substituting for $[T_{11}]$, $[T_{12}]$, $[T_{21}]$ from (A.6b), and for $[T_{22}]^{-1}$ from (B.2), the scattering matrix of the four-port may be expressed in terms of transfer scattering matrix parameters as:

$$[S] = \frac{1}{\Delta} \begin{bmatrix} \begin{bmatrix} t_{13} t_{44} & t_{14} t_{33} \\ t_{14} t_{43} & -t_{13} t_{34} \end{bmatrix} \Delta t_{11} - \begin{bmatrix} t_{31} (t_{13} t_{44} - t_{14} t_{43}) \\ +t_{41} (t_{14} t_{33} - t_{13} t_{34}) \end{bmatrix} \Delta t_{12} - \begin{bmatrix} t_{32} (t_{23} t_{44} - t_{14} t_{43}) \\ +t_{42} (t_{14} t_{33} - t_{13} t_{34}) \end{bmatrix} \\ \begin{bmatrix} t_{23} t_{44} & t_{24} t_{33} \\ -t_{24} t_{43} & -t_{23} t_{34} \end{bmatrix} \Delta t_{21} - \begin{bmatrix} t_{31} (t_{23} t_{44} - t_{24} t_{43}) \\ +t_{41} (t_{24} t_{33} - t_{23} t_{34}) \end{bmatrix} \Delta t_{22} - \begin{bmatrix} t_{32} (t_{23} t_{44} - t_{24} t_{43}) \\ +t_{42} (t_{24} t_{33} - t_{23} t_{34}) \end{bmatrix} \\ t_{44} & -t_{34} & t_{41} t_{34} - t_{44} t_{31} & t_{34} t_{42} - t_{44} t_{32} \\ -t_{43} & t_{33} & t_{43} t_{31} - t_{33} t_{41} & t_{43} t_{32} - t_{33} t_{42} \end{bmatrix} \quad \dots (B.3)$$

APPENDIX C

THEOREMS CONCERNING PROPORTIONAL AND DUAL LINES

The following three theorems concerning NUTLs with proportional and dual distributions will now be proved.

Theorem 1:

The necessary and sufficient conditions for the chain parameters of a lossless NUTL \mathcal{L} of an arbitrary length ℓ to be interrelated as

$$A = D$$

$$B = r^2(\ell)C$$

r being a constant independent of s , is that \mathcal{L} be a proportional line (99), that is, if the distribution of $L(x)$ is given by

$$L(x) = L_0 F(x)$$

then, the distribution of $C(x)$ is

$$C(x) = \frac{L_0}{r^2} F(x) = C_0 F(x).$$

Necessity:

For a lossless line with distributions per unit length $L(x)$ and $C(x)$, where $L(x)$ and $C(x)$ are positive integrable functions of x , it is known that the chain parameters are^(87,88):

$$A = 1 + \sum_{n=1}^{\infty} a_n s^{2n} \quad \dots (C.1)$$

$$B = \sum_{n=0}^{\infty} b_n s^{2n+1} \quad \dots (C.2)$$

$$C = \sum_{n=0}^{\infty} c_n s^{2n+1} \quad \dots (.3)$$

$$D = 1 + \sum_{n=1}^{\infty} d_n s^{2n} \quad \dots (C.4)$$

where

$$a_n = \int_0^{\ell} C(x_{2n}) \int_0^{x_{2n}} L(x_{2n-1}) \dots \int_0^{x_3} C(x_2) \int_0^{x_2} L(x_1) dx_1 dx_2 \dots dx_{2n} \quad \dots (C.5)$$

$$b_n = \int_0^{\ell} L(x_{2n+1}) \int_0^{x_{2n+1}} C(x_{2n}) \dots \int_0^{x_3} C(x_2) \int_0^{x_2} L(x_1) dx_1 dx_2 \dots dx_{2n+1} \quad \dots (C.6)$$

$$c_n = \int_0^{\ell} C(x_{2n+1}) \int_0^{x_{2n+1}} L(x_{2n}) \dots \int_0^{x_3} L(x_2) \int_0^{x_2} C(x_1) dx_1 dx_2 \dots dx_{2n+1} \quad \dots (C.7)$$

$$d_n = \int_0^{\ell} L(x_{2n}) \int_0^{x_{2n}} C(x_{2n-1}) \dots \int_0^{x_3} L(x_2) \int_0^{x_2} C(x_1) dx_1 dx_2 \dots dx_{2n} \quad \dots (C.8)$$

Let for a line of length ξ ($0 \leq \xi \leq \ell$), the total inductance and capacitance be related as

$$\int_0^{\xi} L(x) dx = \mu(\xi) \int_0^{\xi} C(x) dx \quad \dots (C.9)$$

Now, since $A = D$, and $B = r^2(\ell)C$, it is seen from (C.1)-(C.8) that it is necessary that

$$a_1 = d_1 \quad \dots (C.10)$$

and

$$b_0 = r^2(\ell)c_0 \quad \dots (C.11)$$

Hence

$$\int_0^{\ell} C(x_2) \int_0^{x_2} L(x_1) dx_1 dx_2 = \int_0^{\ell} L(x_2) \int_0^{x_2} C(x_1) dx_1 dx_2 \quad \dots (C.12)$$

and

$$\int_0^{\ell} L(x_1) dx_1 = r^2(\ell) \int_0^{\ell} C(x_1) dx_1 \quad \dots (C.13)$$

where x_2 ranges from 0 to ℓ .

Substituting (C.9) in (C.12)

$$\int_0^\ell C(x_2) \mu(x_2) \int_0^{x_2} C(x_1) dx_1 dx_2 = \int_0^\ell L(x_2) \int_0^{x_2} C(x_1) dx_1 dx_2$$

or

$$\int_0^\ell [C(\xi)\mu(\xi) - L(\xi)] \int_0^\xi C(x_1) dx_1 d\xi = 0$$

Since the above expression should hold for any arbitrary ℓ ,

$$C(\xi)\mu(\xi) - L(\xi) = 0 \quad 0 \leq \xi \leq \ell$$

hence

$$L(\xi) = C(\xi)\mu(\xi) \quad \dots (C.14)$$

Thus

$$\int_0^\ell L(\xi) d\xi = \int_0^\ell C(\xi)\mu(\xi) d\xi \quad \dots (C.15)$$

From (C.14) and (C.13)

$$\int_0^\ell C(\xi)\mu(\xi) d\xi = r^2(\ell) \int_0^\ell C(\xi) d\xi$$

for any arbitrary length. Hence

$$\mu(\xi) = r^2(\ell)$$

That is, the function μ should be independent of ξ . Therefore, from

(C.14), it is seen that if the distribution of $L(x)$ is

$$L(x) = L_0 F(x) \quad \dots (C.16a)$$

then the distribution of $C(x)$ is

$$C(x) = C_0 F(x) \quad \dots (C.16b)$$

where

$$r = \sqrt{L_0/C_0} \quad \dots (C.16c)$$

Hence, the necessity of the theorem is established.

Sufficiency:

Assuming the distributions of the line \mathcal{L} to be given by (C.16), it is readily seen from (C.5) and (C.8) that

$$A = D,$$

while from (C.6) and (C.7), it is seen that

$$\frac{b_n}{L_0^{n+1} C_0^n} = \frac{c_n}{C_0^{n+1} L_0^n}, \quad n = 0, 1, 2, \dots$$

or

$$b_n = \frac{L_0}{C_0} c_n = r^2 c_n$$

Hence

$$B = r^2 C$$

Thus the sufficiency is proved.

Theorem 2:

The necessary and sufficient conditions for the chain parameters of two lossless lines \mathcal{L}_1 and \mathcal{L}_2 of equal but arbitrary length ℓ to be interrelated as

$$\begin{aligned} A_1 &= D_2, & D_1 &= A_2 \\ B_1 &= r^2(\ell) C_2, & C_1 &= \frac{B_2}{r^2(\ell)} \end{aligned}$$

r being independent of s , is that \mathcal{L}_1 and \mathcal{L}_2 be dual lines; that is, if the distribution of \mathcal{L}_1 are

$$L_1 = L_{10} F(x) \quad , \quad C_1 = C_{10} G(x) \quad 0 \leq x \leq \ell$$

then the distributions of \mathcal{L}_2 are

$$L_2 = L_{20} G(x) \quad , \quad C_2 = C_{20} F(x) \quad 0 \leq x \leq \ell$$

where

$$r = \sqrt{L_{10}/C_{20}} = \sqrt{L_{20}/C_{10}}$$

Necessity:

Let $L_1(x)$ and $C_1(x)$ be the distributions for line \mathcal{L}_1 and $L_2(x)$ and $C_2(x)$ for line \mathcal{L}_2 , where L_1 , C_1 , L_2 and C_2 are positive integrable functions of x . Then the chain parameters of lines \mathcal{L}_1 and \mathcal{L}_2 may be expressed in terms of the uniformly convergent series in the form

$$A_v = 1 + \sum_{n=1}^{\infty} a_{nv} s^{2n} \quad \dots (C.17)$$

$$B_v = \sum_{n=0}^{\infty} b_{nv} s^{2n+1} \quad \dots (C.18)$$

$$C_v = \sum_{n=0}^{\infty} c_{nv} s^{2n+1} \quad \dots (C.19)$$

$$D_v = 1 + \sum_{n=1}^{\infty} d_{nv} s^{2n} \quad \dots (C.20)$$

where

$$a_{nv} = \int_0^{\ell} C_v(x_{2n}) \int_0^{x_{2n}} L_v(x_{2n-1}) \dots \int_0^{x_2} L_v(x_1) dx_1 \dots dx_{2n} \quad \dots (C.21)$$

$$b_{nv} = \int_0^{\ell} L_v(x_{2n+1}) \int_0^{x_{2n+1}} C_v(x_{2n}) \dots \int_0^{x_2} L_v(x_1) dx_1 \dots dx_{2n+1} \quad \dots (C.22)$$

$$c_{nv} = \int_0^{\ell} C_v(x_{2n+1}) \int_0^{x_{2n+1}} L_v(x_{2n}) \dots \int_0^{x_2} C_v(x_1) dx_1 \dots dx_{2n+1} \quad \dots (C.23)$$

$$d_{nv} = \int_0^{\ell} L_v(x_{2n}) \int_0^{x_{2n}} C_v(x_{2n-1}) \dots \int_0^{x_2} C_v(x_1) dx_1 \dots dx_{2n} \quad \dots (C.24)$$

and $v=1,2$ respectively corresponds to the line \mathcal{L}_1 and \mathcal{L}_2 . For a length of $\xi (0 \leq \xi \leq \ell)$, let the total inductance of \mathcal{L}_1 be related to the total capacitance of \mathcal{L}_2 in the form

$$\int_0^{\xi} L_1(\xi) d\xi = \mu_1(\xi) \int_0^{\xi} C_2(\xi) d\xi \quad \dots (C.25)$$

while the total inductance of \mathcal{L}_2 and total capacitance of \mathcal{L}_1 be related as

$$\int_0^{\xi} L_2(\xi) d\xi = \mu_2(\xi) \int_0^{\xi} C_1(\xi) d\xi \quad \dots (C.26)$$

Since $A_1 = D_2$, $A_2 = D_1$, $B_1 = r^2(\ell)C_2$ and $B_2 = r^2(\ell)C_1$, it is necessary from (C.17)-(C.24) that

$$a_{11} = d_{12} \quad \dots (C.27)$$

$$a_{12} = d_{11} \quad \dots (C.28)$$

$$b_{01} = r^2(\ell)c_{02} \quad \dots (C.29)$$

$$b_{02} = r^2(\ell)c_{01} \quad \dots (C.30)$$

From (C.21)-(C.24) and the above equations, it is seen that

$$\int_0^{\ell} C_1(x_2) \int_0^{x_2} L_1(x_1) dx_1 dx_2 = \int_0^{\ell} L_2(x_2) \int_0^{x_2} C_2(x_1) dx_1 dx_2 \quad \dots (C.31)$$

$$\int_0^{\ell} C_2(x_2) \int_0^{x_2} L_2(x_1) dx_1 dx_2 = \int_0^{\ell} L_1(x_2) \int_0^{x_2} C_1(x_1) dx_1 dx_2 \quad \dots (C.32)$$

$$\int_0^{\ell} L_1(x_1) dx_1 = r^2(\ell) \int_0^{\ell} C_2(x_1) dx_1 \quad \dots (C.33)$$

$$\int_0^{\ell} L_2(x_1) dx_1 = r^2(\ell) \int_0^{\ell} C_1(x_1) dx_1 \quad \dots (C.34)$$

where x_2 ranges from 0 to ℓ .

Substituting (C.25) in (C.31)

$$\int_0^{\ell} C_1(x_2) \mu_1(x_2) \int_0^{x_2} C_2(x_1) dx_1 dx_2 = \int_0^{\ell} L_2(x_2) \int_0^{x_2} C_2(x_1) dx_1 dx_2$$

or

$$\int_0^{\ell} [C_1(\xi) \mu_1(\xi) - L_2(\xi)] \int_0^{\xi} C_2(x_1) dx_1 d\xi = 0$$

Since the above expression should hold for any arbitrary length ℓ

$$C_1(\xi) \mu_1(\xi) - L_2(\xi) = 0 \quad 0 \leq \xi \leq \ell$$

or

$$L_2(\xi) = \mu_1(\xi) C_1(\xi) \quad \dots (C.35)$$

Similarly, using (C.25) in (C.32), it can be shown that

$$L_1(\xi) = \mu_2(\xi) C_2(\xi) \quad \dots (C.36)$$

Integrating (C.35) from 0 to ℓ and using (C.34) for any arbitrary ℓ ,

it is obtained that

$$\int_0^{\ell} L_2(\xi) d\xi = \int_0^{\ell} \mu_1(\xi) C_1(\xi) d\xi = r^2(\ell) \int_0^{\ell} C_1(\xi) d\xi$$

Hence

$$\mu_1(\xi) = r^2(\ell) \quad \dots (C.37)$$

Similarly, from (C.36) and (C.33), it can be shown that

$$\mu_2(\xi) = r^2(\ell) \quad \dots (C.38)$$

Thus, from (C.37) and (C.38)

$$\mu_1(\xi) = \mu_2(\xi) = r^2(\ell)$$

and hence both μ_1 and μ_2 are independent of ξ . Therefore, from (C.35), (C.36) and (C.37)

$$\begin{aligned} L_2(\xi) &= r^2(\ell) C_1(\xi) \\ C_2(\xi) &= \frac{L_1(\xi)}{r^2(\ell)} \quad 0 \leq \xi \leq \ell \end{aligned}$$

Hence, if the distributions of ℓ_1 are

$$L_1(x) = L_{10} F(x) \quad , \quad C_1(x) = C_{10} G(x) \quad 0 \leq x \leq \ell \quad \dots (C.39a)$$

then the distributions of ℓ_2 are

$$L_2(x) = L_{20} F(x) \quad , \quad C_2(x) = C_{20} G(x) \quad 0 \leq x \leq \ell \quad \dots (C.39b)$$

where

$$r = \sqrt{L_{10}/C_{20}} = \sqrt{L_{20}/C_{10}} \quad \dots (C.39c)$$

Thus the necessity is proved.

Sufficiency:

Let the line ℓ_1 and ℓ_2 have distributions as given by (C.39).

Then the various j th coefficients in the different series (C.17)-(C.20) are:

$$a_{j1} = (L_{10}C_{10})^j \int_0^{\ell} G(x_{2j}) \int_0^{x_{2j}} F(x_{2j-1}) \dots \int_0^{x_2} F(x_1) dx_1 \dots dx_{2j} \quad \dots (C.40a)$$

$$b_{j1} = L_{10}^{j+1} C_{10}^j \int_0^{\ell} F(x_{2j+1}) \int_0^{x_{2j+1}} G(x_{2j}) \dots \int_0^{x_2} F(x_1) dx_1 \dots dx_{2j+1} \quad \dots (C.40b)$$

$$c_{j1} = C_{10}^{j+1} L_{10}^j \int_0^{\ell} G(x_{2j+1}) \int_0^{x_{2j+1}} F(x_{2j}) \dots \int_0^{x_2} G(x_1) dx_1 \dots dx_{2j+1} \quad \dots (C.40c)$$

$$d_{j1} = (L_{10}C_{10})^j \int_0^{\ell} F(x_{2j}) \int_0^{x_{2j}} G(x_{2j-1}) \dots \int_0^{x_2} G(x_1) dx_1 \dots dx_{2j+1} \quad \dots (C.40d)$$

and

$$a_{j2} = (L_{20}C_{20})^j \int_0^{\ell} F(x_{2j}) \int_0^{x_{2j}} G(x_{2j-1}) \dots \int_0^{x_2} G(x_1) dx_1 \dots dx_{2j} \quad \dots (C.41a)$$

$$b_{j2} = L_{20}^{j+1} C_{20}^j \int_0^{\ell} G(x_{2j+1}) \int_0^{x_{2j+1}} F(x_{2j}) \dots \int_0^{x_2} G(x_1) dx_1 \dots dx_{2j+1} \quad \dots (C.41b)$$

$$c_{j2} = C_{20}^{j+1} L_{20}^j \int_0^{\ell} F(x_{2j+1}) \int_0^{x_{2j+1}} G(x_{2j}) \dots \int_0^{x_2} F(x_1) dx_1 \dots dx_{2j+1} \quad \dots (C.41c)$$

$$d_{j2} = (L_{20}C_{20})^j \int_0^{\ell} G(x_{2j}) \int_0^{x_{2j}} F(x_{2j-1}) \dots \int_0^{x_2} F(x_1) dx_1 \dots dx_{2j} \quad \dots (C.41d)$$

From the above expressions, it is readily seen that

$$a_{j1} = d_{j2} \quad , \quad d_{j1} = a_{j2}$$

$$b_{j1} = \frac{L_{10}}{C_{20}} c_{j2} \quad , \quad c_{j1} = \frac{C_{10}}{L_{20}} b_{j2}$$

Hence

$$A_1 = D_2 \quad , \quad D_1 = A_2 \quad , \quad B_1 = r^2 C_2 \quad , \quad C_1 = \frac{B_2}{r}$$

Thus, the sufficiency is established.

Theorem 3:

The necessary and sufficient conditions for the chain parameters of two lossless lines ℓ_1 and ℓ_2 of equal but arbitrary length ℓ , to be interrelated as

$$\begin{aligned} A_1 &= A_2, & D_1 &= D_2 \\ B_1 &= r^2(\ell)C_2, & B_2 &= r^2(\ell)C_1 \end{aligned}$$

r being independent of s , is that if the distributions of ℓ_1 are

$$L_1 = L_{10} F(x), \quad C_1 = C_{10} G(x)$$

then the distributions of ℓ_2 are

$$L_2 = L_{20} G(\ell-x), \quad C_2 = C_{20} F(\ell-x)$$

Proof:

It is well known that if (A_2, B_2, C_2, D_2) are the chain parameters of a line of length ℓ , having distributions $L_{20} G(x)$ and $C_{20} F(x)$, then the chain parameters of the line of length ℓ with distributions $L_{20} G(\ell-x)$ and $C_{20} F(\ell-x)$ are (D_2, B_2, C_2, A_2) , since the latter line is nothing but the former looking from right to left. Hence Theorem 3 readily follows from the above result and Theorem 2.